BEHAVIOUR AND DESIGN OF TIMBER-CONCRETE COMPOSITE FLOOR SYSTEM

Ph.D. Thesis

David Yeoh Eng Chuan

2010

Acknowledgements

"I lift up my eyes to the hills – where does my help come from? My help comes from the LORD, the Maker of heaven and earth." Psalms 121: 1-2

Someone once told me to put God first place in my life, and He will bring me to places I never dreamed of. True enough. In this race towards a PhD, God has not only brought me to New Zealand, but He has supplied all my needs according to His riches and met me with good and competent people throughout my journey. Here, I want to say "thank you" to all these special people who have contributed to my success. Without them, I would not have reached the finish line. I pray that God will bless and reward all these people in His time. Ultimately, my help has come from God who has given me grace, health and a strong will to complete the run.

First and foremost, to Jesus Christ, be the glory. His love and grace endures forever.

My beloved wife, Chin Ping, sons, Jonathan and Josiah, has been the greatest cost of my undertaking this race. They have been very patient and understanding despite my long hours at work. In my constant absence, my wife has lovingly cared for our sons, a task far greater than a PhD.

I am indebted to my team of supervisors – Associate Professor Dr Massimo Fragiacomo, Professor Dr Andy Buchanan, and Dr Bruce Deam. They have provided invaluable support, encouragement and insightful advice at all stages of the project. It is an honour to be called also their friend.

Associate Professor Dr Massimo Fragiacomo deserves special acknowledgement. "As iron sharpens iron, so one man sharpens another." A man of noble character is hard to find and I have found one. He was a model mentor and his countless hours sitting with me have given me fundamental insights into the subject matter. His sacrificial commitment to the project is beyond doubt. I am so blessed to have him run this race together with me.

Marta Mazzilli, Mary De Franceschi and Nor Hayati Abd Ghafar were involved directly in the project, constructing and testing of the connection and beam specimens. They have been a wonderful blessing. The extent of their help is greatly appreciated. My officemates who each ran his own race: Min-Ho Chey, Koichi Sugioka, Vinod Kota Sadashiva, and Manoochehr Ardalany who recently started his run. Their persistence in their race has been a constant quiet motivation and encouragement.

I like to thank my friend from University Technology Sydney, Professor Keith Crews for reading my thesis draft and making some helpful observations. Thanks to Norm Pilling and John Maley – technical staffs in the Structures Laboratory for their dedication and assistance in the construction and testing of my test specimens. Other technical staffs I wish to acknowledge are Tim Perigo, Bob Wilsea-Smith, Alan Poynter, Peter Coursey, Richard Newton, Michael Weavers, Stuart Toase, Mosese Fifita, Russell McConchie, and Nigel Dixon. Not forgetting Warwick Banks of Carter Holt Harvey; James Mackechnie from Allied Concrete, formerly a Senior Lecturer at UC; Steve Coll and Antony Cook of Mitek NZ, all of whom have contributed technical support throughout different stages of the project. The kindness of Elizabeth Ackermann who voluntarily assisted me in the last stages is deeply appreciated.

I am grateful to Education New Zealand who granted me a New Zealand International Doctoral Research Scholarship (NZIDRS) and Universiti Tun Hussein Onn Malaysia who provided partial scholarship, which without both, I would not be able to start this race.

Appreciation goes to my sisters, Julie and Jackie for their moral support.

Finally, this success is for my mother, Liew Kam Ooi, who sacrificially and lovingly raised me and gave me education. Her labour and seed sown has borne good fruit. Also for my late uncle, Liew Kam Pong, who has been my spiritual mentor and father.

"This is what the Lord says: 'Let not the wise man boast of his wisdom or the strong man boast of his strength or the rich man boast of his riches, but let him who boasts boast about this: that he understands and knows me, that I am the Lord, who exercises kindness, justice and righteousness on earth, for in these I delight,' declares the Lord." Jeremiah 9:23-24

Abstract

This Ph.D. thesis represents a summative report detailing research processes and outcomes from investigating the ultimate and serviceability limit state short- and long-term behaviour and design of timber-concrete composite floors. The project enables the realization of a semi-prefabricated LVL-concrete composite floor system of up to 15 m long using 3 types of connection. Design span tables which satisfy the ultimate and serviceability limit state short- and long-term verifications for this system form the novel contribution of this thesis.

In quantifying the behaviour of timber-concrete composite floors, 5 different experimental phases have been carried. 9 major achievements in meeting 9 sub-objectives have been concluded:

1) Three best types of connection system for timber-concrete composite floors have been identified.

2) The characteristic strength and secant slip moduli for these connections have been determined.

3) The short-term behaviour of the selected connections defined by their pre- and post-peak responses under collapse load has been established.

4) An analytical model for the strength evaluation of the selected connections based on the different possible modes of failure has been derived.

5) Easy and fast erected semi-prefabricated timber-concrete composite floor has been proposed.

6) The short-term ultimate and serviceability limit state behaviour of timber-concrete composite floor beams under collapse load has been investigated.

7) The long-term behaviour of chosen connections defined by their creep coefficient has been determined.

8) The long-term behaviour of timber-concrete composite floor beams under sustained load at serviceability limit state condition has been investigated.

9) Design example and span tables for semi-prefabricated timber-concrete composite floors that satisfy both the ultimate and serviceability limit state in the short- and long-term using the γ-method have been developed.

Table of Contents

List of Figures

List of Tables

List of Publications

Journal papers:

1) Yeoh D, Fragiacomo M, Buchanan A, Gerber C (2009) Preliminary research towards a semi-prefabricated LVL-concrete composite floor system for the Australasian market. Australasian J Struct Eng 9(3) 225-240.

2) Yeoh D, Fragiacomo M, De Franceschi M, Buchanan A (2009) Experimental tests of notched and plate connectors for LVL-concrete composite beams. J Struct Eng ASCE, submitted August 2009, under review.

3) Yeoh D, Fragiacomo M, De Franceschi M, Koh HB (2009) The state-of-the-art on timber-concrete composite structures – a literature review. J Struct Eng ASCE, submitted August 2009, under review.

4) Yeoh D, Fragiacomo M, Banks W, Newcombe MP (2009) Design and construction of a LVL-concrete composite floor. J Structures and Buildings ICE – Timber special issue, submitted October 2009, under review.

5) Yeoh D, Fragiacomo M, Deam B (2009) Long-term behaviour of LVL-concrete composite connections and beams under sustained load. J Materials and Structures RILEM, submitted December 2009, under review.

6) Yeoh D, Fragiacomo M, Deam B (2010) Experimental limit state behaviour of LVL-concrete composite floor beams. J Eng Struct Elsevier, submitted January 2010, under review.

Publications other than journal papers:

1) Buchanan AH (2007) Timber Design Guide – Chapter 25: Timber flooring by Fragiacomo M, Yeoh D, Davison R, Banks W. New Zealand Timber Industry Federation Inc., Wellington, 275-288.

2) Yeoh D, Fragiacomo M, Aldi P, Mazzilli M, Kuhlmann U (2008) Performance of notched coach screw connection for timber-concrete composite floor system. In:

Proceedings of the 10th World Conference on Timber Engineering, 2-5 June, Miyazaki (Japan), Paper 221, CD copy.

3) Yeoh D, Fragiacomo M, Buchanan A, Crews K, Haskell J, Deam B (2008) Development of semi-prefabricated timber-concrete composite floors in Australasia. In: Proceedings of the 10th World Conference on Timber Engineering, 2-5 June, Miyazaki (Japan), Paper 222, CD copy.

4) Yeoh D, Fragiacomo M, Abd Ghafar H, Buchanan A, Deam B, Crews K (2008) LVL-concrete composite floor systems: an effective solution for multi-storey timber buildings. In: Proceedings of the Australasian Structural Engineering Conference, 26-27 June, Melbourne (Australia), Paper 236, CD copy.

5) Gerber C, Crews K, Yeoh D, Buchanan A (2008) Investigation on the structural behaviour of timber concrete composite connections. In: Proceedings of the 20th Australasian Conference on the Mechanics of Structures and Materials, Queensland (Australia), CD copy.

6) Yeoh D (2008) Timber-concrete composite connections and beams. In: Proceedings of the 7th FIB PhD Symposium, 11-13 September, Stuttgart (Germany), CD copy.

7) Yeoh D, Fragiacomo M, De Francheschi M, Clemente I (2008) Timber-concrete composite connections and beams.In: Proceedings of the VII Italian Workshop on Composite Structures, 23-24 October, Benevento (Italy), CD copy.

8) Koh HB, Mohamad Diah AB, Lee YL, Yeoh D (2008) Experimental study on shear behaviours of timber-lightweight concrete composite shear connectors. In: Proceedings of the 3rd Brunei International Conference on Engineering and Technology, Bandar Seri Begawan (Brunei), CD copy.

9) Yeoh D, Fragiacomo M, Buchanan A, Deam, B (2009) Experimental behaviour at ultimate limit state of a semi-prefabricated timber-concrete composite floor system. In: Proceedings of the International Symposium on Timber Structures from Antiquity to the Present, June 25-27, Istanbul (Turkey), 287-298.

Notations

A	Cross sectional area (with subscripts 1 and 2 for concrete and timber, respectively)
E	Modulus of elasticity (with subscripts 1 and 2 for concrete and timber, respectively)
E_{eff}	Effective modulus (with subscripts 1 and 2 for concrete and timber, respectively)
$(EI)_{eff}$	Effective flexural stiffness of composite beam
$F_{d,u}$	Design maximum load condition at ultimate limit state
$F_{d,p}$	Design quasi-permanent load condition at serviceability limit state
$F_{d,r}$	Design rare load condition at serviceability limit state
F_d^*	Design load combination
F	Shear strength capacity of connection (with subscripts k and d for characteristic and design, respectively)
F^*	Shear force demand in the connection
G	Total dead load/permanent action
G_1	Self-weight dead load
G_2	Superimposed dead load
H	Distance between the centroid of concrete and timber sections
I	Second moment of area (with subscripts 1 and 2 for concrete and timber, respectively)
K	Secant slip modulus of connection (with subscripts s or 0.4 and u or 0.6 for serviceability and ultimate limit states, respectively)
K_{eff}	Effective slip modulus of connection
M^*	Bending moment demand (with subscripts 1 and 2 for concrete and timber, respectively)
M_R	Bending design capacity or resistance

N^*	Axial force demand (with subscripts *1* and *2* for concrete and timber, respectively)
N_R	Tensile design capacity or resistance
P	Point load
Q	Imposed load or variable action
R_m	Mean shear strength of connection obtained from push-out test
V_2^*	Shear force demand in timber
Z	Section modulus
a	Distance between the centroid of the timber-concrete composite section to the centroid of the concrete or timber section denoted by subscripts *1* and *2*, respectively.
b	Section breadth (with subscripts *1* and *2* for concrete and timber, respectively)
f_{cd}	Design compressive strength of concrete
f_{ctd}	Design tensile strength of concrete
f_d	Design strength of timber (with subscripts *t*, *b*, *s* and *p* for tensile, bending, shear and compression perpendicular to grain, respectively)
h	Section depth (with subscripts *1* and *2* for concrete and timber, respectively)
k_2	Duration of load factor for deflection of timber
k_{37}	Duration of load factor for deformation of connection
l	Span length
s	Spacing of connectors (with subscripts *eff*, *min* and *max* for effective, minimum and maximum spacing, respectively)
u	Vertical deflection
v	Slip of connection measured in push-out test
w	Uniformly distributed design load
ϕ	Strength reduction factor

$\phi(t,t_0)$ Creep coefficient (with subscripts *1*, *2* and *f* for concrete, timber, and connection respectively)

γ Gamma coefficient (with subscripts *1* and *2* for concrete and timber, respectively)

ψ_2 Partial factor for quasi-permanent value of a variable load or action

σ Stress due to axial force (with subscripts *1* and *2* for concrete and timber, respectively)

σ_m Stress due to bending moment (with subscripts *1* and *2* for concrete and timber, respectively)

1   Introduction

"By wisdom a house is built, and through understanding it is established; through knowledge its rooms are filled with rare and beautiful treasures. A wise man has great power, and a man of knowledge increases strength."
Proverbs 24:3-5

The focus of this Ph.D. thesis is on the research of behaviour and design of timber-concrete composite (referred to as TCC hereafter in the thesis) floors under short-term and long-term loading. The study undertaken is one that is heavily experimental based involving large amount of time and resources for the planning, construction and testing of connection test specimens and full scale floor beams both in the short- and long-term.

1.1   Background

Timber-concrete composite (TCC) system is a construction technique used for strength and stiffness upgrading of existing timber floors and new construction such as multi-storey buildings and short-span bridges. This technique connects a timber beam, either solid, glued laminated (Glulam) or laminated veneer lumber (LVL), to a concrete slab cast above it, using a connection system to transfer shear forces between timber and concrete. This connection system can be either mechanical fasteners such as nails, screws, and toothed metal plates embedded into the timber, or notches cut from the timber or a combination of both.

TCC floors provide many benefits compared with traditional timber floors such as greater strength and stiffness, less susceptibility to vibration, improved seismic and fire resistance, better acoustic separation and thermal mass. The lower weight than reinforced concrete floors imposes lesser loads on the foundations and thereby reduces the lateral strength required in the structural system in earthquake regions.

In Europe, TCC floors are mainly used for the replacement of old timber floors in historical buildings where acceptable vibration, small deflection and improved load carrying resistance are the motivations. In USA, TCC system has high potential in low-rise construction (Steinberg, 2003). In New Zealand, the construction industry is currently looking for new applications of timber in multi-storey buildings where the opportunity for sustainable materials in building can be expanded. The effort is to venture into the possibility to produce medium to long-span TCC floors of 8 to 15 m using laminated veneer lumber (LVL).

1.2   Objectives

The main objective of this PhD project has been to study and quantify the behaviour of timber-concrete composite floors in the short- and long-term divided into 5 different experimental phases. The short-term herein refers to the response of the composite floors to collapse load in the ultimate limit state (ULS) while long-term refers to the response of the composite floors to sustained load in the serviceability limit state (SLS) condition. The timber concrete shear connection types applied in the composite floors were thoroughly investigated in order to accurately understand and quantify the behaviour of

the system. The final aim of this study has been to develop a simplified and practical limit state design approach for New Zealand through span tables that satisfy both the short- and long-term ultimate and serviceability limit state. In view of this broad aim, the main objective of this largely experimental based research was broken down into 9 sub-objectives:

1) To identify the best types of connection system to be used in TCC floors in New Zealand. The basic criteria of selection are structural performance, ease of manufacturing and cost effectiveness.

2) To determine the characteristic strength and secant slip moduli of the chosen types of connection.

3) To establish the short-term behaviour of the selected connections by defining the pre- and post-peak responses subjected to collapse load.

4) To derive an analytical model for the strength evaluation of the selected connections based on the different possible modes of failure.

5) To propose a semi-prefabricated construction method for TCC floors which ensure easy and fast erection.

6) To investigate the short-term ultimate and serviceability limit state behaviour of TCC floor beams under collapse load, the effects of concrete strength and construction sequence or method such as leaving connection pockets during concreting and grouting them later.

7) To establish the long-term behaviour of chosen connections by determining the creep coefficient.

8) To investigate the long-term behaviour of TCC floor beams under sustained load at serviceability limit state condition considering the effect of environmental changes; propped and un-propped; and concrete with different level of drying shrinkage.

9) To develop design example and span tables for TCC floor beams that satisfy both the ultimate and serviceability limit state in the short- and long-term.

1.3   Scope

Due to the complexity and magnitude of this project, pertinent issues that are within and beyond the scope of this project were clearly outlined during the planning stages. The issues that are inside the scope of this research are:

1) Short-term behaviour – behavioural response of connections and floor beams defined by collapse test with the application of static load.

2) Long-term behaviour – behavioural response of connections and floor beams defined by the application of sustained load for a maximum period of 1 year.

3) Floor beams – refers to simply supported, single span strips of TCC floor beams in T-section.

4) Connections – refers to connection between the timber and concrete elements for the purpose of shear transfer represented by notched coach screw and toothed metal plate connections.

5) Timber – laminated veneer lumber (LVL)

6) Concrete – mainly low shrinkage concrete that is commercially available.

7) Comparisons – only experimental and analytical comparisons were performed.

8) Analytical – the analytical approximations and design carried out were in accordance to either one or both the New Zealand Standards and Eurocodes.

9) Design – the design of TCC floor beams were in accordance to the "γ-method" given in the Annex B of Eurocode 5.

The issues that are beyond the scope of this research but relevant and important for future study are:

1) Numerical analysis – numerical finite element investigations in both the short- and long-term to compare with the experimental findings of this project and to extend the experimental results to composite floors with different geometrical and mechanical properties.

2) Dynamic behaviour – behavioural response of composite floors subjected to seismic loading considering the diaphragm action and floor-to-mainframe connection.

3) Fatigue behaviour – behavioural response of connections and floor beams subjected to 1 to 2 million cycles of repeated loads, for possible applications to short-span bridge decks.

4) Vibrations – behavioural response of medium to long span floors subjected to human-induced vibrations.

5) Acoustic separation – solutions for inter-storey sound and impact transmission.

6) Fire resistance – behavioural response of composite floors to fire.

7) Construction cost – comparison of cost with other available floor systems.

1.4   Flowchart of experimental programme

The experimental research program on LVL-concrete composite floors in the short- and long-term discussed in this thesis has been carried out in five different phases throughout a period of three years starting from July 2006 through to July 2009 before the results are published in different journal papers and reproduced in this thesis. A flowchart of the extensive experimental research programme is given in Fig. 1-1 with the corresponding chapter in this thesis and the period of which each task or phase has been performed.

1.5   Organization of thesis

A brief summary of each chapter in this thesis is given below. The thesis includes six chapters that have been published or submitted to peer-reviewed International Journals, such as the Australasian Journal of Structural Engineering, the ASCE Journal of Structural Engineering, the RILEM Materials and Structures Journal, the Engineering Structures Journal, and the Journal of Construction and Building Materials. These journal papers have been reformatted for this thesis so as to present a consistent style. The references in each paper have been amalgamated and appear in the Reference chapter of the thesis. Although each paper addressed a different aspect and experimental phase of the project, it was essential to allow for some repetition of content amongst the papers in order to provide the reader with an understanding of the flow of the research carried out. However, on the whole, each paper presents a different component of the overall research outcomes to form a complete body of work. Therefore, each paper is both unique and stand-alone but at the same time is complementary to the other papers. Additional information and supporting details that were not included in the papers in order to conform to the publishers' length limitations are provided in the Appendices unless otherwise mentioned.

Chapter 3	Conception and development of experimental research program	July 2006 to March 2007

Chapter 3	Phase 1 Short-term push-out connection test *A parametric investigation*	April 2007 to August 2007

Chapter 4	Phase 2 Short-term push-out connection test *Determination of characteristic strength and mean stiffness values*	January 2008 to May 2008

Chapter 6	Phase 3 Long-term push-out connection test *Determination of creep coefficient*	January 2008 to July 2009

Chapter 7	Design of experimental TCC floor beams	June 2007 to August 2007

Chapter 5	Phase 4 Short-term TCC floor beam test *Investigation of collapse behaviour*	Sept. 2007 to April 2008

Chapter 6	Phase 5 Long-term TCC floor beam test *Investigation of long-term behaviour*	January 2008 to July 2009

Fig. 1-1. Experimental research program flowchart

Chapter 2 presents a comprehensive literature review of the most important references concerning TCC from antiquity to present. Pertinent aspects reviewed includes concept, application and advantages of TCC, different types of connection proposed and investigated, design standards and methods, experimental and numerical research of TCC both in the short- and long-term for connections and floor beams, and various prefabrication systems.

Chapter 3 provides a preliminary of the experimental program carried out in this research project. This chapter introduces a semi-prefabricated LVL-concrete composite floor system developed at the University of Canterbury and discusses the early experimental results of tests performed on connections and beams.

Chapter 4 onwards dwell into the essence of the research objectives. This chapter discusses in detail the experimental procedures and results of short-term connection push-out tests. Central to this discussion are the derivation of the characteristic strength and secant slip moduli of 3 selected types of connection which were used in the design of experimental TCC floor beams described in Chapters 5 and 6. Other highlights of this chapter are the analytical approximation of the pre- and post-peak force-slip relationship for the tested connections, and design formulas in accordance to New Zealand Standards and Eurocodes for strength evaluation of the tested connections.

Chapter 5 reports the outcomes of short-term collapse test performed on eleven 8 and 10 m LVL-concrete composite floor T-beams represented by different variables such as connection types, concrete type, and design level (well- and under-designed) corresponding to number of connections. Experimental-analytical ULS and SLS performance of the tested beams were evaluated.

Chapter 6 presents the outcomes of long-term tests on three types of TCC connections and three 8 m span T-section floor beams under sustained load. The tests lasted for a period of approximately 1.5 years, and were performed in uncontrolled, unheated indoor condition. Important results such as creep coefficients of the connections and mid-span deflections of all the beams including projection to the end of service life are presented.

Chapter 7 describes the design and construction of a novel semi-prefabricated LVL-concrete composite floor that is under development in New Zealand. This system proved to be an effective modular solution that ensures rapid construction. The effective bending stiffness method, also known as the γ-method in accordance with the Annex B of Eurocode 5, was used for the design of the composite floor at ultimate and serviceability limit states. A full worked example compliments this chapter.

Chapter 8 concludes this thesis by presenting the achievements to the 9 sub-objectives outlined in Clause 1.1. Important research needs closes the chapter.

2   Literature Review

The majority of this chapter was submitted to the Journal of Structural Engineering (American Society of Civil Engineering, ASCE) in a paper entitled "The state-of-the-art on timber concrete composite structures – a literature review" (Yeoh et al, 2009f). Additional explanatory text and figures have been included within this chapter to provide a more complete and cohesive review than was possible within the confines of the journal paper.

This chapter provides a comprehensive review of recent research on the behaviour and design of timber-concrete composite (TCC) floors. The literature was carefully selected and presented to outline the fundamental knowledge about TCC structures prior to the contribution provided by the current research project. Aspects reviewed include the concept, application and advantages of TCC, the range of connection types proposed and investigated by others, design standards and methods, experimental and numerical prediction of both the short- and the long-term behaviour of connections and floor beams, and options for prefabrication systems.

Subsequent chapters build on the work reviewed herein, discussing the experimental phases and their outcomes, beginning with preliminary experimental investigations in Chapter 3. As those chapters were also published as stand-alone journal papers, they contain some inevitable repetition of the material presented within this chapter

2.1   Abstract

This chapter presents a survey on the state-of-the-art about timber-concrete composite research. The most important literature references were carefully selected and reviewed to provide an overview and some depth into the development of this construction technique. After highlighting the advantages of the composite system, the standards and design methods currently available are presented. An extensive description of the connection systems developed around the world is also provided. The experimental and numerical investigations performed on connections and beams, in both the short- (at collapse) and long-term (under sustained load) stands out as the primary content of the chapter. Other aspects covered are prefabrication, influence of concrete properties, fatigue tests, fire resistance, vibrations and acoustics.

2.2   Introduction

The timber-concrete composite structure, hereinafter referred to as 'TCC', is a construction technique where a timber beam or deck is connected to an upper concrete flange using different types of connectors. The best properties of both materials can be exploited since bending and tensile forces induced by gravity loads are resisted mainly by the timber, and compression by the concrete topping. Medium to long-span (7 to 15 m) floor systems can be constructed as a result of an effective composite action between the two materials provided through the interlayer connection (interlayer connection is described in Section 2.5).

For this construction technique to be efficient, three fundamental design criteria must be satisfied: (1) the neutral axis of the composite cross-section should be located near the timber-concrete interface in order to ensure both components act efficiently with concrete purely compressed and, therefore, uncracked and the timber mostly subjected to tensile stresses; (2) the connection system must be strong and stiff enough to transfer the design shear force and provide an effective composite action; and (3) the timber part (joist/beam or solid deck made from individual planks nailed together on the edge) must be strong enough to resist bending and tension induced by gravity loads applied on the composite beam. Awareness and familiarity with the behaviour and design methods of TCC are important for this type of construction to permeate into the building industry.

10

After World Wars 1 and 2, there was a shortage of steel for reinforcement in concrete. This has initiated the development of timber concrete composite system in Europe. A system of nails and steel braces to form the connection between concrete slab and timber beams was patented by Muller (1922). Subsequently, in 1939, a patent of steel Z-profiles and I-profiles as interlayer connection system was filed in Switzerland (Schaub, 1939). TCC application was mainly a refurbishment technique for old historical buildings in different European cities such as Leipzig in Germany (Holschemacher et al, 2002). The floors designed at earlier times did not comply with current regulations and failed to meet the requirements of building physics with regards to sound insulation and fire resistance.

In the last 50 years, interest in timber-concrete composite systems has increased resulting in the construction of bridges (United States, New Zealand, Australia, Switzerland, Austria, and Scandinavian countries), upgrading of existing timber floors (Europe), and the construction of new buildings (Natterer et al, 1996). One prime example is the Vihantasalmi bridge built in 1999 in Finland, spanning 168 meters, 11 m wide roadway and 3 m sidewalk (Finnish Road Administration, 1999). Since early 1990s, TCC construction has found important structural applications throughout several European countries including Italy (Turrini and Piazza, 1983a and 1983b). The applications include refurbishment of existing timber floors, floors for new buildings, and deck system for timber bridges (Natterer et al, 1996; Mettern, 2003). Examples of composite bridges can also be found in the United States after composite design and construction were introduced into the American Association of State Highway Officials Specifications in 1944 (Cook, 1976); in New Zealand, where the first experimental bridge was built in 1957 for New Zealand Forest Service across Mangahareke Stream near the northern boundary of Kaingaroa Forest (Cone, 1963); and in Australia, where the first major composite system was built on a highway bridge in the 1950s on the Pacific Highway in New South Wales over the Maria River (Benitez, 2000).

The objective of this chapter is to provide an up-to-date literature review of TCC covering the different aspects related to the interlayer connection, influence of concrete, short- and long-term behaviour, design approach, and numerical modelling. The chapter also gives a general insight into the history and recent developments of TCC systems.

2.3   Advantages of the composite system

Traditional light timber frame floors may suffer from excessive deflection, susceptibility to vibrations, insufficient acoustic separation, and low fire resistance. These problems can be resolved by using TCC floors. The application of TCC extends from bridges, factory buildings, domestic houses to multi-storey timber buildings. TCC construction is still developing at this stage, however it is sufficiently advanced to be applied in different ways (Natterer et al., 1996). There are many advantages of TCC over timber-only or reinforced concrete floors. For new buildings, by connecting an upper concrete slab to timber joists and beams it is possible to: (1) significantly increase the stiffness compared to timber-only floors; (2) considerably improve the acoustic separation; and (3) increase the thermal mass, important to reduce the energy consumption needed to heat and cool the building. On the other hand, by replacing the lower part of a reinforced concrete section, ineffective due to the cracking induced by tensile stresses, with timber joists or a solid timber deck, it is possible to achieve the following advantages: (1) rapid erection of the timber part, particularly if prefabricated off-site, due to its lower weight, with a function of permanent formwork for the concrete topping; (2) reduced load imposed on foundation; (3) reduced mass and, hence, seismic action; (4) possibility to use the timber as a decorative ceiling lining; (5) low embodied energy; and (6) reduced CO_2 emissions since timber is carbon-neutral. For refurbishment of old buildings, the following advantages can be obtained by connecting a concrete topping of about 50 mm to the existing timber floor: (1) increased stiffness and load-bearing capacity; (2) preservation of historical buildings for future generation; and (3) better seismic performance due to the improved diaphragm action. TCC floors are significantly lighter and more economical when compared to their counterparts, reinforced concrete and steel-concrete composite floors, which are characterized by non-regenerative manufacturing process with high energy demand and high emission of carbon dioxide (Kreuzinger, 1999).

2.4   Standards and design methods

Unfortunately, the design of TCC is not addressed by most of the timber standards around the world, hence resulting in the use of this construction technique mainly in some regions of Europe such as Germany, Italy and Finland. Specifically, for TCC, the design provisions are given in Eurocode 5, Part 2, Timber bridges (CEN, 2004c) and Eurocode 5, Part 1, Annex B (CEN, 2004b). Since the interlayer connection is commonly not fully

rigid and will result in a relative slip between the bottom fibre of the concrete and the upper fiber of the timber, the assumption of plane sections remaining plane does not apply to the composite section as a whole. Hence, the method of the transformed section from the conventional principles of structural analysis cannot be used.

Table 2-1. Summary of the state-of-the-art literature for design of TCC structures

Reference	Highlights
Turrini and Piazza, 1983b	Design formulas for TCC floors with glued vertical and inclined rebar connectors
Gelfi et al, 2002	Design formulas for TCC floors with non-glued vertical steel dowels
Ceccotti, 1995 Lukaszewska et al, 2007b	Basics of design of TCC beams using the gamma method and the secant slip moduli of the connection
Frangi and Fontana, 2003	Plastic design of TCC with ductile connection systems
Ceccotti et al, 2002	Detailed description of the design of TCC at ULS and SLS, with emphasis on the influence of creep in the long-term, including two worked examples
Schänzlin, 2003	Extension of the Annex B of EC5 design formulas to account for the effect of concrete shrinkage on the behaviour of TCC structures.
Fragiacomo, 2006	Simplified approach for the design of TCC with allowance for concrete shrinkage, thermal and hygroscopic strains due to environmental variations
Schänzlin and Fragiacomo, 2007	Comparison between two design approaches for the evaluation of the effect of concrete shrinkage on TCC
Buchanan, 2007	Detailed worked examples for the design of an 8 m span TCC beam. This worked example does not include the ultimate limit state (ULS) long-term verifications. The values of connection strength, slip moduli and creep coefficient in this example have been estimated and do not represent the actual tested values.
	This design worked example has been superseded by another worked example found in Yeoh et al (2009a) or Chapter 7 of this thesis. Here, the actual tested values of the connection have been used and the ULS long-term verifications included.

In order to account for the partial composite action resulting from the flexibility of the shear connection, the approximate solution derived by Möhler (1956) for timber-timber composite beams with flexible connection proposed in the Annex B of the Eurocode 5

(CEN, 2004b) is used (Ceccotti, 2002). This approach, which makes use of an effective bending stiffness, is also known as the 'gamma' method. The time-dependent behaviour of the three components in the system, i.e. timber, concrete and connection, resulting in creep, mechano-sorption, drying shrinkage, thermal and hygroscopic strains, adds further complexity to the design of the TCC (Ceccotti, 2002). Hence, the design of TCC involves strength control at ultimate limit state (ULS) of the three component materials, i.e. timber, concrete and connection, and deflection control at the serviceability limit state (SLS).

Both ULS and SLS should be checked in the short- and long-term (the end of the service life). For the short-term (instantaneous) verifications, an elastic analysis based on the use of the gamma method is usually carried out. For the long-term verifications, simplified methods such as the 'Effective Modulus Method' have been proposed in literature (Ceccotti, 2002) in order to account for the effect of creep of the different materials. In such a method, the elastic moduli are divided by one plus the creep coefficient of the material at the end of the service life. The actual non-linear behaviour of most connection systems is accounted for by defining two secant slip moduli, $K_{0.4}$ and $K_{0.6}$, at 40% and 60% of the mean shear strength of the connection measured in shear tests carried out on small composite blocks (the 'push-out' tests). Such quantities are used for SLS and ULS verifications, respectively. More advanced design methods which allows for connection ductility (Frangi and Fontana, 2003), concrete shrinkage, thermal and hygroscopic strains have also been proposed (Schänzlin, 2003; Fragiacomo, 2006; Schänzlin and Fragiacomo, 2007). Table 2-1 provides a summary of the state-of-the-art concerning the design of TCC.

2.5   Interlayer connection systems

The interlayer connectors in a TCC are usually positioned along the beam according to the shear force distribution so that they are concentrated near the supports where the internal shear force is higher and spaced out gradually into the span as the shear force reduces to zero in the middle for a simply supported beam subjected to a uniformly distributed load. The structural efficiency of a TCC system highly depends on the stiffness of the interlayer connection. A connection system that results in high composite action allows a significant reduction of the beam depth and longer span length when compared with a non-composite system. The composite efficiency can be estimated by the quantity E, expressed in percentage, given by (Gutkowski et al., 2008):

$$E = \frac{\Delta_{NC} - \Delta_{PC}}{\Delta_{NC} - \Delta_{FC}}$$ Eq. 2-1

where Δ denotes the mid-span deflection and the subscripts *NC*, *PC*, and *FC* refer to no,

partial and fully rigid connection, respectively.
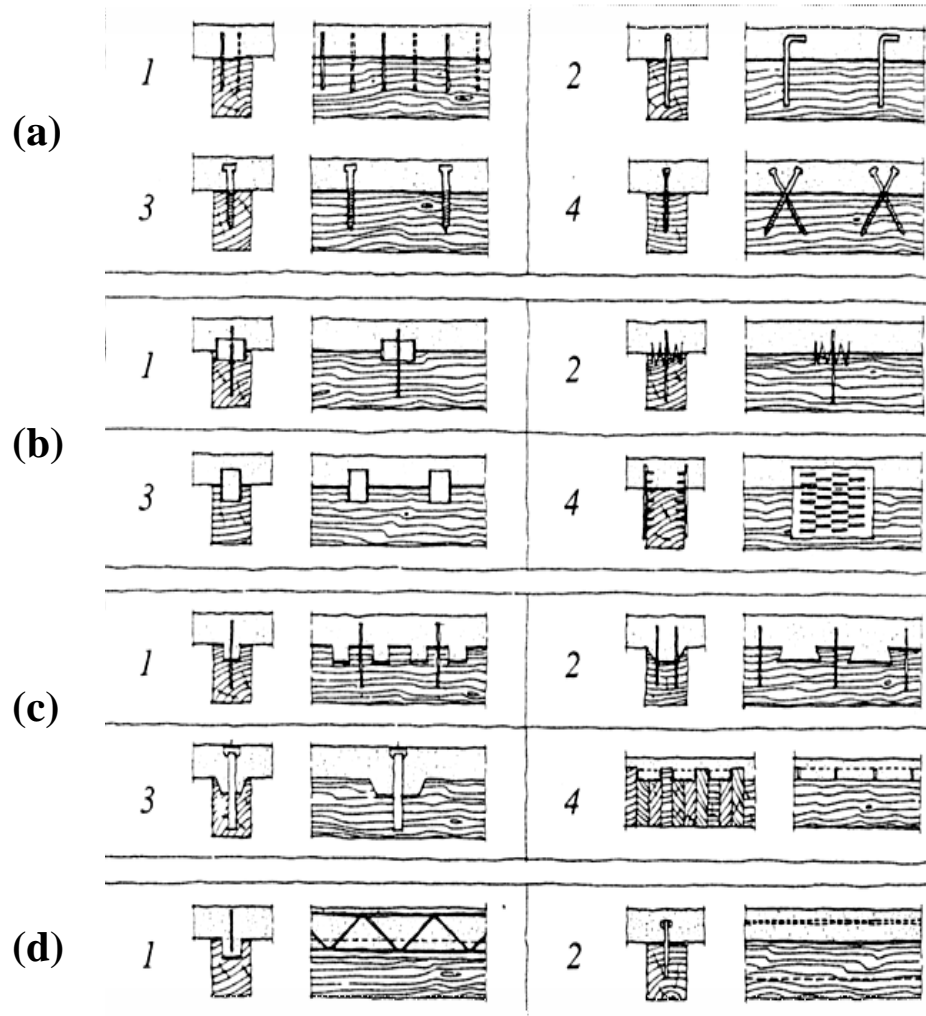
Fig. 2-1. Examples of timber-concrete interlayer connections: (a1) nails; (a2) reinforcement bars, glued; (a3/4) screws; (b1/2) split rings and toothed plates connectors; (b3) steel tubes; (b4) steel punched metal plates; (c1) round holes in timber and fasteners preventing uplift; (c2) square indentation and fasteners; (c3) cup indentation and prestressed steel bars; (c4) nailed timber planks deck and steel shear plates slotted through the deeper planks; (d1) steel lattice glued to timber; (d2) steel plate glued to timber. (Ceccotti, 1995)

Ceccotti (1995) in Fig. 2-1 presented a large number of fasteners that can be used to

connect the concrete slab to the timber, highlighting the different categories of fasteners

in relation to their degree of rigidity ranging from (a) the most flexible to (d) the most

rigid ones. Connection types are grouped in relation to their stiffness: elements connected by nails, screws or dowel shaped fasteners (a), for example, are less rigid than elements connected by surface connectors (b); rigidity can be increased when notches are cut from the timber (c) or when a continuous connector with glue is used (d). Fig. 2-2 provides a comparison of the shear force-slip relationship for different categories of connection system. In order to characterize a connection system, the strength and stiffness are obtained by means of push-out tests carried out in accordance to EN26891 (CEN, 1991). The strength is quantified as the maximum load applied when failure occurs in the push-out test while stiffness is quantified by the slip modulus at 3 different load levels (40%, 60% and 80% of the mean maximum load) corresponding to the service, ultimate and near-collapse load levels.

A wide range of connection systems have been developed in different parts of the world and throughout the century. The connectors can be metal or timber fasteners, or notches cut in the timber and filled by concrete. Based on their arrangement along the beam, the connectors can be categorized in discrete/continuous, and vertical/inclined. They can also be categorized in glued/non-glued, and prestressed/non-prestressed, based on the way they are inserted in the timber.
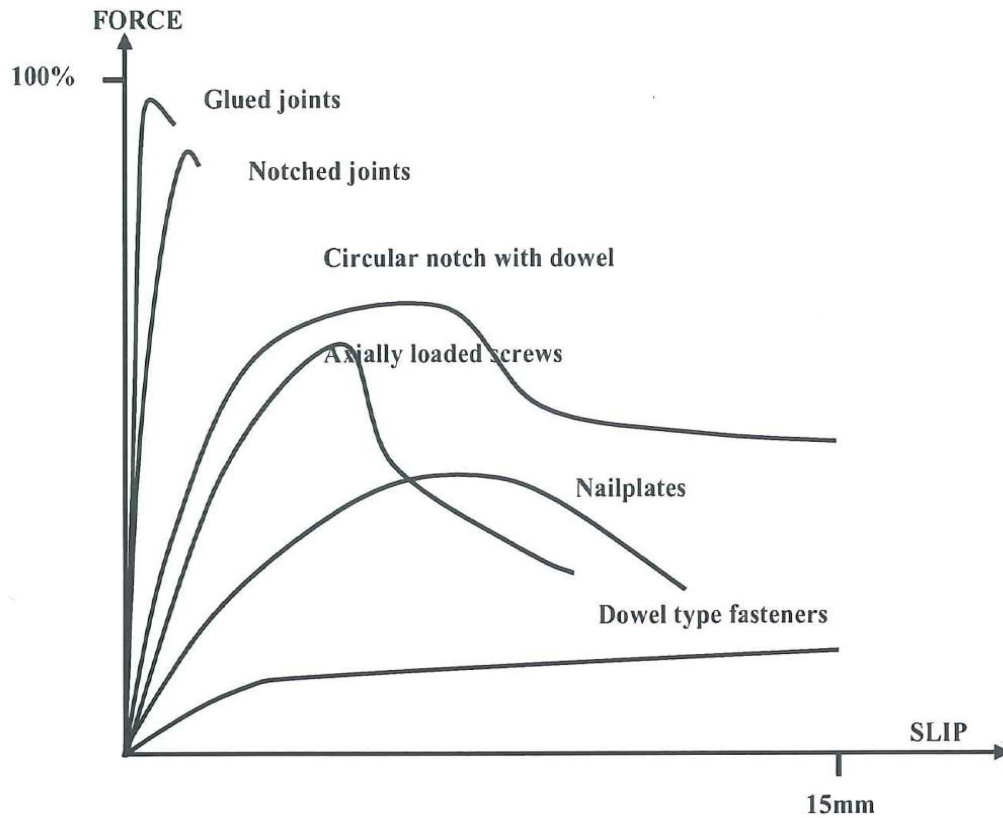
Fig. 2-2. Comparisons of different categories of connection systems (Dias, 2005)
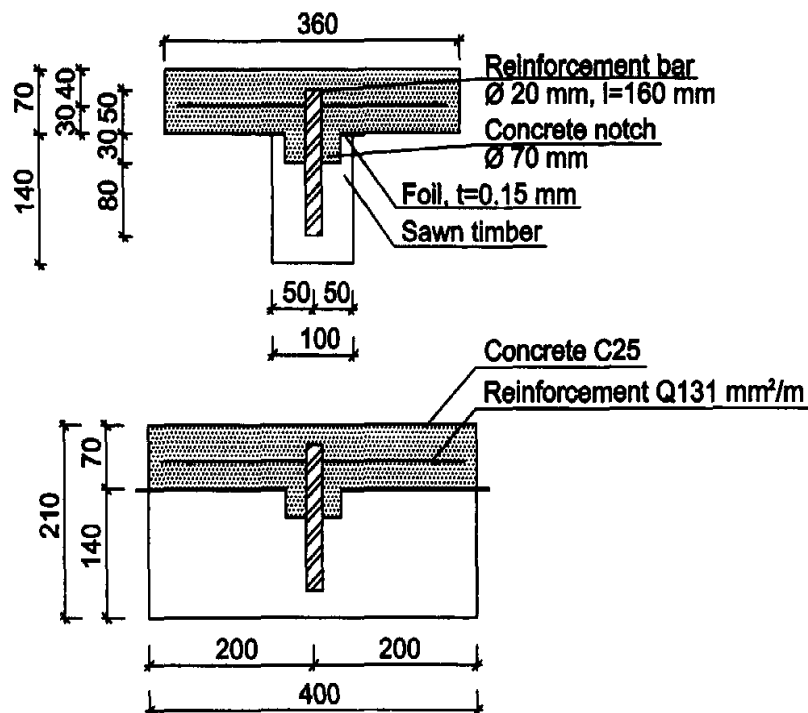
Fig. 2-3. Concrete notch with reinforcement (Van der Linden, 1999)

17

Research and patents on connection systems traced back to as early as 1920s and onwards (Muller, 1922; Schaub, 1939; McCullough, 1943; and Richart and Williams, 1943; Pincus, 1970; Priestley, 1970; and, Pillai and Ramakrishnan, 1977 as summarized in Table 2-2). Notches cut in the timber beam and reinforced with a steel screw or dowel, as illustrated in Fig. 2-3, Fig. 2-4(a) and Fig. 2-4(b), is by far the best connection for TCC with respect to strength and stiffness performance although it may not be altogether economical if the notches had to be cut manually (Kuhlmann and Schänzlin, 2001; Van der Linden, 1999; Seibold, 2004; Deam et al, 2007). The length of the notch, the presence of a lag screw and its depth of penetration into the LVL, were found to be the most important factors affecting the performance of the connection. It was found that the notch length affects the strength and stiffness of the connection while the lag screw provides ductility and improves the post-peak behaviour (Yeoh et al, 2009c or Chapter 3). Notched connection reinforced with dowel or metal anchor that allows tightening after the concrete curing (Fig. 2-5) has the advantage of reducing the gap between the concrete and timber caused by the concrete shrinkage within the notch (Gutkowski et al, 2004).

Alternatively, mechanical connectors such as nailplates (Fig. 2-4(c)) that do not require any cutting in the timber can be used (Aicher et al, 2003 and Yeoh et al, 2009c or Chapter 3). They were found to be efficient in strength and stiffness although significantly less than a notched connection. An important difference between mechanical and notch connections is that in the first case the slip modulus largely depends upon the flexibility of the fastener and the timber in contact with the fasteners; in the second case, conversely, the slip modulus mostly depends on the stiffness of the wood in the inclined surface of the notch, and also on the stiffness of the concrete inside the notch (Balogh and Gutkowski, 2008; and Kuhlmann and Michelfelder, 2006). The post-tensioning of the dowel (Fig. 2-6(a)) increases the strength and stiffness of the connection (Capozucca, 1998), however the relaxation due to creep of timber perpendicular to grain is expected to significantly reduce this benefit over time. The mechanical properties of the connection can be further improved by inclining the dowels to 45º (Fig. 2-6(b)) so as to subject them mainly to axial force instead of shear when inserted vertically as shown by Pillai and Ramakrishnan (1977), Meierhofer (1993), Steinberg et al. (2003), and Grantham et al. (2004).
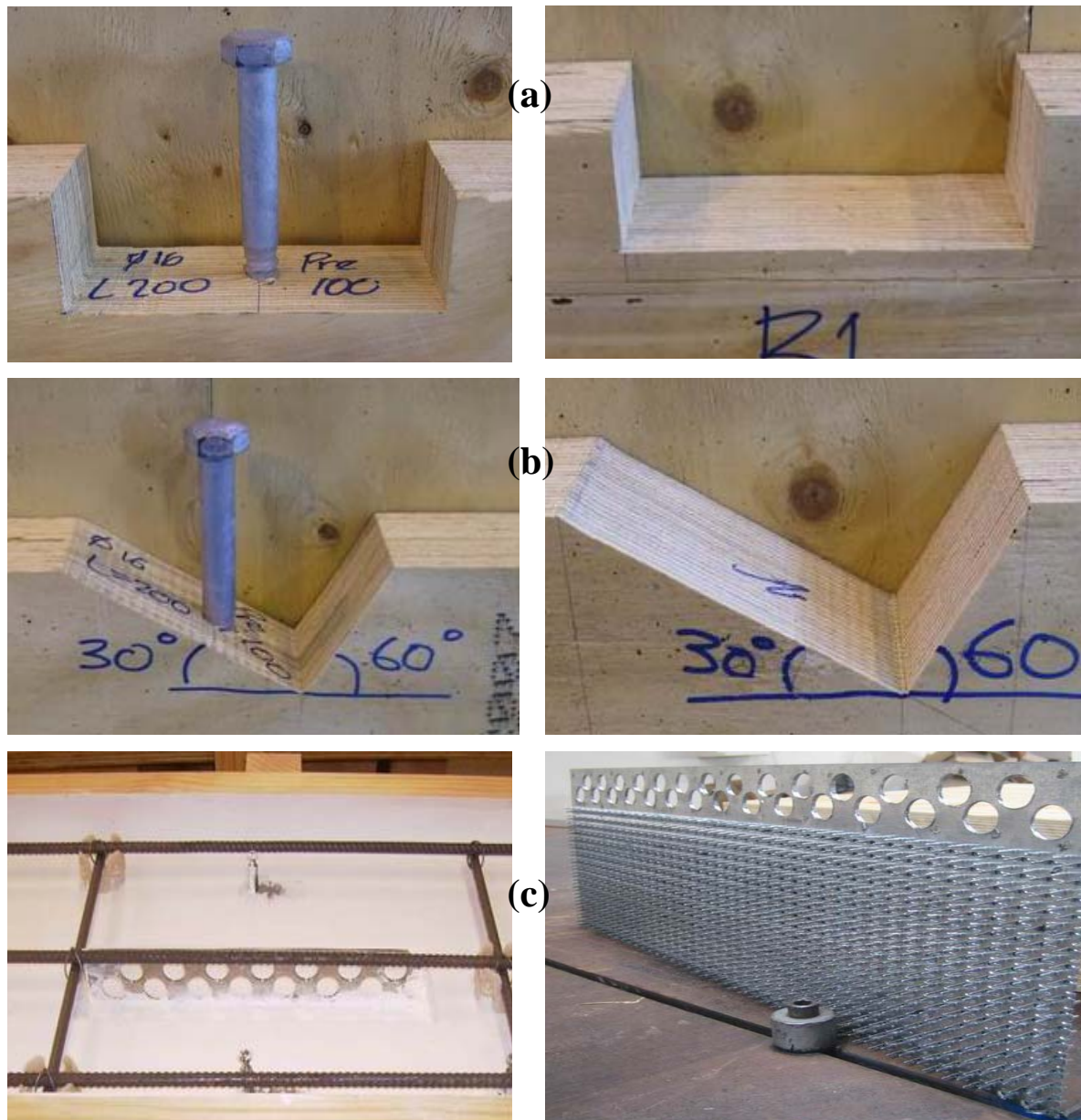
Fig. 2-4 Variations of notched connections with and without coach screws: (a) rectangular; (b) triangular; and (c) toothed plate connection (Yeoh et al, 2009c or Chapter 3)
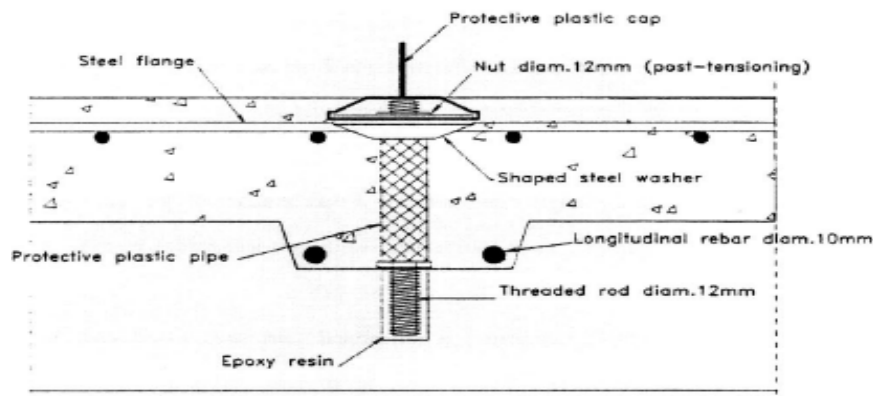
Fig. 2-5. Hilti dowel shear key/anchor (Gutkowski et al, 2004)

The use of glue and epoxy resin in the connection system is not entirely encouraged due to the stringent quality control and complexity of on-site application. However, there has been some research interest over the last few years. Some examples are given in Fig. 2-7, Fig. 2-8 and Fig. 2-9 (Clouston et al, 2005; Brunner et al, 2007; Miotto and Dias, 2008; and, Kuhlmann and Aldi, 2008).

With the aim to develop a fully demountable composite system where the concrete slab is prefabricated off-site, seven types of connector were chosen (Fig. 2-11 and Fig. 2-12) to build 28 asymmetrical shear specimens (Lukaszewska et al, 2008 and Lukaszewska, 2009). Among these connectors, three were investigated for the first time (Fig. 2-12): (1) a steel tube with a welded flange embedded in the concrete slab, with a hexagon head lag screw (SST+S); (2) a modified steel tube with two welded flanges, and a hexagon head lag screw in conjunction with a notch cut in the timber beam (ST+S+N); and (3) a mechanical connector consisting of a pair of folded steel plates embedded into the concrete slab and connected to the glulam beam by means of annular ringed shank nails (SP+N). Due to their simplicity and inexpensiveness, the first and third connector types (SST+S and SP+N) were found to be the most suitable for prefabricated timber-concrete composite system.

A summary of the state-of-the-art concerning different types of connection introduced and tested from early days and over the last two decades is presented in Table 2-2.
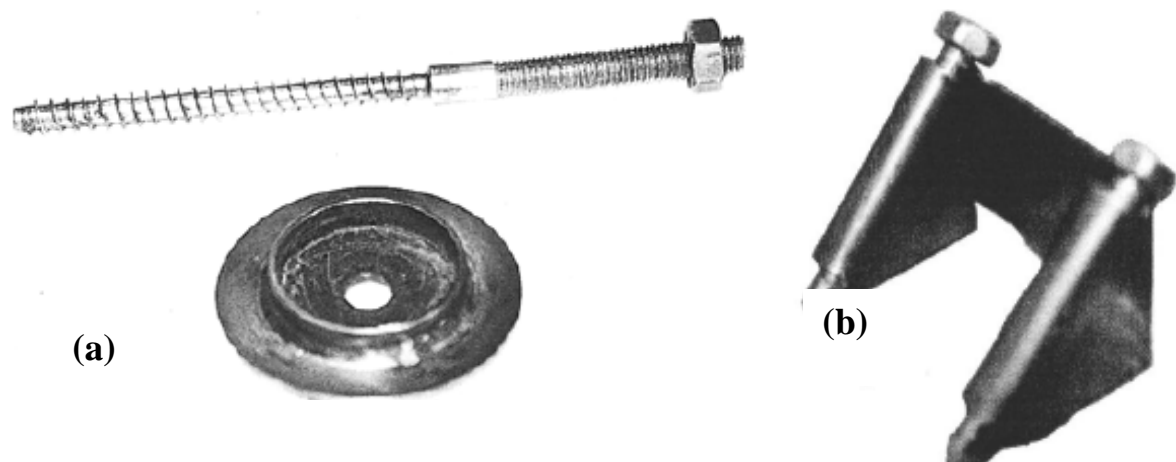
Fig. 2-6. (a) Axial prestressed steel connector (Capozucca, 1998), and (b) upright steel sheet anchored in the timber by two screws at 45° angle (Steinberg et al., 2003)
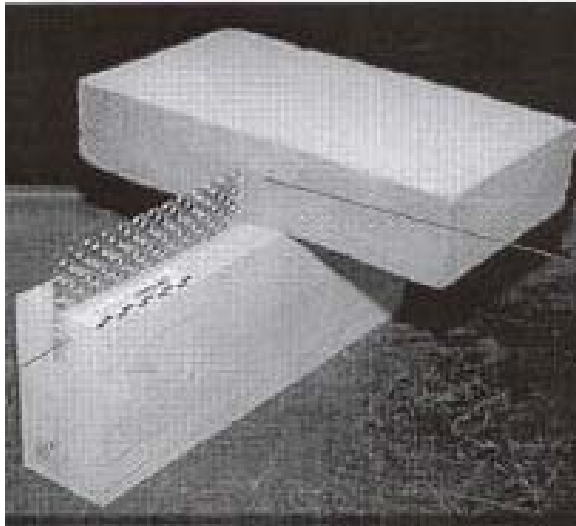
Fig. 2-7. Steel mesh glued slotted into wood (Clouston et al., 2005)

Fig. 2-8. "Perfobond" perforated steel plates (Miotto and Dias, 2008)
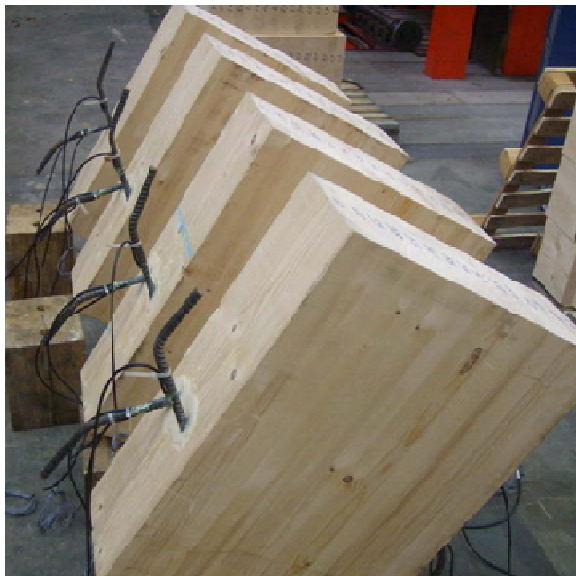
Fig. 2-9. Glued rebars positioned with a 45° angle (Kuhlmann and Aldi, 2008)

Fig. 2-10. Vertical connector by Tecnaria S.p.A (Fragiacomo et al, 2007a)
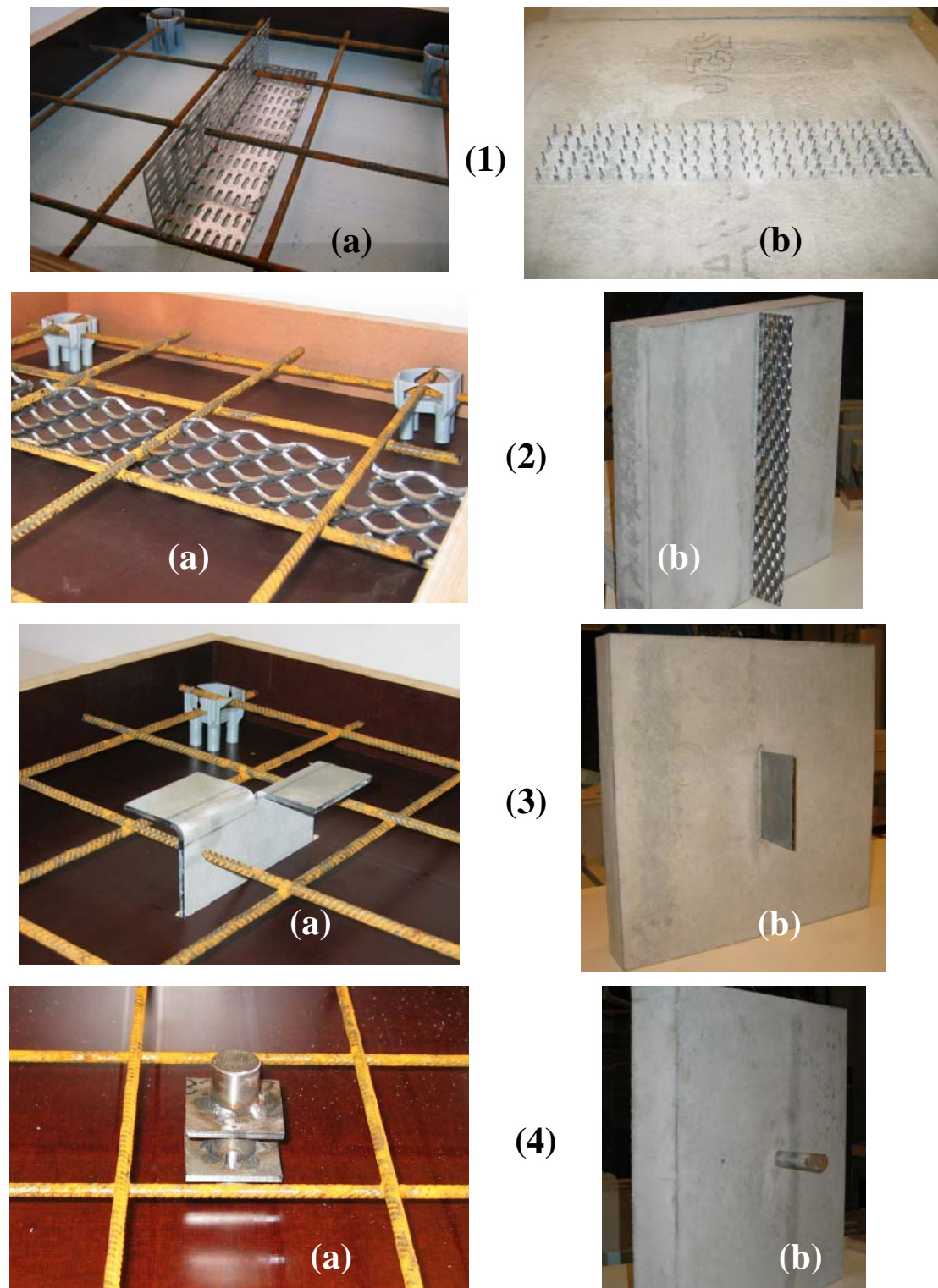
Fig. 2-11. Connectors tested for a prefabricated timber-concrete composite floor in Sweden: (1) Toothed metal plate connector (type SNP): a) in moulding form, b) prefabricated slab with teeth of the plate protruding out ready to be pressed into glulam joist; (2) Epoxy-glued continuous steel mesh (SM): a) in the moulding form, b) prefabricated concrete slab with inserted shear connector; (3) Epoxy-glued folded steel plate (GSP): a) in the moulding form, b) prefabricated slab with inserted shear connector; (4) Epoxy-glued steel dowel with flanges (GDF): a) in the moulding form, b) prefabricated slab with inserted shear connector (Lukaszewska, 2009)
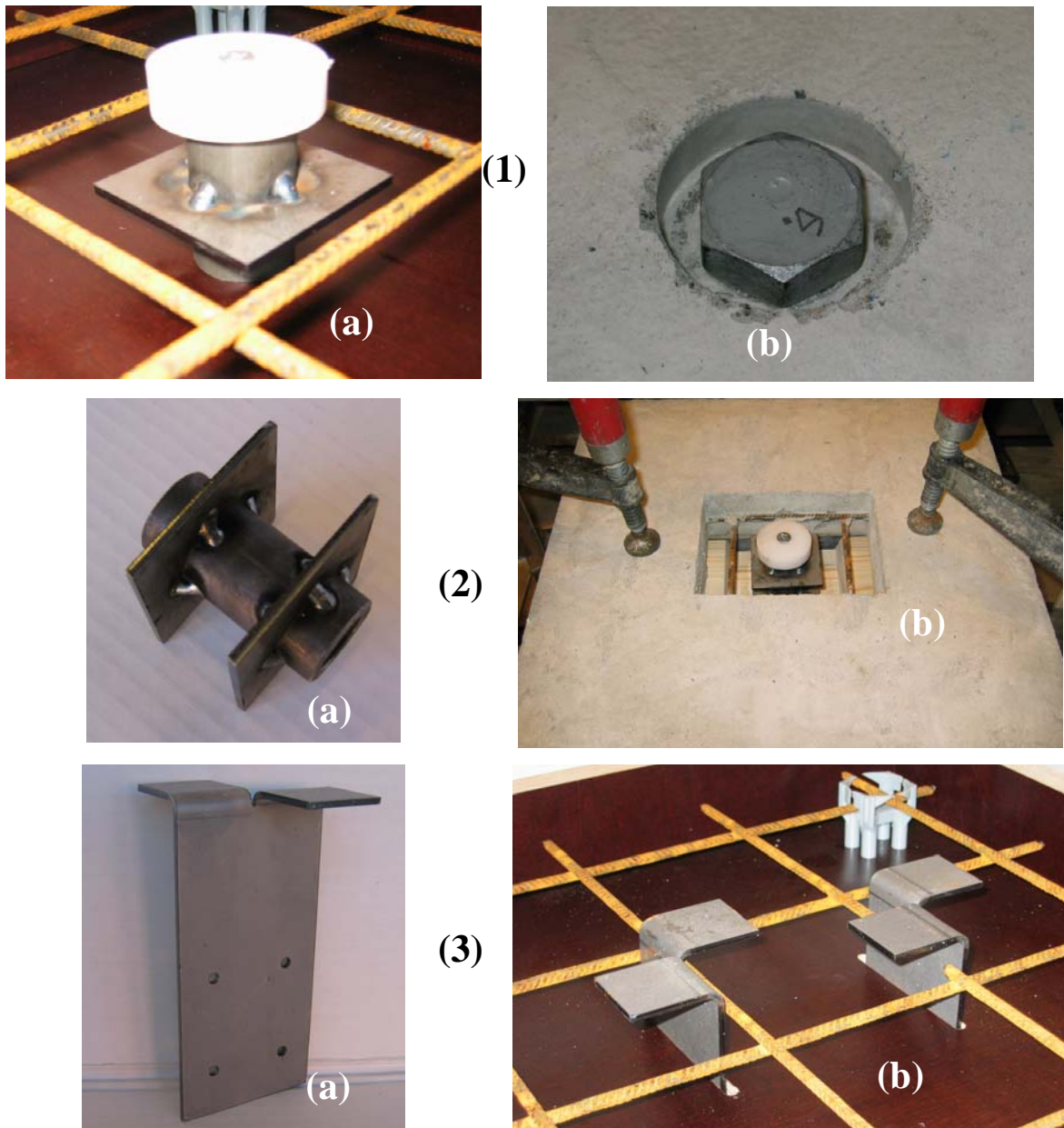
Fig. 2-12. Three types of connector tested for the first time for a prefabricated timber-concrete composite floor in Sweden: (1) Steel tube shear connector SST+S: a) in the moulding form with the screw plastic cap, b) assembled to the glulam beam; (2) Shear type connector ST+S+N: a) steel tube detail, b) prefabricated concrete slab with a 115×120mm^2 rectangular hole placed on top of the glulam member; and (3) Steel plate shear connector SP+N (Lukaszewska, 2009)

Table 2-2. Summary of the state-of-the-art concerning different types of connection

Reference	Connection type	Remarks
Muller, 1922	Nails and steel braces	First use of TCC system and first patent
Schaub, 1939	Steel Z-profiles and I-profiles	Patent in Switzerland
McCullough, 1943	Metal fasteners and pipe dowels	
Richart and Williams, 1943	Triangular plate-spike	Provided full composite action in beam test
Pincus, 1970	Nails without glue	Developed less than 50% composite action
	Nails glued in timber	Enhanced composite action to 100%
Priestley, 1970	Screw spikes, blocks forming castellated surface, screw spike with shear plate, steel tube fitted into bored hole, and cross bar welded to top of tube	Connection with castellated top surface of timber was found to be the strongest. It was recommended that another connector with tension capability be combined, such as screw spikes. Subsequent to connection tests, a full scale T-beam using this castellated surface connection combined with screw spikes was tested to destruction. Flexural failure initiating tensile rupture in the extreme tension fibre of the timber. No shear failure was found.
Pillai and Ramakrishnan, 1977	3-5 mm diameter nails	Inclined 45º nails subjected to tension improved strength and stiffness
Capozucca, 1998	Axially prestressed proprietary steel connector	The prestressing prevented relative slip between timber and concrete even at an elevated load – However main concern is relaxation in the long-term
Mungwa et al, 1999	INSA-Hilti tubular shear connector	Improved global stiffness through a zigzagged cutting edge of the connector into the timber
Van der Linden, 1999	Screws installed at ±45°; nailplates bent at an angle of 90°; reinforcement bar with a concrete notch; and concrete notch in glulam.	The use of plate type connector is suitable for the construction of new composite beams, but not for refurbishment purposes, as it required heavy hydraulic equipment to press the nailplates into the timber. Concrete notch reinforced with bar had high strength

24

Table 2-2. Summary of the state-of-the-art concerning different types of connection (Continued)

Reference	Connection type	Remarks
Steinberg et al, 2003	Vertical connector by Tecnaria S.p.A. and steel sheet anchored in the timber by screws at 45° angle	Connectors using inclined screws subjected to tension were more efficient than vertical screws. Therefore, the load-slip curve was almost linear up to a higher load level as compared to vertical screws even of larger diameter which suffered a significant loss of stiffness before failing
Aicher et al, 2003	Nailplate punched into the timber	Nailplate for TCC connections is 1.5 times larger in mean/characteristic shear capacity and 2.5 to 3 times greater in slip modulus than for timber-timber connections
Gutkowski et al, 2004 Fragiacomo et al, 2007a	Shear key/anchor	Anchors were tightened after concrete curing; the notch detail for interlayer transfer of horizontal forces was found to provide higher composite action and larger strength capacity, while at the same time being relatively inexpensive
Clouston et al, 2005	Continuous steel mesh connector glued to timber	Claimed to nearly obtain 100% composite efficiency. Notable drawbacks in using adhesive – temperature fluctuations (i.e. due to outdoor exposure or fire) may be of concern
Dias, 2005	Variation of notches	A series of test on different types of notches: notches cut from different wood species, notches obtained by gluing and nailing small timber blocks on top of the wood deck in order to obtained a castellated wood-concrete interlayer
Kuhlmann and Michelfelder, 2006	Notches cut in timber deck with and without lag screw	An analytical model to calculate the design resistance of such connection developed from the strut and tie theory is presented
Fragiacomo et al, 2007a	Tecnaria proprietary connector	Plastic hinge occurred in screws inside timber and connector exhibited relatively stiff behaviour at SLS due to the presence of four 'crampons'
Lukaszewska et al, 2008 Lukaszewska, 2009	7 different connections from both types, mechanical fastener and notches	The aim was to develop a fully demountable composite system where the concrete slab is prefabricated off-site. Two connections were found to be the most suitable for prefabricated timber-concrete composite systems because of their simplicity and inexpensiveness

Table 2-2. Summary of the state-of-the-art concerning different types of connection (Continued)

Reference	Connection type	Remarks
Seibold, 2004 Deam et al, 2007 Yeoh et al, 2008b, 2009c (Chapter 3)	Notches cut in LVL with and without lag screw	A long notch improved the strength and stiffness of the connection significantly while the lag screw enhanced the post-peak behaviour of the connection
Brunner et al, 2007	Adhesive connector (wet on wet process)	Claimed to uniformly distribute the shear force evenly over the entire surface preventing local force concentration with 100% efficiency. On-site quality control difficulties are a concern, as well as behaviour in the long-term
Miotto and Dias, 2008	Steel pins and perforated steel plates with glued epoxy adhesive	Steel pins were reported with high ductility while the plates were characterized by superior initial stiffness but fragile rupture
Kuhlmann and Aldi (2008)	Crosswise glued-in rebars	Fatigue push-out test carried out with the intended application in a TCC bridge

2.6   Influence of concrete properties

The influence of concrete properties on the performance of timber-concrete composite connections has been addressed in a number of investigations. In some push-out connection test, Steinberg et al. (2003) used a lightweight concrete with a density of 1.6 kN/m^3 (instead of a normal concrete of 2.4 kN/m^3) in order to minimize the permanent load on the timber. They concluded that timber-lightweight concrete composite structures are affected by the modulus of elasticity of the lightweight concrete which leads to a lower effective bending stiffness of the structure. Consequently, the connectors have to be positioned at a closer spacing in lightweight concrete compared to normal weight concrete. The design, therefore, depends on the compromise between the higher cost due to the use of lightweight concrete and the closer setting of the connectors, and the reduction in permanent load. Koh et al. (2008) tested 12 push-out specimens built from lightweight foamed concrete and Malaysian hardwood connected using different types of

26

nails. Higher grade of lightweight concrete was recommended in order to fully exploit the efficiency of the connection.

The potential upgrade of timber frame buildings using timber-concrete composites has been investigated by Grantham et al. (2004). SFS inclined connectors and lightweight concrete made from recycled sewage sludge with a density of 1760 kg/m^3 were used to reinforce an existing timber floor, which was subjected to full-scale long-term and collapse test. The results highlighted on the one hand the larger sensitivity of lightweight concrete to rheological phenomena compared to normal weight concrete, on the other hand the favourable lower self weight and high strength. On the contrary, in the tests performed by Fragiacomo et al. (2007a) on the head stud proprietary connector marketed as 'Tecnaria' (Fig. 2-10), half of the specimens were constructed using normal weight concrete while, in the remaining half, the slabs were constructed from lightweight aggregate concrete. This variation was found not to significantly affect the performance of the connection system either in the long-term, or in the short-term collapse tests, since the failure took place in both cases in the timber.

In order to reduce the thickness of the concrete slab and, consequently, the self weight, Holschemacher et al (2002) used steel fibre reinforced concrete with wood screws as shear connectors. From a 60 mm thick concrete slab using conventional reinforcement with minimum 20 mm cover, a 48 mm slab thickness was achievable with the application of steel fibre reinforced concrete. Push-out tests showed that the strength of the connection increased 1.3 times and initial stiffness 2.8 times as opposed to the use of normal reinforced concrete.

Shrinkage of concrete during the early days from the time of curing will result in a gap at the outer edge of the connection in the case of a notch cut in the timber. As the concrete shrinks, the notch connection pushes inward causing an undesired initial permanent deflection of the composite beam, particularly in the case of a very stiff connection. In order to prevent this issue, the use of low shrinkage concrete is recommended (Yeoh et al, 2008c, Chapter 3).

2.7   Test to failure of TCC floor beams

Quite a number of short-term collapse tests have been performed to date on TCC floor beams. Collapse tests are important to quantify the actual composite action of the system, the load-bearing capacity and the failure mechanisms. There is in general a close relationship between the collapse load and the failure mechanism, and the type of connection system. A push-out test of the connection should always precede a beam collapse test in order to obtain important information on the mechanical properties of the connection. A summary of the state-of-the-art concerning short-term collapse test of TCC in recent years is presented in Table 2-3.

2.8   Long-term tests

The time-dependent behaviour of TCC requires careful consideration in order to accurately predict the deflection in the long-term. Although long-term tests are expensive and require a lot of preparation, they are needed in order to validate approximate design procedures and calibrate existing analytical and numerical models. Few long-term tests have been performed to date. Long-term tests on connections and floor beams are reviewed hereafter.

2.8.1   On connections

Döhrer and Rautenstrauch (2006) tested nine push-out specimens made from two concrete slabs and one interior timber member, three for each type of connector (notches, vertical stud connectors, and inclined (X) connectors). A sustained load of approximately 30 % of the ultimate load in the short-term test was applied by means of a spring load apparatus so as to simulate the quasi-permanent load condition at serviceability limit state (Fig. 2-13(a)). All specimens were stored in outdoor, sheltered conditions (service class 2 according to Eurocode 5). The elastic slips in the tested connections increased from 10 to 24% after 120 days from the beginning of the test.

Table 2-3. Summary of the state-of-the-art about short-term collapse test of TCC in recent years

Reference	Test description	Remarks
Grantham et al, 2004	Existing timber floor in a full-scale light-frame multi storey platform building converted to a TCC floor using SFS connectors	Long-term test of 34 days under 2.5 kN/m^2 live load with deflection limit of span/333 met and structural collapse at 11.9 times the design imposed load.
Persaud and Symons, 2005	7.3 m span 2 m wide T-beam built from 160×405 mm glulam with 10 vertical lag screw connectors tested under 3-point bending. Collapse load was 173 kN with mid-span deflection 74.9 mm and maximum end slip 5.7 mm.	The composite system was more than 3 times stiffer and almost twice as strong as the one without composite action. Experimental results were compared to 3 different prediction methods: rigorous elastic solution, gamma method and elasto-plastic method. Gamma method was found to overestimate the experimental ultimate strength by 20% while elasto-plastic method showed the closest estimate.
Clouston et al, 2005	Solid glulam deck-concrete system, 10 m long 960 mm wide and 340 mm deep with 3 rows of continuous steel mesh along span, each 1 m long tested under 4-point bending. Ultimate failure occurred at 291 kN with a maximum deflection of over 80 mm.	Near full composite action of the system was reported in the conclusion with a 97% effective bending stiffness with respect to that of a full composite system. Using the gamma method, the failure load was estimated as 312 kN compared to 315 kN for full composite action which is just 1% less.
Ceccotti et al, 2006	Double 6 m span, 1.5 m wide, built from two 125×500 mm glulam T-beam, with 18 corrugated rebars glued to each beam with epoxy resin. Beam was twice loaded and unloaded prior to 4-point bending collapse test after a 5-year long-term monitoring. Collapse load was 2P = 500 kN with a 33.2 mm and 2.47 mm of maximum deflection and end slip, respectively.	Beam collapsed at 2.44 times the service design load due to tension failure in timber with a very stiff behaviour. Composite efficiency of 87 to 93% was reported. No significant plasticization of connection system reported. Experimental results were compared to analytical solutions using the gamma method with the connection secant stiffness at $K_{0.4}$, $K_{0.6}$ and $K_{0.8}$ corresponding to service, ultimate and collapse level, respectively obtained from push-out test. The collapse load was better approximated using $K_{0.8}$.

Table 2-3. Summary of the state-of-the-art about short-term collapse test of TCC in recent years (Continued)

Reference	Test description	Remarks
Gutkowski et al, 2008	Multiple timber-concrete layered beams connected with notch shear/key anchor details, each with a clear span of 3.51 m, were tested to collapse under 4-point bending.	The composite efficiency reported ranged from 54.9 to 77%. The failures were characterized by flexural tensile in the wood. Poor construction of the notch connections resulted in low performance of the system.
Lukaszewska et al, 2009a	Five 4.8 m span full scale T-section TCC floors with 1600×60 mm concrete slab and triple 90×270 mm glulam joists tested to failure in 4-point bending. The concrete slab of specimens was prefabricated off-site with mounted connectors. Three specimens had lag screws surrounded by steel pipes whilst two specimens had metal plates nailed to the glulam joists	Composite action of only 60% and 30% achieved in the beams with lag screws and metal plates, respectively. The use of a notched connection together with the steel pipe and lag screw is a possible way suggested by the authors of improving the connection efficiency.
Yeoh et al, 2009b, 2010 Chapter 5	11 LVL-concrete composite T-beams with 8 and 10 m span, 600 and 1200 mm widths, and notched coach screw and toothed metal plate connections were tested to failure under 4-point bending. Low shrinkage and normal concrete was used.	6 beams were well-designed and 5 beams were under-designed for the targeted non-structural permanent load of 1 kN/m^2 and imposed load of 3 kN/m^2. Composite action of 87.6 to 99.23% at SLS was achieved. Well-designed and under-designed beams collapsed at a range of 2.29-2.91 and 1.17-2.31 times the ultimate design load, respectively.

Further long-term tests in both uncontrolled and controlled climatic conditions were performed on dowel type fasteners and notched connections by Dias (2005). For all the connection types, the creep coefficients after 285 days in uncontrolled climatic condition were approximately twice the values measured in controlled climatic conditions. Capozucca (1998) also used a spring apparatus to investigate the stress losses which might occur in the connector, both in the case of high humidity levels, and when humidity and temperature conditions change. A single connector inserted in untreated wood was kept in tension by a contrast spring, showing a loss of stress estimated about 6 and 10% of the initial load after 3 months. In another specimen with wood treated on the surface using protective resin, no significant difference on the stress loss due to humidity changes was found when compared to the untreated wood.

Bonamini et al. (1990) performed push-out tests in controlled, variable relative humidity conditions on mechanical connectors, recognizing the significant increase in creep coefficient due to variation of moisture content (mechano-sorption). Fragiacomo et al. (2007a) performed long-term tests on the head stud proprietary 'Tecnaria' connector using a lever apparatus to apply a sustained load on twelve push-out specimens (Fig. 2-13(b)). The 2-year test consisted of three phases: (1) Creep tests in constant environmental conditions, to measure the creep coefficient; (2) Creep tests in variable environmental conditions, in order to measure the increase in delayed slip due to the variation of relative humidity (mechano-sorption); and (3) Unloading of the specimens to measure the creep recover. It was found that the connection system is influenced by the hygroscopic behaviour of wood at the interface between the timber and the connector. The creep coefficient at the end of service life (50 years) was estimated as 0.5 in constant relative humidity and 2 in variable humidity.
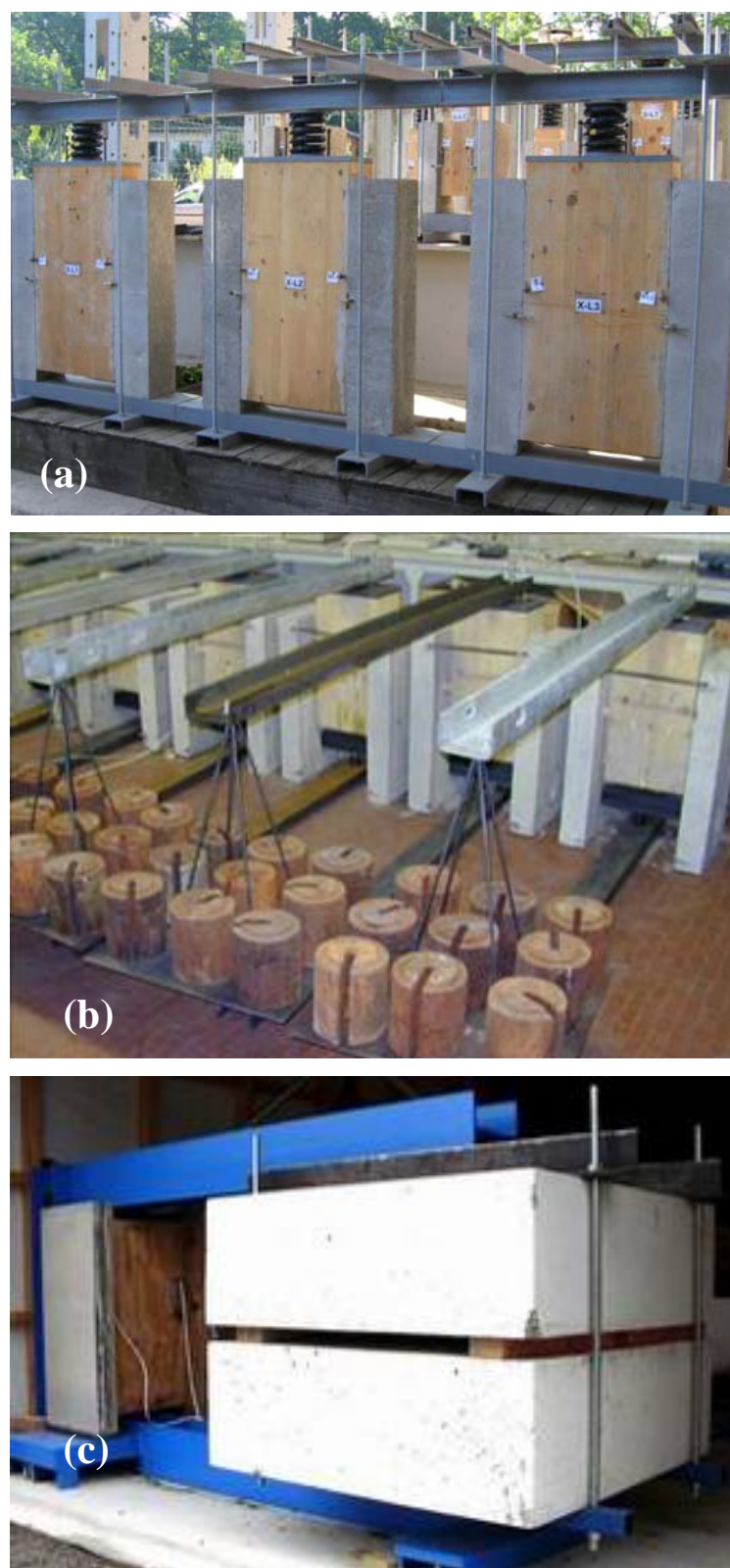
Fig. 2-13. Long-term push-out tests: (a) spring system (Döhrer and Rautenstrauch, 2006); (b) lever apparatus (Fragiacomo et al, 2007a); and (c) "C" shape frame at University of Canterbury (Yeoh et al, 2009d; Chapter 6).

Long-term push-out tests on the notched connection for timber-concrete composite deck systems were performed at the University of Stuttgart under an uncontrolled, only roofed exposed condition (Kuhlmann and Michelfelder, 2004). A creep coefficient of 0.44 and 0.53 for notches with hexagon head and self-drilling timber screw, respectively; and 0.56 for notch without screw was measured after 8 months from the beginning of the test. Push-out long-term tests are also being performed at the University of Canterbury. A different test set up was adopted using a "C" shape lever frame to apply 30% of the ultimate load in the short-term by using concrete weights (Fig. 2-13(c)). The specimens are located in an indoor, unconditioned environment. Three types of connection (rectangular and triangular notches reinforced with a lag screw, and toothed metal plates) were loaded for 1 year with the relative slips being recorded over time. The toothed metal plate connection crept the most under sustained load and rectangular notched coach screw connection the least, with creep coefficients of 3.84 and 0.52 after 1 year, respectively.

2.8.2   On beams

Kenel and Meierhofer (1998) tested for 4 years a composite beam made of solid timber with SFS screw connectors in sheltered outdoor conditions. Some results on a full-scale long-term test performed on a timber floor strengthened with SFS screws and lightweight aggregate concrete was reported by Grantham et al. (2004). Bou Said et al. (2004) monitored for 2 years a composite beam with glued-in mechanical connectors loaded in sheltered outdoor conditions. Fragiacomo et al (2007b) tested 8 deck system beams with shear key connection detail in an uncontrolled indoor environmental condition under sustained load applied the thirds of the span for a period of 133 days. Ceccotti et al (2006) performed a 5-year long-term test on a beam subjected to sustained load in unsheltered outdoor conditions. The mid-span deflection increased in the first two years of the test with fluctuation of all quantities (deflection, relative slip, strains, moisture content, temperature, and relative humidity) throughout the 5-year period of monitoring. The experimental findings were compared to the existing analytical regulations found in Eurocode 5 for different service classes (CEN, 2004b). At the University of Canterbury, a long-term test was performed on three TCC T-beams under sustained load in an indoor, unconditioned environment. Two beams have low shrinkage concrete but different connections, and the other beam has normal concrete. Some primary observations were: (1) the mid-span deflection is still increasing after 1 year; (2) the beam with normal

concrete deflected 6 mm more, corresponding to 25% more than the beam with reduced shrinkage concrete; (3) mid-span deflection increased more during wintertime corresponding to low temperatures; and (4) a fluctuation of all measured quantities as reported by Ceccotti et al (2006) was observed. Also other five TCC T-beams were monitored during construction for the first month after concrete casting in outdoor, unsheltered condition, and still other four T-beams were monitored under sustained load in indoor, uncontrolled environmental conditions (Yeoh et al, 2008a; Chapter 3). Lukaszewska et al. (2009b) tested for one year two TCC beams subjected to sustained load evaluated as 13% of the failure load in the short-term collapse test. The beam specimens were located in an indoor, unconditioned environment, and were made from glulam joists and prefabricated concrete slabs with mounted connectors (steel metal plates nailed to the glulam and metal pipes surrounding lag screws). The specimens increased the instantaneous deflection by about 50 and 80%, whilst the slip increased very little.

2.9   Repeated loading tests

In order to extend the application of TCC to bridges, it is important to quantify any stiffness and strength degradation in the connection system after many fatigue cycles. Limited research has been performed to investigate the behaviour of TCC floors subjected to repeated loading. Weaver et al (2004) carried out 2 million fatigue load cycles on wood-concrete composite bridges and push-out specimens with dowel-type shear connectors. The effect on strength was insignificant but stiffness decreased due to a 5% deflection increment in the tested bridge beam, measured at ultimate load. Döhrer and Rautenstrauch (2006) reported an 8% increase in slip at failure in notched and stud connection push-out specimens after 2 million fatigue cycles. Balogh et al (2008) conducted 21,600 loading cycles on a timber-concrete deck with shear key/anchor connection and found a 9% reduction in stiffness. At the University of Stuttgart, push-out specimens with crosswise glued-in rebars were subjected to fatigue cycles (Kuhlmann and Aldi, 2008). Repeated loading tests up to 2 million cycles on push-out specimens with notched lag screw and toothed metal plate connections were performed at the University of Canterbury (Murray, 2009).

2.10 Finite element modelling

In parallel with experimental tests, FE models to reproduce the behaviour of composite systems both in the short- and long-term were developed. Fragiacomo et al. (2004) and Fragiacomo (2005) presented an accurate uniaxial FE model for, respectively, short- and long-term analyses of timber-concrete composite beams taking into account the flexibility of the connection, the non-linear material behaviour such as concrete cracking and connection plasticization, and the rheological behaviour of the component materials. All phenomena affecting the long-term behaviour of timber, concrete, and connection system, such as creep, mechano-sorptive creep, drying shrinkage, thermal and hygroscopic strains, were fully considered. The influence of moisture content variations in the timber section is rigorously evaluated by using the Toratti's rheological model (Toratti, 1992) and by solving the diffusion problem over the timber section for a given history of environmental relative humidity. This FE model was validated against two experimental tests performed in outdoor, unsheltered conditions providing good accuracy (Fragiacomo and Ceccotti, 2006).

The important influence of environmental thermo-hygrometric variations for beams in outdoor conditions was recognized, and the contribution of such phenomena on deflection and slip of timber-concrete composites was investigated (Fragiacomo, 2006). Schänzlin (2003) developed a uniaxial numerical model based on the finite difference method, which can be used to investigate the time-dependent behaviour of simply supported composite beams with flexible connection exposed to variable environmental conditions. In this case, the Hanhijärvi (2000) rheological model was implemented for timber. Fragiacomo's and Schänzlin's models were compared to each other and to experimental results (Fragiacomo and Schänzlin, 2000) showing close approximation. To (2009) implemented a subroutine in the Abaqus (2000) software package for the 3D time-dependent behaviour of timber and concrete. For timber, To used the Toratti model (1992), whilst the CEB-FIB Model Code (CEB, 1993) was used for concrete creep. Orthotropic/isotropic behaviour was considered for timber/concrete. The moisture content distribution in the timber was computed by solving the diffusion problem for a give history of environmental relative humidity. The advantage of this 3D model over 1D models is the possibility of modelling the connection detail such as a notch cut in the timber and reinforced with a lag screw without the need to perform expensive push-out

tests in order to characterize the connection and identify the values of the slip modulus, shear strength and creep coefficient to be then implemented in 1d models. An experimental-numerical comparison between Fragiacomo's 1D model (Fragiacomo, 2005), To's 3D model (To, 2009), and the outcomes of an experimental test performed in Colorado on a composite beam with notched connection revealed that similar accuracy can be achieved by both models, with the 1D model needing far less computational time. Chassagne et al. (2005) also implemented a user-subroutine in the Abaqus software package for a 3D modelling of timber-concrete composite beams. A rigorous rheological model was implemented for timber and calibrated on results of experimental tests performed by the authors. Apart from FE model of timber-concrete composite beams to study the long-term behaviour, attention was paid to model the connections to predict the mechanical behaviour of a timber-concrete composite connection.

Dias et al (2007b) developed a 3D non-linear FE model for short-term non-linear analyses of composite beams and connections with notches and dowel-type fasteners. In the model, steel and concrete were modelled as an isotropic material, and timber as orthotropic. Good experimental-numerical agreement was found provided the actual material properties are implemented in the model. Aldi (2008) carried out a numerical investigation of notched connections and compared the outcomes with the experimental results. A fairly large scatter of load-bearing capacity and slip modulus was reported.

2.11 Prefabrication

In order to reduce the construction cost and make timber-concrete composite structures more competitive in the market, it is believed that a high degree of prefabrication should be achieved. Lukaszewska and Fragiacomo (2008) introduced a fully demountable TCC system. Here, the off-site prefabrication of a concrete slab with shear connectors already inserted, and the connection to the timber beams at the building site significantly reduce some drawbacks of the traditional system, such as the time needed for the concrete curing, the lower stiffness and higher creep during the concrete curing, the higher cost of a cast-in-situ concrete slab, and potential problems of quality control.

In Germany, a fully prefabricated modular TCC panel (Fig. 2-14) was proposed by Bathon et al. (2006). The panel connected with glued-in metal plates was reported as a

cost effective system able to compete with contemporary reinforced concrete and steel-concrete composite floors. The modular elements can be utilized in floors, walls and roofs in both residential and commercial buildings. More information on the system can be found in TICOMTEC (2007).

concrete

wood

reinforcement

HBV - shear connector
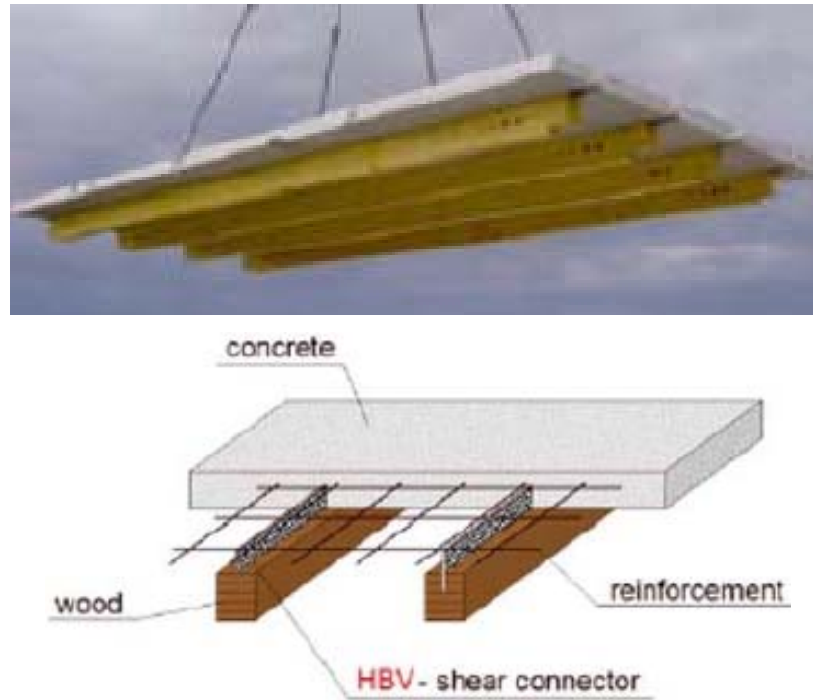
Fig. 2-14. Fully prefabricated TCC panels developed and used in Germany (Bathon et al., 2006)

In Finland, two TCC prefabricated systems labelled SEPA-2000 are currently in production for multi-storey buildings, both using nailplates as shear connectors. The first system is one in cast in-situ floor while the second is a prefabricated floor with the concrete cast upside down in factory without formwork (Fig. 2-15). Investigations on these two systems started in 1997 at the VTT Building Technology, Finland (Toratti and Kevarinmäki 2001, www.sepa.fi).
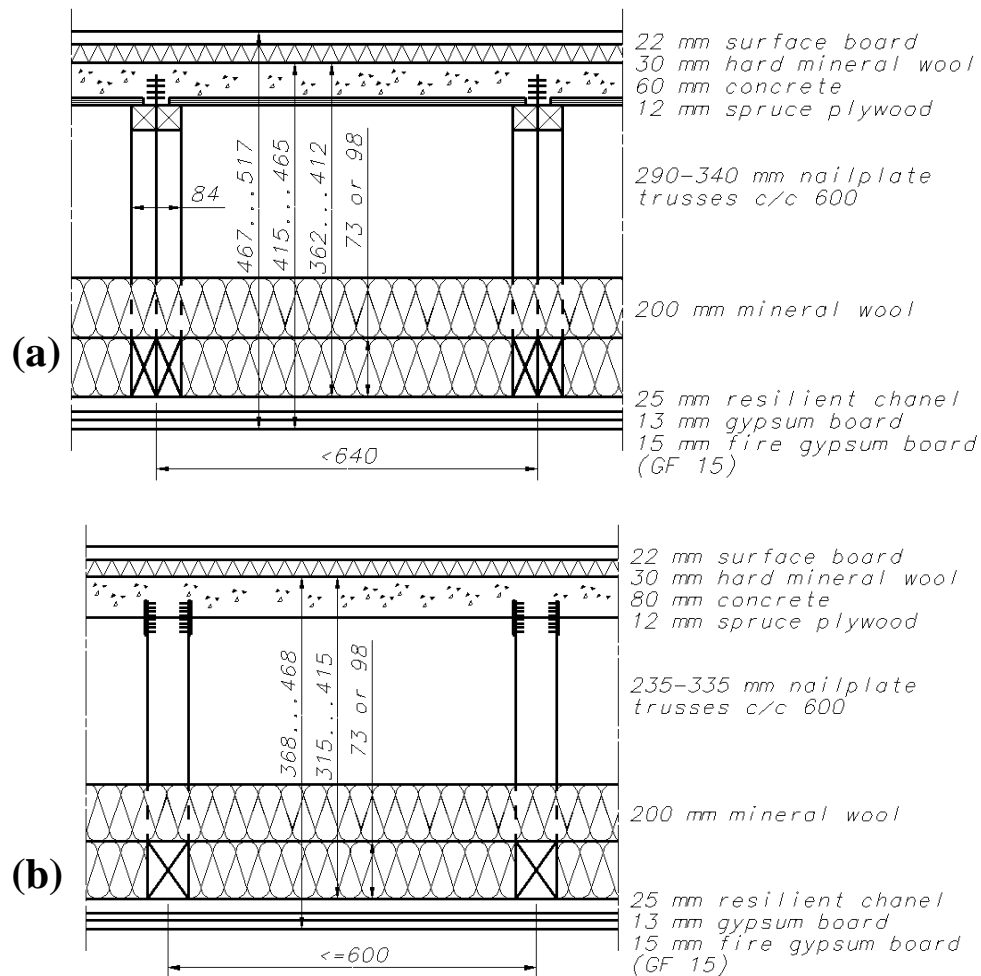
Fig. 2-15. Cross section of SEPA-2000 TCC prefabricated systems in Finland: (a) Cast-in-situ type; and (b) Precast type (Toratti and Kevarinmäki 2001, www.sepa.fi)

A semi-prefabricated floor system (Fig. 2-16) was proposed at the University of Canterbury, New Zealand (Yeoh et al, 2008a, 2009a; Chapter 3 and 7). The system consists of "M" section panels built with LVL joists and a plywood interlayer, prefabricated off-site and then transported to the building site, where the concrete can be poured. Despite the introduction of a "wet" component, advantages of this solution include: (1) ease of transport and lifting of the low weight panels of approximately 1 kN per metre; (2) construction of a monolithic concrete slab with better in-plane strength and stiffness, and no need for additional connections between adjacent panels; (3) high strength and stiffness achievable with reduced number of connectors (6 to 8 connectors), thanks to the effectiveness of the notched connection detail; (4) medium to long-span floors, in the range 6 to 12 m; and, therefore, (5) a system capable of competing with traditional precast concrete solutions.

2.12 Fire, acoustics and vibrations

Issues related to low fire resistance, insufficient acoustic separation and susceptibility to vibrations are met through the use of TCC. The fire performance of a TCC floor is competitive with that of a regular reinforced concrete floors. Natterer (2002) in his paper describing engineered timber structures all across Europe from 1974 to 2001, pointed out that apart from a significant reduction in self-weight, the fire resistance of TCC increased from 60 to 90 minutes when compared to a conventional reinforced concrete slab.

In a TCC structure, the concrete layer acts as a protective cladding for timber, reducing the effect of temperature and delaying the start of charring. On the other hand, the char that develops from the wood of the beams provides insulation to protect the concrete and the connectors against high temperatures (Frangi et al, 2008). In any case, the fire resistance of TCC is significantly increased with respect to that of a timber-only joisted floor.

Two full scale 4 m span TCC M-section floors of 300 and 400 mm deep LVL joist with notched and toothed metal plate connections subjected to 1.56 and 3.06 kN/m^2 gravity load, respectively, were tested under fire in accordance with the fire curve from ISO834 (2000) by O'Neill (2009). The first floor collapsed after 75 minutes and the fire was stopped after 60 minutes for the second floor in order to measure the charring rate (Fig. 2-17).

Frangi and Fontana (2001) developed a simplified method for the calculation of the fire resistance of TCC, and suggested relationships for the reduction of stiffness and strength of connections with the temperature as a function of the connection cover.
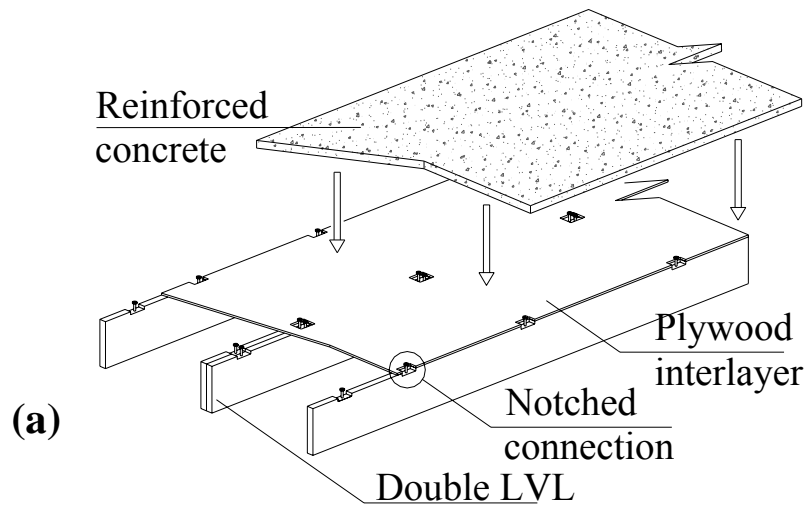
Fig. 2-16. Semi-prefabricated TCC floor system in New Zealand (a) Schematic diagram; (b) Erection of floor units; (c) Floor units in building frame (Yeoh et al, 2009a; Chapter 7)
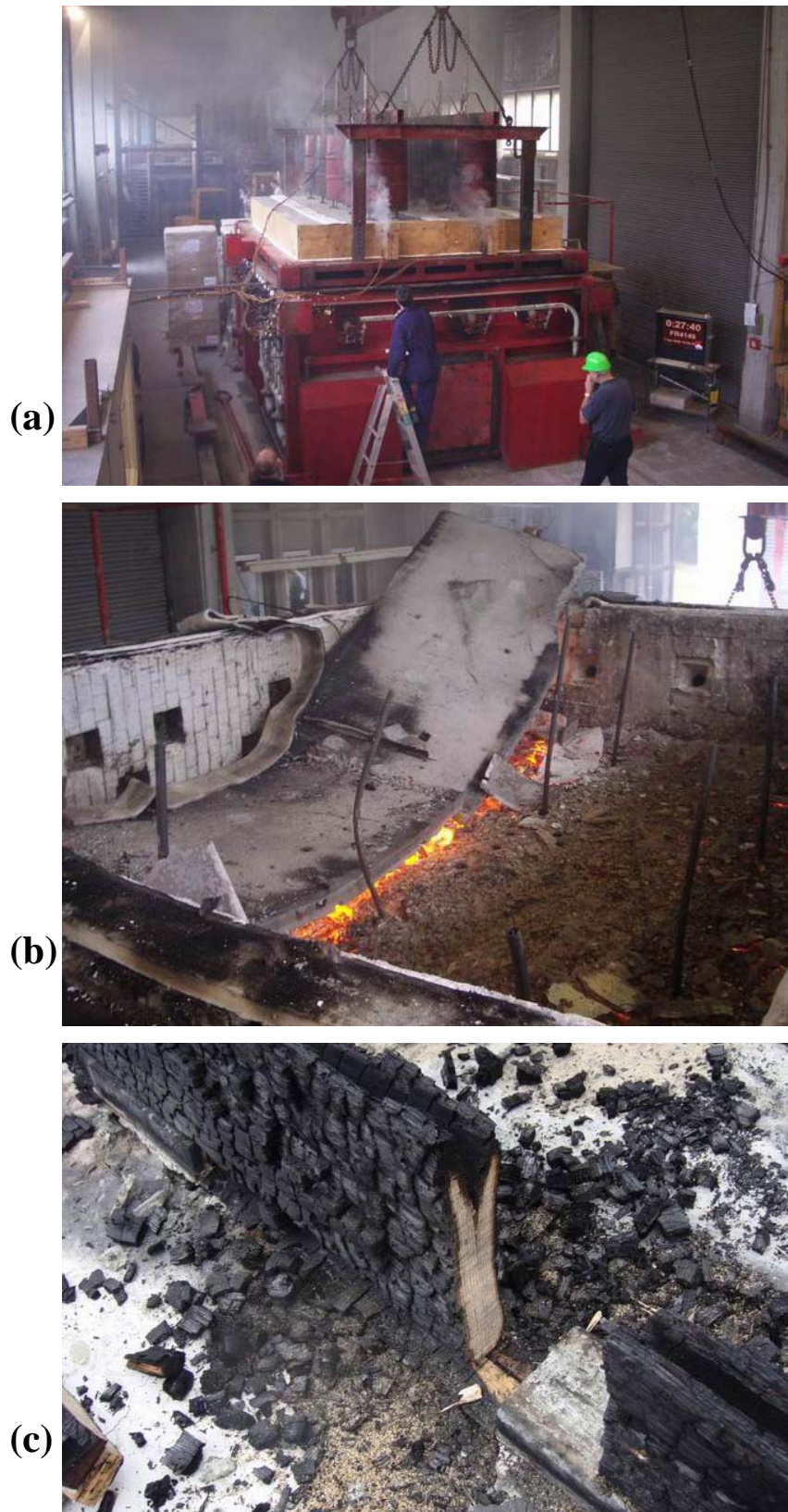
Fig. 2-17. Full scale 4 m span TCC M-section floors: (a) Fire test in progress on floors loaded under service load; (b) 300 mm deep module with notched coach screw connection which collapsed after 75 minutes; and (c) Fire stopped after 60 minutes for 400 mm deep module with toothed metal plate connection to measure charring rate (O'Neill, 2009)

With regards to vibrations and acoustics, the concrete slab increases the mass and stiffness of the timber floor and, thus, improves its overall vibration and impact sound insulation behaviour (Sipari, 2000). Detailed investigations into the dynamic/vibration behaviour of semi-prefabricated LVL-concrete composite floors are ongoing (Abd Ghafar et al, 2008).

2.13 Conclusions

The state-of-the-art on research of timber-concrete composite structures (TCC) has been presented. Several aspects such as the advantages of the system, the standards and design methods available, the types of connections developed around the world, the experimental and numerical investigations performed on connections and beams, in both the short- (at collapse) and long-term (under sustained load) have been discussed. The most important literature references were carefully selected and quoted in the chapter. TCC has a vast potential as a sustainable and effective floor solution, which however is hampered by the lack of awareness in town planners, architects, engineers and builders around the globe. Even though the subject has been investigated at length and considerable knowledge has been acquired, an effective yet economical connection system taking advantage of the prefabrication process characterized by fast erection and complemented with a user-friendly design package is still needed for the TCC to extensively and competitively penetrate into the construction industry. A few prefabricated TCC systems were referenced and briefly described in this chapter. The still limited information on the behaviour of TCC in the long-term deserves further research. Research data on fire resistance, acoustic separation, and susceptibility to vibrations behaviour is almost absent and still needed for implementation of TCC floors in multi-storey buildings.

3   Preliminary Tests on Connections and Beams

This chapter has been reproduced from a journal paper published in the Australian Journal of Structural Engineering entitled "Preliminary research towards a semi-prefabricated LVL-concrete composite floor system for the Australasian market" (Yeoh et al, 2009c).

The purpose of this chapter is to present the preliminary works of this thesis. It discusses the concept of timber-concrete composite floors and introduces a semi-prefabricated LVL-concrete composite medium to long span floor system for the construction of multi-storey timber buildings. The results of Phase 1 push-out test parametric investigations on 15 different types of notched and toothed metal plate connection carried out at the University of Canterbury were presented and compared to similar test results from University Technology of Sydney.

The most important criteria governing the strength and stiffness of the notched connections were identified and the four most promising connection types were decided leading to Phase 2 of the research, discussed in Chapter 4.

Discussion on the first month monitoring of indoor and outdoor floor beams in this chapter provided an understanding of the environmental effect and the significance of low shrinkage concrete application in timber-concrete composite floors. This finding led to plans for long-term test on beams in Chapter 6.

Brief overview of the experimental program on floor beams under Phases 4 and 5 given in this chapter laid the setting to Chapters 5 and 6, respectively.

Supplementary details related to this chapter on material properties, concrete test results, push-out specimen construction details, and short-term connection push-out test results that are presented in the Appendices 1, 2, 3 and 5, respectively.

3.1   Abstract

The choice of floor system has always been a key issue in the design and construction of multi-storey timber buildings. Strict performance requirements such as effective acoustic separation of inter-tenancy floors, thermal mass, fire resistance, limitation of deflection, resistance to vibrations, and effective diaphragm action are very hard to comply with if only timber is used.

The main purpose of this chapter is to present evaluations of short- and long-term experiments carried out mainly at the University of Canterbury, New Zealand for the realization of a semi-prefabricated Laminated Veneer Lumber (LVL)-concrete composite floor system for the local and Australasian market. This chapter discusses a novel semi-prefabricated LVL-concrete composite system where panels made from LVL joists and plywood flooring are prefabricated off-site. Once the panels are lifted onto the supports and connected side-by-side, a concrete topping is cast-in-situ so as to form a continuous slab connecting all the panels. Composite action between the concrete topping and the panels is achieved using different types of connectors such as various forms of notches cut from the LVL joists and reinforced with coach screws or toothed metal plates pressed in the LVL joists.

After outlining the advantages of the proposed system over traditional timber-only and concrete-only floor solutions, this chapter describes short-term push-out tests on connections used in LVL-concrete composite. Tests to failure of small LVL-concrete composite blocks (push-out tests) with different types and shapes of connection systems were performed at the University of Canterbury, New Zealand and at the University of Technology, Sydney. The results were parametrically evaluated and are discussed in detail. The failure mechanism of the notched connection is highlighted together with the strength and stiffness values for each tested connection system. Subsequently, the 4 best connection systems were identified and used in 8-10 m beam specimens.   The experimental program on the beams is presented briefly in order to provide information of the different phases of the project.

3.2 Introduction

The Timber-Concrete Composite (TCC) beam represents a construction technique widely used overseas for new and existing construction (Ceccotti, 2002). This technique consists of connecting an existing or new timber beam or joist with a concrete slab cast above a timber flooring using a connection system (see Fig. 3-1). A steel mesh is placed into the concrete flange in order to resist possible tensile stresses due to slab bending and to reduce the crack width. A plastic membrane is generally laid on the timber flooring in order to prevent concrete leaking during the concrete placement. By interconnecting the lower timber beam with the upper concrete flange a degree of composite action can be achieved.
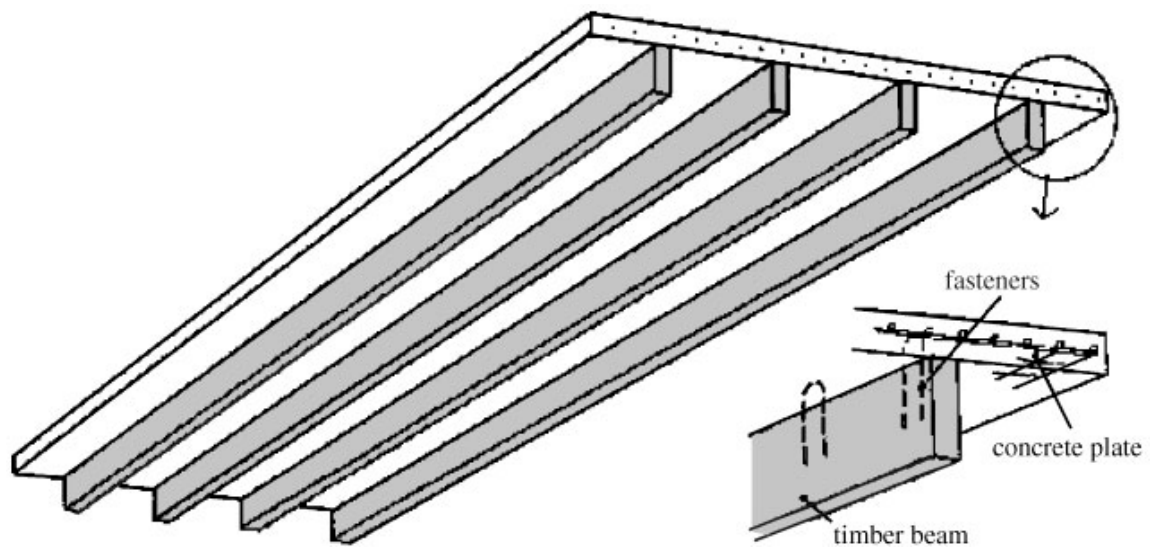
Fig. 3-1. Schematic of a typical timber-concrete composite floor system (Ceccotti, 2002)

A general definition of complete, partial and no composite action is provided in Fig. 3-2. A high degree of composite action is highly desirable in TCC structures as it increases both stiffness and load-carrying capacity, with improved structural performance. In a simple member subjected to bending, the bottom outermost fibres are stressed in tension, whereas the top outermost fibres are stressed in compression. The TCC beam is an attempt to combine the high compressive behaviour of concrete with the tensile and flexural resisting behaviour of timber to provide an improved composite beam. When complete composite action is achieved, the layered beam acts as a one-layer beam with mixed material properties. In this case the beam is stressed such that all or most of the concrete is in compression and all or most of the timber is in tension, depending on the depth of each material. Also there is complete transfer of stresses between the two layers

on the layer interface, and no interlayer slip (relative horizontal movement) occurs (see Fig. 3-2(a)). Complete composite action is the most efficient combination of the two materials in a layered beam configuration.
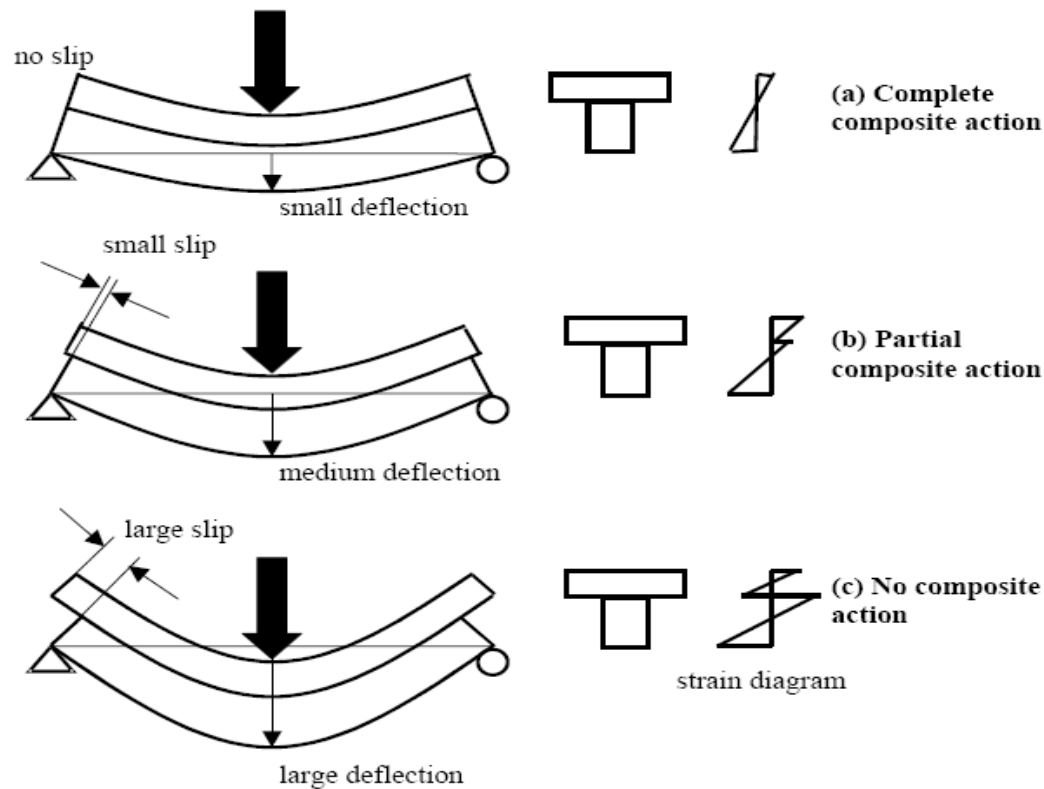
Fig. 3-2. Definitions of composite action

Conversely, when the beam has no composite action, the behaviour of the TCC beam is that of an individual concrete beam deflecting on top of an individual timber beam. In this case, the concrete beam and the timber beam are both stressed in pure bending. Furthermore in beams with no composite action, there is no transfer of stresses between the two layers, and large relative movement of the concrete layer with respect to the wood layer, i.e. significant inter-layer slip, occurs (see Fig. 3-2(c)). As a consequence of that, the beam will deflect more, and the material will be stressed more. When connectors are placed between the concrete layer and the timber layer, partial composite action is generally developed (see Fig. 3-2(b)). Although the different layers are stressed both in tension and compression, the situation is significantly better than that for the case where there is no composite action. Most of the concrete is stressed in compression and most of the wood is stressed in tension. There is limited interlayer slip but it is smaller in magnitude than the slip developed with no composite action. Thus the case of partial

46

composite action falls between the limits of no composite action (worst performance) and complete composite action (ideal performance). Thanks to the composite action, less deflections and larger resistance can be achieved with respect to the timber by itself. Thus providing a connection between timber and concrete improves the structural performance at both serviceability and ultimate limit states. Since complete composite action will lead to the better structural performance, it is important to use stiff connection systems.

3.3   Advantages and disadvantages

The TCC system was originally developed in Europe (primarily in Germany) for strength and stiffness upgrading of existing buildings (Muller, 1922). The possibility of retaining the existing wood floor of historical buildings is, in fact, a significant benefit in ancient buildings of important architectural value. This is achieved by pouring a thin layer of concrete 50 to 75 mm thick on an existing wood floor normally built from large section timber joists that are capable of carrying the extra weight of the concrete. Flexible connections in the form of nails, screws or bolts drilled into the existing floor joists provide the composite action. The concrete topping, in fact, strengthens and stiffens the existing timber floor, allowing the structure to resist larger loads. Important advantages of TCC over timber-only floors are: (1) retaining the original timber structure and simultaneously increasing its stiffness and strength, (2) developing a rigid floor diaphragm, which is important for earthquake-prone regions, (3) enhancing the acoustic separation, thermal mass, and fire resistance of the floor, and (4) reducing the susceptibility to vibration. Thanks to the many benefits with respect to timber-only floors, TCC construction can also be used for new construction and provides a viable solution for multi-storey timber buildings. Notable benefits should be highlighted with respect to the more traditional reinforced concrete slabs: the lower self-weight, the aesthetic appearance of wood, and the better behaviour of the composite section compared to reinforced concrete structures, with all sustainable benefits of wood.

Despite the indisputable merits of the TCC structures, there are still some issues that reduce the diffusion of such a technique. First of all, the use of TCC often prevented by the larger labour cost needed. The total construction cost is significantly influenced by the connection system. The performance of the TCC floor is significantly influenced by the behaviour of the connection system. Stiff and strong shear connectors are required to

provide optimal structural efficiency resulting in a minimum relative slip between the bottom fibre of the concrete slab and the top fibre of the timber beam. Some ductility is desirable since both timber and concrete exhibit quite brittle behaviour in tension and compression, respectively, and the plasticization of the connection is the only source of ductility for the TCC system (Frangi and Fontana, 2003, and Ceccotti et al., 2006). However, the connection system needs to be inexpensive to manufacture and install in order to make TCC floors competitive with other construction systems such as steel and precast concrete floors.
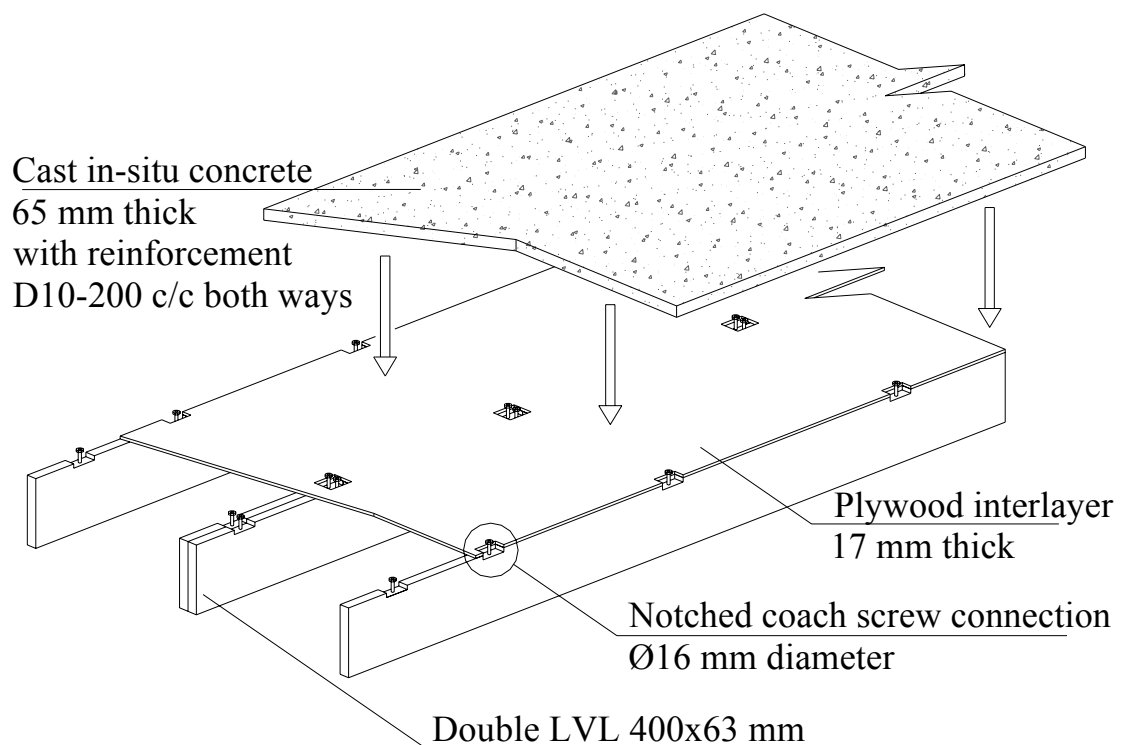
Fig. 3-3. Proposed semi-prefabricated TCC floor system

3.4   Proposed semi-prefabricated TCC floor system

Floors are a crucial part of multi-storey timber buildings. An increasing range of TCC systems have been developed, including cast-in-situ, semi-prefabricated, and fully prefabricated floors. Concrete slabs prefabricated off-site that incorporate shear fasteners are being developed in Sweden (Lukaszewska and Fragiacomo, 2008, and Lukaszewska et al., 2008). Those slabs are then connected with the timber joists on the building site, also providing the potential for fully demountable solutions. Fully prefabricated TCC panels have also been developed and used in Germany (Bathon et al, 2006).

A semi-prefabricated floor system is currently under investigation at the University of Canterbury. The proposed system comprises "M" section panels built with laminated veneer lumber (LVL) beams that act as floor joists and a plywood interlayer as permanent formwork (see Fig. 3-3). The panels can be prefabricated off-site and then transported to the building site, craned into position and connected to the main frame with specially designed joist hangers. Steel mesh is laid above the panels to provide shrinkage control for a 65 mm thick cast in-situ concrete slab. The panels can be propped while the concrete cures. The connection system has notches cut from the LVL joist and reinforced with a coach screw to provide more ductile behaviour during failure and to increase the shear strength. These notches are cut into the beams before the plywood interlayer is nailed on.
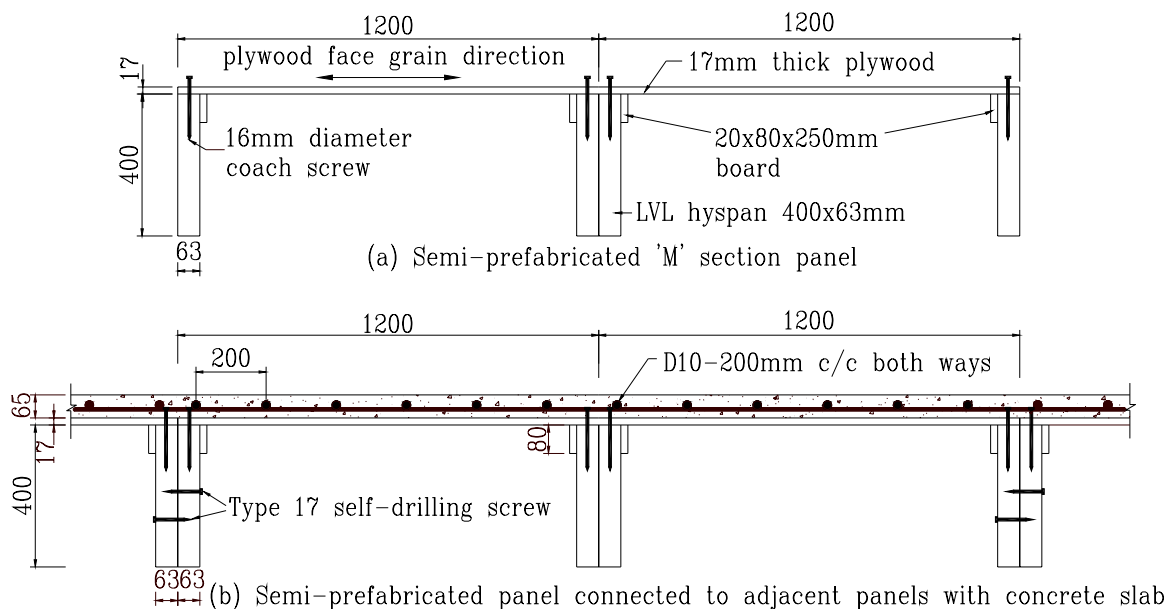
Fig. 3-4. Semi-prefabricated "M" section panel (dimensions in mm)

The 2400 mm wide "M" section panel is built with a single 400 × 63 mm LVL joist on each outer edge and a double LVL joist in the centre. The span of between 8 and 10 m requires 6 to 8 connectors along the length of each joist to provide adequate composite action. Each panel weighs approximately 8 kN, resulting in a lightweight component that is easy to transport and crane. Fig. 3-4 shows the sections of a single panel and how it is joined to the adjacent panels. The design is based on the effective bending stiffness method (the so-called "γ-method") as recommended by Ceccotti (1995) in accordance with the Eurocode 5 (CEN, 2004b). A detailed worked example is found in (Buchanan, 2007).

Advantages of this solution include: (1) ease of transport and lifting of the panels due to low weight; (2) construction of a monolithic concrete slab with better in-plane strength and stiffness, and no need for additional connections between adjacent panels; (3) high strength and stiffness achievable with reduced number of connectors, thanks to the effectiveness of the notched connection detail; (4) medium to long-span floors, in the range 6 to 12 m; and, therefore, (5) a system capable of competing with traditional precast concrete solutions. One disadvantage is the need to introduce a "wet" component (the fresh concrete) on the building site, where all other components are "dry" for a multi-storey timber building.
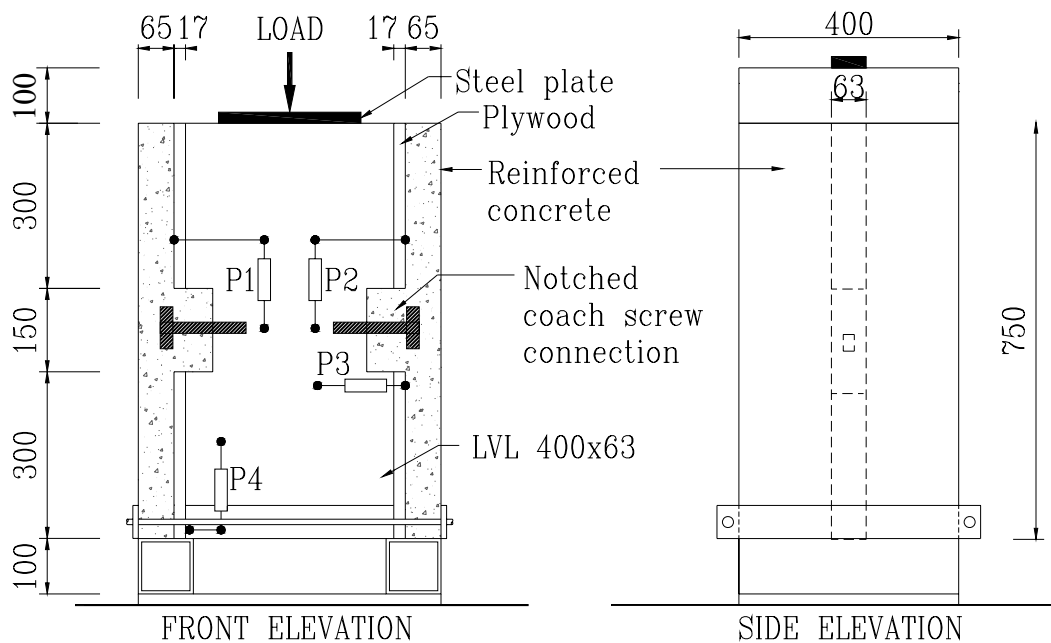
Fig. 3-5. Symmetrical push-out test setup (dimensions in mm)

3.5   Connection push-out tests

An experimental parametric study is essential for the optimization of the notch shape so that the best compromise between labour cost and structural efficiency is achieved. Connection push-out tests were carried out separately both at the University of Canterbury (UC) and at the University of Technology, Sydney (UTS).
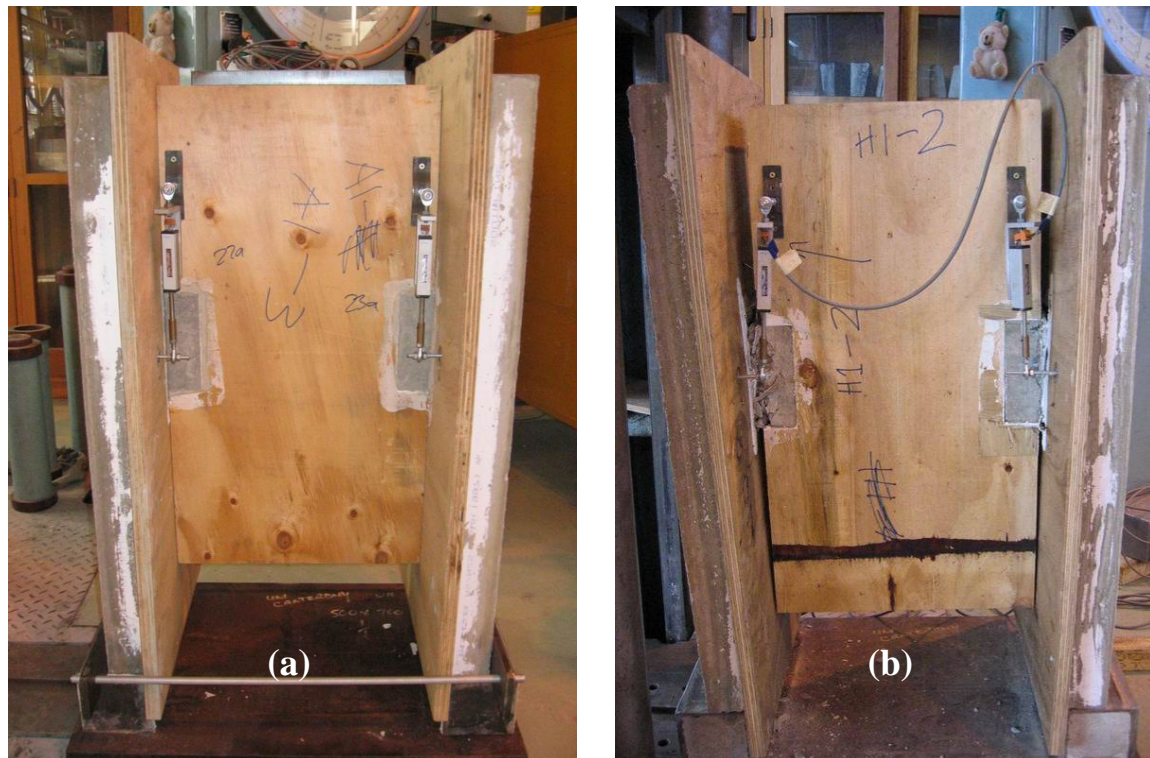
Fig. 3-6. Symmetrical push-out test setup: (a) Specimen before test; and (b) Specimen after test with shear failure along concrete notch causing web-flange separation.
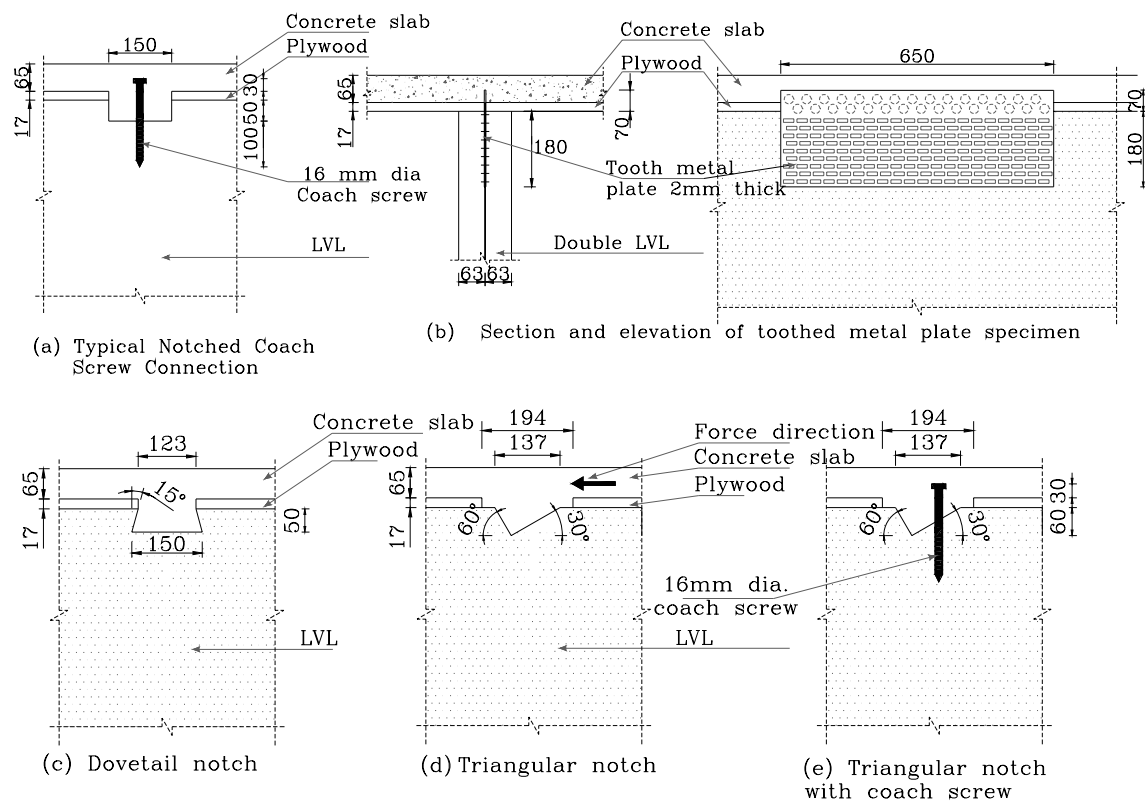
Fig. 3-7. Typical notched coach screw and toothed metal plate connections (dimensions in mm)

51

At UC, the tests were conducted in two phases in accordance with EN 26891 (CEN, 1991) where the connections are loaded in shear and the load-slip relationship recorded using a load cell and potentiometers P1, P2, P5 and P6 (see Fig. 3-5 and Fig. 3-6, potentiometers P5 and P6 are at the same location as P1 and P2 but on the opposite face of the specimen).

[Material properties, concrete test results, push-out specimen construction details and short-term connection push-out test results are presented in the Appendices 1, 2, 3 and 5, respectively]

3.5.1   Phase 1

A total of 15 different types of connection (A1 to H4) were identified in the first phase with two of each connection type tested numbering a total of 30 specimens as presented in Table 3-1. Variations of the typical notched connection included the length, depth, and shapes (dovetail, triangular, rectangular) of the notch are detailed in Fig. 3-7. Coach screws of 12 mm and 16 mm diameters were also inserted in the centre of the notches in some cases, while in other cases no coach screw was used. The depth of penetration of the coach screw into the LVL, and the end distance of the notch from the LVL were also varied. Slightly modified toothed metal plate fasteners (see Fig. 3-7(b)) that are pressed in the lateral side of two adjacent 400×63 mm LVL joists were also investigated and compared with the notched connections.

Fig. 3-8 illustrates the failure mechanism of a typical notched coach screw connection experimentally observed during most of the tests. In general, a shear plane begins to form at *$0.6F_{max}$*. Thereafter, the coach screw starts to act in tension until two plastic hinges were developed. At that stage, the coach screw transfers most of the shear of the connection by rope effect. Further information on analytical and numerical model of the connections can be found in (Yeoh et al., 2008b).

Table 3-1. Strength and stiffness values from first phase push out test at UC

Connection Type (length × depth × width) mm	F_{max} kN Exp.	kN Anal.	$K_{s,0.4}$ kN/mm	$K_{s,0.6}$ kN/mm	$K_{s,0.8}$ kN/mm	$\Delta2/\Delta1$ (%)
A1: Rectangular notch 150×50×63 Coach Screw ϕ16	73.0	68.5	80.2	75.4	61.7	35.5
A2: Rectangular notch 50×50×63 Coach Screw ϕ16	46.0	49.1	38.2	34.5	27.5	13.3
A3: Rectangular notch 150×25×63 Coach Screw ϕ16	71.8		113	102	76.1	26.1
90d-150/25-CS[+] (identical to A3)	68.9	-	-	-	-	-
B1: Rectangular notch 150×50×63	48.3	56.7	105	59.3	41.3	73.9
C1: Rectangular notch 150×50×63 Coach Screw ϕ12	66.0	66.3	77.9	74.5	62.3	38.8
C2: Rectangular notch 150×50×63 Coach Screw ϕ16 depth 140mm	84.2	87.8	211	145	95.5	36.5
D1: Doves tail notch 150×50×63	20.5		51.1	28.1	33.5	37.0
E1: Triangular notch 30°_60° 137×60×63	40.2		101	57.3	37.9	34.1
E2: Triangular notch 30°_60° 137×60×63 Coach Screw ϕ16	82.6		123	104	75.4	36.5
B-60d/60-CS[+] (identical to E2)	66.48	-	-	-	-	-
F1: Rectangular notch short end 150×50×63 Coach Screw ϕ16	74.4		92.7	91.1	73.6	49.0
G1: Rectangular notch LSC 150×50×63 Coach Screw ϕ16	68.8		67.0	66.9	56.1	49.3
H1: Rectangular notch 2-LVL 150×50×126 Coach Screw ϕ16	128		218	183	119	42.1
H2: Double toothed mp 650 mm	163.9	163	378	276	127	44.0
H3: Double toothed mp 325 mm	81.1	81.7	480	508	53.4	33.3
H4: Double toothed mp 150 mm	47.9	37.7	54.3	38.7	31.2	37.5

[+] *These specimens were tested at UTS.*
LSC *for Low Shrinkage Concrete*
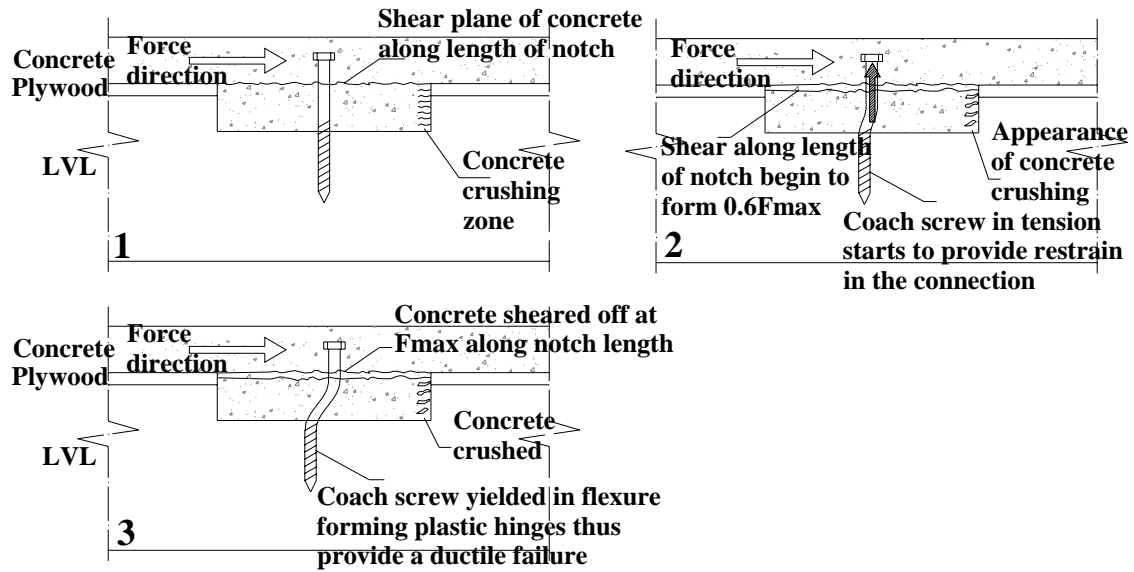
Fig. 3-8. Experimental failure mechanism of notched connection with coach screw

The relationship between shear force and relative slip is presented in Fig. 3-9 for the selected specimens most representative of the different connector shapes. The results in terms of shear strength (F_{max}), secant stiffness (also defined as slip modulus) at serviceability limit state or 40% ($K_{S,0.4}$), at ultimate limit state or 60% ($K_{S,0.6}$) and at collapse or 80% ($K_{S,0.8}$) of the strength are summarized in Table 3-1 as an average of the values measured on two specimens. The strength, F_{max} is defined as the largest value of shear force monitored during the test for slips not larger than 15 mm. In order to provide some information on the post-peak behaviour and the level of ductility, the ratio Δ_2/Δ_1 is introduced, defined as the ratio of strength difference at peak and at 10 mm slip (Δ_2), to the strength at peak (Δ_1), reported in Table 3-1. The lower the Δ_2/Δ_1 ratio, the better the post-peak behaviour and the higher the ductility. For definition purpose, a ratio below 50% would be considered as a ductile connection or otherwise a brittle connection.

The connection strength is significantly influenced by the length of the notch. This is observed in a 50 mm length notch (A2=46 kN) which exhibited approximately 60% of the strength of a 150 mm notch (A1=73 kN). Similar agreement is also found when comparing the notches without coach screws but have different length at the mouth of the notch, ie. B1, rectangular notch 150 mm length (48.3 kN strength); E1, triangular notch with 137 mm length (40.2 kN strength); and D1, dovetail notch with 123 mm length (20.5 kN strength).
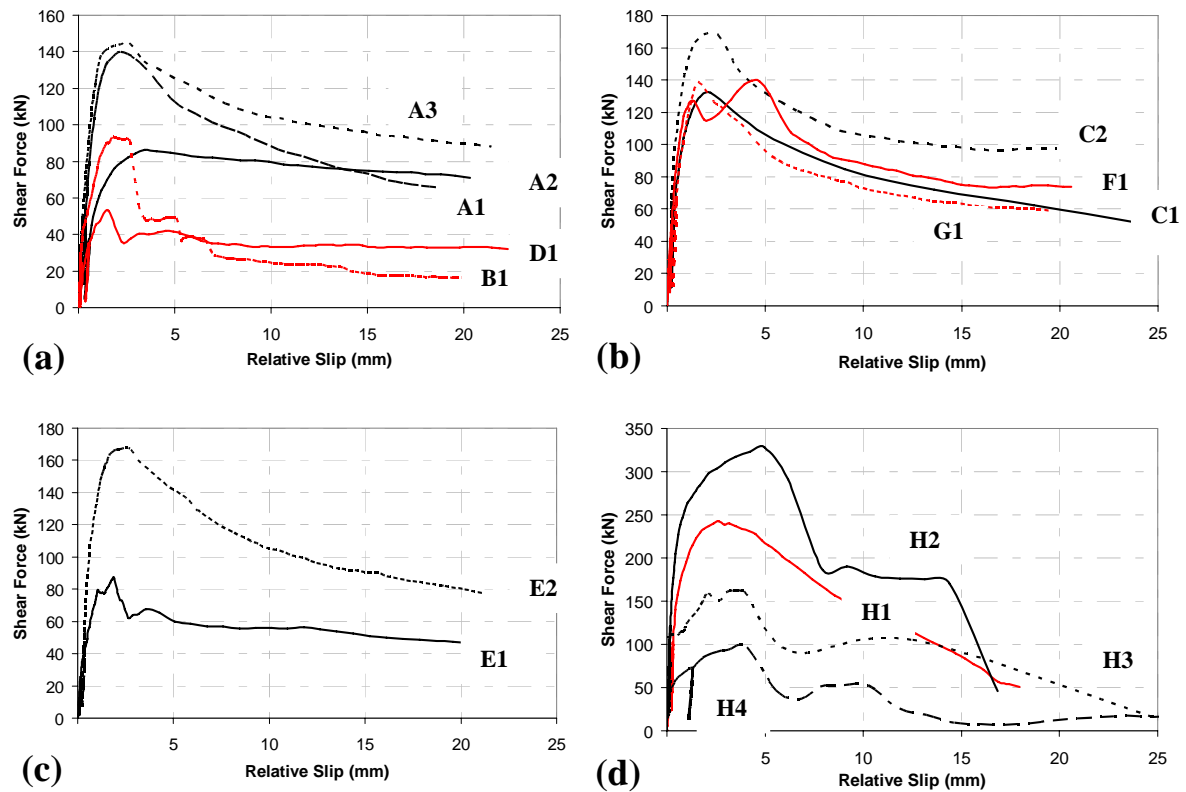
Fig. 3-9. Relationship between shear force and relative slip for 15 connection systems tested in first phase push-out test at UC.

The presence of a coach screw also significantly affects both the strength and stiffness of the connection. It increases the strength of a connection by 1.5 to 2 times the strength without coach screw. For instance, connection E2 with a coach screw is 2 times stronger than E1 without one. Fig. 3-9(a) shows a similar trend by comparing connections A1 and B1. The initial stiffness as shown in Fig. 3-9(c) is not enhanced significantly by a coach screw (compare E1 and E2), however, the coach screw is important to prevent the stiffness deteriorating after the serviceability limit, taken as 40% of the maximum shear force. It appeared that the only source of ductility was provided by the coach screw, which also significantly increased the resistance.

It is observed in 2 cases for B1 and E1 that the stiffness after the attainment of the serviceability limit and the post-peak behaviour markedly degraded in the absence of a coach screw. The size of coach screw was found to only affect the strength and not the stiffness as seen in A1 and C1, while the penetration depth in excess of 20 mm increased the strength slightly but caused a large increase in stiffness as can be observed by

comparing C2 and A1 (see Fig. 3-9(b)). The depth of notch has no effect on either the strength or the stiffness properties (compare A1 and A3). Generally, all of the specimens failed by shear in the concrete (Fig. 3-10(a)), hence a longer length of notch is essential to improve the shear strength. The performance of the triangular shaped notch was similar to that of a rectangular notch of similar length (compare F_{max} for specimens A1, 73 kN, and E2, 83 kN), making it a more viable option as it is much easier to manufacture. The double sided 2 mm thick toothed metal plate connection (specimens H2, H3 and H4) exhibited a ductile plate tearing failure with high strength and stiffness as presented in Fig. 3-10(b). The strength of this connection can be easily determined from the plate's yield strength and length. Furthermore, the connection demonstrated an encouraging result as shown in Fig. 3-9(d) making it by far the most practical connection type apart from the rectangular and triangular notches with coach screw connections.
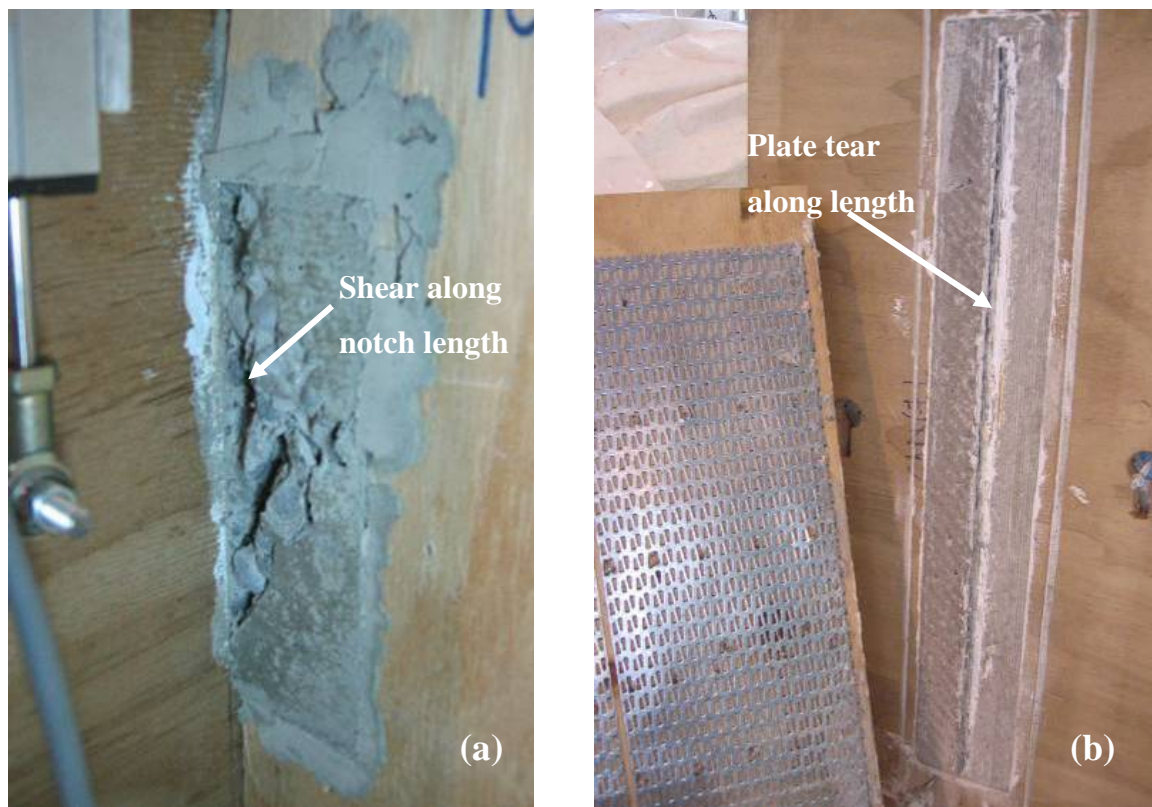
Fig. 3-10. (a) Rectangular notched connection failure – shear in concrete length, and (b) Toothed metal plate connection failure – plate tearing along length of plate

3.5.2 Phase 2

Based on the observations from the experimental tests to failure, and taking into account the ease of construction, the four most promising connection systems were found to be: (1)

150 × 25 mm rectangular notch reinforced with 16 mm diameter coach screw; (2) 300 × 50 mm rectangular notch reinforced with 16 mm diameter coach screw; (3) 150 mm long triangular notch reinforced with 16 mm diameter coach screw; and (4) 2 × 333 mm toothed metal plate connector. The latter 3 connections were tested for the characteristic values of strength and stiffness in the second phase of push-out tests at UC. The results to this push-out test are presented in Chapter 4.

3.5.3 Push-out test at UTS

At UTS, a series of push-out tests were performed involving different variations in notched connections such as: (1) square rectangular notch of 90º facets; (2) bird-mouth or triangular notch; (3) slant notch with 15º, 25º, 35º and 45º facets; and (4) curve notch with a radius (Fig. 3-11). The strength results of the tested connections are presented and discussed in the following sub-section. Comparisons were made between the results obtained at UC and UTS for connections that are identical.
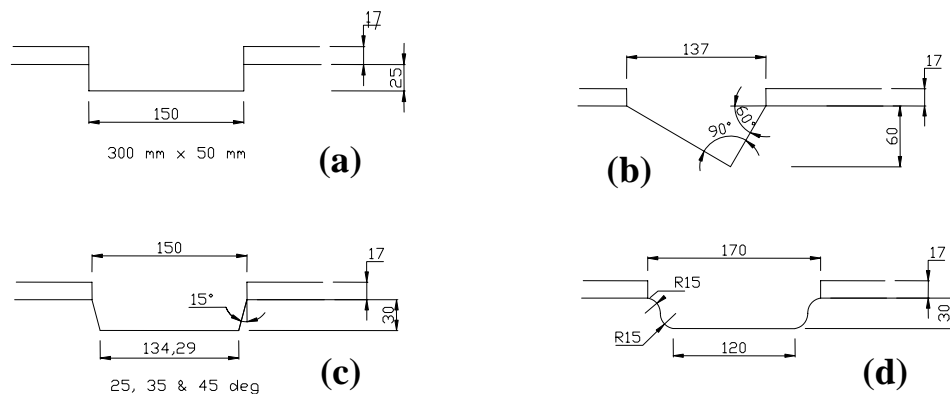
Fig. 3-11. Detailing of the shear connections tested at UTS– (a) square notch (90° facets), (b) bird-mouth, (c) slant notch (15°, 25°, 35° and 45° facets) and (d) curve notch

Similar agreement concerning the use of a coach screw was found in the UTS test results. A comparison of relative strength of each of the connection types is presented graphically in Fig. 3-12 (coach and wood screws are labelled as CS and WS in the specimen name respectively), where the strength of each connection is expressed as a percentage of the strength achieved for the strongest connection (90d- 150/25-CS) – which corresponds to 100%. The notation given for the type of connection can be read as, for instance 90d-150/25-CS: 90d for 90º facet, 150 for notch length, 25 for depth of notch and CS for coach screw. Other notations used are B for bird mouth and S for slanted facet. It can be

clearly seen that the connections with a CS achieve higher strength than that with WS's. In addition, two distinct groups of performance bands can be identified; the first one includes 90d-150/25-CS, B-60d/60-CS and S-170/30-CS (these three series offering high strength), whilst the second one includes the slanted-facet connection, with these series achieving about 50% of the strength of 90d-150/25-CS. More details of the investigations carried out at UTS are presented in (Gerber et al., 2008).
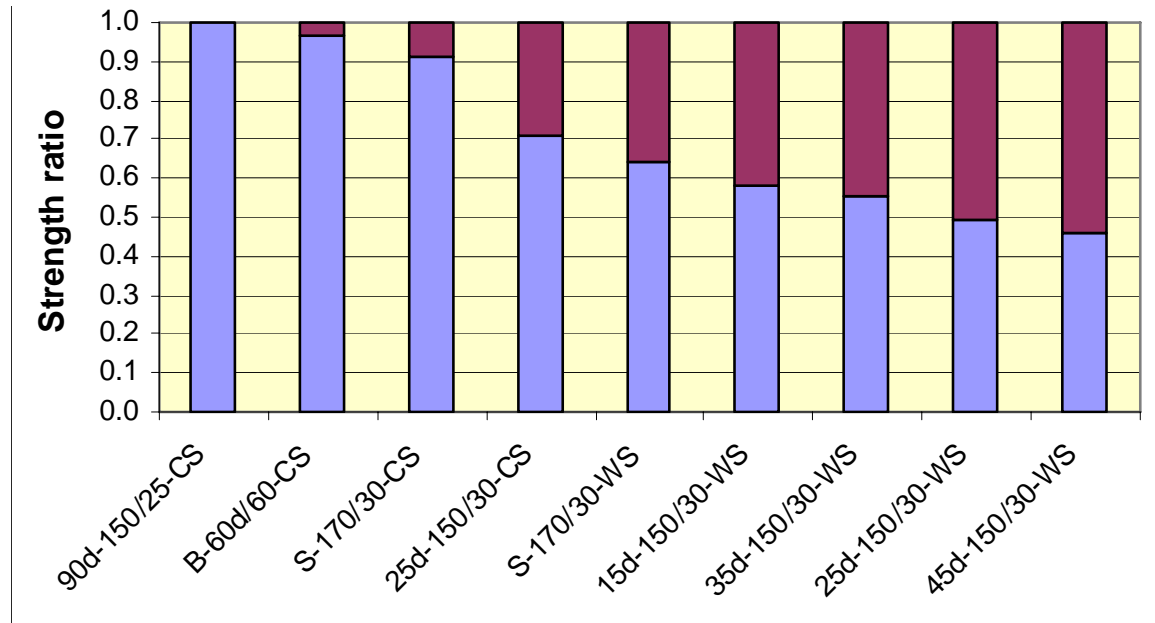
Fig. 3-12. Strength comparison of push-out tests at UTS

The significant difference of strength and stiffness values of the same connection tested in UC and UTS as presented in Table 3-1 is largely attributed by the strength and quality of concrete. For instance, honeycomb due to lack of compaction was observed in the 300 mm length rectangular notch in UTS. The mean compressive strength at UTS was 32.73 MPa as oppose to 42.71 MPa at UC. The failures in the notches are predominantly due to concrete shear along the length of the notch and therefore the concrete compressive strength is an important indicator.

3.6   Composite Beam Experimental Program

An extensive experimental program on full-scale T-strips of TCC floor spanning 8 and 10 m is currently ongoing at the University of Canterbury in collaboration with the University Technology of Sydney which involves 5 phases: (1) short-term monitoring of

beams outdoor and indoor, in unconditioned environment, where the deflections of 9 beams have been monitored for a period of 1 month after the concrete placement to investigate the effects of the construction process and the environmental changes; (2) short-term monitoring of beams indoor in unconditioned environment, where 4 beams are being monitored for a period of 3 months with the quasi-permanent load condition $G_k+0.4Q_k$ applied using water buckets after 28 days (Fig. 3-13(a)) from the concrete placement in order to investigate the time-dependent behaviour during construction and the first months of life of the structure; (3) repeated loading of selected beams under 2 millions cycles, so as to investigate the possibility of using the proposed system for short-span bridges; (4) test to failure of all the beams in (1) and (2) under four-point bending static load (Fig. 3-13(b) and Fig. 3-14); and (5) long-term monitoring of 3 beams under quasi-permanent load condition for a period of 1 year followed by unloading for 3 months to assess the creep coefficient during loading and unloading periods.

The four most promising types of connectors for the beam specimens were identified using the push-out tests detailed in the previous section. Different numbers of connectors corresponding to two scenarios, well-designed and under-designed according to the Eurocode 5 provisions, have been considered for each type of connection. Well-designed herein refers to full compliance of all inequalities at both the ultimate and serviceability limit state verifications while under-designed refers to a beam design where the demand of maximum shear force in the connection exceeds approximately 1.3 times the shear force resistance of the connection at the ultimate limit state. The method of effective bending stiffness (also known as γ-method) for ultimate and serviceability limit state was adopted in the design, with the slip moduli $K_{S,0.4}$ at serviceability limit state and $K_{S,0.6}$ at ultimate limit state, and strength values, F_{max} obtained from the aforementioned push-out tests for the selected connection type.
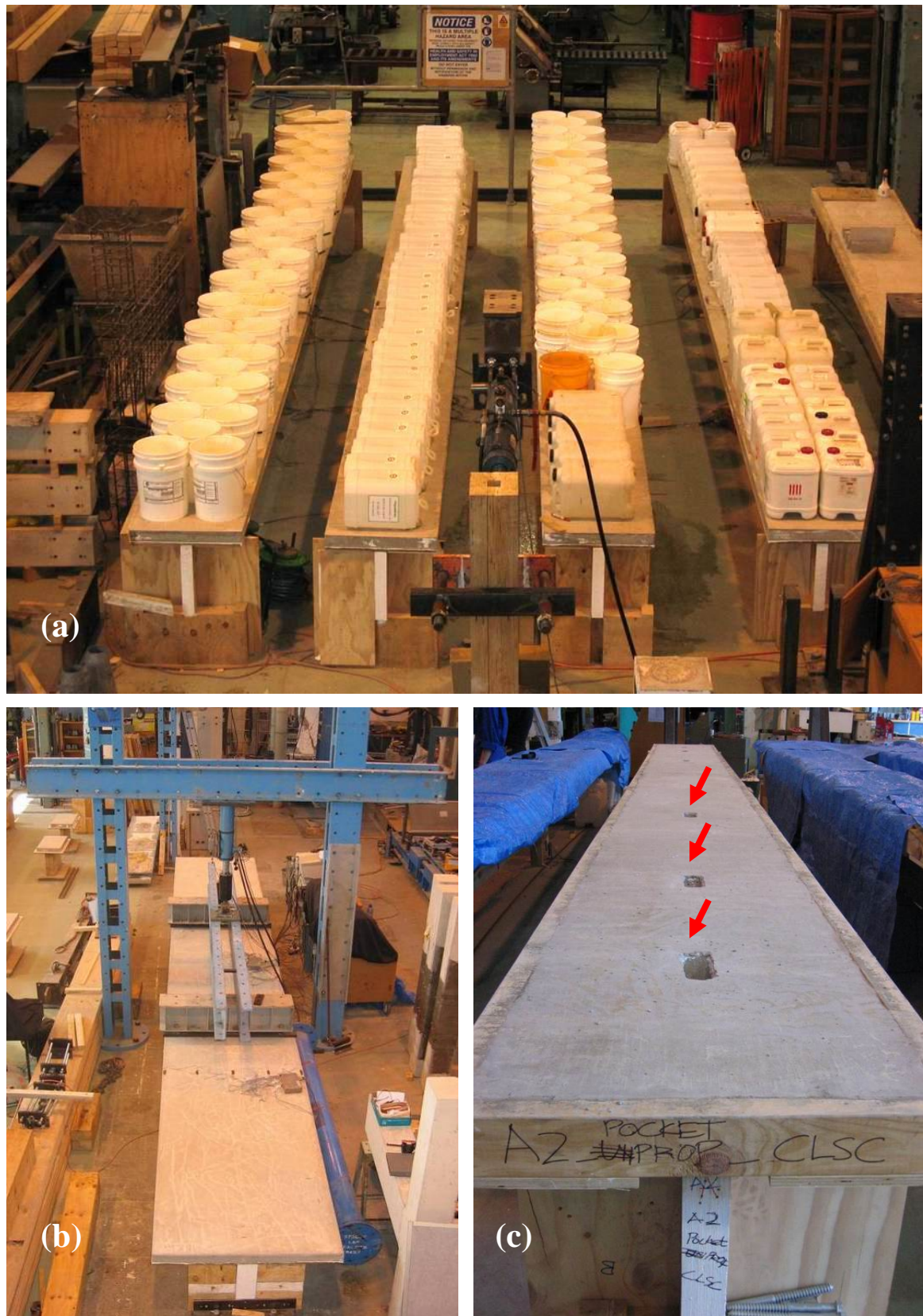
Fig. 3-13. Full scale TCC T-beams at the University of Canterbury, (a) 4 beams under service loads using buckets of water, (b) An 8 m beam 1200 mm width ready for collapse test at 4 point bending, and (c) Arrows pointing to connection pockets in beam
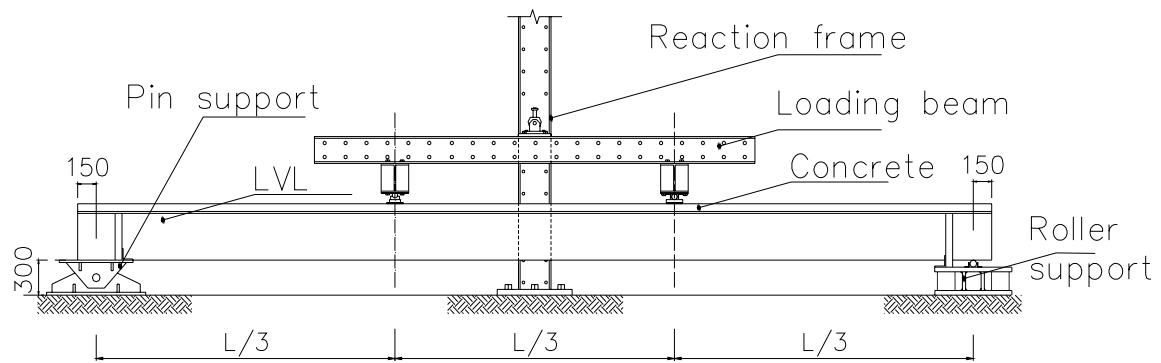
Fig. 3-14. Four-point bending test setup for collapse test of TCC beams (dimensions in mm)

Two span lengths were tested: 8 m and 10 m. Construction variables include the number of days of propping (0, 7 and 14) and curing (1 and 5), and whether the notches were cast at the time of the concrete placement or grouted 7 days later. The grouted notches required a void or pocket (see Fig. 3-13(c)) at the time of concrete placement that was filled later with high strength grout (with shrinkage compensation). The type of concrete was carefully selected as shrinkage may induce excessive deflection on the TCC beam due to the high stiffness of the connection (Fragiacomo et al., 2007b). A commercially available low shrinkage concrete (CLSC) of 35 MPa, 650 microstrain with special admixture (Eclipse), 13 mm size aggregate and 120 mm slump was used. Fig. 3-15 illustrates a typical TCC T-strip beam with a 300 mm length notched coach screw connection.

BEAM D span = 8 m
CONNECTION TYPE: A1mod 50x300 NCS16
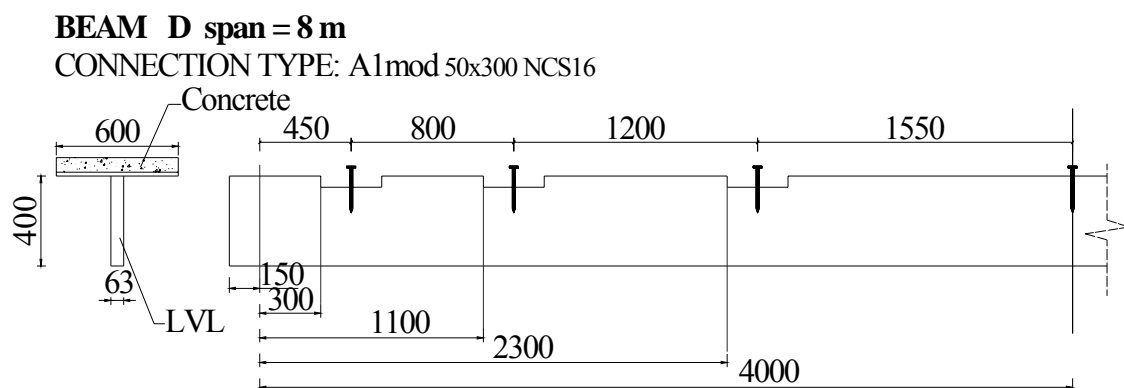
Fig. 3-15. A typical 8 m TCC beam with a 300 mm length rectangular notched connection (dimensions in mm)

3.7   First Month Monitoring of Beams

This section reports the first phase of the beam experimental program. 5 beams were constructed outdoor and another 4 beams constructed indoor. Mid-span deflection of the beams was monitored using potentiometer during the first month after the concrete placement (see Table 3-2). The sampling rate was every five minute during concrete casting, and subsequently every hour after the concrete has set. Relative humidity and temperature were automatically recorded with 4 key events noted overtime: (1) concrete placement, (2) concrete set, assumed as 6 hours after casting, (3) prop removal, and (4) 28 day. The aim of this short-term monitoring is to investigate the effects of environmental changes and type of construction on the beams deflection.

Table 3-2. Short-term 1 month beams monitoring schedule

Beam Notation and (Location)	Connection and (Number of connectors) in mm	Span and (Width) in metre	Propped (Days) or Unpropped	Design level and (Concrete Type)
A1 (Indoor)	25dx150l NCSϕ16 (6 numbers)	8 (0.60)	Propped (14)	Under-designed (CLSC)
C1 (Outdoor)	30º_60º TriNCSϕ16 (10 numbers)	8 (0.60)	Propped (7)	Well-designed (CLSC)
D1 (Outdoor)	50dx300l NCSϕ16 (6 numbers)	8 (0.60)	Propped (7)	Well-designed (CLSC)
D2 (Outdoor)	50dx300l NCSϕ16 (6 numbers)	8 (0.60)	Unpropped	Well-designed (CLSC)
E1 (Indoor)	50dx300l NCSϕ16 (6 numbers)	10 (0.60)	Propped (7)	Under-designed (CLSC)
E2 (Indoor)	50dx300l NCSϕ16 (6 numbers)	10 (0.60)	Propped (7)	Under-designed (NC)
F1 (Outdoor) double LVL	Plate_2x333l Staggered (8 numbers)	8 (1.20)	Propped (7)	Well-designed (CLSC)
F2 (Outdoor) double LVL	Plate_2x333l Staggered (8 numbers)	8 (1.20)	Unpropped	Well-designed (CLSC)
G1 (Indoor) double LVL	2x25dx150l NCSϕ16 (6 numbers)	8 (1.20)	Propped (7)	Well-designed (CLSC)

Note: NCS - Notched Coach Screw, CLSC - Commercial Low Shrinkage Concrete, NC - Normal Concrete, d – depth, l – length

62
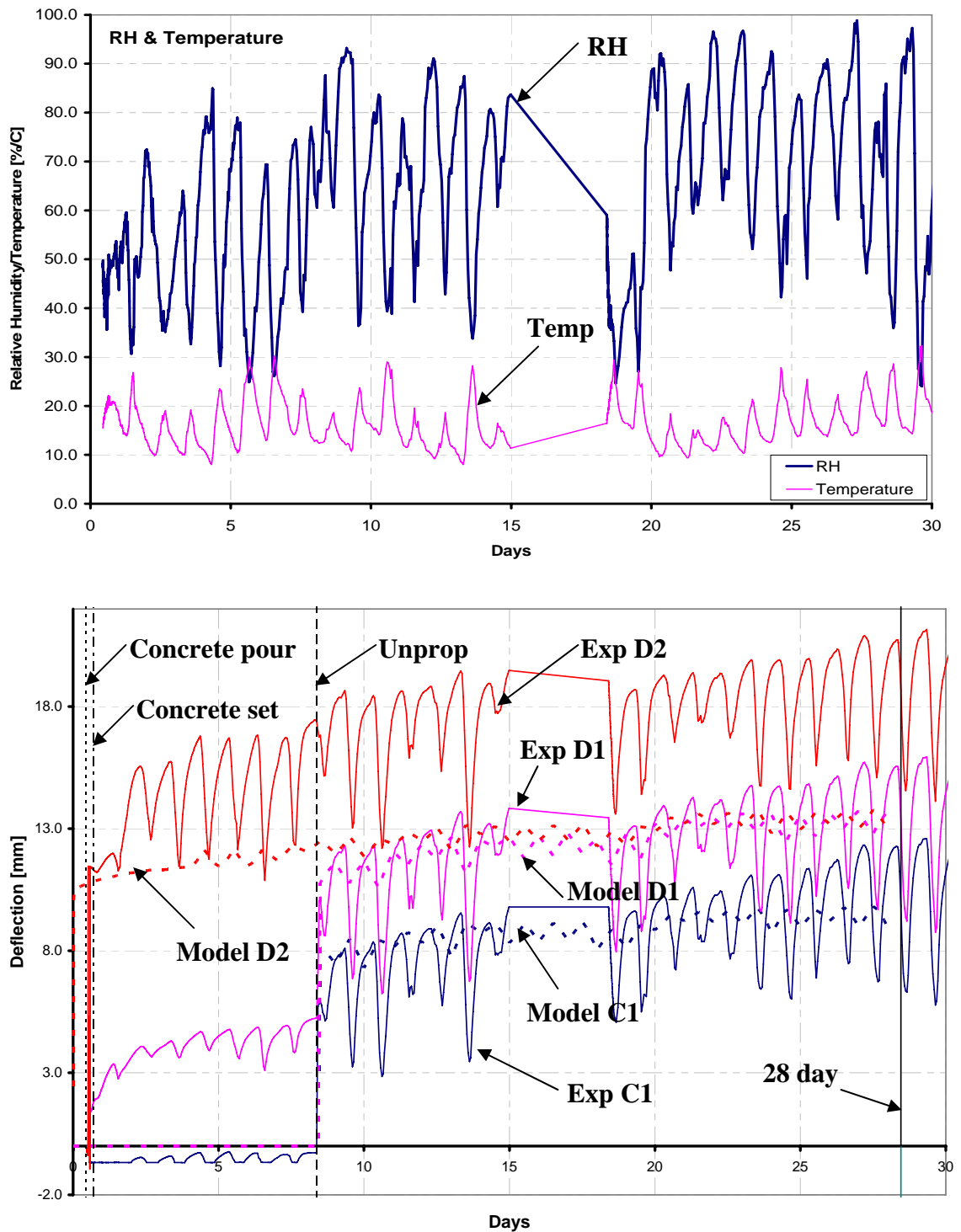
Fig. 3-16. History of mid-span deflection for outdoor beams (bottom) with corresponding RH and temperature histories

Fig. 3-16 shows the history of mid-span deflection for selected outdoor TCC beams (C1, D1 and D2) in an unconditioned environment. Overall, the deflection plots of all the beams throughout the monitoring period had a periodic pattern that reflected

environmental fluctuations. The relative humidity (RH) peaked at the same time as the minimum daily temperature. The fluctuation of deflection was found in all plots to be consistent with the peaks of relative humidity and minimum values of temperature. Basically, the deflection fluctuation was within the range of 4 to 6 mm, and took place between day and night.

Unpropped beam (D2) sagged 11 mm at the time of casting. Uneven and soft outdoor grounds have caused invalid deflection in propped beams (C1, D1) which had to be corrected. Props were removed after 7 days in propped beams. An instantaneous 6 to 10 mm deflection increment was recorded when the prop was removed although the final deflection at 28 day was in the range of 5 mm less than the unpropped beams, corresponding to span/1600. On the whole, propping of beams at mid- span was important to minimise permanent deflection and enable initial composite action to be developed before sustaining the full self-weight of the concrete slab. Nevertheless, after the removal of props, deflection fluctuations in all beams follow a similar trend due to RH and temperature changes which were also observed in unpropped beams. Fig. 3-17 displays the indoor experimental-numerical comparisons in terms of mid-span deflection for selected TCC beams (E1, E2). The environmental fluctuations were not as prominent as in outdoor conditions and, therefore, the day-to-night deflection variations were insignificant. Low shrinkage concrete (in E1) was effective in reducing the total deflection by 5 mm at 28 day when compared to normal weight concrete (in E2). The concrete shrinkage, in fact, increases the overall deflection of composite beams, especially when the connection is very stiff like in the case under study.

The temperature and relative humidity experienced during these tests were not as adverse as it would be in many regions of Australia which will impose high fluctuations. Therefore it is crucial that further test be carried out to monitor the behaviour of the system under more severe conditions.
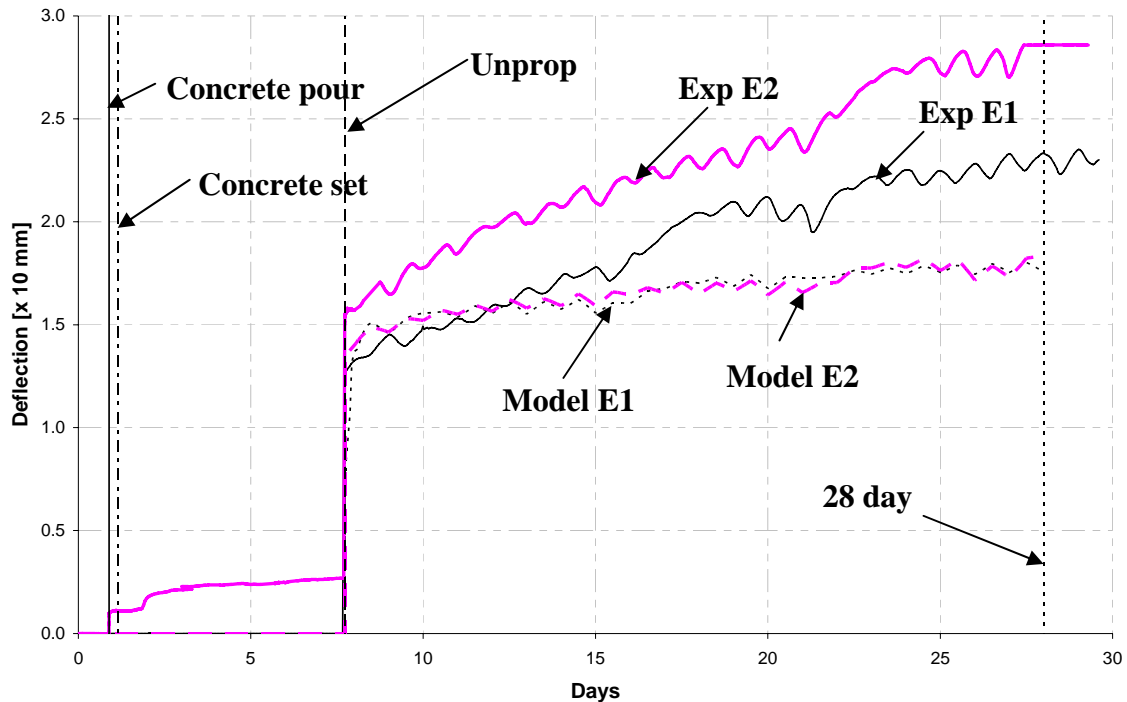
Fig. 3-17. History of mid-span deflection for indoor beams

3.8   Conclusions

The important issue with such composite system addressed in this chapter is the large deflections experienced over the service life of the structure. In order to minimize these deflections, it is recommended that reduced shrinkage concrete be used and spans be propped at mid span as carried out in this project. Other possible method of reducing the deflections is by pre-cambering the floor joist, and in this case of pre-cambering the LVL, it involves a modification in the cutting of the LVL at the factory.

This chapter has presented the preliminary outcomes of a broad experimental program ongoing at the University of Canterbury, New Zealand, and University of Technology Sydney, Australia, also with the participation of overseas institutions such as the University of Sassari, Italy. This joint research program is aimed to develop a floor solution suitable for medium to large span floors in multi-storey timber buildings. The performance requirements of effective acoustic separation, adequate fire resistance, and reduced susceptibility to vibrations indicated the use of a concrete topping as highly desirable.

In order to exploit the stiffness and strength contribution of the concrete, a shear connection system should be used, so as to obtain composite action between the concrete topping and the timber beam. The proposed solution is therefore a semi-prefabricated timber-concrete composite system where timber panels made from LVL joists and plywood sheets are prefabricated off-site, craned into position, and used as permanent form for the concrete topping which is poured on site. This solution has the advantages of the prefabrication and allows, at the same time, the construction of a monolithic floor from the concrete topping poured on site.

Composite action is obtained by cutting notches from the LVL joists and relying on the bearing at the timber-to-concrete interface, or using tooth metal plates pressed on the side faces of the LVL joists. Different notch shapes have been investigated by performing push-out tests on small composite blocks, and the four most promising systems identified. The failures in the notches are predominantly due to concrete shear along the length of the notch and therefore the concrete compressive strength is an important indicator. The mechanical properties of the connectors (shear strength and slip moduli) needed for the design of the floor were then evaluated. Based on those values, strips of 8 m and 10 m composite floors for office buildings were designed, constructed and tested. The tests, discussed in Chapters 5 and 6, include long-term, repeated (this study is beyond the scope of this thesis) and monotonic loading.

4 Short-term Connection Push-out Test and Design Formulas for Strength Evaluation

This chapter has been reproduced from a journal paper submitted to the Journal of Structural Engineering (American Society of Civil Engineering, ASCE) with the title of "Experimental tests of notched and plate connectors for LVL-concrete composite beams" (Yeoh et al, 2009e).

It focuses specifically on short-term push-out test of 3 selected best connections carried out under Phase 2: (1) 300 mm long rectangular notch cut in the LVL joist and reinforced with a 16 mm diameter coach screw (termed as "lag screw" in this chapter); (2) triangular notch reinforced with the same coach screw; and (3) two 333 mm long toothed metal plates pressed in the lateral surface of two adjacent LVL joists.

The experimental procedures and results are presented exhaustively together with analytical approximations for the strength of the connections derived in accordance with New Zealand Standards and Eurocodes. Fundamental understanding of the connections' behaviour and their derived characteristic strength and stiffness values were essential for the design of the composite floor beams that have been tested in the subsequent phases, discussed in Chapters 5 and 6.

Supplementary details related to this chapter on material properties, concrete test results, push-out specimen construction details, notched connection strength evaluation analytical model and short-term connection push-out test results that are presented in the Appendices 1, 2, 3, 4 and 5, respectively.

4.1   Abstract

This chapter reports the experimental results of symmetrical push-out tests performed on notched and toothed metal plate connectors for laminated veneer lumber (LVL)-concrete composite floor systems. The characteristic shear strength and slip moduli were evaluated for three types of connectors: (1) a 300 mm long rectangular notch cut in the LVL joist and reinforced with a 16 mm diameter lag screw; (2) a triangular notch reinforced with the same lag screw; and (3) two 333 mm long toothed metal plates pressed in the lateral surface of two adjacent LVL joists. The rectangular notch was found to be very stiff and strong, and therefore inexpensive to use in composite beams. The triangular notch, although less stiff and strong, has the advantage of being easier to construct as it requires only two cuts. Also the metal plates are less stiff and strong, however the construction does not require any cut and may be preferred if industrial presses are available. The shear force-relative slips relationships are presented together with an analytical pre-peak and post-peak approximation which can be used to carry out non-linear finite element analyses of LVL-concrete composite beams. The failure mechanisms of the notched connections are also discussed. Analytical design formulas for shear strength evaluation of notched connections derived in accordance with New Zealand Standards and Eurocodes are proposed based on the possible failure mechanisms and experimental behaviour. Good approximation was found if a slight modification of the Eurocodes formulas is introduced.

4.2   Introduction

Timber-concrete composite floors consist of two parts, an upper concrete slab tied to a lower timber beam by means of shear connectors. The shear connectors transmit the shear and prevent or reduce the relative movement ('slip') between the lower fibre of the slab and the upper fibre of the timber beam depending on the efficiency of the connection. The concrete flange, mainly subjected to compression, takes advantage of the high compression strength and stiffness of concrete. The timber web, mainly subjected to tension and bending, benefits from the high tension strength to weight ratio of timber, particularly in the case of LVL. A wide range of shear connectors have been developed in the world particularly in Europe and each of these connectors varies in its rigidity and strength. Ceccotti (1995) presented a large number of fasteners that can be used to

connect the concrete slab to the timber, and sorted them in different categories in relation to their degree of rigidity. The shear strength and stiffness (or 'slip modulus') of the shear connectors at serviceability and ultimate limit state are important parameters required for the design of a timber-concrete composite floor.

Literature on timber-concrete composite connections was found as early as 1922 with a patent filed by Muller for connections formed by a system of nails and steel braces; 1939 where Schaub (1939) filed a patent of steel Z-profiles and I-profiles as interlayer connection system; and 1943 (McCullough, 1943) where connections built from different metal fasteners and pipe dowels were tested. Shear transfer devices in the form of triangular plate-spike were found to provide full composite action in a beam (Richart and Williams, 1943) while on the contrary Pincus (1970) reported that mechanical shear fastener such as nails developed less than 50% composite action between the timber and concrete T-beam. Pincus also confirmed that nails epoxied to timber were possible to achieve full composite action up to failure. Pillai and Ramakrishnan (1977) carried out connection shear tests on a series of 3-5 mm diameter nails and reported that the arrangement of the nails at an inclination of 45° with the head pointing towards the closest support resulted in higher strength and lower slip.

Fragiacomo et al (2007a) reported results of tests to failure and under sustained load of a proprietary head stud connector screwed to the timber marketed by the 'Tecnaria SpA' (www.tecnaria.it). The connector was found to perform well both in the short- and long-term. Lukaszewska et al (2008) in an effort to develop a fully demountable timber-concrete composite system with concrete slab prefabricated off-site chose seven types of connector to build 28 asymmetrical push-out specimens. Among these connectors, three were investigated for the first time: (1) a steel tube with a welded flange embedded in the concrete slab, and a hexagon head coach screw; (2) a modified steel tube with two welded flanges, and a hexagon head coach screw in conjunction with a notch cut from in timber beam; and (3) a mechanical connector consisting of a pair of folded steel plates embedded into the concrete slab and connected to the glulam beam by means of annular ringed shank nails. Due to their simplicity and inexpensiveness, the first and third connector types were used in prefabricated timber-concrete composite beams tested to failure (Lukaszewska et al, 2009a). Nailplate or toothed metal plate is another connection system

extensively used in timber construction due to the ease of assembly and reasonably good performance. Aicher et al (2003) reported tests on two series of nailplates embedded in the concrete and nailed to the timber with equal width and length dimensions of 114 × 266 mm and compared the results with timber-timber connection. The conclusion was that a nailplate used in timber-concrete composite beams is approximately 1.5 times stronger and 2.5 to 3 times stiffer than if used in timber-timber connections.

In recent years, a comprehensive investigation on timber-concrete composite connections has started at the University of Canterbury, New Zealand with the aim to develop a semi-prefabricated LVL-concrete composite systems for medium to long span floors (Yeoh et al, 2008a; Chapter 3). Research carried out and ongoing includes performance of connections and full-scale beams in the short- and long-term, susceptibility to vibrations, and tests under repeated loading behaviour of such medium to long-span floor system. The load-bearing capacity of composite systems markedly depends upon the level of composite action that is developed by the shear connectors. Since the cost and constructability of the system depends upon the ease of production of these shear connectors, it is crucial to develop connectors that are stiff and strong yet easy to manufacture and assemble. This chapter reports the outcomes of short-term (failure) push-out tests carried out on the three best connectors selected based on the outcomes of previous research (Seibold, 2004; Deam et al, 2007 and Yeoh et al, 2009c or Chapter 3). The objective of these tests was the evaluation of the characteristic strength and stiffness (also termed as slip modulus) values to be used in design of composite floors. The chapter reports the experimental program, discusses the experimental and analytical behaviour of the connectors, and presents an analytical model for the shear strength evaluation of the connectors.

4.3   Background of the short-term push-out research program

The short-term push-out research program was carried out in different phases at the University of Canterbury from year 2006 to 2008. The choice of using a notched connection reinforced with lag screw was based on early work reported by Deam et al (2007) where small LVL-concrete composite blocks incorporating different types of connectors were tested to failure and their performance compared to each other. Connectors investigated included round and rectangular concrete plugs with and without

screw and steel pipe reinforcement, proprietary (SFS) screws, lag screws with different diameters, sheet brace anchors, and framing brackets. The comparison clearly showed the best performance of the rectangular concrete plug reinforced with a lag screw. Such a connector type was then successfully implemented by Deam et al. (2008) in LVL-concrete composite beams, some of which were prestressed with unbonded tendons. Following those former investigations, Yeoh et al (2009c) carried out a parametric experimental study in order to investigate the effect of notch geometrical variations such as depth and length, presence of lag screw reinforcement, size and penetration depth of lag screw on the strength and stiffness performance (presented in Chapter 3). Factors related to the ease of production, labour and material costs were carefully considered in order to achieve an optimized notch shape that provides the best compromise between structural efficiency and labour cost. The next phase of the research, described in this chapter, commenced at the end of year 2007 where three types of connections were chosen and tested in order to evaluate their characteristic strengths and mean slip moduli at serviceability and ultimate limit states. Materials used were laminated veneer lumber (LVL), normal weight and low shrinkage concrete grade 35, obtained from a commercial batching plant, steel reinforcement and lag screws. A 3D finite element model of the selected connections using ANSYS software package (ANSYS, 2007) is currently under development at the University of Stuttgart, Germany, with the purpose to predict the strength and stiffness of the connections (Yeoh et al, 2008b).

4.4   Experimental program

The three best types of connection displayed in Fig. 4-1 were tested in shear to determine their characteristic strength and slip moduli: (1) $300l \times 50d \times 63w$ mm rectangular notch reinforced with 16 mm diameter lag screw (R); (2) $30°\_60°$ $137l \times 60d$ mm triangular notch reinforced with 16 mm diameter lag screw (T); and (3) two $333l \times 136d \times 1t$ mm staggered toothed metal plates (P) where l, d, w, and t are the length, depth, width and thickness, respectively. Nine specimens were tested per type of connection while another three specimens with the triangular notched connection were built and tested in the weak direction, i.e. with the notch inverted ($60°\_30°$) with respect to the direction of the shear force (TT).

71
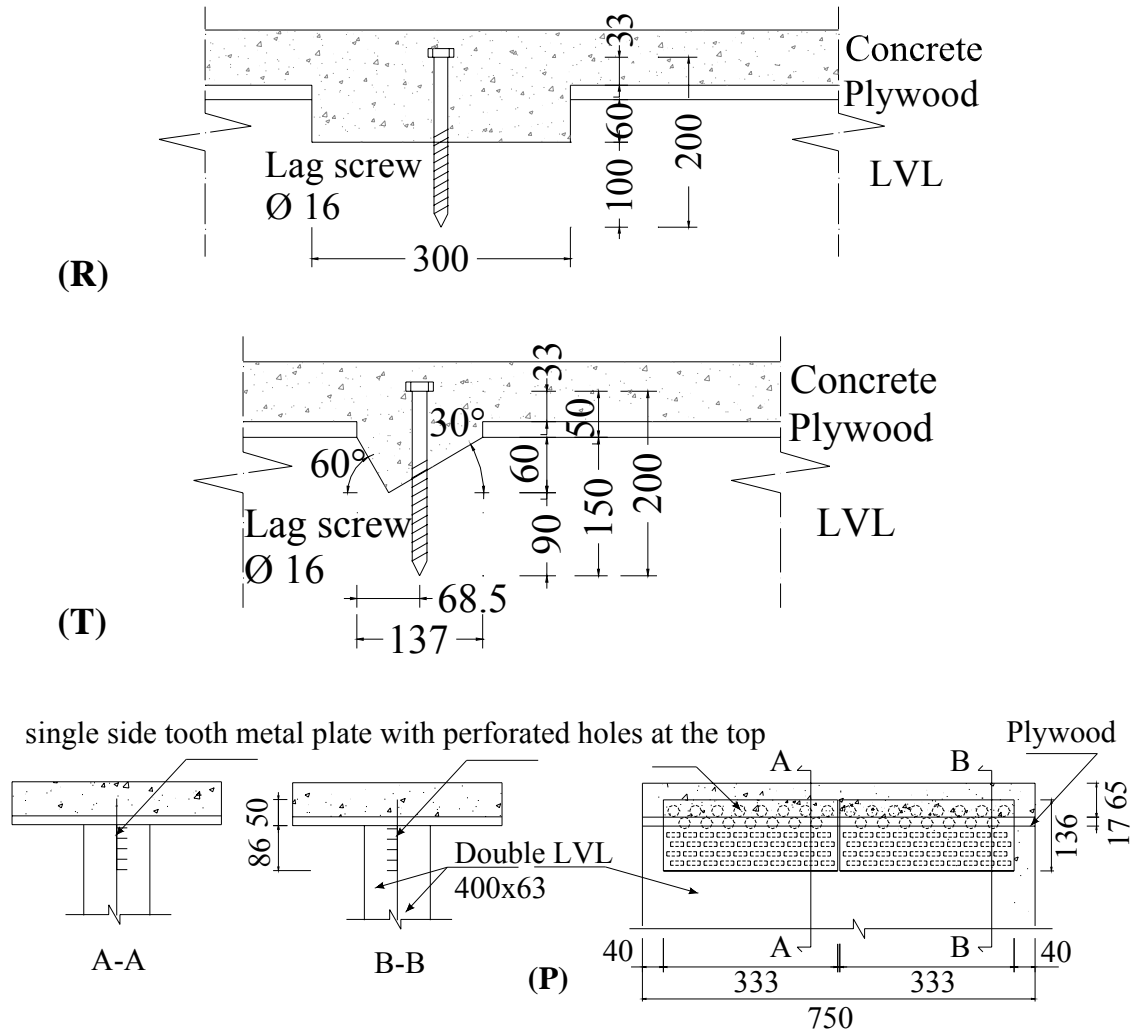
Fig. 4-1. Three types of connection (R, T, and P) tested in push-out tests (dimensions in mm)

A total of 30 specimens were constructed. Fig. 3-5 shows the test set up of the symmetrical push-out test carried out in accordance with EN 26891 (CEN, 1991) under a Universal Testing Machine. It must be pointed out that specimens R, T and TT had only one LVL joist, whereas specimens P had two LVL joists to sandwich the two toothed metal plates (see Fig. 4-1). The connections were loaded in shear and the load-slip relationship recorded using a load cell and 50 mm potentiometers P1, P2, P5 and P6 (Fig. 3-5, potentiometers P5 and P6 are at the same location as P1 and P2 but on the opposite face of the specimen). The connections were loaded at a rate of *0.2F$_{est}$* kN per minute in shear with the load applied onto the LVL web section of the specimen until the connection failed. The loading protocol requires an initial estimate of the strength of the specimen, *F$_{est}$* which was determined on the basis of experience, preliminary tests, or

calculation. This was then adjusted for the second specimen using the new actual F_{est} from the first tested specimen. The specimen was first loaded to *0.4F_{est}* and held for 30 seconds, then unloaded to *0.1F_{est}* and maintained for 30 seconds. Thereafter the specimen was loaded to failure or to a maximum slip of 20 mm, whichever occurred first. The purpose of the initial loading-unloading phase was to eliminate any internal friction in the connection, and to ensure any initial slip or slack present in the connection does not affect the final results. The slip measurements were recorded for each test specimen using potentiometers that were mounted adjacent to the connections. The slip at maximum load, F_{max}, defined as the shear strength, was also recorded.
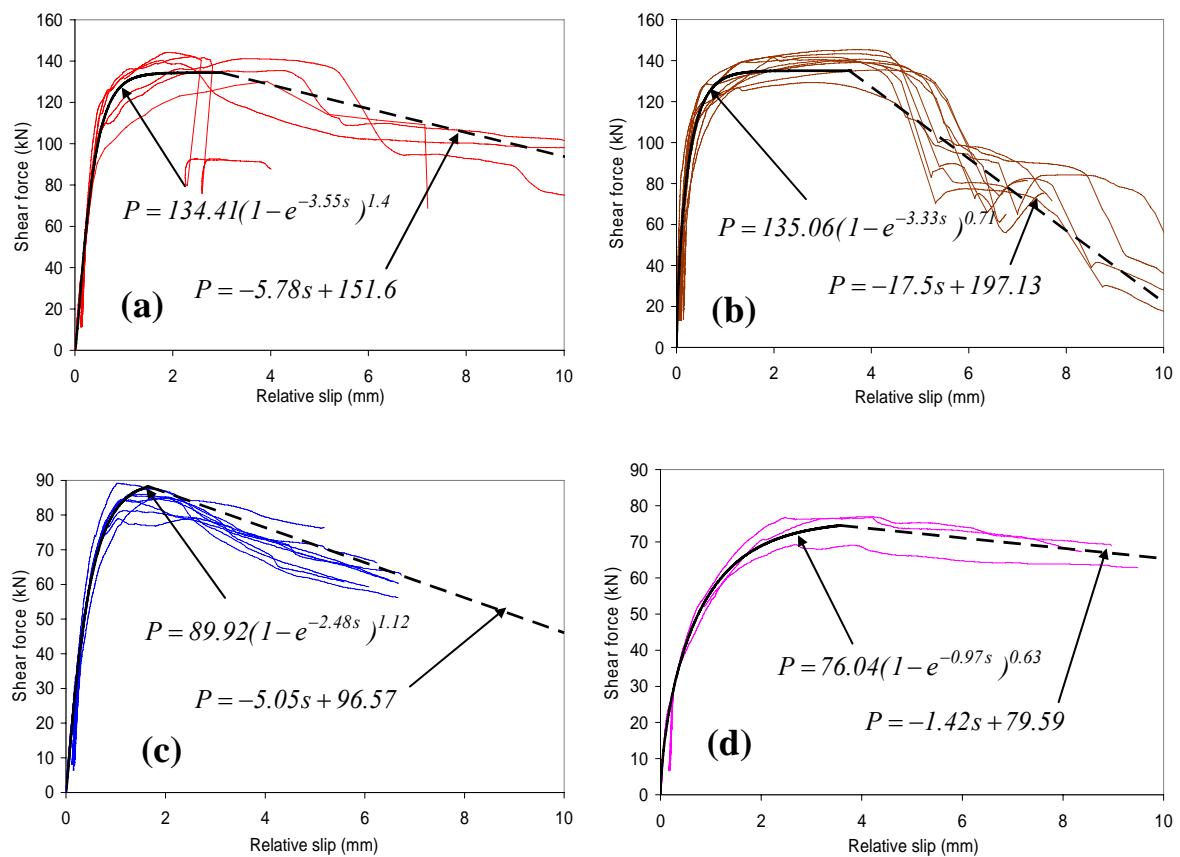
Fig. 4-2. Single connection experimental load-slip curves with analytical pre- and post-peak best-fit curves for connections (a) R; (b) P; (c) T and (d) TT

[Material properties, concrete test results, push-out specimen construction details and short-term connection push-out test results are presented in the Appendices 1, 2, 3 and 5, respectively]

73

4.5   Results

EN 26891 (CEN, 1991) provides specifications for the derivation of the connection shear strength and secant slip moduli at 40% (assumed as the serviceability limit state load level - SLS), 60% (assumed as the ultimate limit state load level - ULS) and 80% (near the collapse load level) of the shear strength. Load-slip curves are presented for all connections in Fig. 4-2. Table 4-1 shows the average values of shear strength (F_{max}) and secant slip moduli at 40% ($K_{s,0.4}$), 60% ($K_{s,0.6}$) and 80% ($K_{s,0.8}$) of the shear strength. The standard deviation (σ), coefficient of variation (CV) and characteristic strength (R_k) at 5th percentile for each tested connection are also reported. In order to provide some information on the post-peak behaviour and the type of failure (ductile or brittle), the ratio Δ_2/Δ_1 is introduced, defined as the ratio of the strength difference at peak and at 10 mm slip (Δ_2), to the strength at peak (Δ_1), reported in Table 4-1. The lower the Δ_2/Δ_1 ratio, the better the post-peak behaviour and the higher the ductility. For definition purposes, a ratio below/above 50% would be considered as a fairly ductile/brittle connection.

4.6   Discussion

4.6.1   Connection behaviour

Similar mode of failures and behaviour were observed for all the tested connections as reported in Yeoh et al (2009c) or Chapter 3. Both the rectangular and triangular notched connections failed primarily due to the shear in concrete along the shear plane while plate tearing occurred in the toothed metal plate connection (Fig. 3-10). The lag screw enhanced the post-peak behaviour of the rectangular and triangular connections as expressed by the calculated Δ_2/Δ_1 ratio (Δ_2/Δ_1 = 33.9 and 49.7% respectively) in Table 4-1 and in the shear force vs. relative slip plots (Fig. 4-2(a), (c) and (d)). On the contrary, the toothed metal plate connection exhibited a ratio Δ_2/Δ_1 = 80.7% characterized by brittle behaviour, as can be observed in Fig. 4-2(b) where a sudden load reduction after the attainment of the peak load) is evident. Such a value of the Δ_2/Δ_1 ratio disagrees with the outcomes of the preliminary tests presented in Yeoh et al (2009c) where the range of 33-44% was obtained. Such a difference could be attributed to the reduction of the plate thickness from 2 mm to 1 mm, to the use of single sided teeth instead of double sided teeth, and to the use of a two separate staggered plates instead of a continuous plate length.

Table 4-1. Shear strength and secant slip moduli values for a single connector

Type of connection $((\Delta_2/\Delta_1))$	Values	Slip moduli			Shear strength
		$K_{s,0.4}$ (kN/mm)	$K_{s,0.6}$ (kN/mm)	$K_{s,0.8}$ (kN/mm)	F_{max} (kN)
T (1-LVL) (49.7%) Low ductility	Range	128-177	122-168	94.3-140	79.0-89.2
	Ave [R_k]	146	139	116	84.8 [70.4] { 2 }
	σ (CV %)	13.5 (9.3)	12.7 (9.1)	12.1 (10.4)	3.1 (3.7)
TT (1-LVL) (12.6%) Ductile	Range	107-114	65.3-89.0	44.9-53.7	69.2-77.0
	Ave [R_k]	110	78.9	50.4	74.3 [61.7]
	σ (CV %)	3.3 (3.0)	12.3 (15.6)	4.8 (9.5)	4.4 (6.0)
R (1-LVL) (33.9%) Fairly Ductile	Range	217-286	205-282	114-259	130-144
	Ave [R_k]	247	241.4	194	139 [115] { 1 }
	σ (CV %)	27.4 (11.1)	28.0 (11.6)	51.2 (26.4)	5.2 (3.7)
P (2-LVL) (80.7%) Brittle	Range	249-590	239-511	182-363	129-145
	Ave [R_k]	464 [2]	395	257	139 [116] { 3 }
	σ (CV %)	132 (28.5)	100 (25.4)	63.1 (24.5)	5.0 (3.6)

Note: { } Strength rank for 2-LVL

Tearing of the plate was the failure mechanism detected in the toothed metal plate connection. The high slip recorded for this connection could be attributed to the progressive tearing of the plate and possibly the slippage of the teeth from the LVL (Fig. 3-10(b)). The ultimate load was reached with a relatively gradual increase of strength, due to the steel plate ductility and the reinforcement in the concrete slab. Subsequently, two load reductions were observed for almost all the tested specimens, corresponding to the progressive tearing of the first plate and then of the second plate.

The rectangular notched connection resulted in the stiffest connection with the additional benefit of a fairly ductile behaviour due to the presence of the lag screw. However, the behaviour of the specimens was not homogeneous due to the segregation of the concrete in some of the notches, and LVL shear failure in two specimens. As such, they were

disregarded in the statistical evaluation of strength and slip moduli. The triangular notched connection showed less stiffness and strength. The maximum strength and stiffness decreased whereas ductility improved when the triangular notched connection was tested in the opposite or weak direction (TT type specimens). The triangular notched connection was also found to possess a relatively stable post-peak behaviour as observed in a gradual and uniform reduction of load after failure for all the tested specimens (Fig. 4-2(c)).

4.6.2   Strength and slip moduli comparisons

In order to make a direct comparison with the toothed plate connection which had a double LVL joist, the strength and slip moduli for the rectangular and triangular notched connections (R and T) were doubled. As such, in terms of strength, the rectangular notched connection ranks the first ($115.3 \times 2 = 230.6$ kN), second the triangular notched connection ($70.4 \times 2 = 140.8$ kN) and third the toothed metal plate connection (115.6 kN) as presented in Table 4-1. The coefficient of variation for strength was found to be in the range of 3.6 to 6% hence this was an accurate determination. However the coefficient of variation for the slip moduli exceeded 10% in most cases with the plate connection having a coefficient variation between 24.5 to 28.5%. By referring to the slip modulus at serviceability limit state ($K_{s,0.4}$), the triangular notched connection ranks the last ($145.8 \times 2 = 291.6$ kN/mm), second the plate connection (463.7 kN/mm) and first the rectangular notched connection ($247.2 \times 2 = 494.4$ kN/mm). A doubled triangular notched connection exhibited a slightly higher strength than the toothed plate connection but only approximately half the slip moduli of the toothed plate connection.

The length of the notch significantly affects the shear strength of the notched connection while the presence of a lag screw maintains a good stiffness after the attainment of the serviceability limit state load level ($0.4F_{max}$) and provides ductility in the post-peak stage. The 300 mm rectangular notched connection is by far the best connection in terms of strength, slip moduli and post-peak behaviour. On the other hand, the toothed metal plate connection has the advantage of not requiring any cut of the timber, and thereby may allow the achievement of speed in construction and reduction in labour cost. Although the triangular notched connection is not as strong and stiff as the rectangular notch, it is nevertheless characterized by simpler construction which involves only two cuts of the

timber. Such connection may be preferred particularly when computer aided cutting machines are not available.

4.6.3   Influence of lag screw and length of notch on the connection performance

In order to investigate the effect of cutting a rectangular notch in the LVL, two additional push-out specimens with only lag screws and no notches were built and, tested. Comparisons were made between this connection, a 150l × 50d mm rectangular notch without lag screw, the same notch with 12 and 16 mm diameter lag screw, and a 300l × 50d mm rectangular notch with a 16 mm screw as reported in Table 4-2. The connection without a notch was the weakest in strength and stiffness while the 300 mm notch with lag screw connection was the strongest. The 300 mm notched lag screw connection was 3 times stronger and 8.5 times stiffer than the connection with just a lag screw. Hence, the importance of the concrete notch is emphasized here as a major contributor to both strength and stiffness.

Table 4-2. Comparison of mean strengths and secant slip moduli for different connectors

Type of connection	Slip moduli (kN/mm)		Shear strength (kN)
	$K_{s,0.4}$	$K_{s,0.6}$	F_{max}
ϕ16 lag screw only	28.9	6.3	46.44
150 mm notch only	105	59.3	48.3
150 mm NLS ϕ12	77.9	74.5	66
150 mm NLS ϕ16	80.2	75.4	73
300 mm NLS ϕ16	247.2	241.4	138.9

Note: NLS = Notched connection reinforced with Lag Screw

The absence of a notch brought about an approximately 80% reduction in slip modulus from 28.96 kN/mm at serviceability limit state ($K_{s,0.4}$) to 6.30 kN/mm at ultimate limit state ($K_{s,0.6}$). A 20% and 40% reduction in slip modulus at ultimate limit state ($K_{s,0.6}$) and strength respectively, was evident in the notch without lag screw with respect to the same notch reinforced with lag screw. The notch without lag screw only achieved 80% of stiffness compared to one reinforced with a lag screw. The 300 mm rectangular notch was found to be 1.9 times stronger and 3 times stiffer than the 150 mm rectangular notch. There was no significant difference in terms of strength and stiffness by changing the size

of lag screw from 16 mm to 12 mm diameter (see also Yeoh et al, 2009c or Chapter 3). Regarding the notch length, the increment of shear strength was found to be roughly linear while the increment of stiffness varied exponentially.

4.6.4   Characteristic strength

The characteristic strength of the connection is required for the design of a timber-concrete composite beam at ultimate limit state. Both the notched connection types failed by shear in the concrete, hence a ratio which relates the characteristic strength of the connection to the characteristic compressive strength of the concrete calculated using the mean strength obtained from the concrete cylinder tests is proposed. Concrete is assumed to follow a normal distribution and, because due to its homogeneity as opposed to timber, in the statistical analysis the level of confidence is assumed to be 90% (while for timber it is 75%). From the concrete compressive cylinder tests performed on 3 series of 2 cylinders (corresponding to 3 concrete castings), a *ratio coefficient* for the prediction of the characteristic strength of a notched connection is determined.

Table 4-3. Compressive strength of concrete

Cast	f_c (N/mm^2)	$f_{c,ave}$ (N/mm^2)	R (N/mm^2)	σ (N/mm^2)
1	45.14 45.65	45.39	0.51	0.45
2	46.54 48.20	47.37	1.66	1.48
3	43.61 40.80	42.20	2.81	2.50
Mean Value		44.99		1.48

The procedure is summarized in Table 4-3, where (1) Range, *R,* is the difference between the compressive strengths of the two specimens, f_c, at 28 days; (2) Standard deviation, σ, is estimated as *0.89 × R* on the basis of 2 test specimens. The characteristic compressive strength of concrete can then be calculated as $f_{c,k} = f_{c,ave} - 5.31\sigma = 37.15 \ N/mm^2$ where the coefficient *k* = 5.31 relates to the number of concrete castings (3 castings in our case) tested (Owen, 1963). Hence, the *ratio coefficient* of *0.83* is calculated by dividing the

characteristic compression strength of concrete, $f_{c,k}$, by the mean value of the compressive strength, $f_{c,ave}$. The ratio is expected to get close to 0.9 with a high number of specimens. This *ratio coefficient*, multiplied by the mean strength of the connection, provides the characteristic strength of the notched connections, R_k, presented in Table 4-1. Although the failure of the toothed metal plate connection was not triggered by shear in the concrete, the same *ratio coefficient* was conservatively used to derive the characteristic strength. These characteristic strengths can then be used for the design of timber-concrete composite beams.

Table 4-4. Analytical pre- and post-peak shear force vs. relative slip relationship for a single connector

Connector type	Pre-peak behaviour			Post-peak behaviour		Slip	
	P_{max} (kN)	α	β (mm^{-1})	a (mm)	b (kN)	s_p (mm)	s_u (mm)
TT	76.0	0.63	0.97	-1.42	79.6	3.58	10
T	89.9	1.13	2.48	-5.05	96.6	1.65	10
R	134	1.40	3.55	-5.78	1520	3.01	15
P	135	0.71	3.33	-17.5	197	3.54	10

4.6.5   Analytical approximation of the shear-slip curves, and failure mechanisms

The experimental shear force vs. relative slip curves of each connection type tested were fitted with an average analytical curve comprising of a pre-peak and a post-peak behavior (Fig. 4-2). The pre-peak behaviour is based on the nonlinear analytical model proposed by Ollgard et al (1971) and described by Eq. 4-1, whereas the post-peak behaviour is described by a linear curve with negative slope given by Eq. 4-2. The corresponding parameters are listed in Table 4-4. Such a nonlinear shear force-slip relationships can be used in advanced uniaxial finite element beam models such as that developed by Fragiacomo et al. (2004) for non-linear analyses to failure of timber-concrete composite beams, as reported by Ceccotti et al. (2006).

$$P = P_{max}(1 - e^{-\beta s})^{\alpha} \text{ for } s < sp \qquad \text{Eq. 4-1}$$

$$P = as + b \text{ for } sp < s < su \qquad \text{Eq. 4-2}$$

where s is the relative slip, s_p is the slip at P_{max}, s_u is the maximum slip at the lower end of the post-peak curve, P_{max} is the maximum load reached by the approximating curve, α, β, a and b are constants. It is important to remember that the toothed metal plate connection (P) is regarded as a double LVL while the other connections, triangular (T and TT) and rectangular notched (R) as a single LVL.

Fig. 4-3 shows the typical pre-peak and post-peak behaviour of a tested connection and Fig. 4-4 illustrates the corresponding failure mechanisms and behaviour of a notched connection. In general, a shear plane begins to form at $0.6F_{max}$ as indicated by (1) in Fig. 4-3 and Fig. 4-4. At this stage, the concrete notch began to shear and crushing of concrete occurred due to the compression of the notched connection under the force of $0.6F_{max}$. As the load reaches the peak value, the concrete notch is almost completely sheared and the compression zone of the concrete becomes very obvious. Here, the lag screw starts to carry most of the load by rope effect acting in shear and tension resulting in the formation of two flexural plastic hinges as the load decreases gradually with an increase in the slip (see (2) in Fig. 4-3, Fig. 4-4 and Fig. 4-5). The slope of the load descent highly depends upon the size of the lag screw and the depth of the penetration in the case of a notched connection.
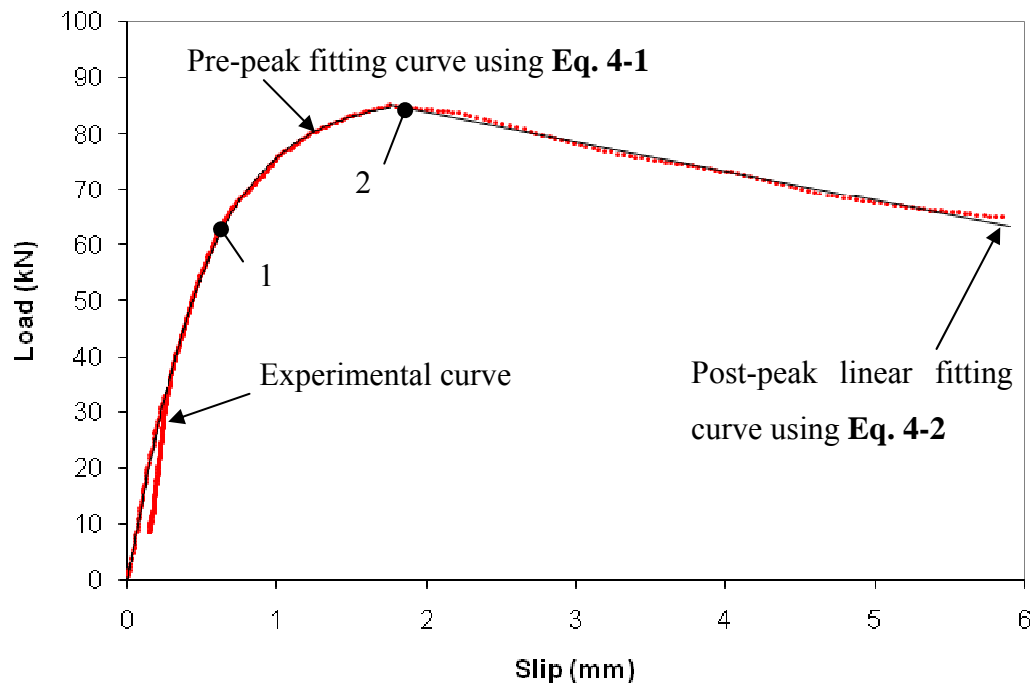
Fig. 4-3. Typical pre-peak and post-peak behaviour
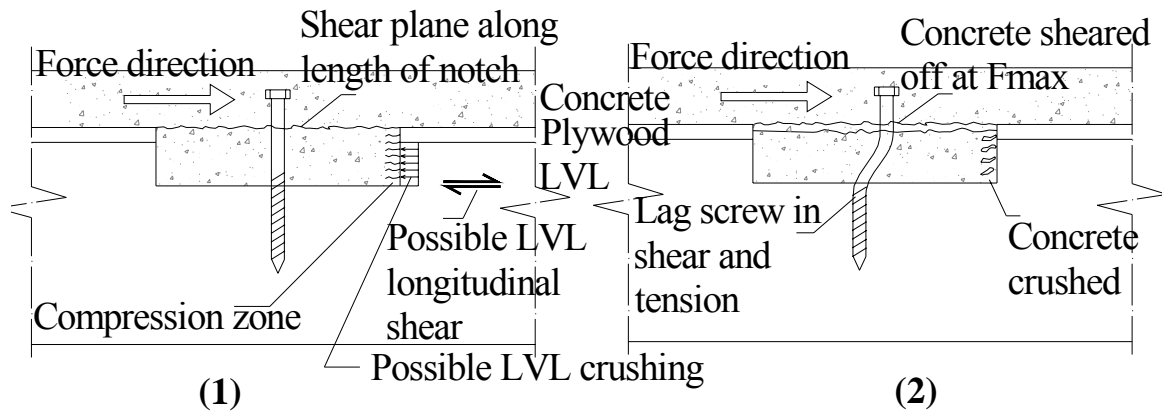
Fig. 4-4. Experimental failure mechanisms and behaviour of a notched connection reinforced with a lag screw

Fig. 4-5. (a) Formation of flexural plastic hinges in lag screw; and (b) Lag screw under tension in the direction of force

4.7   Derivation of design formulas for notched connection strength evaluation

A simplified analytical model for strength evaluation of the notched connection is proposed in Eq. 4-3 to Eq. 4-6. The notched connection is regarded as a concrete corbel protruding into the LVL joist subjected to shear coming from the shear load applied to the connection. The lag screw acts as reinforcement for the concrete corbel, and contributes to the shear transfer from timber to the concrete. The formulas were compared with the experimental results and were found to predict the failure load with acceptable accuracy in most cases. The model is based on the control of all possible failure mechanisms that may occur in the connection region (see also Kuhlmann and Michelfelder, 2006): (1) failure of concrete in shear in the notch; (2) crushing of concrete in compression in the notch; (3) failure of LVL in longitudinal shear between two consecutive notches or between the last notch and the end of the LVL beam; and (4) failure of LVL in crushing parallel to the grain at the interface with the concrete corbel, as illustrated in Fig. 4-4 and

discussed in the previous section. Analytical design formulas in accordance with New Zealand Standards and Eurocodes were derived. By comparing the outcomes from the different standards, it was found that New Zealand Standards overestimate the maximum shear strength, while Eurocodes are quite conservative with the actual experimental results in between. An alternative approach based on the introduction of a reduction factor, β^*, to be used in the Eurocodes formulas was then derived and compared with the experimental results, showing the best accuracy.

4.7.1   According to New Zealand Standards (NZS method)

The corresponding formulas, reported herein after, were derived in accordance with provisions from New Zealand Standards for both timber (SNZ, 1993) and concrete structures (SNZ, 2006). The formulas are based on the four possible failure mechanisms described above:

$$F_{conc,shear} = 0.2f_c'bl + nk_1pQ \qquad\qquad \text{Eq. 4-3}$$

$$F_{conc,crush} = f_c'A_c \qquad\qquad \text{Eq. 4-4}$$

$$F_{LVL,shear} = k_1k_4k_5f_sLb \qquad\qquad \text{Eq. 4-5}$$

$$F_{LVL,crush} = k_1f_cbd \qquad\qquad \text{Eq. 4-6}$$

where $F_{conc,shear}$ is the nominal shear strength of concrete for a notched connection reinforced with a lag screw, $F_{conc,crush}$ is the nominal compressive strength of concrete in the crushing zone, $F_{LVL,shear}$ is the nominal longitudinal shear strength of LVL between two consecutive notches or between the last notch and the end of the timber beam, and $F_{LVL,crush}$ is the compressive strength of LVL in the crushing zone. f_c' is the compressive strength of concrete, b and l are the breadth of the LVL joist and the length of notch, respectively, n is the number of lag screws in the notch, k_1 is the modification factor for duration of loading for timber, p is the depth of penetration of lag screw in the timber, and Q is the withdrawal strength of the lag screw in Eq. 4-3. A_c is the crushing zone effective area, i.e. $b \times d$ in Eq. 4-4 where d is the depth of the notch. k_4 and k_5 are

the modification factors for load sharing (taken as 1.0 for material with properties of low variability such as LVL), f_s is the LVL strength for longitudinal shear, and L is the shear effective length, i.e. the distance between two consecutive notches or between the last notch and the end of the timber beam in Eq. 4-5. f_c is the LVL compressive strength parallel to the grain in Eq. 4-6. The design value of the shear strength is obtained by using the characteristic values of material strengths f_c', Q, f_s and f_c in Eq. 4-3 to Eq. 4-6, and by multiplying the minimum among the four values reported above by the strength reduction factor, ϕ.

4.7.2 According to Eurocodes (EC method)

Based on the Eurocodes for both timber (CEN, 2004b) and concrete structures (CEN, 2004a), the shear strength of concrete for a notched connection reinforced with a lag screw when modelled as a corbel can be calculated using the following formula:

$$F_{conc.shear} = \beta 0.5 b_n l_n v f_c + n_{ef} (\phi_{cs} d_{ef} \pi)^{0.8} f_w \qquad \text{Eq. 4-7}$$

where β is the reduction factor of the shear force taken as 0.25 which corresponds to the loading distance from the edge of the support in the case of the notch treated as a corbel; b_n and l_n are the breadth of the joist and the length of the notch, respectively; v is a strength reduction factor for concrete cracked in shear, assumed as 0.516; f_c is the compressive strength of concrete; n_{ef} is the effective number of lag screws, assumed equal to the actual number of screws in the notch if they are spaced enough; ϕ_{cs} is the diameter of the lag screw, d_{ef} is the pointside penetration depth less one screw diameter; and, f_w is the withdrawal strength of the screw perpendicular to the grain. The other three failure mechanisms are governed by design equations similar to Eq. 4-4 to Eq. 4-6, the only difference being that the coefficients k_4 and k_5 are replaced by k_{sys} and k_5, which is assumed as one for LVL, and the coefficient k_1 is replaced by k_{mod}. The design value of the shear strength is then obtained by using the design values of the material strengths f_{cd}, f_{wd}, etc., which are obtained by dividing the characteristic values by the material strength coefficients, γ, in the design equations, and by taking the minimum of the four values of design strength strengths so obtained.

4.7.3   Reduction factor, β^* method (EC* method)

A new reduction factor, β^*, given in Eq. 4-8, was introduced as to replace the existing reduction factor, β in Eq. 4-7 in order to account not only for the loading distance but also for the length of the notch, l_n, which was found to have a significant effect in the experimental tests, and the diameter of the lag screw, ϕ_{cs}. This method was found to be in close proximity with the experimental mean strength values.

$$\beta^* = \frac{l_n - 2\phi_{cs}}{2l_n}$$
Eq. 4-8

Table 4-5 provides a comparison of the experimental mean strength for the rectangular and triangular notched connections with the three analytical strength evaluation methods. For all connector types, the governing design formula was found to be Eq. 4-3 and Eq. 4-7 for concrete shear, which agrees well with the failure mechanism detected in the experimental tests. The EC method was found to be the more conservative than the NZS method while the EC* method shows a prediction very close to the experimental outcomes in all the cases.

Table 4-5. Experimental-analytical comparison of connector shear strength

Type of connection	Mean strength (kN)			
	Experimental	Analytical method		
		NZS	EC	EC*
TT	74.3	94.0	70.7	83.4
T	84.8	94.0	70.7	83.4
R	139	186	99.1	140

[Notched connection strength evaluation analytical model calculation are presented in Appendix 4]

4.8   Conclusions

This chapter reported the outcome of experimental push-out tests carried out on three connector types for LVL-concrete composite beams. The connectors were 300l × 50d × 63w mm rectangular notches cut in the LVL and reinforced with a 16 mm diameter lag

screw, 30°_60° × 137*l* × 60*d* mm triangular notches reinforced with the same diameter lag screw, and two 333*l* × 136*d* × 1*t* mm toothed metal plates pressed on the lateral surface of the LVL joist, where *l*, *d*, *w*, and *t* are the length, depth, width and thickness, respectively. The aim of the push-out tests was to determine the characteristic values of the shear strength, and the mean values of the slip modulus, which are important design properties. To this purpose, 30 symmetric push-out specimens were constructed and tested to failure. It was found that the length of the notch significantly enhances the strength performance of the connection while a lag screw improves the slip modulus at ultimate limit state, the post-peak behaviour, and enables a more ductile failure to take place. The 300 mm notch reinforced with a lag screw is 3 times stronger and 8.5 times stiffer than a connection without a notch but just with the lag screw; 1.9 times stronger and 3 times stiffer than a 150 mm reinforced notch connection. The 300 mm long rectangular reinforced notch connection stands out as the best connection among those tested due to the high strength and slip moduli, while the 2 × 333 mm toothed metal plate connection appeared to be the most practical and labour cost effective since it does not involve any notching. However, this connection system requires a readily available hydraulic press of industrial size for this system to be used in floor construction. On the other hand, the triangular notch reinforced with a lag screw has the advantage of easier and faster construction requiring only two cuts. Neither of the notched connections exhibited a brittle failure due to the use of the lag screw, whereas a brittle failure was observed in the toothed metal plate connection characterized by tearing of the plate.

Analytical pre-peak and post-peak approximations for the load-slip relationship of three selected connections were presented and related to the failure mechanism and behaviour of the connections. Considering all possible failure mechanisms, analytical formulae for the strength evaluation of the notched connection were derived according to New Zealand Standards and Eurocodes. The formulas were found to predict the experimental failure load with acceptable accuracy in all cases, with the closest agreement achieved when a new reduction factor was introduced in the Eurocodes formulas to take into account the length of the notch and the diameter of the lag screw. The failure in the notched connections is primarily due to shearing of the concrete in the shear plane. Therefore the characteristic strength of the three selected connections was calculated using a ratio coefficient of 0.83 derived statistically from the cylinder compressive strength test results.

5   Short-term Collapse Test on Beams

This chapter has been reproduced from a journal paper submitted to the Engineering Structures (Elsevier) entitled "Experimental behaviour of LVL-concrete composite floor beams at strength limit state" (Yeoh et al, 2010).

Four types of connection tested and selected in Chapters 3 and 4 were used in the design and construction of eleven 8 and 10 m floor beams. This chapter discussed the outcomes of short-term tests on these beams tested under 4-point bending carried out in Phase 4 of the experimental framework. The design method and calculation example are presented exhaustively in Chapter 7. Long-term test of connections and another three 8 m beams under sustained load are given in Chapter 6.

Supplementary to this chapter are Appendix 6 which contains photographs of the construction of short-term beams, and Appendix 7 which contains photographs and experimental graphs of short-term beam tested to collapse.

5.1   Abstract

This chapter reports the outcomes of short-term collapse tests performed on eleven LVL (laminated veneer lumber)-concrete composite floor T-beams. Different variables such as span length (8 and 10 m), connection and concrete type, and design level (well- and under-designed) in terms of connector numbers were investigated. During the tests, mid-span deflection, connection slips and strains were measured. Connection types investigated include triangular and rectangular (150 mm and 300 mm long) notches cut in the timber and reinforced with a coach screw, and modified toothed metal plates pressed on the edge of the LVL joists. All of the beam specimens were designed using the effective bending stiffness or γ-method according to Annex B of Eurocode 5. The same method was used for an analytical-experimental comparison of the beams performance at ultimate (ULS) and serviceability (SLS) limit state. All well-designed beams exhibited more than 95% degree of composite action even though only few connectors (e.g. six 300 mm long notches on the 8 m span beam) were used. Their ULS and SLS live load capacity was found to be approximately 0.9 times to that of a full composite beam. A 15% increment correction factor to the deflection or a 13% reduction to the effective bending stiffness calculated using the transformed section method can be proposed for all well-designed beams, i.e. beams designed using the γ-method according to Annex B of Eurocode 5. Although the γ-method was found to significantly underestimate the maximum imposed load at ULS, it provided an accurate prediction of the deflection in the short-term. In terms of connection type, the best performance was achieved using the 300 mm rectangular notches, which exhibited high stiffness and strength even beyond the ULS load level and, therefore, less number of connectors along the beam. The triangular notch is another viable alternative which require more connectors but is easier and faster to cut. Metal plate connectors are practical in construction but the beam stiffness was found to rapidly deteriorate beyond the ULS load level.

5.2   Introduction

Timber-concrete composite (TCC) systems are a construction technique used for strength and stiffness upgrading of existing timber floors and new construction such as multi-storey buildings and short-span bridges. By combining two different materials it is possible to exploit their best qualities since the timber is positioned in the tension region

of the composite section while the concrete is used in the compression region. The presence of timber, due to its lower density in comparison with reinforced concrete, decreases the weight of this flooring system, implying several advantages over reinforced concrete floors such as higher efficiency in terms of load carried per self-weight, better seismic performance, and lower carbon footprint. The concrete topping increases the thermal mass and fire resistance, improves the acoustic separation, and enhances the in-plane rigidity, very important in seismic regions, compared to an only-wood floor. All the aforementioned advantages can be achieved only if the composite system is structurally effective by means of a stiff and strong shear connection system. A wide range of connection systems is available, each with different level of rigidity (Ceccotti, 1995). Seven types of connectors were tested in shear by Lukaszewska et al. (2008), out of which the best two systems were used to build five fully prefabricated TCC floors tested to failure under 4-point bending (Lukaszewska et al, 2009a and Lukaszewska, 2009).
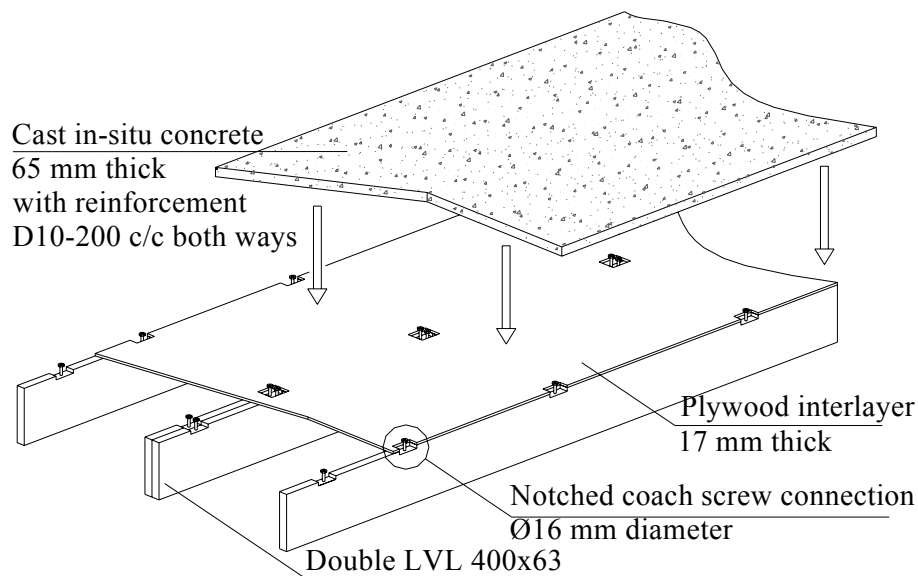
Fig. 5-1. Proposed semi-prefabricated LVL-concrete composite system

A semi-prefabricated LVL-concrete composite system has been developed at the University of Canterbury, New Zealand, comprising of "M" section panels built with laminated veneer lumber (LVL) beams acting as floor joists and a plywood interlayer as permanent formwork (Fig. 5-1). The panels can be prefabricated off-site and then transported to the building site, craned into position and connected to the main frame with specially designed joist hangers (Yeoh et al, 2009a and Smith et al, 2009). Steel mesh is

88

laid above the panels to provide shrinkage control for a 65 mm thick cast in-situ concrete slab. The panels can be propped while the concrete cures or alternatively pre-cambered to minimise deflection. The connection system has notches cut from the LVL joist and reinforced with a coach screw to increase the shear strength and provide more ductile behaviour. These notches are cut in the beams before the plywood interlayer is nailed on. The outcomes of the experimental push-out test carried out on different shear connectors can be found in Yeoh et al (2009e) and Deam et al (2007), whilst tests to failure of TCC beams prestressed with unbounded tendons are discussed in Deam et al (2008). The design of LVL-concrete composite system is discusses at length in Yeoh et al (2009a).

This chapter reports the outcomes of the experimental tests to failure performed on eleven full-scale T-beams representative of semi-prefabricated LVL-concrete composite floor strips. The specimens were 8 and 10 m long, and had different connection systems. The experimental results are critically discussed and compared with an analytical design method which accounts for the flexibility of the connection system.
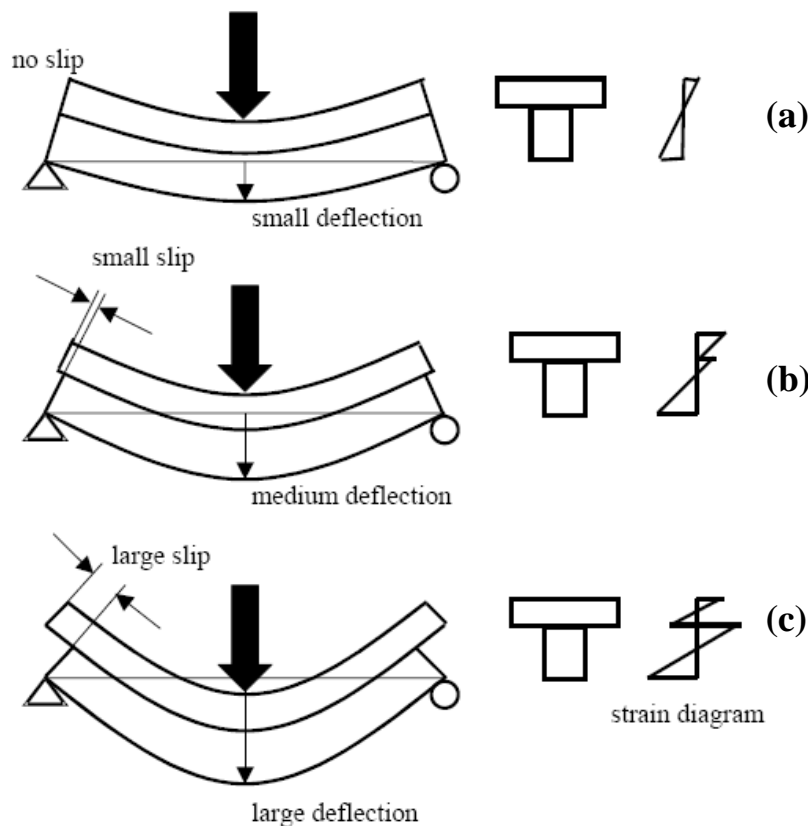
Fig. 5-2. Flexural behaviour of composite beam: (a) full composite action; (b) partial composite action; (c) no composite action

5.3   Concept of composite action

The interconnection of a timber beam web member with an upper concrete flange produces a degree of composite action which is illustrated in Fig. 5-2. Two extreme limits of stiffness can be identified: (1) a lower limit, termed as 'no composite action' where there is no horizontal shear force transfer between the two layers resulting in large interlayer slip and deflection; (2) an upper limit, termed as 'fully composite action' where there is complete shear force transfer between the two layers resulting in zero interlayer slip and small deflection. The flexural behaviour of a real composite system is usually intermediate between these two limits and termed as 'partial composite action'. In this case, the amount of interlayer slip and deflection in the composite beam highly depend upon the strength and stiffness of the interlayer connection system.

The degree of composite action (DCA) quantified as percentage is given in Eq. 5-1, where ΔN, calculated theoretically, signifies the deflection of the composite beam with no connection (lower limit); ΔR, calculated theoretically, signifies the deflection of the composite beam with fully rigid connection (upper limit); and ΔF, measured experimentally, signifies the deflection of the composite beam with the actual flexible connection (Gutkowski et al, 1999).

$$DCA = \frac{\Delta_N - \Delta_F}{\Delta_N - \Delta_R} \times 100$$

Eq. 5-1

Maximising the *DCA* is important to increase the stiffness and the strength of the composite beam. This may require, however, the use of many connectors, leading to a system which might be uneconomical. A right compromise between structural efficiency and cost must therefore be found. The desired characteristics for the proposed semi-prefabricated LVL-concrete composite system are: (1) medium to long span, from 6 to 12 m; (2) minimum number of connectors, so as to minimize construction cost; (3) high *DCA*; and (4) acceptable deflection in the long-term. The choice of a strong and stiff connection is therefore crucial to achieve the aforementioned requirements, since the stiffer the connection, the lesser the deflection of the composite system. Very stiff connections, in fact, ensure a complete composite action of timber beam and concrete slab, with little or no slip at the interface beam-concrete interface and small deflection.

5.4   Experimental programme

5.4.1   Beam specimens

The 'M' section semi-prefabricated LVL-concrete composite system had 2400 mm breadth and was built with a single 400 × 63 mm LVL joist on each outer edge and a double LVL joist in the centre (Fig. 5-3a). Such M section was reduced to the inner 'T' section made from the double LVL joist with a 1200 mm wide flange shown in Fig. 5-3a within dashed lines and in Fig. 5-3b. This 'T' section was further scaled down to a single LVL joist with a 600 mm wide flange for the test beams (Fig. 5-3c). Each beam specimen was designed and constructed by varying a number of parameters: (1) the type of connection, (2) the number of connectors, (3) the span length, (4) the type of construction, and (5) the type of concrete. Construction variables include the number of days the prop was left in place at mid-span (0, 7 and 14 days), and whether the notches were cast at the time of the concrete placement or grouted 7 days later (in the case of beam A2, see Table 5-1).
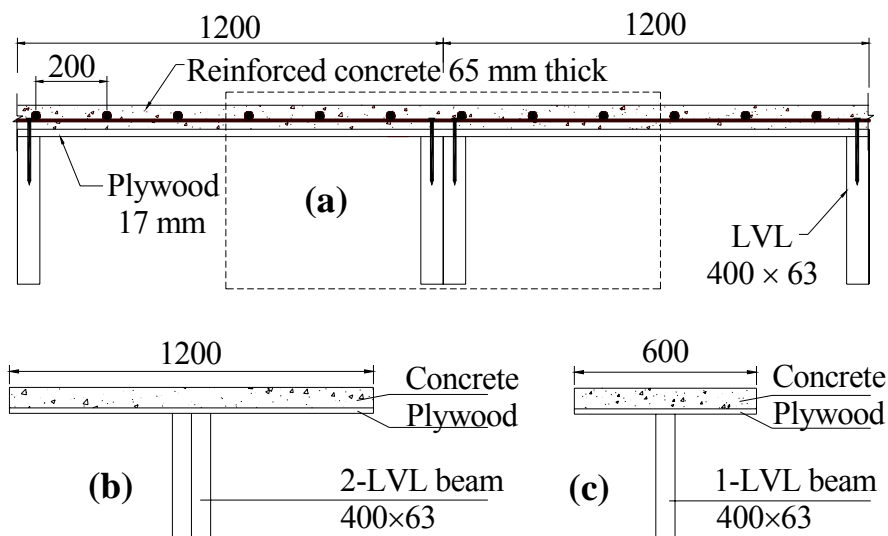
Fig. 5-3. (a) Semi-prefabricated "M" section panel; (b) Reduced T-section; (c) Further reduced T-section (dimensions in mm)

Eleven beam specimens of 8 and 10 m span were designed, built and tested to collapse under four-point bending load. Table 5-1 provides a description of the floor beams. Beam G1 was a reference beam built from double LVL joists and 1200 mm wide flange (Fig. 3b) while all other beam specimens had a further reduced section of a single LVL joist and 600 mm wide flange (Fig. 3c). Beam F1 with toothed metal plate connection was an exception as it required two LVL joists to sandwich the plates leading to a double LVL

section with 1200 mm flange (Fig. 3b). Eight beams (A1, A2, B1, B2, C2, E1, E2, G1) were constructed indoor while three beams (C1, D1, F1) outdoor. Beams A1, B1, B2 and C2 were first subjected to the quasi-permanent service load *G + 0.4Q* according to the AS/SNZ (2002) for 3 months prior to collapse test which was part of a separate long-term behaviour investigation (Yeoh et al, 2009c or Chapter 3). Beam A2 was cast with pocket notches which were grouted on day 7 with high strength low shrinkage SIKA 212 grout (SIKA, 2008). The prop on this beam was removed at day 11 (which was 3 days after pocket grouting) as grout was assumed to have achieved sufficient strength according to manufacturer's specifications.

[Construction of short-term beams in the form of photographs are given in Appendix 6]

Table 5-1. Description of beam specimens tested to collapse

Beam specimen	Span in m {Flange breadth in mm}	Number and type of connectors	Design level	Time the prop was left in place
A1 (indoor)	8 {600}	6-R150	Under	7d
A2 (indoor)	8 {600}	6-R150	Under	10d
B1 (indoor)	8 {600}	10-R150	Well	7d
B2 (indoor)	8 {600}	10-R150	Well	7d
C1 (outdoor)	8 {600}	10-T	Well	7d
C2 (indoor)	8 {600}	10-T	Well	No
D1 (outdoor)	8 {600}	6-R300	Well	7d
E1 (indoor)	10 {600}	6-R300	Under	7d
E2 (indoor)	10 {600}	6-R300	Under	7d
F1 (outdoor)	8 {1200}	8-P	Under	7d
G1 (indoor)	8 {1200}	10-R150	Well	7d

Four types of connectors (Fig. 5-4) were used to construct the composite beam specimens: (1) Rectangular notches 150 mm long reinforced with a coach screw (R150); (2) Rectangular notches 300 mm long reinforced with a coach screw (R300); (3) Triangular notches reinforced with a coach screw (T); and (4) Modified toothed metal plates pressed in the edge of the LVL joist (P). Such connectors were chosen based on the outcomes of a parametric experimental study which included push-out tests to failure carried out on 15 different connector types (Yeoh et al, 2009c). The average and characteristic shear

strengths, R_m and R_k, and secant slip moduli $K_{0.4}$, $K_{0.6}$, and $K_{0.8}$ at 40%, 60% and 80% of the collapse shear load, respectively, are given in Table 5-2 as a result of the push-out tests to failure carried out on the four connector types (Yeoh et al, 2009e).
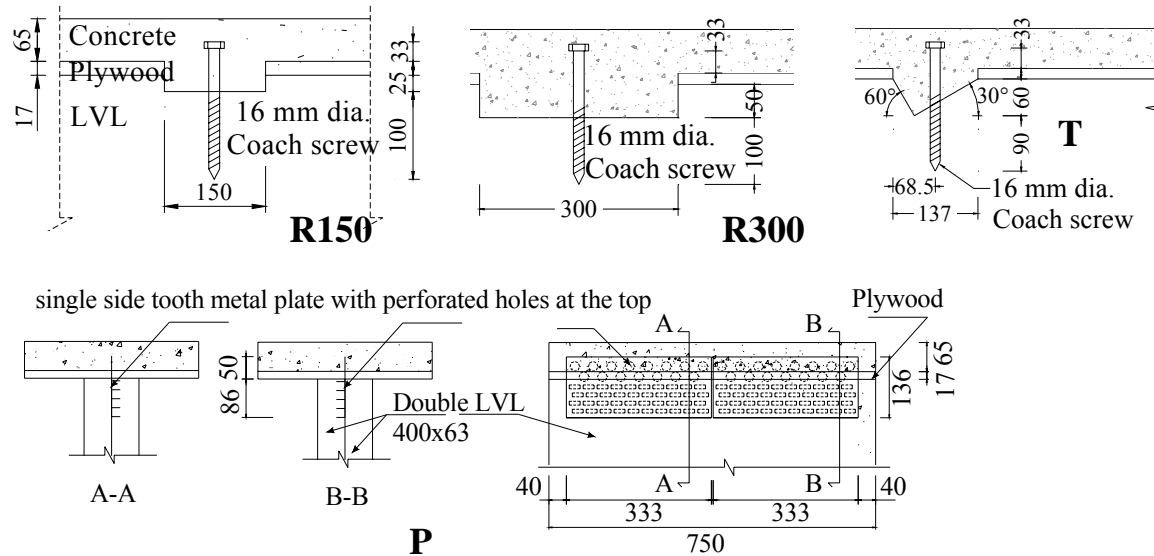
Fig. 5-4. Four types of connectors used to construct the composite beam specimens (dimension in mm)

Table 5-2. Average shear strength and secant slip moduli values for a single connector (Yeoh et al, 2009e or Chapter 4)

Type of connection	Secant slip moduli (kN/mm)			Shear strength (kN)	
	$K_{0.4}$	$K_{0.6}$	$K_{0.8}$	R_k	R_m
R150 (1-LVL)	80.2	75.4	61.7	60.6	73
T (1-LVL)	146	139	116	70.4	84.8
R300 (1-LVL)	247	241	194	115	139
P (2-LVL)	464	395	257	115	139

All of the beams were designed at ultimate (ULS) and serviceability (SLS) limit state in accordance with the design procedure suggested by Ceccotti (1995). This procedure, also known as the 'γ-method', is based on the use of the formulas for composite beams with flexible connections provided by the Annex B of the Eurocode 5 (CEN, 2004b) for the evaluation of the effective bending stiffness. Such a quantity is calculated using the secant slip moduli $K_{0.4}$ and $K_{0.6}$ for ULS and SLS verifications in the short-term, respectively. For verifications in the long-term, the effect of creep is accounted for by dividing the elastic moduli of concrete and LVL, and the slip modulus of the connector, by one plus

the corresponding creep coefficient, as described at length in Yeoh et al (2009a) or Chapter 7. The characteristic shear strength R_k is used for ULS verifications of the connection. For each beam configuration, two different numbers of connectors were identified. Such numbers correspond to two design levels: well- and under-designed, depending on whether all design inequalities at ULS and SLS are satisfied or not. The most critical design criterion for the well-designed beams was SLS in the long-term, followed by shear strength of connection at ULS in the short- and long-term. In the under-designed beams, the demand of shear force in the most stressed connector was about 30% more than the design resistance at ULS in the short- and long-term. An imposed load Q of 3 kN/m^2 for office buildings and a total permanent load $G = G_1 + G_2$ of 3 kN/m^2, with G_1 and G_2 signifying the self-weight and the superimposed permanent load, assumed as 2 and 1 kN/m^2, respectively. The purpose for the variations in the design level was to investigate the actual strength and composite action achievable by the beam specimens, and to verify the accuracy of the analytical γ-method used in design.

5.4.2   Materials

Three different types of concrete were carefully selected as shrinkage was expected to induce significant deflection on the composite beam in the long-term due to the high stiffness of the connection. A commercially available low shrinkage concrete (CLSC) was used for all the beams apart from beam B2 which was built using a special low shrinkage concrete (SLSC) and beam E2 where normal weight concrete (NWC) was used. Both CLSC and NWC were supplied by a commercial batching plant. The CLSC specifications given to the supplier were: 35 MPa characteristic strength, 650 microstrain shrinkage at 28 day with Eclipse admixture, 13 mm size aggregate and 120 mm slump workability. The SLSC was batched in the laboratory with a 35 MPa characteristic strength mix design using limestone aggregates which produced a lower drying shrinkage. The NWC was a 25 MPa characteristic strength concrete accepted from other existing job.

Concrete material testing such as slump test, cylinder compressive strength test and drying shrinkage test were conducted based on NZ3112 (SNZ, 1986) for each batch of concrete used. Some CLSC specimens had more than 120 mm slump. This compromise was accepted in order to reflect the actual construction scenario in the research. Fig. 5-5 shows a comparison of the shrinkage measured on the different concrete mixes and their

slump. A significant part of the shrinkage occurred in the first 50 days after casting. It is evident that concrete mixes with high slump have also high shrinkage. The mean values of these quantities are summarised in Table 5-3. The average compressive strength of CLSC at 28 day and at the day of beam test were 44.31 MPa and 53.74 MPa, with a coefficient of variation of 8.22% and 7.58%, respectively. The measured average density of CLSC was 2405 kg/m^3 while the average Young's modulus at the day of beam test can be estimated as 33.40 GPa based on NZS 3101 equation (SNZ, 2006).
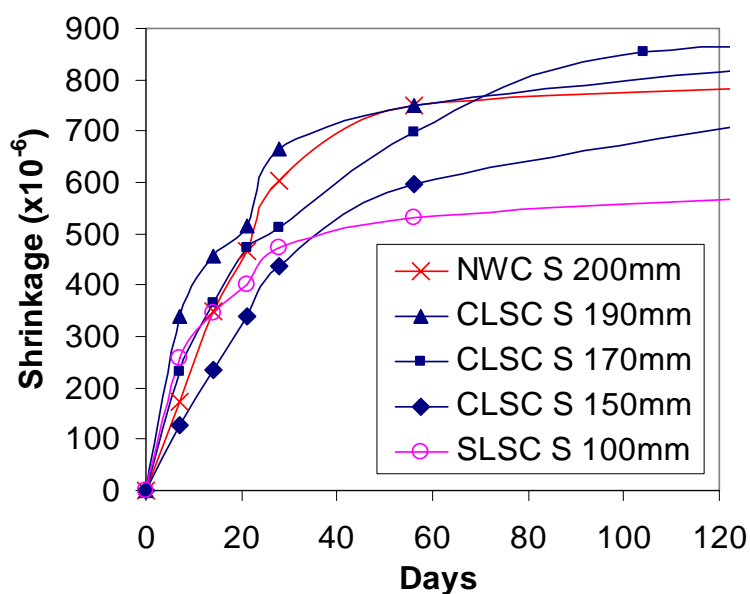
Fig. 5-5. Shrinkage of concrete mixes with different slump (S)

Table 5-3. Experimental mean properties of concrete

Beam specimens	Concrete type	Slump (mm)	Shrinkage at 28d ($\times 10^{-6}$)	Compressive strength (MPa)	
				At 28d	At day of beam test
A1, A2, B1, C2	CLSC G35	150	436	49.6	58.0
C1, D1	CLSC G35	170	512	42.6	54.4
E1, G1	CLSC G35	190	667	41.5	48.2
F1	CLSC G35	220	-	43.4	54.4
B2	SLSC G35	100	474	28.0	38.8
E2	NWC G25	200	602	25.4	31.0
Pocket	SIKA 212		394	-	80.3

The LVL used was 400×63 mm Truform recipe with mean Young's modulus of 11.34 GPa (CHH, 2007a). For LVL members subjected to combined bending and tension, which is the case for the LVL joists in a composite floor, a strength domain given by Eq. 5-2 can be assumed (CEN, 2004b and Buchanan, 1986):

$$\left(\frac{\sigma_b}{f_b}\right) + \left(\frac{\sigma_t}{f_t}\right) \leq 1 \qquad \text{Eq. 5-2}$$

where σ_b, σ_t signify the flexural and tensile stress component due to the load (strength demand), and f_b, f_t signify the bending and tensile strength of LVL, respectively (strength capacity). Eq. 5-2 can be manipulated so as to express the inequality in terms of maximum tensile stress in the bottom fibre of the LVL beam:

$$\sigma_{max} = \sigma_b + \sigma_t \leq f_m(M/N) = \frac{1 + \dfrac{\sigma_t}{\sigma_b}}{\dfrac{f_t}{f_b} + \dfrac{\sigma_t}{\sigma_b}} f_t \qquad \text{Eq. 5-3}$$

where σ_{max} and f_m signify the strength demand and strength capacity, respectively. The average strength capacity f can be calculated by assuming the average values of f_b and f_t for LVL, estimated as 46.84 MPa and 33.38 MPa, respectively, on the basis of the statistical properties measured by the manufacturer on small test specimens as corrected for size effect (CHH, 2007b). The stress ratio σ_t/σ_b depends on the M/N ratio in the LVL joist, which is affected by the stiffness ratios between concrete and timber, and by the slip modulus of the connection system. Using the γ-method for each tested beam, the stress ratio σ_t/σ_b was found in the range from 0.773 to 0.906. By substituting those values inside Eq. 5-3, a mean LVL strength f_m of 39.45 MPa was obtained for the beam specimens under investigation.

[Material properties and concrete test results are presented in the Appendices 1 and 2, respectively]

5.4.3   Experimental setup

All beams were tested approximately at 4 to 5 months from construction. Every beam was simply supported and subjected to four point bending test to failure using a 400 kN static ram under displacement control (Fig. 5-6). The loading protocol followed during the test

was similar to that recommended for connection testing (CEN, 1991). The beam was first loaded to 0.4F_{est}, held for 30 seconds, unloaded to 0.1$F_{es}t$, held for 30 seconds and finally loaded up to the collapse of the beam at a constant rate of 0.2$F_{es}t$ per minute, $F_{es}t$ being the estimated failure load of each composite beam predicted first hand using the γ-method. The load applied on the beam (*2P*) and deflection at mid-span (*Δ$_{max}$*) were measured for every beam. The relative slip between concrete slab and LVL beam (*ΔH*) was measured at every connection location. During the test, the following observations were made: (1) presence of visual cracks in the connections; (2) time and level of load when the first crack was detected either by hearing or visually; (3) nature and mode of failure; and (4) condition of connection prior to failure and after collapse.
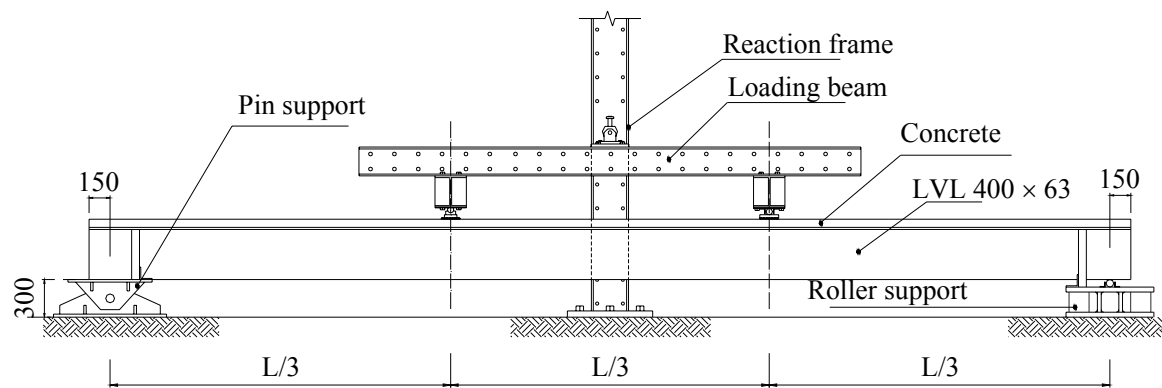
Fig. 5-6. Typical four point bending test set-up (dimensions in mm)

Fig. 5-7. Different types of failure mechanisms detected in the composite beams: (1) fracture in tension of LVL; (2) failure for concrete shear and crushing in 300 mm rectangular notch coach connection

[Photographs and experimental graphs of short-term beam tested to collapse are presented in Appendix 7]

5.5   Results and discussion

Two types of failure mechanisms were detected: (1) fracture in tension of LVL under loading points at one-third of the span (Fig. 5-7a) with no apparent sign of failure in connections, for well-designed beams; and (2) for under-designed beams, failure of connection in shear and/or crushing of concrete with plasticization of the coach screw in the case of notched connections (Fig. 5-7b), or plate tearing in the case of metal plate connections. The failure pattern of notch connectors was similar to that detected in push-out tests (Yeoh et al, 2009e or Chapter 4) where concrete strength was found to significantly influence the shear strength of the connection and, therefore, the load-bearing capacity of the composite beam. In most cases, the first crack sound was heard at approximately 60% of the collapse load F_{max} indicating the start of connection yielding which was followed by further plasticization as the screeching sound became louder. The failure hierarchy observed for under-designed beams was as follows: (1) crack sound in one or multiple connections as an early warning; (2) failure of the first connector, usually near the support; (3) consecutive failures of the other connectors moving towards the middle of the beam due to redistribution of the shear force; (4) when all connectors have failed, the load is resisted only by the LVL beams with zero composite action and final fracture of LVL in tension.

The results of the tested beams are summarized in Table 5-4. Several beams were not tested to complete destruction to enable vibration tests to be performed, which was a study under a separate project. The maximum or collapse total load, F_{max}, corresponding to the resultant of the points load, $2P_c$, and the maximum mid-span displacement at collapse, Δ_{max}, are reported in Table 5-4. The total load-midspan deflection curves are displayed in Fig. 5-8 for all the beams where the F_{max} values for single LVL beams were doubled to allow immediate comparison with the double LVL beams with 1200 mm concrete flange width. In the same figure, also the upper limit of a full composite beam, the lower limit of no composite beam, and the case of only LVL beams with no concrete slab were plotted.

Table 5-4. Summary of collapse TCC floor beam results

Beam	F_{max}	M_{exp}	w_{eq}		Δ_{max}	$K_{fi,beam}$	Load (kN)		DCA_{SLS} (%)		
	$2P_c$		Exp.	Anal			ULS	SLS	Exp	Anal	Ratio
	kN	kNm	kN/m	kN/m	mm	kN/mm	$2P_u$	$2P_s$		$K_{0.4}$	Exp/Anal
A1s i	87.3	116	14.6	8.28	64.1	1.36	46.4	30.9	86.8	96.5	0.90
A2s*i	75.3	100	12.5	8.28	63.2	1.19	40.0	26.7	90.1	96.5	0.93
B1s*i	105	140	17.5	11.3	63.1	1.67	72.2	48.1	97.3	97.8	0.99
B2s i	97.5	130	16.3	11.3	73.8	1.53	67.0	44.6	96.2	97.8	0.98
C1s o	89.7	119	15.0	12.9	58.3	1.54	61.6	41.1	95.5	98.0	0.98
C2s*i	110	147	18.3	12.9	66.7	1.65	75.5	50.4	96.1	98.0	0.98
D1s*o	80.8	108	13.5	13.6	48.1	1.68	55.5	37.0	96.3	98.4	0.98
E1s i	79.6	133	10.6	7.65	93.8	0.85	42.3	28.2	99.9	98.8	1.01
E2s i	55.4	92.3	7.38	-	66.9	0.84	29.4	19.6	98.9	98.8	1.01
F1d*o	174	232	28.9	15.5	95.6	1.82	92.2	61.5	98.1	98.7	0.99
G1d i	201	268	33.5	22.5	69.4	2.90	138	92.0	96.6	97.1	0.99

* indicates beams not tested to complete destruction to allow for vibration tests; s for single LVL 600 mm wide flange; d for double LVL 1200 mm flange; i for beams constructed indoor; o for beams constructed outdoor.

The experimental equivalent uniformly distributed load, w_{eq}, in kN/m was calculated by equating the experimental maximum bending moment such that $wL^2/8 = (2P_c)L/3$. The corresponding w_{eq} analytical value was calculated using the γ-method (Ceccotti, 1995) with connection secant slip moduli of $K_{0.6}$. The load w_{eq} is defined as the maximum load such that all LVL, concrete and connection pass the short-term verifications at ULS. The mean values of mechanical properties (modulus of elasticity and strength) of materials were used in the analytical prediction of w_{eq} to compare it with the experimental value. The experimental final beam stiffness, $K_{fi,beam}$, was calculated at the maximum or collapse load, F_{max}.

The derivation of load at ULS depends on the experimental failure mechanism. Based on the experimental maximum or collapse load, F_{max}, the ULS load was estimated using the formula (Ceccotti et al, 2006) $2P_u = (f_d/f_m) \times 2P_c \times k_{mod} = 0.687(2P_c)$ for beams with fracture tensile failure (in the case of well-designed beams) or $2P_u = (R_k/R_m) \times 2P_c \times k_{mod}/\gamma_M = 0.531(2P_c)$ for beams with connection shear failure (in the case of under-

designed beams). The SLS load was estimated by $2Ps = 2P_u/\gamma_Q = 0.458(2P_c)$ for well-designed beams and $0.354(2P_c)$ for under-designed beams. The properties were assumed as follows: LVL design strength, $f_d = 33.85$ MPa (from Eq. 5-3, assuming the design values of f_t and f_b provided by the manufacturer); LVL mean strength, $f_m = 39.45$ MPa; connection strength characteristic/mean ratio, $R_k/R_m = 0.83$ (Yeoh et al, 2009e or Chapter 4); partial factor for connection, $\gamma_M = 1.25$; partial factor for variable action, $\gamma_Q = 1.5$; and load duration modification factor, $k_{mod} = 0.8$ (where imposed load refer to an office building, for which a medium term load duration applies in a real floor in a building although $k_{mod} = 1.0$ should have been used to represent the actual test load which was a short term load). The use of $k_{mod} = 1.0$ would only have increased the ULS load of the well-designed beams by 25%. This increase would be irrelevant because the design of all beams were governed by deflection (SLS) as will be discussed in Section 5.7.
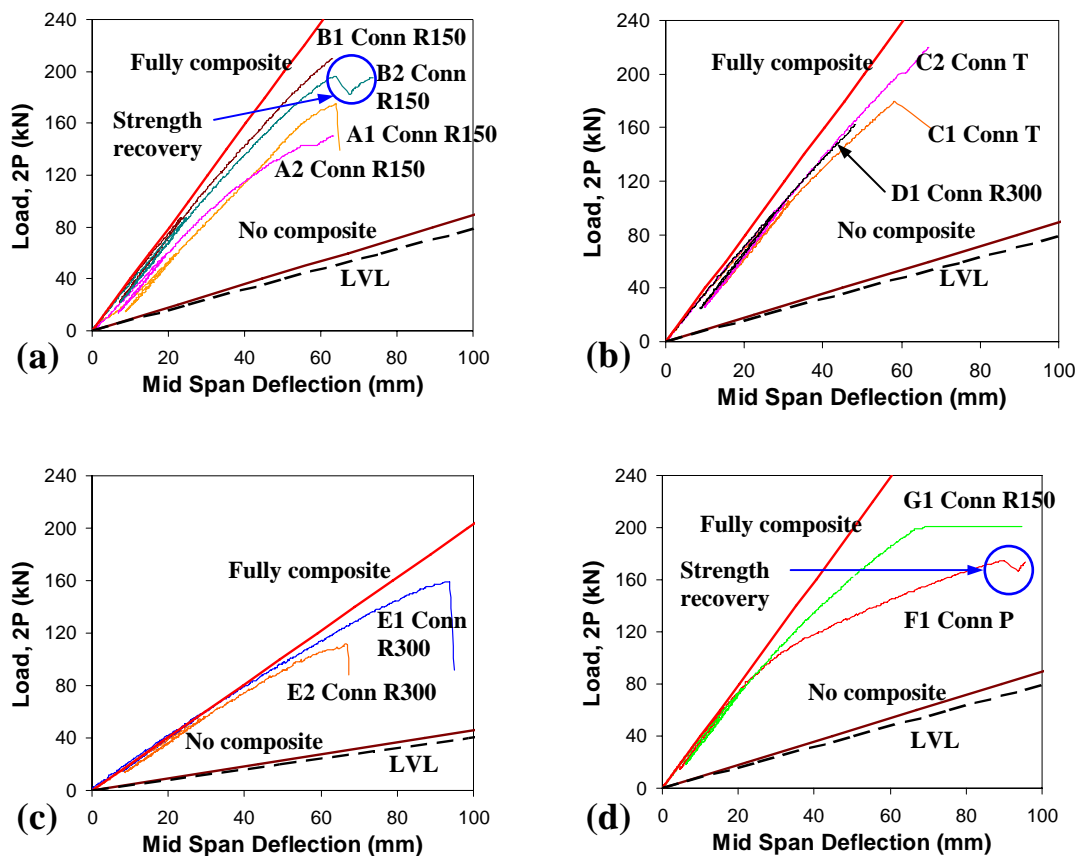
Fig. 5-8. Experimental load-deflection plots reflecting double LVL 1200 mm wide flange section for all beams (refer Table 5-1 and Fig. 5-4 for beam and connection description)

5.6   Short-term performance at ULS

Fig. 5-9 presents analytical-experimental comparisons of load capacity at ULS in the short-term in terms of imposed load for tested beams built from commercial low shrinkage concrete (CLSC), LVL-only and fully composite beams. The analytical design imposed load in kN/m^2 was predicted such that all the ULS short-term inequalities were satisfied using the γ-method with connection secant slip modulus $K_{0.6}$ where concrete, LVL and connection strength design values were used. In all cases, the connection strength inequality was governing.
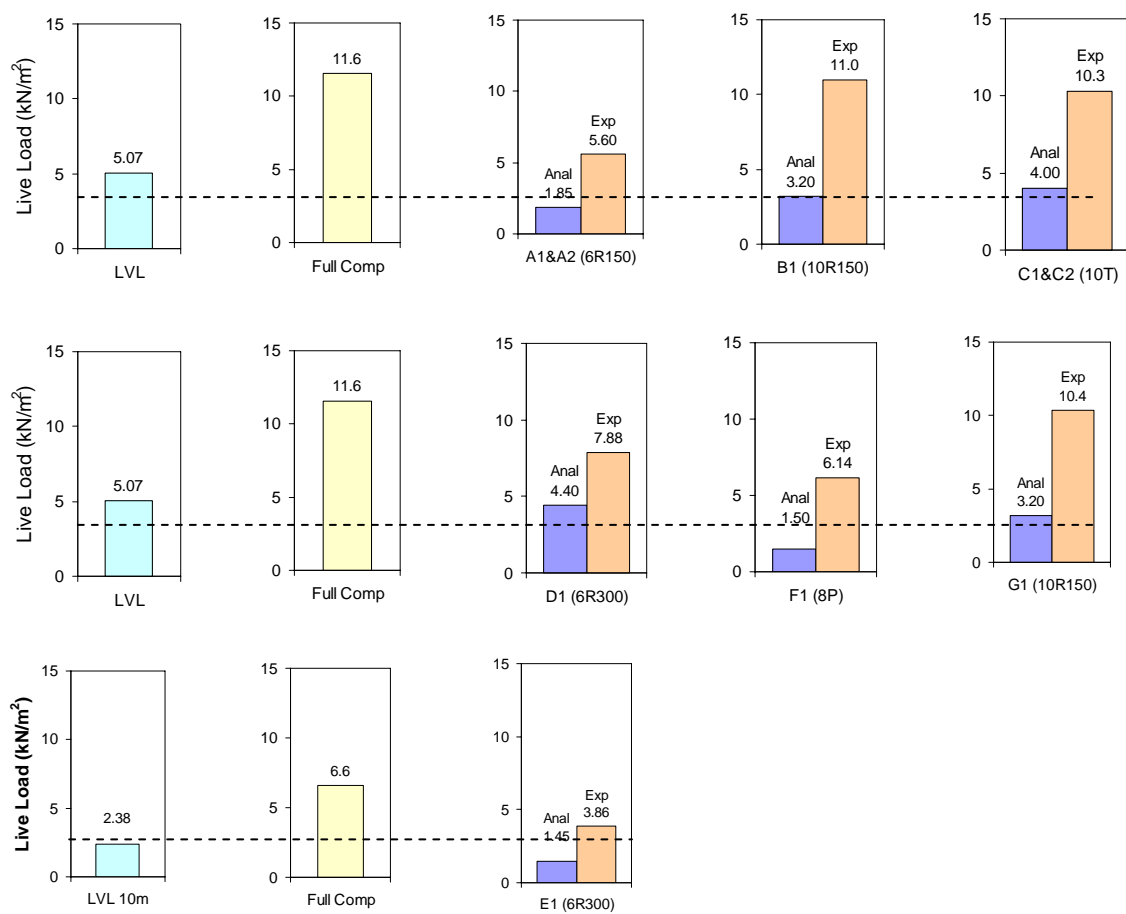
Fig. 5-9. Analytical-experimental short-term ULS live load capacity of tested TCC beams compared to LVL-only and fully composite TCC. Dashed line shows the design live load (3 kN/m^2)

The experimental live load, Q, in kN/m^2 was converted from ($2P_u$) in Table 5-4 using the equivalence of the bending moments, i.e. $w_u L2/8 = P_u L/3$. w_u was considered as the ultimate design load consisting of the dead and live load components, i.e. $w_u = 1.2G + 1.5Q$. w_u was solved for Q, where $G = 3$ kN/m^2, divided by the LVL joist spacing (600 or

1200 mm) for kN/m^2, i.e. $w_u = 1.2(3 \times 0.6) + 1.5(Q \times 0.6) = 2.16 + 0.9Q$ for 600 mm wide units. The fully composite live load capacity was determined using the γ-method with γ_1=1.0.

Important observations from Fig. 5-9 are:

1. All well-designed beams (B1; average of C1 and C2; and G1) exhibited an experimental load capacity very close to that of a fully composite (approximately 0.9 times). This is true for beams with large degree of composite action (Table 5-4). Note that beam D1 was not tested to complete collapse making 7.88 kN/m^2 not the actual collapse load.

2. All experimental live load capacities were about 3 times larger than the analytical capacities for all under-designed and well-designed beams. In other words, the γ-method underestimated the short-term ULS capacity for all cases in this experiment. It is important to note that for all cases, the design governing condition was deflection in the long-term.

5.7   Short-term performance at SLS

The analytical and experimental capacities at SLS in terms of imposed load in kN/m^2 corresponding to the deflection limit of span/300 in the short-term is given in Fig. 5-10 for all tested beams, fully composite and LVL-only beams. The analytical imposed loads were predicted using the effective bending stiffness, EI, obtained from the γ-method with connection secant slip modulus $K_{0.4}$ and mean Young's moduli of concrete and LVL such that the aforementioned deflection limit was satisfied. The experimental live load was determined from the experimental load-deflection curve as the load corresponding to the deflection limit quoted above. The experimental load in kN was converted to kN/m and then to kN/m^2 using a deflection equivalent criterion, i.e. *5wL^4/384EI = Pa(3L^2-4a^2)/24EI* where *a=L/3*, and then by dividing *w* by the flange width (600 or 1200 mm). The fully composite imposed load capacity was determined using the γ-method with γ_1=1.0 or using the transformed section method so that the short-term deflection limit was satisfied. The mean Young's modulus of concrete and LVL were used.
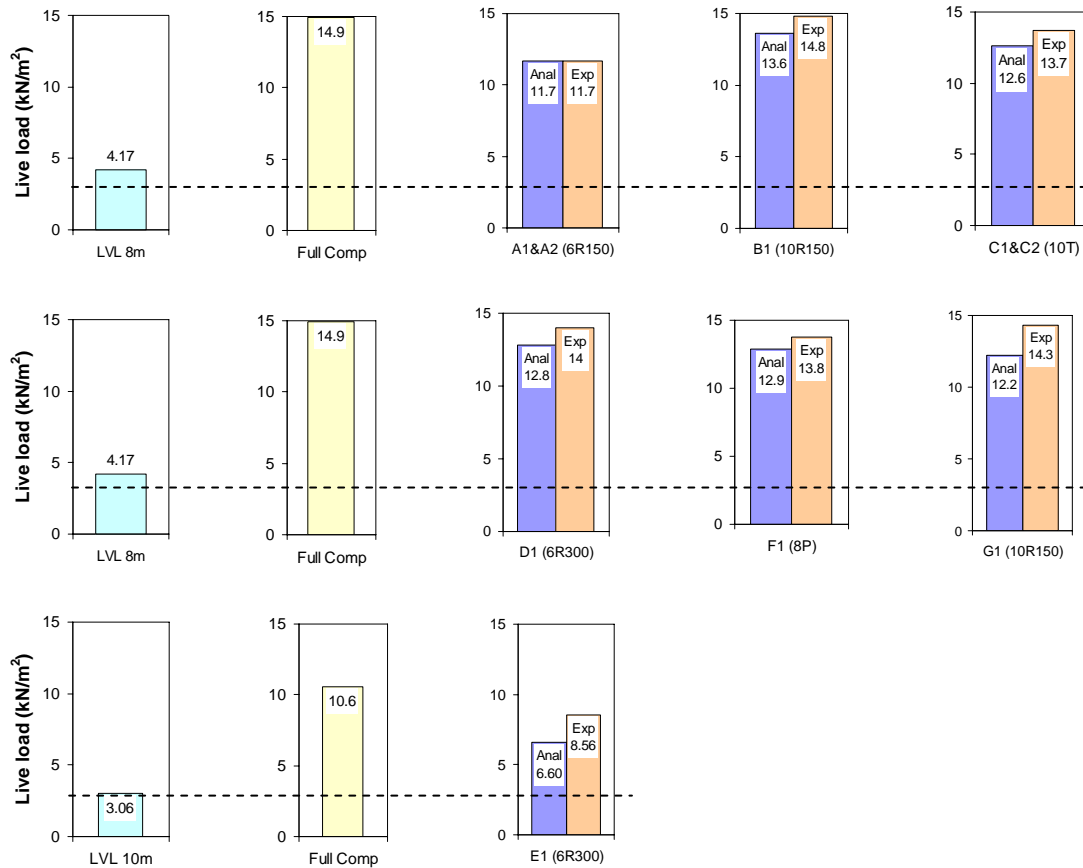
Fig. 5-10. Analytical-experimental comparison of live load capacity in the short-term at SLS for tested TCC beams, LVL-only and fully composite TCC. Dashed line shows the design imposed load (3 kN/m²)

Important observations from Fig. 5-10 are:

1. In most cases, the analytical prediction underestimated the experimental live load by about 10%. The γ-method, therefore, provided an accurate and conservative prediction of the live load at SLS.

2. The experimental load capacities of well-designed beams are only 10% less than that of fully composite beams.

3. The actual design live load of 3 kN/m² is approximately one-fourth of the analytical and experimental live load capacity. This is due to deflection in the short-term not being the governing design criterion for the beams under investigations, which were governed mostly by deflection in the long-term.

The experimental degree of composite action at SLS, DCA_{SLS}, was calculated using Eq. 5-1 with the experimental deflection obtained from the corresponding SLS load in Table

5-4 using the γ-method and the connection slip modulus $K_{0.4}$. All the beams exhibited high level of composite action within the range of 86.8 to 99.9%. This is observed in Fig. 5-8 where all the load-deflection curves were in close proximity to the fully composite curve. In all cases, the analytical γ-method closely estimated the experimental values within 1 to 10% difference.

By comparing the imposed load capacities at SLS of fully composite and experimental beams (Fig. 5-10), the difference was only less than 10% particularly for well-designed beams (B1, C1, C2, D1, G1). This indicated that the transformed section method can be used with some correction factor to design composite beams such as those investigated in this study characterized by a high degree of composite action (Table 5-4).

Table 5-5. Deflection at SLS load (*2P_s*) and effective bending stiffness of fully composite (FuC), experimental and analytical beams built from commercial low shrinkage concrete (CLSC)

Beam	Deflection, Δ (mm)					Ratio (EI)	
	FuC	Exp.	Anal.	Exp/FuC	Exp/Anal	Exp/FuC	Exp/Anal
A1	15.6	22.7	17.5	1.45	1.30	0.69	0.77
A2	13.5	18.0	15.1	1.34	1.19	0.75	0.84
B1	24.3	26.5	26.1	1.09	1.02	0.92	0.98
C1	20.7	23.9	22.1	1.15	1.08	0.87	0.92
C2	25.4	28.8	27.1	1.13	1.06	0.88	0.94
D1	18.7	21.1	19.7	1.13	1.07	0.88	0.93
E1	27.8	27.8	28.9	1.00	0.96	1.00	1.04
F1	15.5	16.6	16.2	1.07	1.02	0.93	0.98
G1	23.2	25.9	25.5	1.12	1.02	0.89	0.98

In an attempt to quantify this correction factor for design at SLS, experimental fully composite beam deflections at SLS load level (*2P_s*) were compared, as presented in Table 5-5. The analytical deflection determined using the γ-method with the connection secant slip modulus $K_{0.4}$ was also included in the comparison. For the well-designed beams, the experimental deflection was 1.09 to 1.15 times the fully composite deflection, and 1.02 to 1.08 times the analytical deflection. Taking a conservative approach, this finding is

indicative of a 15% increment correction factor to the deflection or, equivalently, a 13% reduction to the flexural stiffness (EI) calculated using the transformed section method.

5.8   Comparisons among different beams

5.8.1   Reference beam (G1) and reduced T-section beam (B)

Beam G1 was a reference beam with a double LVL joist and 1200 mm wide concrete flange. All other beams with notch connection were constructed with a reduced sectional geometry made of a single LVL joist and 600 mm wide concrete flange, and the same span and notch length. In order to confirm that this sectional reduction does not affect the actual strength and stiffness properties, the experimental results of the two beams were compared. The stiffness, $K_{fi,beam}$, and collapse load, F_{max}, of beam B1 were doubled and found to be 15% and 5% larger than beam G1, respectively (see Table 5-4 and Fig. 5-8).

The degree of composite action calculated for the two beams was less than 1% difference. The differences were deemed to be within acceptable limit considering possible variations in the concrete for the two beams. It can therefore be concluded that the single joist LVL composite beam with 600 mm wide concrete flange is fully representative of the entire semi-prefabricated composite panel 2400 mm wide, the load bearing capacity and stiffness of which can be simply evaluated by multiplying by four the values measured on the 600 mm wide beam specimens.

5.8.2   Effect of pocket notches (beams A1 and A2)

Beams A1 and A2 had the same connection design and were built indoor. The notched connections in beam A2 were left pocketed during the concrete pouring as opposed to the casting of the whole slab including the notches in the case of beam A1 and all the other beams. The pockets were grouted on the 7th day with high strength low shrinkage SIKA 212 grout which had a drying shrinkage of 394 microstrain and 80 MPa compressive strength on the day of beam testing as compared to 436 microstrain and 58 MPa of concrete used in beam A1, respectively (Table 5-3). Although the compressive strength and shrinkage properties of the pockets in beam A2 were better, the beam exhibited lower stiffness (12% less) and collapse load (14% less) compared to beam A1 (Table 5-4 and Fig. 5-8). The actual reason for this difference is not fully known. Insufficient propping

days (3 days according to SIKA 212 manufacturer recommendation) before the grouted notches developed enough strength could be a possible reason.

5.8.3   Effect of design level (beams A and B)

To investigate the effect of the design level in TCC beams, two beams were compared, both with similar connection (R150): beams A, under-designed (with 6 connectors), and beams B, well-designed (with 10 connectors). The well-designed beams were approximately 1.2 times stiffer and stronger (collapse load, F_{max}) than the under-designed beams. A redistribution of shear force after the first connection yielding was evident in a well-designed beam because of the sufficient number of connectors in the beam. This is particularly evident in the load-deflection curve of beam B2 (Fig. 5-8a) where there was a recovery of strength after the load decreased at about 200 kN following the yielding of a connector. This is an important outcome as it ensures a moderate ductile behaviour of the composite beam which may allow sufficient time for evacuation in the case of an emergency. Such recovery was not seen in the under-designed beams. The high degree of composite action exhibited by the well-designed beams implied that deflection is minimal.

5.8.4   Effect of connection type

Beam B1 with 150 mm rectangular notch connection (R150) was compared with beam C2 with triangular notch connection. Both beams have the same number of connectors. No significant differences in strength, stiffness and composite action can be recognized (Table 5-4). This shows that different types of notched connection used in TCC beams do not affect the structural performance as long as the connectors have similar mechanical properties (see Table 5-2).

Comparing beams with notched connections (in particular beam A1 with R150) to metal plate connected beam (F1), similar strength (174.6 kN by doubling the collapse load of A1, and 174 kN for F1, Fig. 5-8a and Fig. 5-8d) was observed. Beam F1 showed slightly better initial stiffness (3.68 kN/mm) than A1 which, however, declined rapidly (1.82 kN/mm) after $0.6F_{max}$. Such behaviour was not evident in beams with notched connections. This was likely due to the yielding and tearing of the metal plate connections which were more ductile than the coach screws in the notched connections. Consequently,

past $0.6F_{max}$, these connections slipped more than notched connections causing larger beam deflection. It was also observed that a metal plate connected beam, although under-designed, exhibited a sort of strength recovery, unlike under-designed notch-connected beams. In order to improve the post-peak stiffness of beam F1 and prevent the final brittle failure of the plate connection due to tearing, it is recommended that the plate thickness be increased (Yeoh et al, 2009e or Chapter 4).

5.8.5   Effect of notch length

Beams with rectangular notch connectors of different lengths but the same design level were compared: beam B1 with 10 notches 150 mm long (R150) and beam D1 with 6 notches 300 mm long (R300). Both beams had the same design level, i.e. they were designed for the same load. Both the stiffness and degree of composite action of the beams were almost identical (1.67 kN/mm and 97.3% for B1; 1.68 kN/mm and 96.3% for D1, respectively, in Table 5-4). The actual maximum load of the beams was not known as the test was stopped before collapse occurred to enable vibration testing of the beams.

By comparing beams with the same number of notch connectors (six) and different notch length (150 mm in beams A, and 300 mm in beam D1), it is evident that the beam with longer notch (D1) performed better in stiffness (30% more) and composite action (10% more). No actual maximum load can be compared since beam D1 was not tested to complete destruction. The use of longer notches is preferable to improve the performance of the composite beam as the length of the concrete notch itself increases the shear strength and stiffness of the connection as found in push-out tests (Yeoh et al, 2009e or Chapter 4).

5.8.6   Effect of concrete type (beams E1 and E2)

Beam E1 was built with grade 35 low shrinkage concrete (measured f_{cm} = 48 MPa) and beam E2 with grade 25 normal concrete (measured f_{cm} = 31 MPa). Beam E1 (79.6 kN) exhibited 40% higher collapse load than beam E2 (55.4 kN) (Table 5-4 and Fig. 5-8) with the same stiffness and degree of composite action. Essentially it was the concrete in the notched connections that provided the shear transfer capacity between the concrete and

LVL. Therefore this comparison indicates that compressive strength of the concrete is crucial to achieve beams with high strength performance.
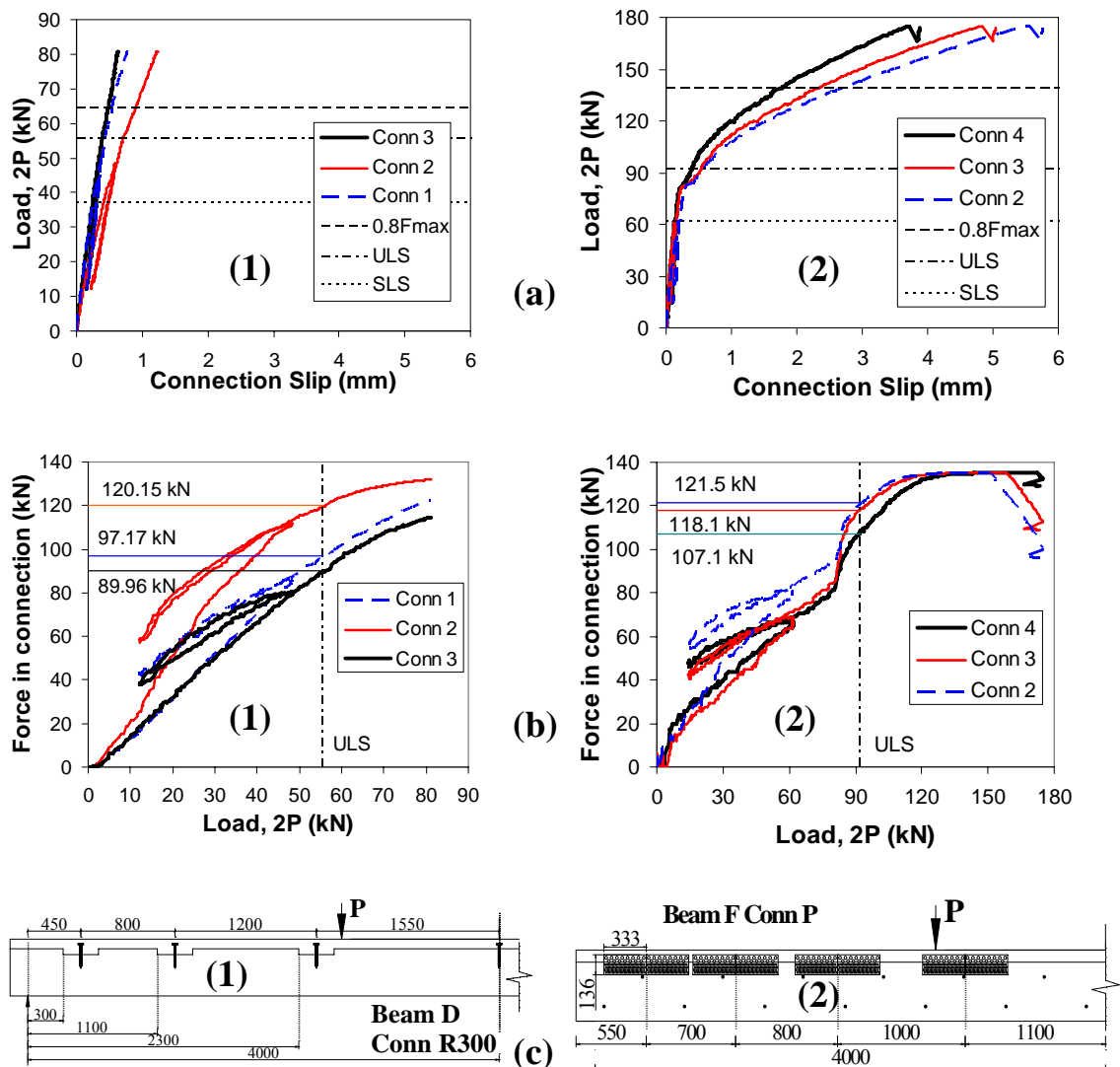
Fig. 5-11. Load-connection slip curves (a); the corresponding shear force in connection (b); and position of connectors with respect to loading point where Conn 1 is located nearest to left support and Conn 4 nearest to mid-span (c); for (1) beam D1 with single LVL (connection R-300); and (2) beam F1 with double LVL (connection P). (Refer to Fig. 5-4 for connection types)

5.8.7   Effect of environmental exposure before collapse test (indoor and outdoor)

Beams C1 (outdoor) and C2 (indoor) were compared. Note that beam C1 was left outdoor without any imposed load subjected to environmental changes (corresponding to spring and summer seasons) for 4 to 5 months. Beam C2 (110 kN, 1.65 kN/mm) was found to be

20% stronger and 10% stiffer than beam C1 (89.7 kN, 1.54 kN/mm). No difference was found in the degree of composite action.

5.9   Horizontal slip of shear connection

The relative slip between the concrete slab and the LVL joist were monitored during the tests at the connector location. The slips of beams D1 and F1 with 300 mm rectangular notches (R-300) and metal plates (P) are presented in Fig. 5-11(a1) and (a2), respectively, together with the corresponding shear force plotted in Fig. 5-11(b1) and (b2). The shear forces were obtained from load-slip curves measured in the connection push-out tests (Yeoh et al, 2009e or Chapter 4). The amount of slip is indicated for different load levels at SLS, ULS and $0.8F_{max}$. The largest slip occurred, normally, in the inner connector nearest to the outer edge of the point load, for example Conn 2 in beam D1.

Connection R-300 in beam D1 behave relatively stiff even past the ULS load level. Connection P exhibited high initial stiffness, but slip markedly increased after the ULS load indicating yielding of the plate. Fig. 5-11(b2) shows that the shear force in all connectors of beam F1 reached a plateau and eventually dropped indicating complete failure in the connections and beam. Such behaviour was not observed in beam D1 since connection R-300 has a different failure mode (Yeoh et al, 2009e or Chapter 4).

5.10   Conclusions

Short-term collapse tests were conducted on eleven 8 and 10 m span laminated veneer lumber (LVL)-concrete composite floor T-beams. Several variables such as connection types, concrete type, and design level corresponding to number of connections were investigated. Mid-span deflections and connection slips were measured during the tests. The types of connectors were triangular and rectangular (150 mm and 300 mm long) notches cut in the LVL and reinforced with coach screws, and modified toothed metal plate connectors. Different concrete was used including normal weight, commercial low shrinkage, and special low shrinkage concrete.

The effective bending stiffness method or γ-method according to Annex B of Eurocode 5 (CEN, 2004b) was used to design the beams under 3 kN/m^2 design imposed load and 1

kN/m^2 design permanent load in addition to the self weight. Six beams were well-designed and five were under-designed. Well-designed beams refer to beams that fully comply with all design inequalities at ULS and SLS. Under-designed beams refer to beams where the maximum demand of shear force in the connection was about 1.3 times the resistance at ULS.

All well-designed beams exhibited more than 95% degree of composite action regardless of the type of connection used. They also showed redistribution of shear force in the connectors thus enabling strength recovery in the event the outer connections fail. Therefore, a well-designed system is highly recommended.

The use of 300 mm rectangular notch with coach screw connection in the composite beam is recommended for two main reasons: (1) High stiffness and strength even beyond the ULS load level; and (2) Less number of connectors along beam and, therefore, less cost. Triangular notched connection is another alternative. Although it may require more connectors to that of a 300 mm notch for the same design level, a triangular notch is easier and faster to cut, particularly if CNC machines are not available. Metal plate connection is practical in construction, however a disadvantage was the quick decrease in stiffness beyond the ULS load level. Such behaviour can be improved by increasing the plate thickness so as to postpone the brittle failure for tearing.

No significant difference was found in the short-term performance among beams with different shrinkage properties of concrete. However, the strength of concrete is important especially in notch-connected beams since the concrete within the notches provides the shear transfer between the LVL and the concrete slab.

Based experimental-analytical comparisons of the short-term performance at ULS and SLS, the following conclusions can be made:

1. All well-designed beams with high degree of composite action exhibited experimental imposed load capacities at ULS and SLS very close to that of a fully composite beam (approximately 10% less).

2. Therefore, a 15% increment correction factor to the deflection or a 13% reduction to the effective bending stiffness, (EI), calculated using the transformed section method can be proposed for all well-designed beams.

3. All experimental imposed load capacities at ULS are about three times larger than the analytical capacities for all under- and well-designed beams. In other words, the γ-method underestimated the short-term capacity at ULS in all cases. It is important to note that for all cases, the design governing condition was deflection in the long-term.

4. In most cases, the analytical prediction underestimated the experimental imposed load at SLS by about of 10%. In other words, the γ-method provided a reasonably accurate and conservative prediction of the imposed load at SLS.

6   Long-term Tests on Connections and Beams

This chapter has been reproduced from a journal paper submitted to the Materials and Structures RILEM Journal entitled "Long-term behaviour of LVL-concrete composite connections and beams under sustained load" (Yeoh et al, 2009d).

Three selected best types of connection concluded in Chapter 4 and three floor beams were tested in the long-term under sustained load for 1.5 years. This chapter discussed the outcomes of these long-term tests. These tests were planned and carried out in Phase 3 for connections and Phase 5 for beams, of the whole experimental framework. The results of these tests, in particular the connection tests, were used for the design of timber-concrete composite floor beams presented in Chapter 7.

Supplementary to this chapter are the design and construction of long-term push-out test frames in Appendix 8, and, construction and setup of beams for long-term test in Appendix 9.

6.1   Abstract

The long-term behaviour and creep mechanism in timber-concrete composite (TCC) structures are known to be very complex because the three components, timber, concrete and connection, creep differently and at a different rate depending on the environmental conditions. This chapter reports the outcomes of long-term tests on three types of TCC connections and three 8 m span T-section floor beams under sustained load, where the timber beam was made from laminated veneer lumber (LVL). The tests lasted for a period of approximately 1.5 years, and were performed in uncontrolled, unheated indoor condition. Important results such as the creep coefficients of the connections and the mid-span deflections of all the beams including projection to the end of service life are presented. The environmental condition which the beam specimens were exposed to was marginal to service class 3 according to Eurocode 5. The predicted final long-term deflections exceeded the span/200 deflection limit, which were indicative of the expected deflection level for TCC structures exposed to similar somewhat severe environmental conditions. Reducing the initial deflection in the system by propping and/or pre-cambering the timber beam, together with the use of low shrinkage concrete or precast concrete slabs which are allowed to shrink first before connecting to the timber beams are some of the possible solutions to reducing long-term deflection for long-span applications.

6.2   Introduction

Timber-Concrete Composite (TCC) floors represent a construction technique where a concrete slab is connected on top of timber joists using different types of connector. The three components of TCC floors, timber, concrete and connection, are characterized by different time-dependent behaviour, which depends upon several factors such as stress level, moisture content, temperature and relative humidity of the environment. The main long-term design parameter that must be considered for TCC floors is deflection. It is possible to control the long-term deflection of timber beams and joists by application of surface treatment against moisture (Ranta-Maunus, 2000). However, the long-term performance of TCC floors is more complex and depends upon a number of phenomena which occur within the structural components that make up the TCC system. Phenomena such as creep, drying shrinkage and thermal strains of concrete; creep, timber and moisture strains of timber; and creep of connection, affect strength, stiffness and

113

deflection of TCC in the long-term. Timber can be regarded as a linear-viscoelastic material in a stable environment characterized by constant relative humidity if the stresses are less than 35% of the short-term strength. In a variable environment, the stress threshold reduces and the viscoelastic behaviour of timber is no longer linear because the change in humidity conditions highly increases the deformations under load as compared to a constant condition. As such, the mechano-sorptive creep or creep due to variation in the moisture content has to be considered. Factors such as timber size, surface properties, loading type, length of environmental cycle, and moisture diffusion also indirectly affect the long term behaviour of TCC floors (Toratti, 2004).

Few long term tests on TCC structures and connections have been performed to date (Bou Said et al, 2004; Ceccotti et al, 2006; Fragiacomo et al, 2007a and 2007b; Grantham et al, 2004). Numerical (Fragiacomo and Ceccotti, 2006; Fragiacomo, 2006; Schänzlin, 2003) and analytical (Fragiacomo and Ceccotti, 2004; Schänzlin and Fragiacomo, 2007) models have been proposed to predict the long-term behaviour of TCC structures. Bou Said et al (2004) tested a TCC beam of 8 m span with glued-in connections over a period of two years in a sheltered outdoor condition. The relative humidity exceeded 85% over a number of days. The short term deflection estimated using Eurocode 5 (CEN, 2004b) was significantly exceeded during the two year period and consequently the prescribed limitation on the long term deflection was also exceeded.

Ceccotti et al (2006) tested a TCC floor system of 6 m span with glued-in connections under a uniformly distributed load over a period of 5 years in unsheltered, outdoor conditions. The moisture content did not exceed the 20% limit over the tested period, however, relative humidity exceeded 85% over a number of weeks. The TCC beam was classified as service class 3 and whilst the test results were best approximated by coefficients for service class 3, the test results were still above the Eurocode 5 (CEN, 2004b) predictions.

Fragiacomo et al (2007b) monitored the behaviour of eight TCC beams with notched shear key and Hilti dowel connections over a period of 133 days after load application in uncontrolled sheltered laboratory conditions. The experimental result was used to verify a finite element model which in turn was used to predict the behaviour of the beams over a period of 50 years (Fragiacomo, 2006). A deflection of 1/100 of the beam length was

predicted after 50 years based on the finite element model. Reduction factors recommended by Eurocode 5 (CEN, 2004b) under-predicted the test results while the finite element and analytical results were in good correlation with the test results.

Grantham et al (2004) monitored upgraded TCC floor over a period of 40 days. The tests, however, were aimed at evaluating the benefits of propping the composite floor during pouring of concrete and as such, are not really applicable for determination of long term creep deflections.

Kavaliauskas et al. (2005) evaluated the long-term deflection of a TCC beam based on Eurocode 5 (CEN, 2004b) recommendation by doubling the creep coefficient k_{def} for the connection. Because the Eurocode method only gives initial and final deformation and experimental results indicate that the final deformation is often exceeded within the first year for medium and long span floors. Kavaliauskas et al. (2005) proposed calculating the creep of concrete and timber separately, with concrete creep deformation calculated using on Eurocode 2 (CEN, 2004a) and the timber creep deformation calculated using an exponential law proposed by Le Govic (Kavaliauskas et al, 2005). Results from the proposed method showed that the initial deflection prediction was twice that predicted by Eurocode 5 (CEN, 2004b) and reached almost the its final value over a period of 60 days. The calculated final deflection was 1.5 times that predicted by Eurocode 5 (CEN, 2004b). Schänzlin and Fragiacomo (2007) introduced two rigorous approaches to evaluate long-term deflections. One approach uses material creep coefficients and rigorous closed form solutions to evaluate the effect of inelastic strains such as concrete shrinkage (Fragiacomo and Ceccotti, 2004). Their other approach uses the effective creep coefficients of the different materials instead of the pure material creep coefficients so as to account for their different creep rates over time. Concrete shrinkage and climatic strains are transformed into an equivalent uniformly distributed load so as to enable the use of the Eurocode 5 (CEN, 2004b) formulas for composite beams with flexible connections (Schänzlin and Fragiacomo, 2007). This approach was found to further improve the prediction of the long-term deflection.

This chapter reports the outcomes of long-term tests on three types of TCC connections and three 8 m span, T-section floor beams subjected to sustained load for a period of approximately 1.5 years in an unheated and poorly insulated detached building. The most

crucial quantities were logged, including relative connections slips, mid-span beams deflections, relative humidity, temperature and moisture content. Important results are presented herein, including connection creep coefficients and mid-span deflections of all the beams. These are also extrapolated to the end of service life. The influence of environmental changes and experimental results are critically discussed and compared with analytical approximations based on the use of Eurocode 5 (CEN, 2004b) and the extended approach recommended by Schänzlin and Fragiacomo (2007). Experimental extrapolation and analytical prediction of the final long-term deflection were attempted and compared to each other.

6.3   Material properties

The LVL used for the construction of the connection and floor beam specimens was 400d × 63w mm sections where d and w are the depth and width, respectively. The mean Young's modulus of the LVL was 11.34 GPa and the characteristic bending strength was 48 MPa, based on independent quality control testing (Gaunt and Penellum, 2004). A commercially available, low shrinkage concrete (CLSC) with Eclipse admixture was used for all the specimens except for one beam which used normal weight concrete (NWC). Both types of concrete were ordered to provide the following properties: 35 MPa characteristic compressive strength, 13 mm aggregate, and 120 mm slump. Cylinder compressive strengths tests to NZS3112 Part 2 (SNZ, 1986), gave 28 day compressive strengths of 45 MPa for both concrete types. The mean drying shrinkages were 400 and 910 microstrain at 28 days for CLSC and NWC, respectively.

[Material properties are presented in Appendix 1]

6.4   Connection and beam tests

Three types of connection were tested. For each connection type, pairs of symmetrical push-out specimens were built: one was subjected to a sustained load of approximately 0.3F_{max}, which represents the quasi-permanent part of the serviceability design load, where F_{max} is the maximum strength of the connection determined from short-term push-out test (Yeoh et al, 2009c and 2009e or Chapters 3 and 4). The second specimen of each pair was used as control specimen with no external loads in order to monitor the relative

slip due environmental variations. The types of connection tested were: (1) a 300*l* × 50*d* × 63*w* mm rectangular notch reinforced with 16 mm diameter coach screw (R); (2) a 30°_60° 137*l* × 60*d* mm triangular notch reinforced with 16 mm diameter coach screw (T); and (3) a pair of 333*l* × 136*d* × 1*t* mm staggered toothed metal plates (P) where *l*, *d*, *w*, and *t* are the length, depth, width and thickness, respectively, as illustrated in Fig. 6-1. These connections were selected on the basis of the strength and stiffness performance achievable, the ease of production, and the labour and material costs (Yeoh et al, 2009c or Chapter 3).
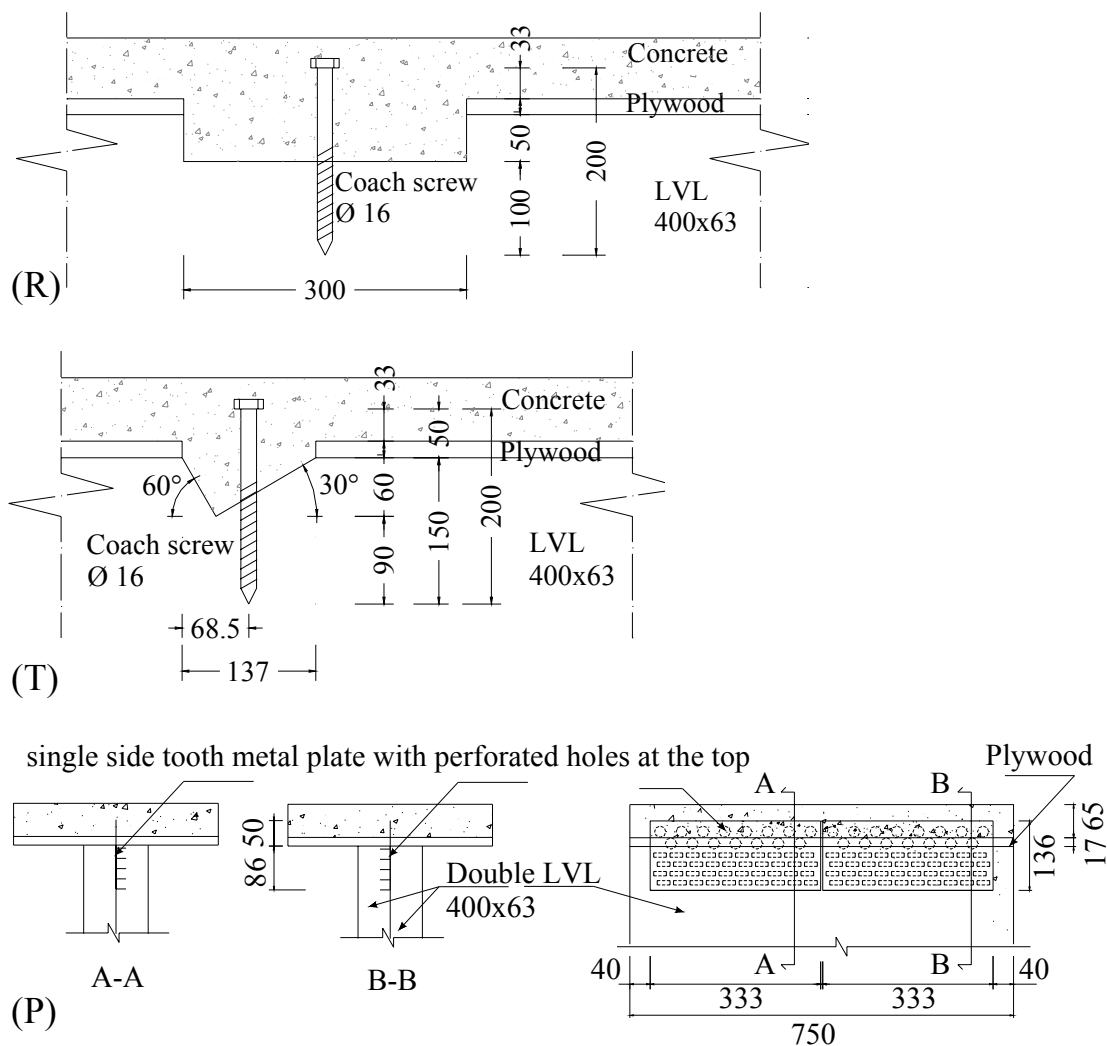
Fig. 6-1. Three types of connection (R, T, and P) tested in push-out tests (dimensions in mm)
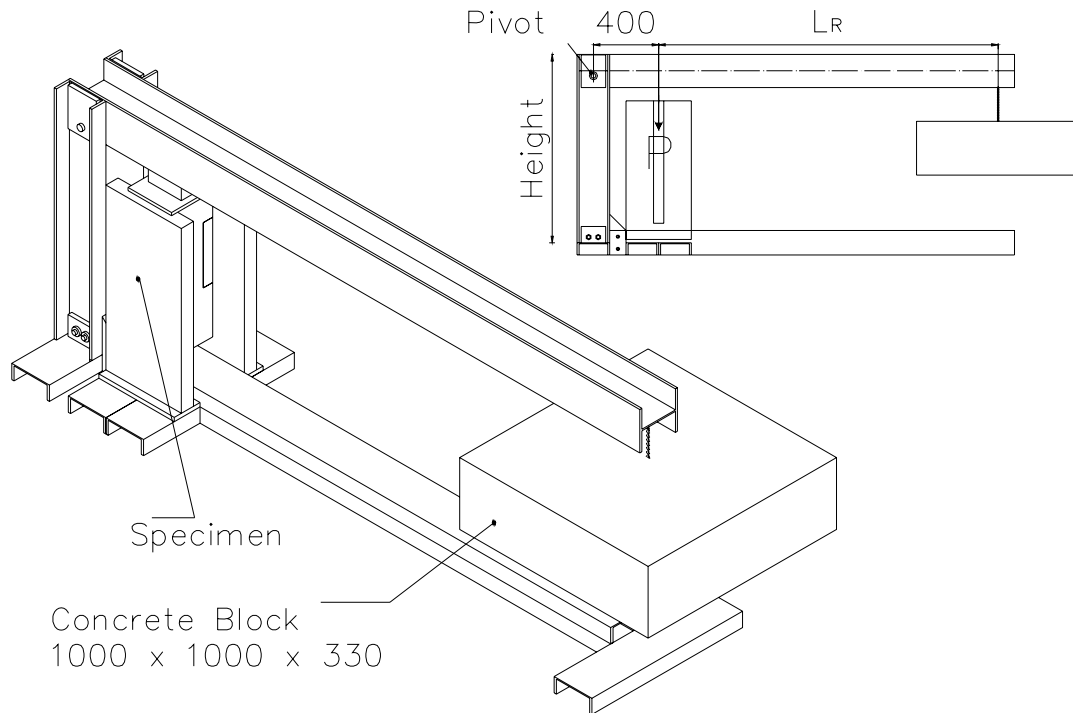
Fig. 6-2. "C" shape lever frame for sustained load test of connection (dimensions in mm)

Table 6-1. Details of connection long-term push-out frames (F_{max} is the mean shear strength of a pair of connections)

Frame #	F_{max} (kN)	$0.3F_{max}$ (kN)	Concrete Weight (kN)	L_R (mm)
1 for T	165	50	8.07	2680
2 for R	240	72	8.07	3770
3 for P	276	83	16.1	2260

Each of the loaded push-out specimens was set-up in a specially designed "C" shape lever frame built from parallel flange channels and universal columns as shown in Fig. 6-2. Concrete blocks weighing 8.07 kN each were used to provide the sustained load. The length (L_R) of each frame housing the 3 connections were calculated based on the weight of the concrete block so that the force exerted on the push-out specimen was equivalent to approximately $0.3F_{max}$ as summarized in Table 6-1, F_{max} being the mean shear strength of the corresponding connection system. All the loaded and control specimens were placed in a detached garage building in Christchurch, New Zealand, which provided an indoor, unheated, uncontrolled condition (Fig. 6-3). Loads were first applied on the 20th May 2008 (approaching winter), after approximately 4 months after had been fabricated. The quantities measured and logged were relative slips on each side of the connections as

shown in Fig. 6-4, using 30 mm potentiometers (P1 and P2 in the front and, P3 and P4 in the rear side of the specimen), relative humidity and temperature, using HIH-4000 Series humidity sensors and LM-35 temperature sensors, respectively. The sampling rate was every minute for the first 24 hours after loading and every hour for the remainder of the long-term test duration.

Fig. 6-3. Garage to house connections and floor beams long-term tests
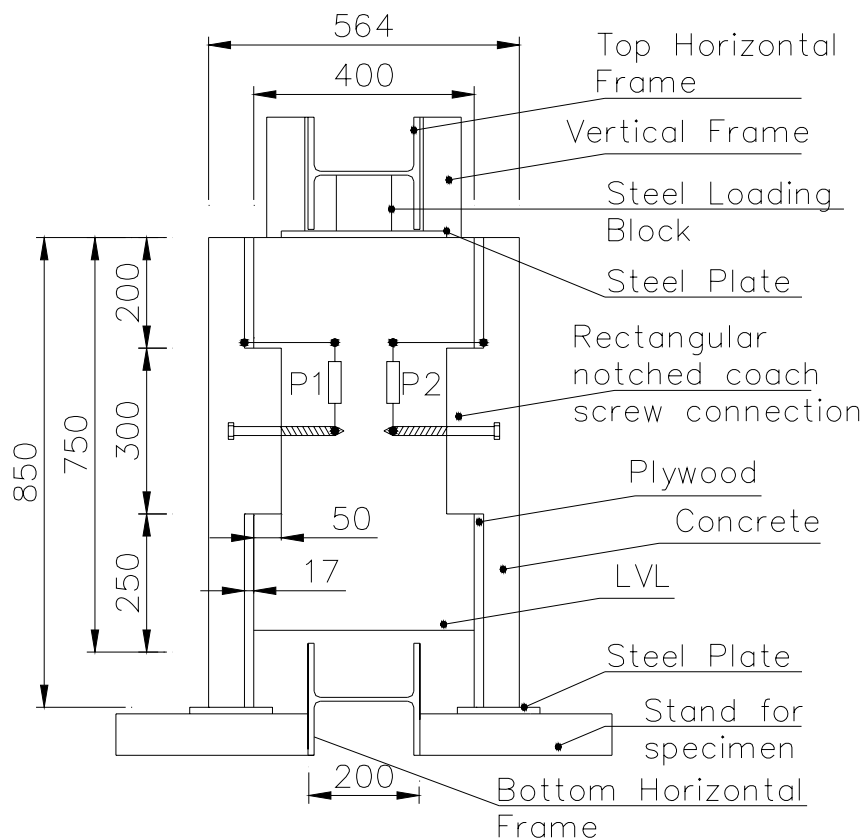
Fig. 6-4. Set-up of specimen in lever frame and locations of potentiometers (dimensions in mm)

[Design and construction of long-term push-out test frames are presented in Appendix 8]

Three 8 m span, T-section floor beams (designated as H, I and J), were built in the same garage as the push-out specimens. These were simply supported on seats built from LVL so that the seats were loaded parallel their grain (Fig. 6-5(a)). Two beams, H and I, had a single LVL joist, a 600 mm wide slab and 6 type R connectors along the span (Fig. 6-5(b)). Beam H was cast with normal weight concrete and beam I with low shrinkage concrete. Beam, J, had a double LVL joist, a 1200 mm wide low shrinkage concrete slab and 8 type P connectors along the span (Fig. 6-5(c)). Beam H was cast on the 25th February 2008 (towards the end of summer) and beams I and J the next day.
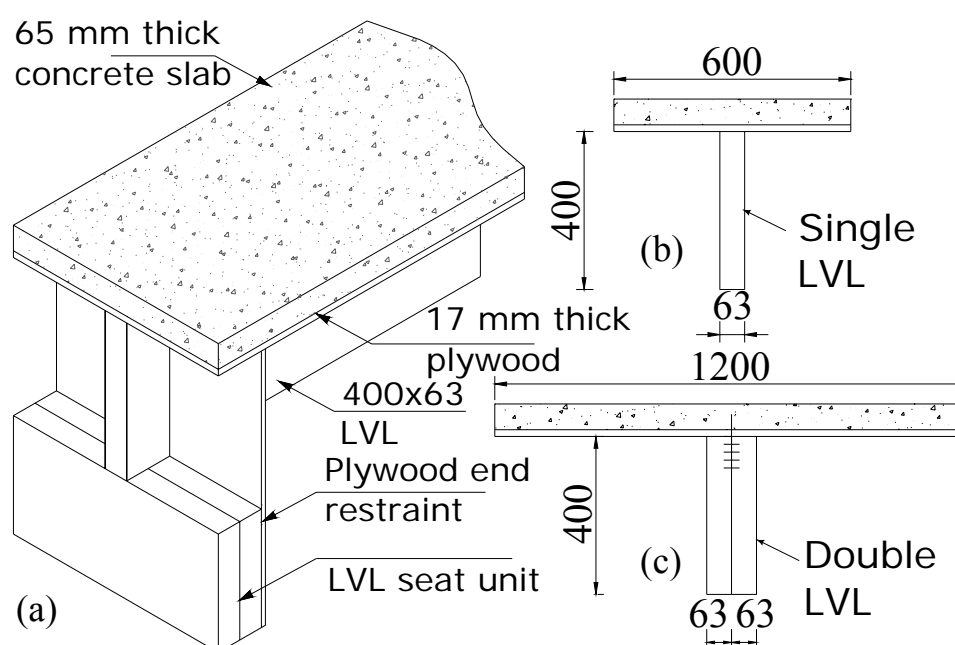
Fig. 6-5. 3-D view and cross-sections of beam specimens: (a) beam on LVL seat support; (b) single LVL beam with connection type R; and (c) double LVL beam with connection type P (dimensions in mm)

All the beams were propped at mid-span for the first seven days. The concrete was cured for 5 days after setting (approximately 6 hours after pouring) using damp Hessian sacks, and at day 36 (1st April 2008, autumn) a superimposed load of 2.2 kN/m^2 was applied using sealed buckets of water (Fig. 6-6) as the quasi-permanent part of G + 0.4Q for the serviceability limit state loading. Mid-span and support displacements were measured every minute during casting and loading for the initial 24 hours and every hour for the remainder of the long-term test. Mid-span displacements were corrected to remove

support settlements (e.g. due to compression of the seats) by subtracting the average support displacements. Environmental conditions such as relative humidity and temperature were recorded in the same manner as for the long-term connection tests.

A moisture content block from the same batch of LVL was placed under the slab of one of the floor beams, adjacent to the LVL joist. The weight of this block was recorded periodically, including the beginning and end of the long-term test, by placing it on a digital scale. The oven-dried moisture content of the LVL block was obtained and end of the long-term test. The periodical moisture contents of the LVL were calculated from the oven-dried weight of the block.

[Construction and setup of beams for long-term test are presented in Appendix 9]

Fig. 6-6. Floor beam specimens loaded with buckets of water in the garage
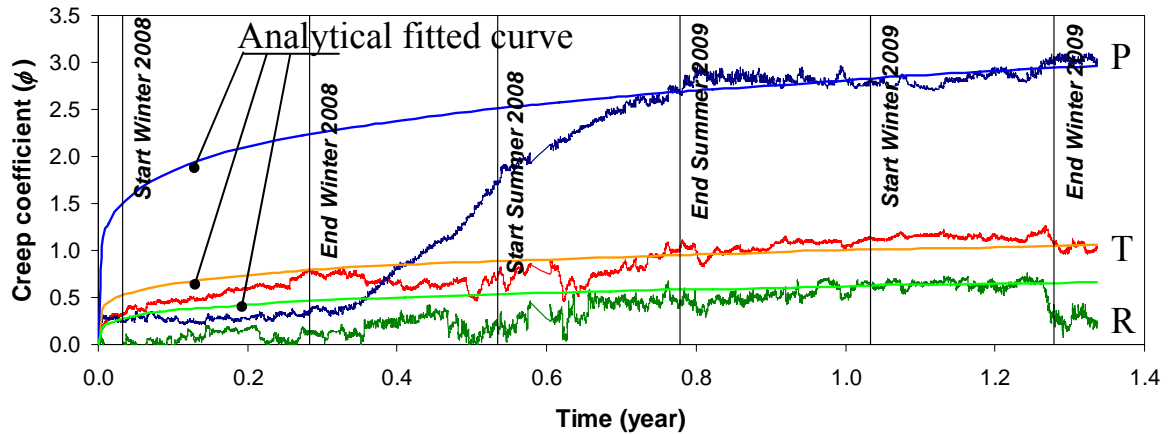
Fig. 6-7. Experimental creep coefficient and analytical fitted curve using power-type function for connections T, R and P from 20th May 2008 to 20th September 2009 (refer to Fig. 6-1 for connection description)
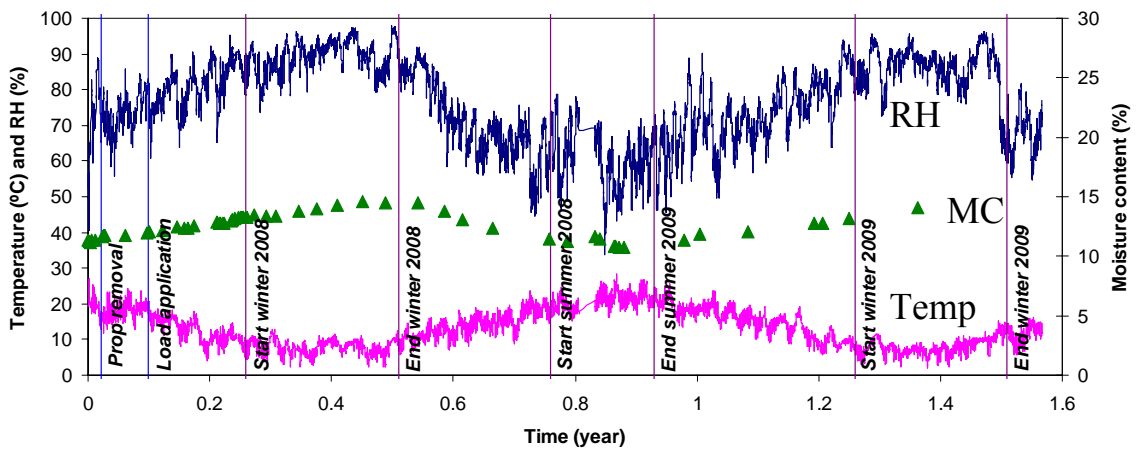
Fig. 6-8. Relative humidity, temperature, and average LVL moisture content changes throughout the beam long-term tests (from 25th Feb 2008 to 20th Sept 2009)
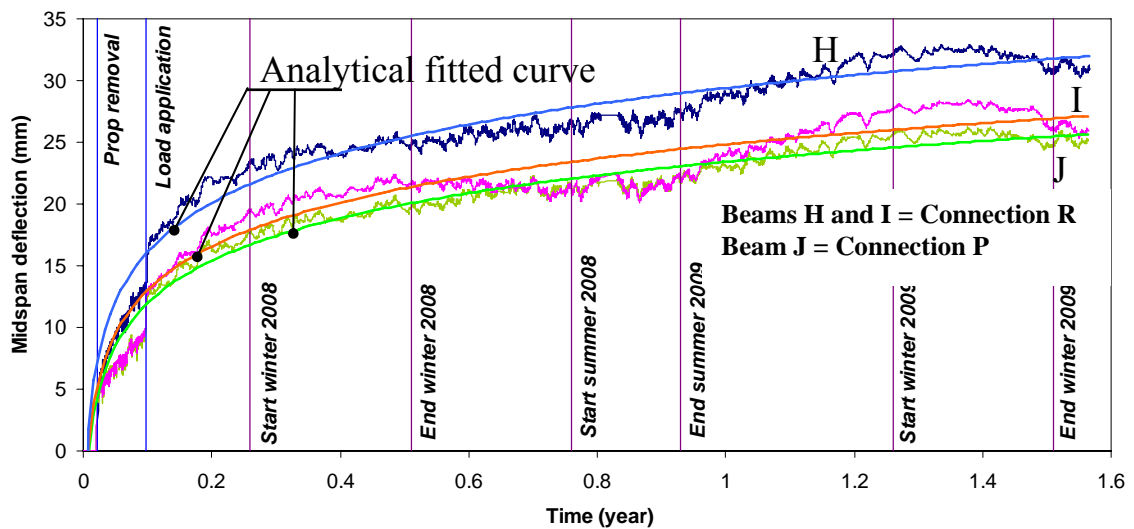
Fig. 6-9. Mid-span deflection of beams H, I and J (from 25th Feb 2008 to 20th Sept 2009) under sustained load and analytical fitted curve using logarithmic function equation

6.5   Creep coefficient for the connections

The connection creep coefficient, $\phi(t)$, subtracts potential environmentally induced variations in the connection, based on control specimen measurements, as given by:

$$\phi(t) = \frac{[\Delta(t) - \Delta_d(t)] - \Delta_{el}}{\Delta_{el}}$$

(Eq. 6-1)

where $\Delta(t)$ denotes the relative slip of the connection at time t, subscript d refers to slip of the control specimen, and subscript el denotes the instantaneous elastic slip immediately after the application of load.

Test data was processed at 488 days (or 1.34 year, from 20th May 2008 to 20th September 2009) and fitted with power functions (Fig. 6-7) in order to extrapolate the creep coefficient to 50 years, $\phi(50y)$. The extrapolated coefficients were then converted to the k_{37} creep factor required for design using the New Zealand Timber Structures Standard, NZS 3603 (SNZ, 1993). The relationship between the two is given by (Eq. 6-2)   (Eq. 6-3). The creep factor may then be used to modify the effective slip modulus for the connection, for both the ultimate and serviceability limit states, using (Eq. 6-2)   (Eq. 6-3).

$$k_{37} = 1 + \phi(t) \qquad\qquad K_{eff} = \frac{K}{k_{37}}$$

(Eq. 6-2)   (Eq. 6-3)

The creep coefficient increased uniformly with time for all the connections except the type P connection, which unexpectedly increased from $\phi(0.34\ y) = 0.42$ (0.34 y = 124 days) to $\phi(t) = 2.84$ and than stabilized again after 0.8 year (292 days). The abrupt change in the type P connection was possibly due to rigid slip within the steel plates. While the precise mechanism is unknown, the change occurred between the end of winter 2009 and the end of summer 2009, when there was a significant increase in average temperature (from 8 °C to 28 °C) and decrease in relative humidity (from 90% to 50%, Fig. 6-8).

After 1 year, the creep coefficients for all the connections appeared to reach a plateau until 1.26 year (460 days) when a small descent occurred in connections T and R. This

was possibly caused by the 23% drop in relative humidity and approximately 2 °C temperature increase at the end of winter.

Table 6-2. Average slips, creep coefficients and creep factors of connections

Conn. type	$\Delta(1y)$	$\Delta_{el}(1y)$	$\Delta_d(1y)$	$\phi(1y)$		Diff. %	Fitting curve	$\phi(50y)$	k_{37}
				Exp	*Anal*				
T	0.43	0.21	0.01	1.05	1.00	+4.99	$\phi(t)=0.328t^{0.189}$	2.10	3.10
R	0.39	0.24	0.02	0.54	0.62	−12.7	$\phi(t)=0.154t^{0.237}$	1.57	2.57
P	1.11	0.28	0.07	2.81	2.81	+0.07	$\phi(t)=0.959t^{0.182}$	5.73	6.73

Table 6-2 summarises the average slips, creep coefficients and creep factors for the tested connections. The creep coefficients predicted using the fitted curves are within 6% of the experimental values at 1 year. The plate connection (P) had the largest creep coefficient of $\phi(50\,y) = 5.7$, followed by the triangular notch (T) with $\phi(50\,y) = 2.1$ and the rectangular notch (R) with the smallest of $\phi(50\,y) = 1.6$. The reasons for the differences are unclear but are likely to be related to the distribution of stress within the connection region.

6.6   Floor beams test results

The mid-span deflection trends for floor beams H, I and J until 570 days or 1.56 years (from 25th February 2008 to 20th September 2009 and in an uncontrolled indoor environment) are presented in Fig. 6-9, along with a logarithmic function fitted to the experimental results. The mid-span deflections for the beams at different key events such as at the removal of the prop, load application, and the start and end of winter and summer, are summarized in Table 6-3. The test is on-going.

There was significant mid-span deflection during the first quarter year (90 days) after the props were removed. There were only gradual increases after that quarter, with yearly fluctuations most likely due to the environmental changes in the garage, although there were quasi-plateaus between the end of winter 2008 (0.5 year) and the end of summer in 2009 (0.9 year) and in the middle of winter 2009. The 5.0 to 6.2 mm initial beam deflections ($\Delta_{G,inst}$) were caused by the self-weight of the floors after the removal of the props. These were near the 5.8 to 5.9 mm deflections predicted using the Eurocode 5 (CEN, 2004b) formulas for composite beams with flexible connections and the slip

modulus recommended by Ceccotti (1995) for the serviceability limit state. Prior to the application of the superimposed load at 36 days, this deflection had increased by approximately 7.8 mm for beam H, 4.8 mm for beam I and 5.1 mm for beam J. Application of the superimposed load initially increased the deflections ($\Delta_{Q,inst}$) by approximately 1.6 to 2.6 mm, about 30% to 50% of the initial self weight deflections ($\Delta_{G,inst}$). The use of low shrinkage concrete (beam I) was shown to reduce the deflection by approximately 5 mm compared to normal weight concrete (beam H), corresponding to span/1600. The deflection for beams H, I and J observed to date (1.56 years) were 31.0 mm, 26.0 mm and 25.2 mm, respectively.

Table 6-3. Mid-span deflections of beams in long-term test at different key events

Key events	Time		Mid-span deflection of beams (mm)		
			H	I	J
Concrete casting	0d		0	0	0
Prop removal	7d	$\Delta_{G,inst}$	6.20	4.97	4.99
Live load application	36d	Δ_{before}	14.0	9.83	10.1
		Δ_{after}	15.9	12.4	11.7
$\Delta_{Q,inst}= \Delta_{after}$-$\Delta_{before}$			1.98	2.60	1.61
Ratio $\Delta_{Q,inst}$ /$\Delta_{G,inst}$			0.32	0.52	0.32
Start winter 2008	0.27y		22.9	19.2	17.3
End winter 2008	0.52y		24.7	21.3	19.5
Start summer 2008	0.77y		26.6	21.1	21.2
End summer 2009	0.94y		27.6	22.4	22.3
To-date	1.56y	Δ_{to_date}	31.0	26.0	25.2
Fitted logarithmic function			$\Delta = 5.778Ln(t)$ $+ 29.39$	$\Delta = 5.126Ln(t)$ $+ 24.82$	$\Delta = 4.985Ln(t)$ $+ 23.42$
			$R^2 = 0.9423$	$R^2 = 0.9179$	$R^2 = 0.9666$
End of service life	50y	Δ_{50}	52.0	44.9	42.9
Ratio Δ_{to_date} /($\Delta_{G,inst}$+ $\Delta_{Q,inst}$)			3.78	3.44	3.81
Ratio Δ_{50}/($\Delta_{G,inst}$+ $\Delta_{Q,inst}$)			6.36	5.93	6.50

6.7 Influence of environmental fluctuation and moisture content

The physical environment for the beams is represented by the relative humidity (RH) and temperature data plotted in Fig. 6-8. This can be characterized as either low temperature

with high RH or high temperature with low RH as presented in Fig. 6-10. The minimum, average and maximum temperatures of the colder months (averaged between winter of 2008 and 2009) were 2.1 ºC, 7.8 ºC and 14.1 ºC; and warmer months in summer 2008 were 13.4 ºC, 20.3 ºC and 28.4 ºC, respectively. This gives an average difference of 12.7 ºC between the two seasons. The daily fluctuations of the two quantities are important because the beams were in indoor, unheated conditions, particularly the temperature in the colder months and the RH in the warmer months. For example, during winter, the maximum differences in daily temperature and RH were observed to be 5.8 ºC and 13.3%, and in summertime, 7.0 ºC and 29.7%, respectively.
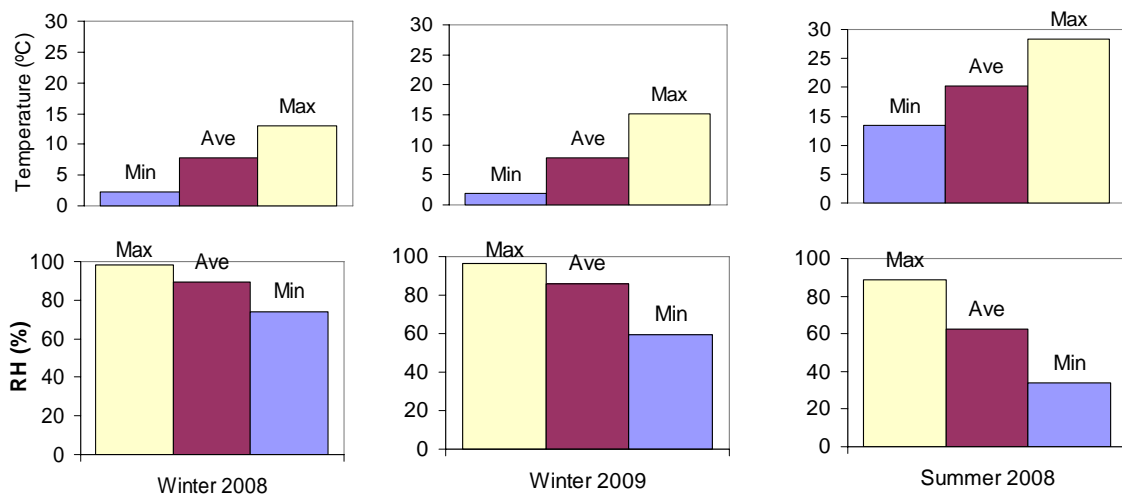
Fig. 6-10. Minimum, average and maximum temperature and relative humidity data monitored in the colder and warmer months

An attempt to draw a relationship between the RH, temperature and deflection of the beams with the moisture content (MC) of the LVL is presented in Fig. 6-11. The average MC of the LVL monitored from February 2008 to July 2009 ranged between 10.7 to 14.6%. It is clear that low temperatures and high RH increased the MC of the LVL and consequently caused the deflection increases between July – August 2008. During this period, temperatures fell to the lowest (2.6 ºC), RH was highest (92.5%) and MC highest (14.6%) and the beam deflections were largest for the 2008 year. The temperature then escalated to peak at 26 ºC with RH lowest (48.7%) in January 2009 when the MC descended to 10.8%. During this time, the deflections in all the beams remained in a quasi-plateau before the pattern repeated for the following year. Analysis of the experimental environmental data using the CSIRO equilibrium moisture content (EMC)

126

chart (Blakemore, 2003) indicated that the EMC in the garage varied considerably and was particularly high in the cooler months – varying between approximately 7% in the warmer months to more than 25% in the cooler months. This compares with the 8% to 12% range normally experienced in heated, indoor conditions.
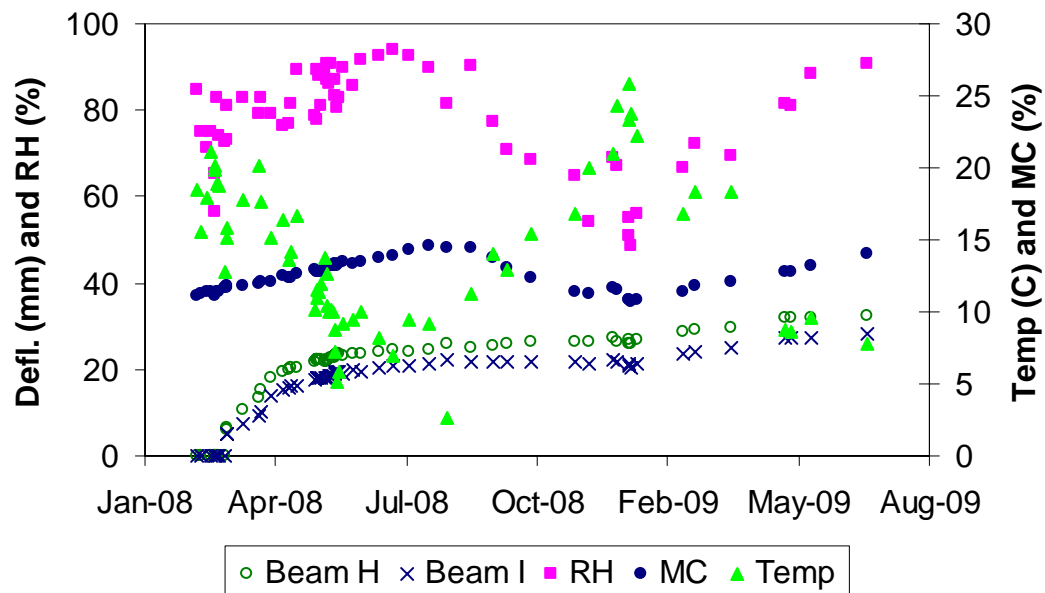
Fig. 6-11. Relationships between beam deflection and relative humidity and between temperature and moisture content

Although the MC of the LVL remained below 20% throughout the whole test, the measured RH was more than 75% for approximately 18 weeks during winter each year. These limits make the environmental condition for the beams equivalent to Eurocode 5 marginal to service class 3 (CEN, 2004b) or to a NZ3603 (SNZ, 1993) long-term duration factor of $k_2 = 3$. The significant EMC variation may contribute to the higher creep. For example, it is well established that it is not just the level of moisture content that affects creep deflections. The rate of change and number of cycles of moisture content and therefore EMC can have a more significant effect on creep behaviour, with rapid changes in EMC producing more severe creep under bending loads (mechano-sorptive creep (Toratti, 2004).

It is also evident that the creep mechanism is worse for longer spans where the stiffness of the floor is much more dependent on composite action between the concrete and the timber beams. Based on the review of literature available on TCC floors, it can be seen

that the effect of variation in EMC is significant on the long-term behaviour of TCC floors. Concrete creep and the various interactions of shrinkage and creep, shrinkage or swelling in the LVL, and creep of the connection system, contribute to significant additional deformation in TCC floor structures Five year long-term tests on TCC beams using glued-in rebars as connectors had most of the deflection develop during the first two years, after which creep deflections tended to either plateau or increase much more slowly (Ceccotti et al, 2006). However, another test on TCC beams with inclined proprietary (SFS) connectors showed a distinct increase through a 5-year experiment, with minimal reduction in the rate of deflection increase after the end of the second year (Kenel and Meierhofer, 1998).

When interpreting the data plotted in Fig. 6-8 and Fig. 6-9, it is important to note that the daily deflection fluctuations at any one point were attributed to the changes in relative humidity and temperature. The increase in deflection over time appeared to be accentuated by the cold weather, or, more specifically the low temperature, noting that the lowest temperatures during the winter months caused the greatest deflection. This is explained by the different thermal expansion rates and conductivities of the timber and the concrete. During winter the timber moisture content increased, leading to an expansion of the timber beam and, because this is mostly in tension for TCC, increasing deflections. Conversely, in the warmer months after winter, the gradual reduction in timber moisture content maintained the deflections for all the beams until the next cold period and its accompanying deflection increase. This mechanism is consistent with the behaviour observed in other experimental tests and numerical modelling (Ceccotti et al, 2006; Fragiacomo, 2006; Kenel and Meierhofer, 1998).

The results, for comparatively extreme environmental fluctuations, are expected to be indicative of the upper limits of long-term deflections that can be expected for TCC structures. More research needs to be undertaken for TCC floors in the more uniform indoor, air conditioned or heated environments.

6.8   Prediction of the long-term behaviour

The connection creep factor was found to have no direct effect on the deflection of TCC beams. For example, the connection creep factor, k_{37}, at 1.5 years for connection type P

used in beam J was approximately 2.5 times larger than that of connection type R in beams H and I (Table 6-2). No similar increment was observed in the deflections for the three beams corresponding to the differences of the creep factor in the connections. A larger creep factor results in a smaller effective slip modulus, which will increase the long-term deflection. However, since the creep coefficients of timber and concrete are the same in all the specimens, a decrease of 2.5 times in creep factor of connection does not necessarily imply an increase in deflection of 2.5 times. Recall that also the slip modulus and connector spacing is different in the 2 beams, I and J.

The experimental beam deflections (up to 1.5 years) are compared in Fig. 6-12 with the deflections expected for service classes 2 and 3 according to the Eurocode 5 (CEN, 2004b). The total creep factor $k_{2,eq}$ is defined as the ratio between the total deflection and the sum of the instantaneous deflections measured when the props were removed and when the live load was applied. Since the composite beam is statically indeterminate internally, with three components characterized by different creep coefficients, the $k_{2,eq}$ factor will not be a real creep coefficient. Instead, it can be regarded as a system property that depends on the interactions between the materials, and which is also affected by thermal, moisture strains, and drying shrinkage of concrete.

In the Eurocode 5, the creep coefficient is $k_{def} = 0.8$ and $k_{def} = 2$ for service classes 2 and 3, respectively. The analytical deflections were calculated with the "gamma" method, using the effective bending stiffness proposed in Annex B of Eurocode 5 (CEN, 2004b). In order to account for the effect of creep in the concrete, timber and connection, effective moduli were calculated for each material by dividing its Young's modulus by one plus its material creep coefficient. This simplified method, introduced by Ceccotti (1995) and known as the "Effective Modulus Method", uses the pure creep coefficients of the different components. The Fig. 6-12 experimental-analytical comparison shows that the experimental deflections for all the beams near 1.5 years were in closer proximity (within ± 5% as illustrated by the error bars in Fig. 6-12) to the analytical deflections calculated using service class 3 conditions, hence proving that the environmental conditions that the beams were subjected to can be better represented by the service class 3. This method, however, does not account for the effect of inelastic strains on the internal forces and the deflection of TCC caused by the different thermal expansion and shrinkage of concrete

and timber. As such, the analytical deflection approximation at the end of service life (50 years) underestimated the actual value as described in the following paragraph.

(a)

(b)
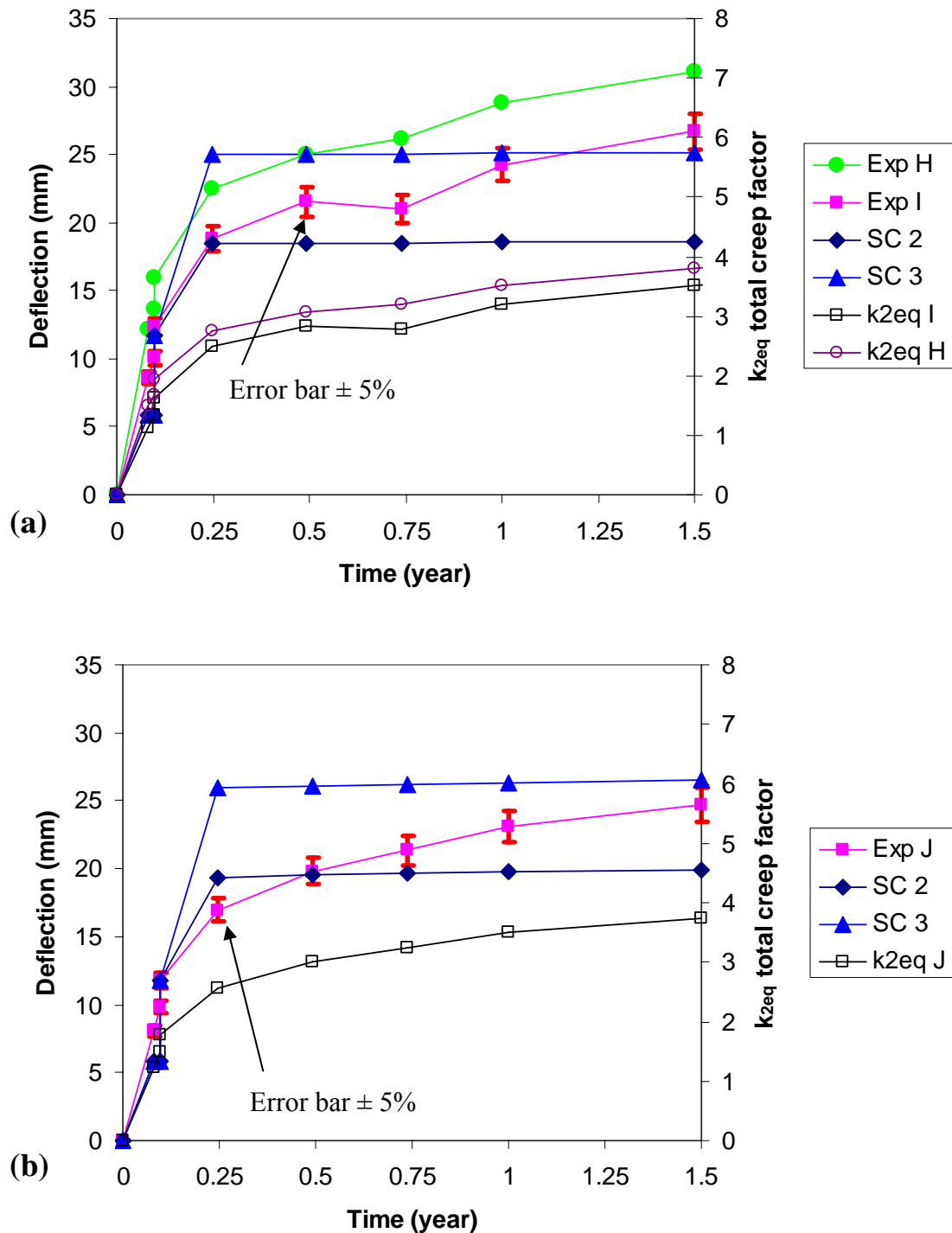
Fig. 6-12. Experimental-analytical deflection of beams up to 1.5 years with their corresponding total creep factor, $k_{2,eq}$: (a) Beams H and I; and (b) Beam J. (SC = Service Class)

In order to predict the long-term final maximum deflection of the beams at the end of service life (50 years), the experimental deflection-time plot of the beams in Fig. 6-9 were fitted with the logarithmic functions given in Table 6-3, with the final maximum deflections for beams H, I, and J of 52.0 mm, 44.9 mm and 42.9 mm, respectively. While these all exceed the Eurocode long-term deflection limit of span/200 = 40 mm, the cyclic environmental variations are likely to overestimate the final deflection. The cyclic trend, in fact, spoils the typical creep trend over time, characterized by increasing value with reduced rate, and makes the best fit curve somewhat less reliable. Advanced numerical models (Schänzlin, 2003; Fragiacomo, 2005; To, 2009) can separate the cyclic yearly variation from the typical creep trend, so these and continuing the experiment for another couple of years are therefore recommended as means of checking the accuracy of the 50-year predictions.

The "Effective Modulus Method" was used to compute the analytical final maximum deflections for service classes 2 and 3 as presented in Table 6-4. This analytical approach underestimated the experimental results by factors of 2.33 and 2 for service class 2, and by 1.74 and 1.52 for service class 3 in beams I and J, respectively. A possible reason for this underestimation is that the effects of drying shrinkage of concrete and, shrinkage/swelling of concrete and timber due to thermal expansion were neglected as mentioned earlier. This is further explained in the following.

Table 6-4. Analytical deflections using pure and effective creep coefficients compared to experimental deflections at 1 and 50 years (measures in mm)

Time	Beam I				Beam J			
	Pure creep coef.		Eff. creep	Exp	Pure creep coef.		Eff. creep	Exp
	SC 2	SC 3	SC 3	(Exp fit)	SC 2	SC 3	SC 3	(Exp fit)
1 y	18.6	25.1	-	24.3	19.8	26.4	-	23.1
50 y	19.2	25.8	30.1	(44.9)	21.5	28.2	33.7	(42.9)

SC = Service Class

The stresses vary over time within the statically indeterminate system built from three different materials with different creep behaviours. Timber creeps more slowly than

concrete. Based on the models of Hanhijarvi (1995) and Toratti (1992), Schänzlin and Fragiacomo (2007) found that timber creeps about 60% between 3 to 7 years while concrete creeps about 95% within the same timeframe. The more rapidly creeping material (in this case, the concrete) will become softer than the slower material (timber). This will redistribute the internal forces from the concrete to the timber. However, while over time the concrete reduces its elastic strains (and stresses) and timber increases its elastic strains (and stresses), the connection creep absorbs the differences so the system maintains an internal equilibrium.

Since the creep coefficient of concrete and its rate are different from that of timber and from that of the connection, both at the end of service life and over time, and for the phenomena described in the previous paragraph, an effective creep coefficient for each of the materials, was introduced by Schänzlin and Fragiacomo (2007) to better approximate the long-term effects for TCC structures. The effective creep coefficients for timber, concrete and connection were obtained by multiplying the pure creep coefficient by a ψ coefficient for timber and concrete, and by a constant of one for connection, as given in (Eq. 6-4) to (Eq. 6-6), respectively.

$$E_{t,eff} = \frac{E_t}{1 + \psi_t k_{def}} \qquad \text{(Eq. 6-4)}$$

$$E_{c,eff} = \frac{E_c}{1 + \psi_c \phi_c} \qquad \text{(Eq. 6-5)}$$

$$K_{eff} = \frac{K_s}{1 + \phi_{conn}} \qquad \text{(Eq. 6-6)}$$

where, $\psi_t = 1.0$ (for $t = 50$y) or 0.5 (for $t = 3$ to 7y) and $\psi_c = 1.82 - 0.24\gamma_1^{3.51}$ (for $t = 50$y) with $\gamma_1 = 0.552$ (beam I) and 0.579 (beam J).

The deflections at 50 years for beams I and J predicted using this method (Table 6-4) were also found to underestimate the extrapolated experimental deflections by 1.49 and 1.27 times for beams I and J, respectively. This method, with an effective creep coefficient, underestimated the experimental values less than the averages of 1.63 and 1.38 predicted using the pure creep coefficient.

The long-term deflection was found to be important for the three beam specimens as it is likely to exceed the limit of span/200 generally accepted by codes of practice. Possible methods of minimizing the long-term deflection include reducing the initial deflection with fresh concrete by propping the timber joist, using a pre-cambered timber joist, and using low-shrinkage concrete. Alternatively, the concrete slab could be precast and allowed to shrink before being connected to the timber joist.

6.9   Conclusions

Long-term tests were conducted in an uncontrolled, unheated indoor environment using three different types of TCC connections and three 8 m span TCC beams. Test results from sustained loading durations of 1.34 and 1.56 years, respectively, were presented in this chapter. The specimens were exposed to environmental conditions characterized by either low temperature with high relative humidity or high temperature with low relative humidity, conditions considered to be reasonably severe with relatively high daily fluctuations of temperature in the cooler months (maximum of 5.8 ºC) and of relative humidity in the warmer months (maximum of 29.7%). The equilibrium moisture content dropped to approximately 7% in the warmer months and rose to approximately 25% in the cooler months, which exposed the specimens to an environmental condition classed as marginal to service class 3 according to Eurocode 5. The relative connection slips and beam deflections fluctuated in response to the environmental changes. Large slips and deflections were induced by the low temperatures and equivalent high equilibrium moisture content during the cooler months, while in the warmer months with higher temperatures and low equilibrium moisture content, they remained more consistent.

The creep coefficients, $\phi(t,t_0)$, for the connection specimens were extrapolated to the end of service life (50 years). The corresponding creep coefficients were, k_{def} = 2.1 for the triangular notched and coach screw connection (T), k_{def} = 1.6 for the rectangular notch and coach screw connection (R) and k_{def} = 5.7 for the toothed metal plate connection (P).

Two of the beam specimens had connection type R. Of these, beam H had normal weight concrete and beam I had low shrinkage concrete, with half the drying shrinkage of normal weight concrete. The third, beam J, had connection type P and low shrinkage concrete.

Beam I, with low shrinkage concrete deflected 5 mm less than beam H with normal weight concrete corresponding to span/1600.

Superimposed load induced an instantaneous 30 to 40% increase in beam deflections. A significant portion of the deflection occurred in the first quarter of the year and, most of the remainder (with annual fluctuations) until 1.2 years after which the deflections remained constant. The mid-span deflections were extrapolated to the end of service life (50 years), with the final deflection for the beams predicted to be 52.0, 44.9 and 42.9 mm for beams H, I and J, respectively. Although the predicted final long-term deflections exceeded the commonly accepted limit of 40 mm (span/200), the environmental conditions were deliberately severe. Also, the extrapolation was based on a relatively short duration experiment and there was difficulty fitting a logarithmic curve to fluctuating experimental results which are likely to introduce additional error.

Two analytical methods were compared to the extrapolated experimental deflections at the end of the service life. The "Effective Modulus Method", using the separate material creep coefficients for the timber, concrete and connection proposed by Ceccotti (1995) significantly underestimated the extrapolated experimental deflections. The "effective creep coefficient method" recommended by Schänzlin and Fragiacomo (2007) underestimated deflections by 40 to 60%.

The time-dependent behaviour and creep mechanism in TCC are known to be very complex because the timber, concrete and connection all creep differently. Some creep rates are affected by environmental conditions so stresses are redistributed within the three components. Creep is inevitable so the long-term deflections of TCC structures are most effectively minimized by reducing initial deflections as much as possible by propping or pre-cambering the timber joist, and by using low shrinkage concrete. The other alternative is to precast the concrete slab and allow it to shrink before being connected to the timber joist.

It is recommended that long-term tests continue for at least another two years, and that advanced numerical models be used to extrapolate experimental results to the end of the service life in order to provide more conclusive experimental-analytical comparisons and more confidence in design recommendations. In addition, a long-term test should be

conducted in a more representative service environment, with an equilibrium moisture content of 8 to 12% found in air-conditioned and heated buildings.

7   Design and Construction of LVL-Concrete Composite Beams

This chapter has been reproduced from a journal paper submitted to the Structures and Buildings ICE Journal – Timber Special Issue with the title of "Design and construction of a LVL-concrete composite floor" (Yeoh et al, 2009a).

The purpose of this chapter is to present the design procedure for timber-concrete composite floor system in accordance to the γ-method proposed by the Annex B of Eurocode 5. This design procedure which applies the connection's strength and stiffness values derived in Chapter 4, and connection's creep coefficient derived in Chapter 6, satisfies the short- and long-term ultimate and serviceability limit states verifications. A full worked example compliments this chapter.

Supplementary to this chapter is Appendix 10 presenting the span tables of semi-prefabricated LVL-concrete composite floors of up to 15 m long. The span tables are ready for use by a practicing engineer without needing to carry out long design calculations. It is an important contribution of this thesis to the construction industry with the main objective to promote the use of timber-concrete composite floor systems in multi-storey timber buildings. The span tables give the safe live load in kN/m^2 for M-section modules (first mentioned in Chapter 3) with 3 connection types: (1) 300 mm long rectangular notch cut in the LVL joist and reinforced with a 16 mm diameter coach screw (R-300); (2) triangular notch reinforced with the same coach screw (T); and (3) two 333 mm long toothed metal plates (P) discussed in Chapter 4.

7.1   Abstract

This chapter describes the design and construction of a novel semi-prefabricated LVL-concrete composite floor that is under development in New Zealand. In this solution, the floor units made from LVL joists and plywood are prefabricated in the factory and transported to the building site. The units are then lifted onto the supports and connected to the main frames of the building and to the adjacent units. Finally, a concrete topping is poured on top of the units in order to form a continuous slab connecting all the units. Rectangular notches cut from the LVL joists and reinforced with coach screws provide the composite action between the concrete slab and the LVL joists. This system proved to be an effective modular solution that ensures rapid construction. The effective bending stiffness method, also known as the 'gamma method' in accordance with the Annex B of Eurocode 5, is used for the design of the composite floor at ultimate and serviceability limit states. The design procedure of the semi-prefabricated composite floor in the short- and long-term is presented in the chapter and explained with a detailed worked example.

7.2   Introduction

Timber-concrete composite (TCC) floor system is a construction technique where a concrete slab is mechanically connected to its supporting timber joists using either notches cut from the timber or suitable mechanical fasteners. The concrete can be cast in-situ or, alternatively, the fasteners can be inserted into a prefabricated concrete slab to provide on-site connection to the timber. The shear connectors provide composite action which utilizes the advantages of both materials: tensile and bending resistance of timber, and compressive strength of concrete (Ceccotti, 1995). In an effort to introduce new applications of timber in multi-storey buildings in New Zealand, medium to long-span TCC floors of 8 to 10 m using laminated veneer lumber (LVL) have been proposed. There is currently an extensive research program ongoing at the University of Canterbury aimed to develop a semi-prefabricated LVL-concrete composite floor system (Yeoh et al, 2009b, 2009c, or Chapter 3). This chapter reports the design and construction of the proposed semi-prefabricated composite system.

The design of TCC is not found in most of the timber standards around the world other than the Eurocodes, hence resulting in the use of this construction technique mainly in

137

Europe. Specifically, for TCC, the design provisions are given in Eurocode 5, Part 2 (CEN, 2004c) and Eurocode 5, Part 1, Annex B (CEN, 2004b). Because the connection between the interlayer, concrete and timber, is normally semi-rigid which will result in a relative slip between the bottom fibre of the concrete and the upper fibre of the timber, the assumption of plane sections remaining plane does not apply to the composite section as a whole. Therefore, the method of the transformed section from the conventional principles of structural analysis cannot be used. In order to account for the partial composite action resulting from the flexibility of the shear connection, the approximate solution using an effective bending stiffness (also known as the 'gamma' method) derived by Möhler (1956) for timber-timber composite beams with flexible connection proposed in the Annex B of the Eurocode 5 (CEN, 2004b) is used (Ceccotti, 2002).

7.3   Semi-prefabricated LVL-concrete composite floor

Floors are a crucial part of multi-storey timber buildings. The advantages of TCC floors over timber-only floors are many such as greater stiffness, less susceptibility to vibrations, better seismic performance, higher fire resistance and, last but not least, better acoustic separation. An increasing range of TCC systems has been developed, including cast-in-situ, semi-prefabricated, and fully prefabricated floors (Yeoh et al, 2009f or Chapter 2).

A semi-prefabricated composite floor system built with LVL beams which act as floor joists and a plywood interlayer as permanent formwork is proposed for the New Zealand building industry (Fig. 7-1). The connection system has notches cut from the LVL joist and reinforced with a coach screw to provide more ductile behaviour during failure and to increase the shear strength. These notches are cut in the beams before the plywood interlayer is nailed on. Toothed metal plate is another preferred connection where no cutting of notches is required which allows fast and easy installation of the connection with the help of an industrial hydraulic press (Yeoh et al, 2009c or Chapter 3). This floor system is comprised of a typical 2400 mm wide "M" section unit with one 63 × 400 mm LVL joist on each side and a double LVL in the centre and spans between 8 to 12 m requiring 6 to 10 connectors along the length of each joist to provide adequate composite action. Each unit weighs approximately 8 kN, resulting in a lightweight component that is easy to transport and crane. The system was used as floors in a large two-third scale, two-storey, experimental post-tensioned timber building (Fig. 7-2) that is under development

through a combined initiative of the University of Canterbury and STIC (Structural Timber Innovation Company Ltd). The building was constructed to aid the development of connection details, to provide cost and construction sequencing information, and to evaluate the earthquake performance of the structural system. The floor units were prefabricated and delivered on-site by commercial Glulam (glue laminated timber) manufacturers. New Zealand timber fabricators do not have fully mechanized production capability and rely mainly on handheld tools which resulted in high fabrication costs for the floor units. Approximately 25% of the total fabrication cost was attributed to labour which calls for an improvement in the New Zealand timber manufacturing processes. Overall, the floor units contributed to 42% of the total construction cost. On-site assembly was rapid (Fig. 7-3). Each floor unit was held by overhead crane for approximately 2 minutes, equating to a floor coverage rate of 486 m^2/hour. Floor units were light enough to be manoeuvred manually.
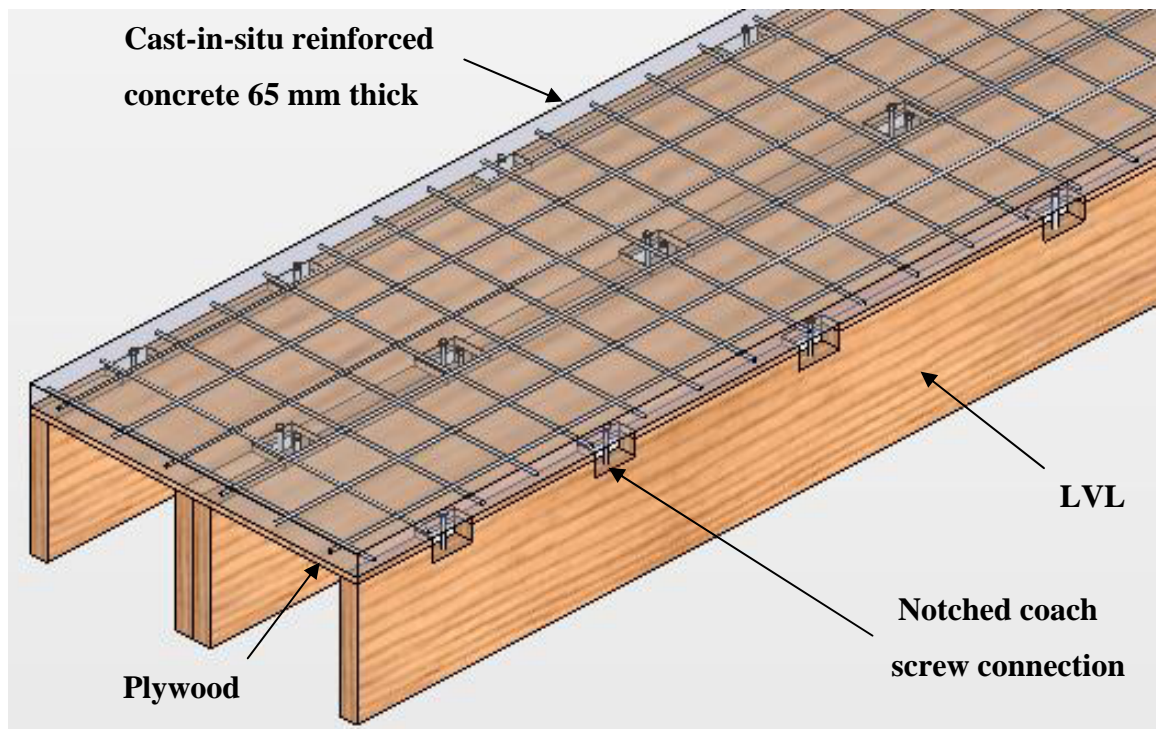
Fig. 7-1. "M" section semi-prefabricated LVL-concrete composite floor system
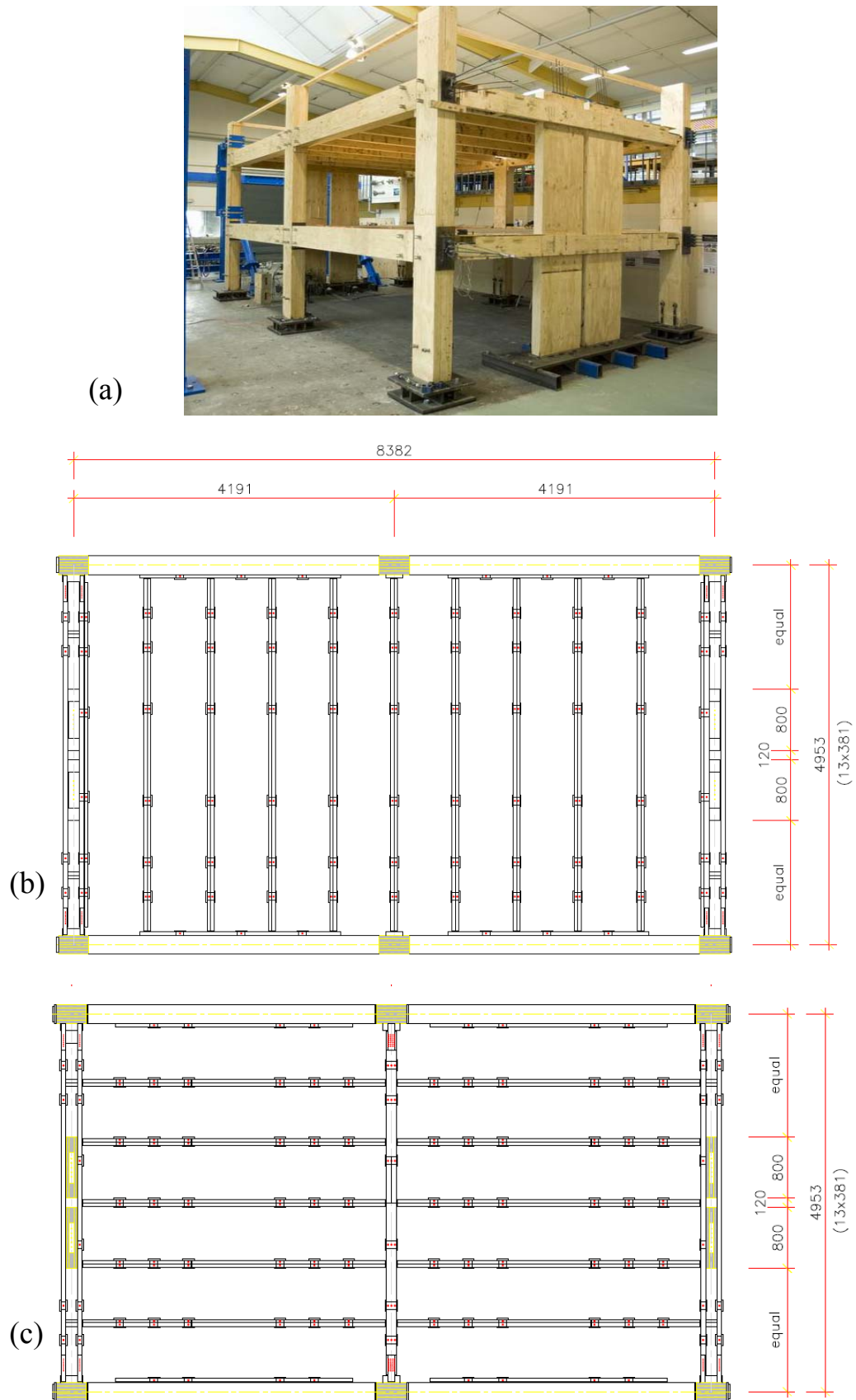
Fig. 7-2. Experimental post-tensioned timber building 3-D view in (a), floor plan of level 2 and 3 in (b) and (c), respectively.

(a)

(b)

(c)
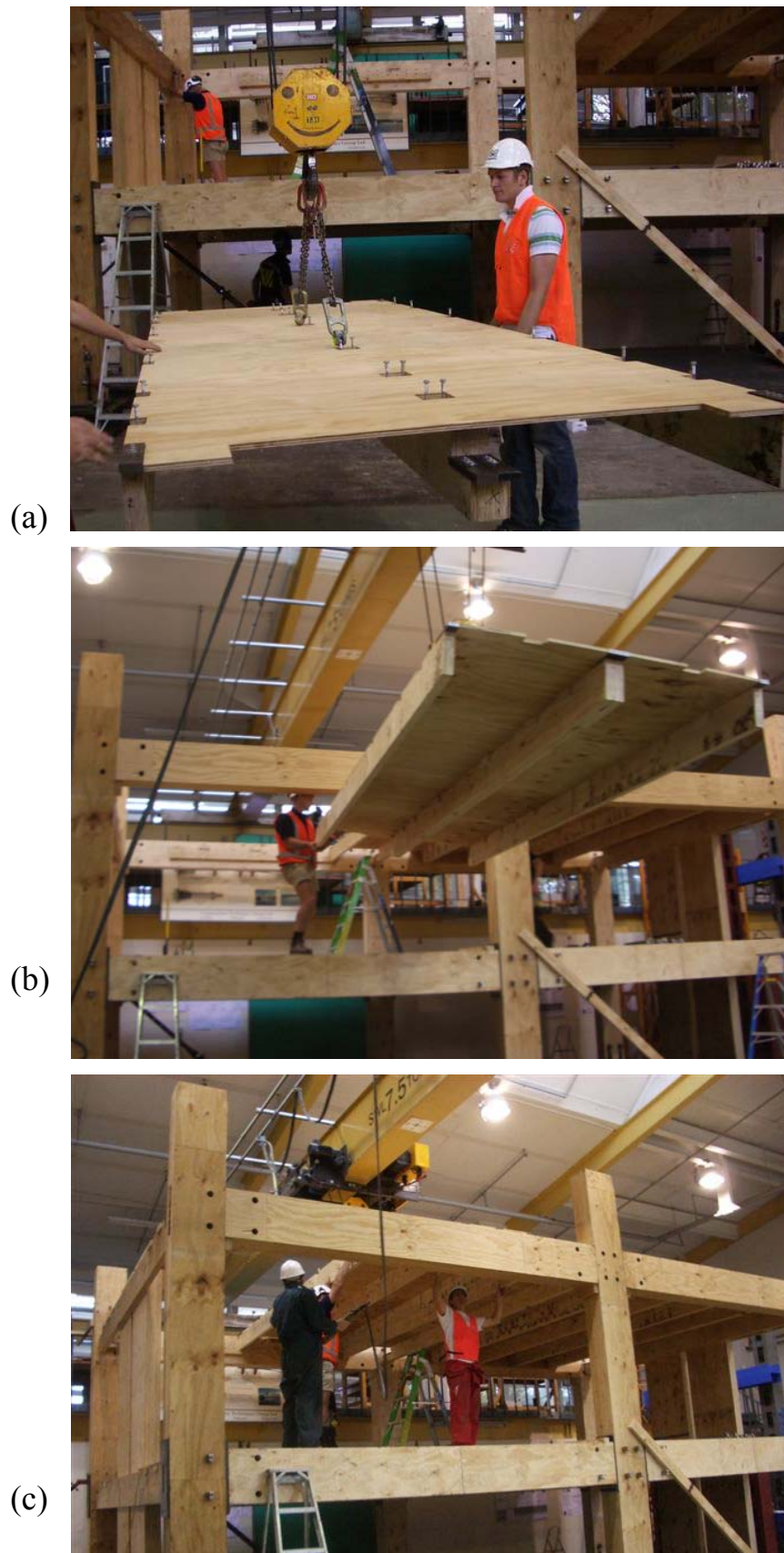
Fig. 7-3. On-site assembly of floor unit: (a) Lifting of "M" section floor unit; (b) Unit craned to position; and (c) Units were manually adjusted without the help of the crane
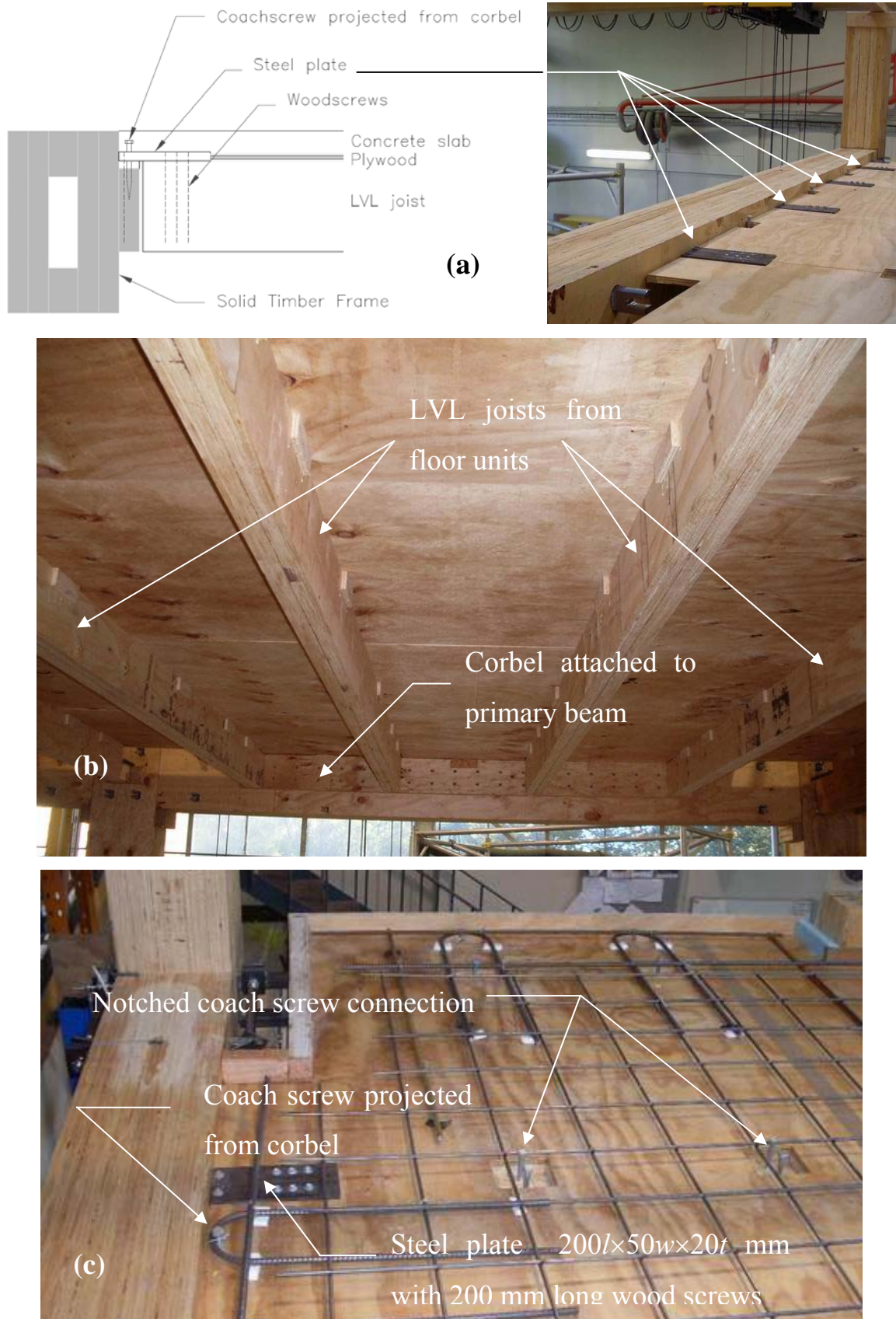
Fig. 7-4. Support connection details: (a) Schematic diagram; (b) Underside of floor units sitting on corbel; and (c) Floor unit with details of 20 mm thick steel plate locked onto corbel

The floor units were supported on specially designed corbel seat consist of 20 mm thick steel plates and 200 mm long 14 gauge type 17 wood screws (Fig. 7-4) that allows fastening of the connections from the top which further increases the construction rate and ensure a modular system (Carradine et al, 2009). Such support seating is able to accommodate large seismic deformations and maintain significant in-plane seismic forces to meet the New Zealand earthquake requirements (Newcombe et al, 2009). Joist hanger support connection with Type 17 screws and in-plane floor shear transfer using either coach screws inserted in the lateral face of the beam or reinforcing bars connected to fasteners in the solid wall using threaded couplers have been proposed in literature (Smith et al, 2008 and 2009). Steel mesh is used to provide shrinkage control for a typical 65 mm thick cast in-situ concrete slab.

The units can be propped while the concrete cures or alternatively in an unpropped solution, the LVL joists can be pre-cambered so that the mid-span deflection is marginalized by dead and construction loads. Propping of the joists will incur extra cost and interruption to the builders on site. Conversely, precambering of the joists will perform the same result although it is not particularly practical. Precambering of the LVL joists can be achieved in two methods: (1) cutting a radius in the LVL joist during the production of the LVL; or (2) during the prefabrication of the units, the LVL joists are clamped downwards at each end over a central support, forcing the joints to bend, then the permanent formworks, in this case, the plywood, are nailed or screwed to the LVL flange. Another available solution is to increase the size of the LVL joist in order to minimise the effect of an unpropped floor. The final choice, however, would depend on the cost and savings achievable from each of the aforementioned solutions.

Advantages of this solution include: (1): ease of transport and lifting of the panels due to their low weight; (2) fast installation and ease of positioning the panels without the need of a crane once they are lifted in place; (3) construction of a monolithic concrete slab with better in-plane strength and stiffness, and no need for additional connections between adjacent panels; (4) high strength and stiffness achievable with reduced number of connectors, thanks to the effectiveness of the notched connection detail; (5) possibility to construct medium to long-span floors, in the range of 8 to 12 m; and, therefore, (6) a system capable of competing with traditional precast concrete solutions. One

disadvantage is the need to introduce a "wet" component (the fresh concrete) on the building site, where all other components are "dry" for a multi-storey timber building.

7.4   Basics of design

The design of TCC beams has to be carried out in order to satisfy both serviceability (SLS) and ultimate limit states (ULS) in the short- and long-term (the end of the service life). The ULS is checked by comparing the maximum shear force in the connection, the maximum stress in concrete, and the combination of axial force and bending moment in timber with the corresponding resisting design values. The most important serviceability verification is the control of maximum deflection, which is used also for an indirect verification of the susceptibility of the floor to vibration, as suggested by AS/NZS 1170 Part 0 (AS/SNZ, 2002). Two types of problem have to be addressed when evaluating stress and deflection for a TCC beam: (1) the flexibility of connection which leads to partial composite action; and (2) the time-dependent behaviour such as creep, mechano-sorption, shrinkage/swelling, thermal and moisture strains of timber and concrete, and creep and mechano-sorption of the connection system. An elastic analysis using the gamma method is applied for the short-term (instantaneous) verifications, while the 'Effective Modulus Method' recommended by Ceccotti (2002) is used for the long-term verifications in order to account for the effect of creep of the different materials.

The limit state design of TCC beam considering both short- and long-term verifications is illustrated in Fig. 7-5 The complete design procedure should cover the following verifications (Ceccotti et al, 2002): (1) ULS in the short-term, where the structure is under maximum load (i.e. $F_{d,u} = 1.2G + 1.5Q$ in accordance with the AS/NZ Standards) applied instantaneously just after construction; (2) SLS in the short-term, where the deflection is verified upon the application of imposed load (i.e. only Q that is not factored); (3) ULS in the long-term, where the quasi-permanent load condition (i.e. $F_{d,p} = G + 0.4Q$ in accordance with the AS/NZ Standards) is applied throughout the service life of the structure, and the remaining part of the ultimate load (i.e. $\Delta F = F_{d,u} - F_{d,p} = 0.2G + 1.1Q$) is applied at the end of the service life; and (4) SLS in the long-term at the end of the service life, where the time dependent phenomena (creep) in the materials are evaluated under the quasi-permanent load condition ($F_{d,p} = G + 0.4Q$) considered as applied throughout the service life, and the instantaneous effects are produced by the difference

144

between the rare ($F_{d,r} = G + Q$) and the quasi-permanent ($F_{d,p} = G + 0.4Q$) load condition ($F_{d,r} - F_{d,p} = (1 - 0.4)Q$).
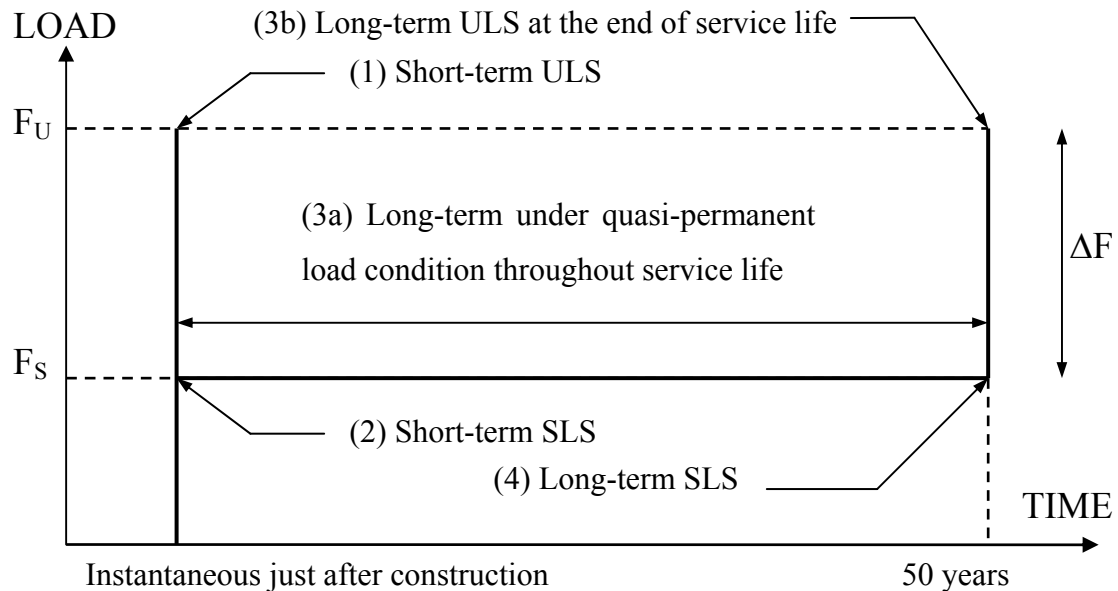
Fig. 7-5. Limit state design of TCC beams for verifications in the short- and long-term

The ULS long-term verifications are theoretically indispensable for the reason that TCC structures are internally statically indeterminate structure made from three components, concrete, timber and connection, each of them characterized by a different creep coefficient. Since the creep coefficients have different trend in time, they will lead to a redistribution of strains and stresses over time in the different materials. This implies the dependency of the load bearing capacity on the time when it is evaluated and, therefore, the need to carry out ULS verifications at different times (the assembling time, where no creep deformation has developed, and the end of the service life, when all materials have crept differently and a stress redistribution has taken place in the composite beam). Furthermore, the concrete shrinkage and environmental variations will induce additional stresses and deflections which have not been considered in the design and for which some studies are in progress (Fragiacomo 2006, Schänzlin and Fragiacomo, 2007, 2008). On the other hand, the SLS verifications in the long-term considering both the quasi-permanent and rare combinations have been recommended by Eurocode 5, Part 1 (CEN, 2004b) assigning a limit between 1/150 to 1/300 of the span length. However, SLS limits are less stringent than ULS limits depending on the function of the structure and requirement of the client.

145

7.5   Flexibility of connection

Since most of the connection systems exhibits non-linear shear force-relative slip relationship, Ceccotti (1995) proposed to define two different values of slip modulus:

$$K_s = \frac{0.4R_m}{v_{0.4}}$$ $$K_u = \frac{0.6R_m}{v_{0.6}}$$ Eq. 7-1   Eq. 7-2

where R_m is the mean shear strength obtained from a push-out test, $v_{0.4}$ and $v_{0.6}$ are slips measured under a shear load equal to $0.4R_m$ and $0.6R_m$ respectively. The quantities K_s and K_u are therefore secant slip moduli that are employed, respectively, for serviceability and ultimate limit state verifications (Fig. 7-6). They should be evaluated by performing push-out experimental tests on small TCC blocks in accordance with EN 26891 (CEN, 1991) such as those found in literature (Lukaszewska et al, 2007a and Yeoh et al, 2009e or Chapter 4).
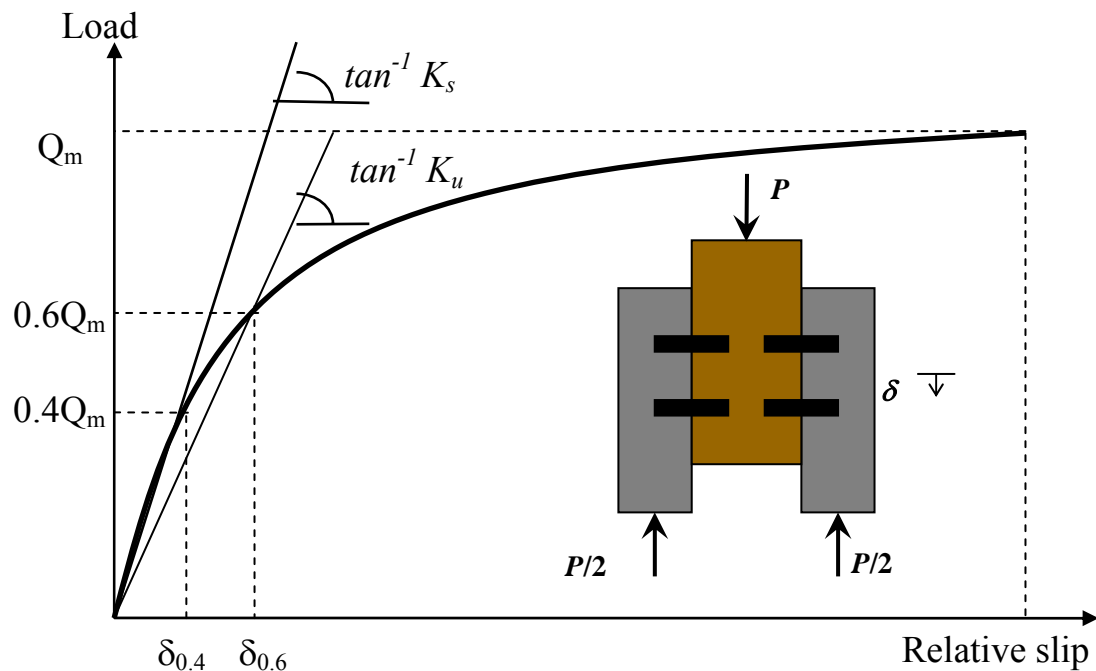
Fig. 7-6. Evaluation of the secant slip moduli of connection for serviceability and ultimate limit states by performing a push-out test

If experimental results for the connection properties are not available, Eurocode 5, Part 1-1 (CEN, 2004b) provides some formulas for timber-timber connection systems based on

the European Yielding Model. Those formulas are then extended by Eurocode 5, Part 2 (CEN, 2004c) to TCC connections by doubling up the former values of slip moduli and by increasing of 20% the former values of shear strength. Studies recently performed (Ceccotti et al, 2007, Lukaszewska et al, 2007), however, showed that significant errors may be introduced using the analytical approach based on the European Yielding Model, and recommended that experimental push-out tests be performed to fully characterize the connection system.

7.6   Design formulae

The elastic formulas for solving the TCC beam are reported herein after:

$$(EI)_{ef} = E_1 I_1 + E_2 I_2 + \gamma_1 E_1 A_1 a_1^2 + \gamma_2 E_2 A_2 a_2^2 \qquad \text{Eq. 7-3}$$

$$\gamma_1 = \frac{1}{1 + \dfrac{\pi^2 E_1 A_1 s_{ef}}{K l^2}} \qquad \text{Eq. 7-4}$$

$$\gamma_2 = 1 \qquad\qquad A_i = b_i h_i \ \text{ with } i = 1,2 \qquad \text{Eq. 7-5} \qquad \text{Eq. 7-6}$$

$$I_i = \frac{b_i h_i^3}{12} \ \text{ with } i = 1,2 \qquad a_1 = \frac{\gamma_2 E_2 A_2 H}{\gamma_1 E_1 A_1 + \gamma_2 E_2 A_2} \qquad \text{Eq. 7-7} \qquad \text{Eq. 7-8}$$

$$a_2 = \frac{\gamma_1 E_1 A_1 H}{\gamma_1 E_1 A_1 + \gamma_2 E_2 A_2} \qquad H = h_1 / 2 + a + h_2 / 2 \qquad \text{Eq. 7-9} \qquad \text{Eq. 7-10}$$

$$s_{ef} = 0.75 s_{min} + 0.25 s_{max} \qquad u = \frac{5 F_d^* l^4}{384 (EI)_{ef}} \qquad \text{Eq. 7-11} \qquad \text{Eq. 7-12}$$

$$\sigma_{m,i}(x) = \frac{1}{2} \cdot \frac{E_i a_i M^*(x)}{(EI)_{ef}} \qquad \sigma_1(x) = -\frac{\gamma_1 E_1 a_1 M^*(x)}{(EI)_{ef}} \qquad \text{Eq. 7-13} \qquad \text{Eq. 7-14}$$

$$\sigma_2(x) = \frac{\gamma_2 E_2 a_2 M^*(x)}{(EI)_{ef}} \qquad\qquad N_i^*(x) = \sigma_i(x)\cdot A_i \qquad\qquad \text{Eq. 7-15 \quad Eq. 7-16}$$

$$M_i^*(x) = \sigma_{m,i}(x)\cdot Z_i \qquad\qquad V_2^*(x) = V^*(x) \qquad\qquad \text{Eq. 7-17 \quad Eq. 7-18}$$

$$F^*(x) = \frac{\gamma_1 E_1 A_1 a_1 s(x)}{(EI)_{ef}}\cdot V^*(x) \qquad\qquad \text{Eq. 7-19}$$

where the subscripts *1* and *2* refer to concrete and timber, respectively (see also Fig. 7-7 for notations): E and K are the Young's modulus of material and slip modulus of connection, respectively; A and I are the area and the second moment of area of the *ith* cross-section, respectively; Z is the section modulus of the *ith* cross-section; $(EI)_{ef}$ is the effective flexural stiffness of the composite beam; u is the mid-span vertical displacement, evaluated for simply supported beams, the most common case; F_d^* is the design load combination, uniformly distributed along the beam; σ_1 and σ_2 are the stress components due to the axial force in concrete and timber, respectively; $\sigma_{m,1}$ and $\sigma_{m,2}$ are the maximum stress components due to the bending moment in concrete and timber, respectively; N_i^* and M_i^* are the demand of axial force and bending moment in the *ith* component, respectively; V_2^* is the shear force demand in timber, evaluated by assuming that the timber beam resists the entire shear force of the composite beam; F^* is the shear force demand in the connection system; s is the spacing between the connectors; V^* and M^* are the demand of shear force and bending moment in the composite beam, respectively; x is the abscissa along the beam axis where the stresses and internal forces are being evaluated; and, s_{min}, s_{max} and s_{ef} are the minimum, maximum and effective spacing of connectors, respectively. Eq. 7-3 to Eq. 7-19 are used for design in the short-term of the composite beam. The different stiffness properties of the connection system due to the non-linear mechanical behaviour are taken into account by using the slip modulus K_s given by Eq. 7-1 for serviceability limit state verifications, whilst the slip modulus K_u given by Eq. 7-2 is used for ultimate limit state verifications.
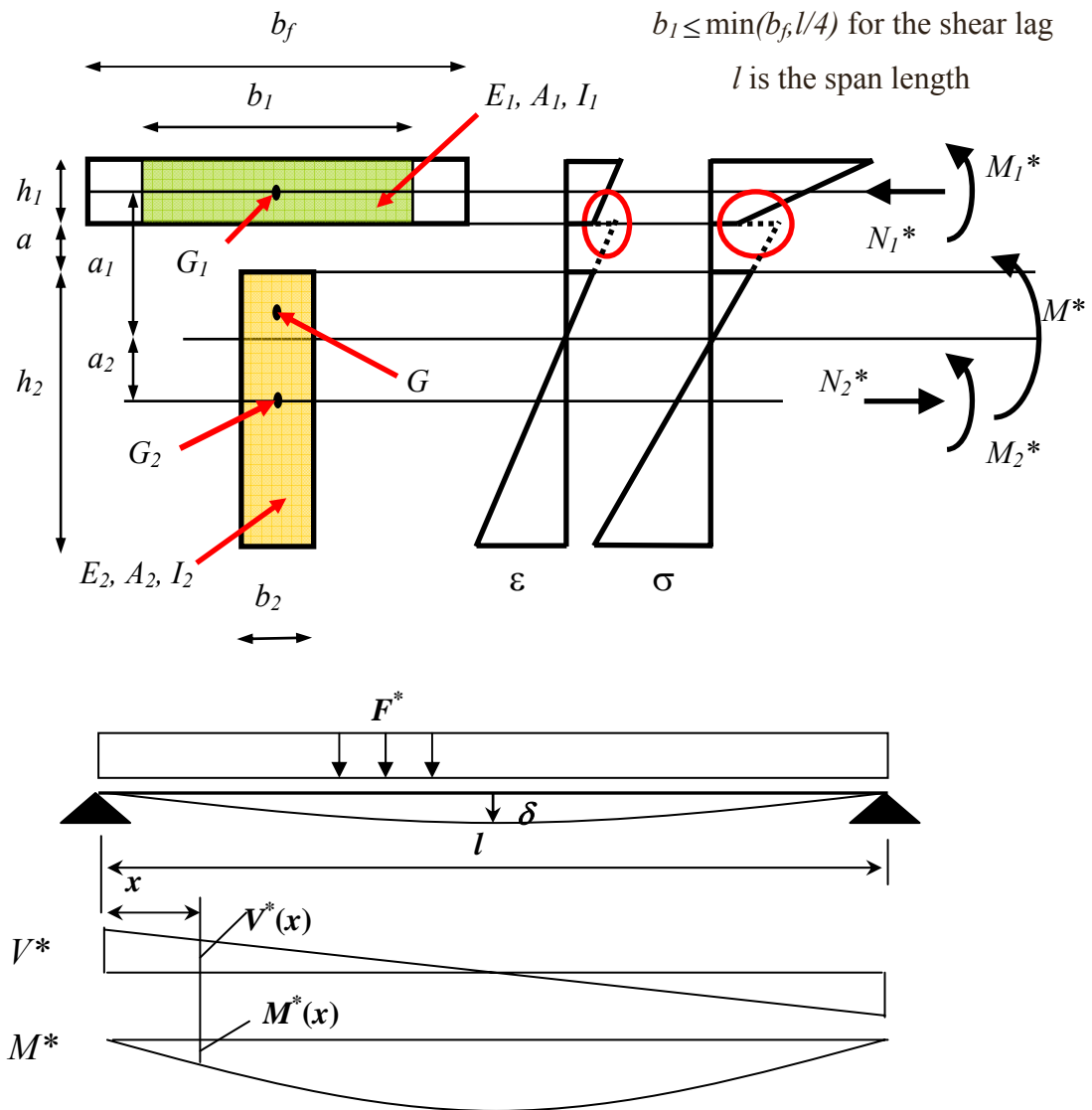
Fig. 7-7. Symbols used in the elastic formulas of composite beams with flexible connection

7.7   Time-dependent behaviour

The creep of the concrete flange, timber beam, and connection system can be accounted for, in long-term verifications, by replacing the elastic moduli of concrete E_1 and timber E_2, and the slip modulus of connection K with the effective moduli $E_{1,eff}$, $E_{2,eff}$ and K_{eff} given by:

$$E_{1,eff} = \frac{E_1}{1 + \phi_1(t,t_0)}$$

Eq. 7-20

$$E_{2,eff} = \frac{E_2}{1 + \phi_2(t - t_0)}$$

<div align="right">Eq. 7-21</div>

$$K_{eff} = \frac{K}{1 + \phi_f(t - t_0)}$$

<div align="right">Eq. 7-22</div>

where $\phi_1(t, t_0)$, $\phi_2(t - t_0)$ and $\phi_f(t - t_0)$ are, respectively, the creep coefficient of concrete, timber, and mechanical connection system, t and t_0 are, respectively, the final time of analysis (the end of the service life, usually 50 years) and the initial time of analysis (the time of application of the imposed load). The creep of timber and connection is provided by NZS 3603 (SNZ, 1993) as k_2 and k_{37} coefficients, respectively, given by:

$$k_2 = 1 + \phi_2(t - t_0) \qquad\qquad k_{37} = 1 + \phi_f(t - t_0)$$

<div align="right">Eq. 7-23   Eq. 7-24</div>
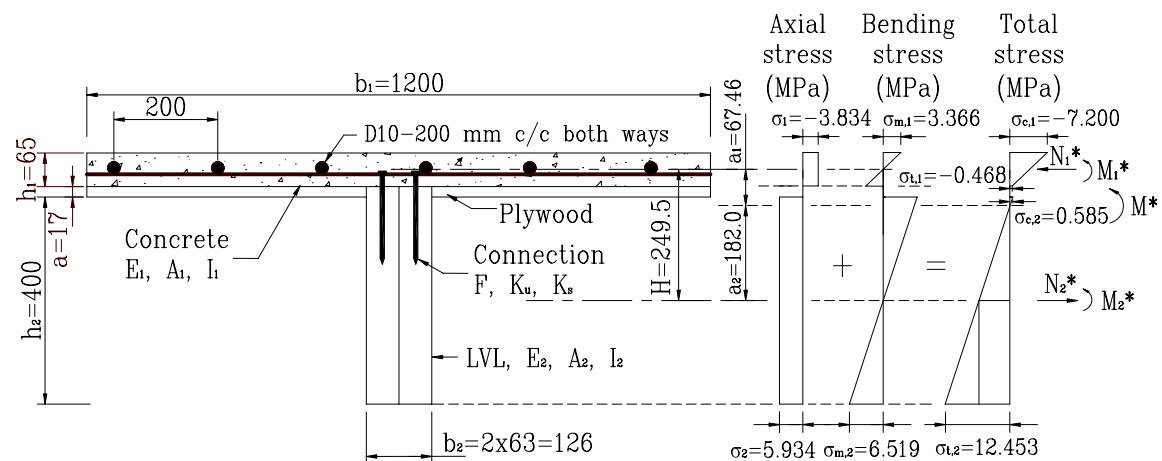
Fig. 7-8. Geometrical properties and stress diagrams of LVL-concrete composite section (length unit in mm, stress unit in MPa)

7.8   Design worked example

The design of a simply supported LVL-concrete composite floor spanning 8 m for a commercial office building in accordance with NZ Standard is presented in this section. The floor is made of double LVL joists which are spaced at 1200 mm centres with 65 mm thick concrete slab. Plywood of 17 mm thickness is used as a permanent formwork which separates the concrete and the LVL. A notched connection detail reinforced with coach screw provides the composite action between concrete and LVL. The geometrical

<div align="center">150</div>

properties of the composite section are given in Fig. 7-8 together with the stress diagrams of the section at short-term ultimate limit state being outcomes of the design example.

This design worked example which includes ultimate and serviceability limit state short and long-term verifications supersedes the one published in Buchanan (2007). The connection strength, slip moduli and creep coefficient obtained from experimental tests presented in Yeoh et al (2009e) or Chapter 4 and Yeoh et al (2009d) or Chapter 6, respectively, have been used in this worked example.

Design data on loads:

Imposed load			=	4.5	kN/m^2
Permanent load (finishes and services)			=	1	kN/m^2
Superimposed permanent load (self-weight and construction load)		=	2	kN/m^2
Total permanent load, G	=	$(1 + 2) \times 1.2$	=	3.6	kN/m
Total imposed load, Q	=	4.5×1.2	=	5.4	kN/m

ULS short-term load combinations,

for uniformly distributed load, w = 1.2G + 1.5Q	=	12.4	kN/m
design bending moment, $M_d = wL^2/8$	=	99.4	kNm
design shear force, $V_d = wL/2$	=	24.8	kN

SLS load combinations,

for short-term deflection, Q	=	5.4	kN/m
for long-term deflection, G + 0.4Q	=	5.76	kN/m
for vibration	=	1	kN

Design data on connection:

The connection slip moduli and strength were determined by experimental push-out test (Yeoh et al, 2009e or Chapter 4) for rectangular notched coach screw of 126(*w*) × 50(*d*) × 300(*l*) where *w*, *d*, and *l* as the width, depth and length in mm, respectively (See Fig. 7-9 for definition of connection spacing):

Connection slip modulus for ULS, K_u	=	483	kN/mm
Connection slip modulus for SLS, K_s	=	494	kN/mm
Characteristic strength of connection, F_k	=	231	kN
Maximum spacing of connection, s_{max}	=	1394	mm

| Minimum spacing of connection, s_{min} | = | 831 | mm |
| Effective spacing of connection, $s_{eff} = 0.75s_{min} + 0.25s_{max}$ | = | 972 | mm |
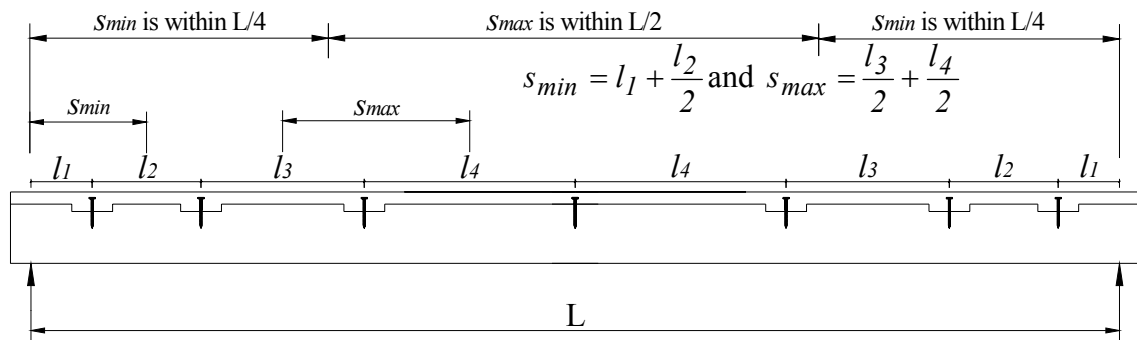
Fig. 7-9. Typical TCC beam showing indicative spacing of notched connection for the definition of s_{min} and s_{max}

Design data on creep:

Concrete design creep coefficient, $\phi_1(t,t_0) = k_2\ k_3\ k_4\ k_5\ \phi_{cc,b} = 3.16$ according to NZS3101 (SNZ, 2006)

> Hypothetical thickness, $t_h = 2A_g/u_e = 130$ mm;
>
> Basic creep coefficient, $\phi_{cc,b} = 3.18$ for $f'_c = 35$ MPa;

where A_g is the gross cross sectional area of the member;

u_e is the exposed perimeter;

and modification factors, for thickness, $k_2 = 1.39$ (depends on hypothetical thickness, t_h);

for maturity, $k_3 = 1.1$;

for environment, $k_4 = 0.65$ in dry indoor condition;

and for high strength, $k_5 = 1$ for $f'_c < 50$ MPa

Timber duration of load factor for long-term creep, $k_2 = 2.0$ according to NZS 3603 (SNZ, 1993)

Rectangular notched connection creep coefficient, $\phi_f(t - t_0) = 1.57$ obtained from experimental long-term push-out test (Yeoh et al, 2009d or Chapter 6)

Strength Capacity for Timber – Truform LVL (Gaunt and Penellum, 2004) :

Young's modulus of LVL, $E_2 = 10700$ MPa

Timber design tensile strength, $f_{t,d} = \phi\, k_1\, k_4\, k_{24}\, f'_t$

$\qquad = 0.9 \times 0.8 \times 1 \times 0.85 \times 30 = 18.4\ \text{N/mm}^2$

Timber design bending strength, $f_{b,d} = \phi\, k_1\, k_4\, k_5\, k_8\, k_{23}\, k_{24}\, f'_b$

$\qquad = 0.9 \times 0.8 \times 1 \times 1 \times 1 \times 1 \times 0.95 \times 48 = 32.8\ \text{N/mm}^2$

Timber shear design strength, $f_{s,d} = \phi\, k_1\, k_4\, k_5\, f'_s$

$\qquad = 0.9 \times 0.8 \times 1 \times 1 \times 5.3 = 3.82\ \text{N/mm}^2$

Timber compression perpendicular to grain design strength, $f_{p,d} = \phi\, k_1\, k_3\, k_5\, f'_p$

$\qquad = 0.9 \times 0.8 \times 1 \times 1 \times 12 = 8.64\ \text{N/mm}^2$

where modification factors $k_1 = 0.8$ for medium duration of load;

$k_3 = 1$ for bearing area;

$k_4,\ k_5,\ k_6 = 1$ for load sharing, grid system;

$k_8 = 1$ for stability;

$k_{23} = 1$ for curvature;

$k_{24} = 0.95$ for bending and 0.85 for tension parallel to grain (size factor) where LVL depth is greater than 300 mm;

and strength reduction factor, $\phi = 0.9$ for LVL (CHH, 2009)

Tensile design capacity, $N_R = f_{t,d}\, A_2 = 18.4 \times 126 \times 400 = 925\ \text{kN}$

Bending design capacity, $M_R = f_{b,d}\, Z_2 = 32.8 \times \dfrac{126 \times 400^2}{6} = 110\ \text{kNm}$

Strength capacity for concrete:

Young's modulus of concrete, $E_1 = \quad 34000\ \text{MPa}$

Concrete design compressive strength, $f_{cd} = \phi \times f_{ck} = 0.85 \times 35 = 29.8\ \text{N/mm}^2$

Concrete design tensile strength, $f_{ctd} = \phi \times f_{ctk} = 0.85 \times 2.2 = 1.87\ \text{N/mm}^2$

Strength capacity for connection:

Characteristic strength of connection, $F_k = 231\ \text{kN}$

Design strength of connection, $F_d = \phi\, k_a\, k_b\, F_k = 129\ \text{kN}$

$\qquad$ where $\phi = 0.7$, $k_a = 1.0$ for dry timber and $k_b = 0.8$ for medium term load

Solution:

Verifications performed in this worked example are:

(1) Ultimate limit state in the short-term;

(2) Serviceability limit state in the short-term;

(3) Ultimate limit state in the long-term; and

(4) Serviceability limit state for long-term.

In general, the calculation has been carried out in the following order for each of the verifications on ultimate limit state, (1) and (3):

(a) Bending stiffness properties for ultimate limit state in the short or long term verifications to calculate the effective flexural stiffness value, $(EI)_{ef}$.

(b) Timber strength demand and inequalities.

(c) Concrete strength demand and inequalities.

(d) Connection strength demand and inequalities.

In general, the calculation has been carried out in the following order for each of the verifications on serviceability limit state, (2) and (4):

(a) Bending stiffness properties for serviceability limit state in the short or long term verifications to calculate the effective flexural stiffness value, $(EI)_{ef}$.

(b) Deflection inequalities.

(1) Verifications for ultimate limit state in the short-term:

(a) Bending stiffness properties for ultimate limit state short term verifications:

Concrete gamma coefficient,

$$\gamma_1 = \frac{1}{1+\dfrac{\pi^2 E_1 A_1 s_{ef}}{K_u l^2}} = \frac{1}{1+\dfrac{\pi^2(34000)(65 \times 1200)971.75}{482860(8000)^2}} = 0.55$$

a_1 distance,

$$a_1 = \frac{E_2 A_2 H}{\gamma_1 E_1 A_1 + \gamma_2 E_2 A_2} = \frac{10700(63 \times 400)(249.5)}{0.549(34000)(65 \times 1200)+1(10700)(63 \times 400)} = 67.5 \text{ mm}$$

where $H = h_1 / 2 + a + h_2 / 2 = \dfrac{65}{2} + 17 + \dfrac{400}{2} = 250$ mm

a_2 distance, $a_2 = \dfrac{\gamma_1 E_1 A_1 H}{\gamma_1 E_1 A_1 + E_2 A_2}$ or $a_2 = H - a_1 = 250 - 67.5 = 182$ mm

Effective flexural stiffness,

$$(EI)_{ef} = E_1 I_1 + E_2 I_2 + \gamma_1 E_1 A_1 a_1^2 + E_2 A_2 a_2^2$$

$= 34000(2.75 \times 10^7) + 10700(6.72 \times 10^8) + 0.55(34000)(78000)(67.5)^2 +$
$(10700)(50400)(182)^2$

$= 3.26 \times 10^{13}$ Nmm^2 where $I_1 = \dfrac{b_1 h_1^3}{12}$ and $I_2 = \dfrac{b_2 h_2^3}{12}$

(b) Timber Strength Demand and Inequalities:

Timber axial stress due to axial force,

$$\sigma_2(x) = \dfrac{E_2 a_2 M(x)}{(EI)_{ef}} = \dfrac{(10700)(182.0)(99.36 \times 10^6)}{3.262 \times 10^{13}} = 5.93 \text{ N/mm}^2$$

Timber axial stress due to bending moment,

$$\sigma_{m,2}(x) = \dfrac{1}{2} \cdot \dfrac{E_2 h_2 M(x)}{(EI)_{ef}} = \dfrac{0.5(10700)(400)(99.36 \times 10^6)}{3.262 \times 10^{13}} = 6.52 \text{ N/mm}^2$$

Corresponding timber axial force,

$$N^* = \sigma_2 A_2 = 5.93 \times 126 \times 400 = 299 \text{ kN}$$

Corresponding timber bending moment,

$$M^* = \sigma_{m,2} Z_2 = 6.52 \times \dfrac{126 \times 400^2}{6} = 21.9 \text{ kNm}$$

Combined bending and tension ratio, $N^*/\phi N_R + M^*/\phi M_R <= 1$

$$= \frac{299.1}{0.9(925.3)} + \frac{21.90}{0.9(110.3)} = 0.58 < 1 \qquad \therefore \text{ satisfactory}$$

Timber shear stress,

$$\tau_{max} = 1.5 \; \frac{V_d}{A_2} \; = 1.5 \; (\frac{49.68 \times 10^3}{50400}) = 1.48 \; \text{N/mm}^2 < f_{s,d} = 3.82 \; \text{N/mm}^2 \qquad \therefore \text{ satisfactory}$$

Bearing of timber at support where bearing length, l_b, is 50 mm,

$$\sigma_{t,90} = \frac{V_d}{l_b b_2} = \frac{49.68 \times 10^3}{50 \times 126} = 7.89 \; \text{N/mm}^2 < f_{p,d} = 8.64 \; \text{N/mm}^2 \; \therefore \text{satisfactory}$$

(c) Concrete strength demand and inequalities:

Concrete axial stress due to axial force,

$$\sigma_1(x) = \frac{\gamma_1 E_1 a_1 M(x)}{(EI)_{ef}} \; = \frac{0.549(34000)(67.46)(99.36 \times 10^6)}{3.261 \times 10^{13}} = 3.83 \; \text{N/mm}^2$$

Concrete axial stress due to bending moment,

$$\sigma_{m,1}(x) = \frac{1}{2} \cdot \frac{E_1 h_1 M(x)}{(EI)_{ef}} \; = \frac{0.5(34000)(65)(99.36 \times 10^6)}{3.261 \times 10^{13}} = 3.37 \; \text{N/mm}^2$$

Concrete total upper fibre stress, $\sigma_{c,tot} = - \sigma_1 - \sigma_{m,1}$

$$= -3.83 - 3.37 = -7.20 \; \text{N/mm}^2 < f_{cd} = 29.8 \; \text{N/mm}^2 \; \therefore \text{satisfactory}$$

Concrete total lower fibre stress, $\sigma_{t,tot} = - \sigma_1 + \sigma_{m,1}$

$$= -3.83 + 3.37 = -0.47 \; \text{N/mm}^2 \; (\text{compression}) < f_{ctd} = 1.87 \; \text{N/mm}^2 \; \therefore \text{satisfactory}$$

(d) Connection strength demand and inequalities:

Shear force in connection at maximum shear, $F_{(x=0)} = \dfrac{\gamma_1 E_1 A_1 a_1 s_{min}}{(EI)_{ef}} \cdot V_{max}$

$$= \frac{0.549(34000)(78000)(67.46)(831)}{3.261 \times 10^{13}} \times 49.68 \times 10^3 \ = \ 124 \ \ \text{kN} \ < \ F_d \ = \ 129 \ \ \text{kN}$$

$\therefore$ satisfactory

Shear force in connection at L/4, $F_{(x=L/4)} = \dfrac{\gamma_1 E_1 A_1 a_1 s_{max}}{(EI)_{ef}} \cdot V_{L/4}$

$$= \frac{0.549(34000)(78000)(67.46)(1394)}{3.261 \times 10^{13}} \times 24.84 \times 10^3 \ = \ 104 \ \ \text{kN} \ < \ F_d \ = \ 129 \ \ \text{kN}$$

$\therefore$ satisfactory

(2) Verification for serviceability limit state in the short-term:

(a) Bending stiffness properties for serviceability limit state short term verifications:

Concrete gamma coefficient,

$$\gamma_1 = \frac{1}{1 + \dfrac{\pi^2 E_1 A_1 s_{ef}}{K_s l^2}} \ = \ \frac{1}{1 + \dfrac{\pi^2 (34000)(65 \times 1200)971.75}{494460(8000)^2}} = 0.56$$

a_1 distance,

$$a_1 = \frac{\gamma_2 E_2 A_2 H}{\gamma_1 E_1 A_1 + \gamma_2 E_2 A_2} = \frac{10700(63 \times 400)(249.5)}{0.555(34000)(65 \times 1200) + 1(10700)(63 \times 400)} = 66.9 \ \text{mm}$$

a_2 distance,

$$a_2 = \frac{\gamma_1 E_1 A_1 H}{\gamma_1 E_1 A_1 + \gamma_2 E_2 A_2} \ \text{ or } \ a_2 = H - a_1 = 250 - 66.9 = 183 \ \text{mm}$$

Effective flexural stiffness,

$$(EI)_{ef} = E_1 I_1 + E_2 I_2 + \gamma_1 E_1 A_1 a_1^2 + \gamma_2 E_2 A_2 a_2^2$$

$$= 34000(2.75 \times 10^7) + 10700(6.72 \times 10^8) + 0.56(34000)(78000)(66.9)^2 +$$
$$(10700)(50400)(183)^2$$

$= 3.27 \times 10^{13}$ Nmm^2

(b) Deflection inequalities:

Deflection under 1 kN load for vibration, $u_{vibration} = \dfrac{Pl^3}{48(EI)_{ef}} = \dfrac{1000(8000)^3}{48(3.269 \times 10^{13})}$

$= 0.33$ mm $<$ allowable deflection for vibration of 1 to 2 mm $\therefore$ satisfactory

Instantaneous deflection just after the application of live load,

$$u_{ins\tan t} = \frac{5Ql^4}{384(EI)_{ef}} = \frac{5(5.4)(8000)^4}{384(3.269 \times 10^{13})} = 8.81 \ \ mm \ < \ u_{allow} = \frac{span}{300} = 26.7 \ \ mm$$

$\therefore$ satisfactory

(3) Verification for ultimate limit state in the long-term:

Fictitious effective moduli accounting for time dependent effects at final time, *t*, of analysis (the end of the service life, usually 50 years),

Effective modulus for concrete, $E_{1,eff} = \dfrac{E_1}{1 + \phi_{cc}(t, t_0)} = \dfrac{34000}{1 + 3.155} = 8182$ N/mm^2

Effective modulus for timber, $E_{2,eff} = \dfrac{E_2}{k_2} = \dfrac{10700}{2} = 5350$ N/mm^2

Effective modulus for connection, $K_{eff} = \dfrac{K_s}{k_{37}} = \dfrac{K_s}{1 + \phi_f(t - t_0)}$

$= \dfrac{494466}{1 + 1.569} = 192474$ N/mm^2

(a1) Bending stiffness properties for ultimate limit state long term verifications throughout the service life of the structure:

Concrete gamma coefficient,

$$\gamma_1 = \frac{1}{1 + \dfrac{\pi^2 E_{1,eff} A_1 s_{ef}}{K_{eff} l^2}} = \frac{1}{1 + \dfrac{\pi^2 (8181.98)(65 \times 1200)971.75}{192474(8000)^2}} = 0.67$$

a_1 distance,

$$a_1 = \frac{E_{2,eff} A_2 H}{\gamma_1 E_{1,eff} A_1 + E_{2,eff} A_2} = \frac{5350(63 \times 400)(249.5)}{0.668(8181.98)(65 \times 1200) + (5350)(63 \times 400)}$$

$$= 96.64 \text{ mm}$$

a_2 distance, $a_2 = \dfrac{\gamma_1 E_{1,eff} A_1 H}{\gamma_1 E_{1,eff} A_1 + E_{2,eff} A_2}$ or $a_2 = H - a_1 = 250 - 96.7 = 153$ mm

Effective flexural stiffness,

$$(EI)_{ef} = E_{1,eff} I_1 + E_{2,eff} I_2 + \gamma_1 E_{1,eff} A_1 a_1^2 + E_{2,eff} A_2 a_2^2$$

$$= 8182(2.75 \times 10^7) + 5350(6.72 \times 10^8) + 0.67(8182)(78000)(96.7)^2 + (5350)(50400)(153)^2$$

$$= 1.410 \times 10^{13} \text{ Nmm}^2$$

Quasi-permanent load combination, $F_{d,p}$

$$F_{d,p} = G + 0.4Q = 3.6 + (0.4 \times 5.4) = 5.76 \text{ kN/m}$$

Design bending moment, $M_d = \dfrac{F_{d,p} l^2}{8} = \dfrac{(5.76)(8)^2}{8} = 46.1$ kNm

Design maximum shear force, $V_d = \dfrac{F_{d,p} l}{2} = \dfrac{(5.76)8}{2} = 23.0$ kN

Design shear force at L/4, $V_{L/4} = \dfrac{V_d}{2} = \dfrac{23.04}{2} = 11.5$ kN

(a2) Bending stiffness properties for ultimate limit state long-term verifications at the end of service life (similar to the bending stiffness properties for ultimate limit state short-term):

Effective flexural stiffness,

$$(EI)_{ef} = E_1 I_1 + E_2 I_2 + \gamma_1 E_1 A_1 a_1^2 + E_2 A_2 a_2^2 = 3.26 \times 10^{13} \text{ Nmm}^2$$

Difference between ultimate and quasi-permanent load combinations, $F_{d,u} - F_{d,p}$

$$F_{d,u} - F_{d,p} = (1.2G + 1.5Q) - (G + 0.4Q) = 0.2G + 1.1Q$$

$$= (0.2 \times 3.6) + (1.1 \times 5.4) = 6.66 \text{ kN/m}$$

Design bending moment, $M_d = \dfrac{(F_{d,u} - F_{d,p})l^2}{8} = \dfrac{(6.66)(8)^2}{8} = 53.3 \text{ kNm}$

Design maximum shear force, $V_d = \dfrac{(F_{d,u} - F_{d,p})l}{2} = \dfrac{(5.76)8}{2} = 26.6 \text{ kN}$

Design shear force at L/4, $V_{L/4} = \dfrac{V_d}{2} = \dfrac{26.64}{2} = 13.3 \text{ kN}$

(b) Timber Strength Demand and Inequalities:

Timber axial stress due to axial force for $F_{d,p}$ load combination,

$$\sigma_2(x) = \frac{E_{2,eff} a_2 M(x)}{(EI)_{ef}} = \frac{(5350)(152.8)(46.08 \times 10^6)}{1.410 \times 10^{13}} = 2.67 \text{ N/mm}^2$$

Timber axial stress due to axial force for $F_{d,u} - F_{d,p}$ load combination,

$$\sigma_2(x) = \frac{E_2 a_2 M(x)}{(EI)_{ef}} = \frac{(10700)(182.0)(53.28 \times 10^6)}{3.262 \times 10^{13}} = 3.18 \text{ N/mm}^2$$

Total timber axial stress due to axial force,

$$\sigma_{2,tot} = 2.672 + 3.182 = 5.854 \text{ N/mm}^2$$

Timber axial stress due to bending moment for $F_{d,p}$ load combination,

$$\sigma_{m,2}(x) = \frac{1}{2} \cdot \frac{E_{2,eff} h_2 M(x)}{(EI)_{ef}} = \frac{0.5(5350)(400)(46.08 \times 10^6)}{1.410 \times 10^{13}} = 3.50 \text{ N/mm}^2$$

Timber axial stress due to bending moment for $F_{d,u} - F_{d,p}$ load combination,

$$\sigma_{m,2}(x) = \frac{1}{2} \cdot \frac{E_2 h_2 M(x)}{(EI)_{ef}} = \frac{0.5(10700)(400)(53.28 \times 10^6)}{3.262 \times 10^{13}} = 3.50 \text{ N/mm}^2$$

Total timber axial stress due to bending moment,

$$\sigma_{m,2,tot} = 3.496 + 3.496 = 6.992 \text{ N/mm}^2$$

Corresponding timber axial force,

$$N^* = \sigma_{2,tot} A_2 = 5.854 \times 126 \times 400 = 295 \text{ kN}$$

Corresponding timber bending moment,

$$M^* = \sigma_{m,2,tot} Z_2 = 6.992 \times \frac{126 \times 400^2}{6} = 23.5 \text{ kNm}$$

Combined bending and tension ratio,

$$N^*/\phi N_R + M^*/\phi M_R = \frac{295.0}{0.9(925.3)} + \frac{23.49}{0.9(110.3)} = 0.59 < 1 \therefore \text{ satisfactory}$$

Timber shear stress for $F_{d,p}$ load combination,

$$\tau_{max} = 1.5 \frac{V_d}{A_2} = 1.5 \left(\frac{23.04 \times 10^3}{50400}\right) = 0.69 \text{ N/mm}^2$$

Timber shear stress for $F_{d,u} - F_{d,p}$ load combination,

$$\tau_{max} = 1.5 \frac{V_d}{A_2} = 1.5 \left(\frac{26.64 \times 10^3}{50400}\right) = 0.79 \text{ N/mm}^2$$

Total timber shear stress,

$$\tau_{max,tot} = 0.686 + 0.793 = 1.479 \text{ N/mm}^2 < f_{s,d} = 3.82 \text{ N/mm}^2 \therefore \text{ satisfactory}$$

Bearing of timber at support where bearing length, l_b, is 50 mm for $F_{d,p}$ load combination,

$$\sigma_{t,90} = \frac{V_d}{l_b b_2} = \frac{23.04 \times 10^3}{50 \times 126} = 3.66 \text{ N/mm}^2$$

Bearing of timber at support where bearing length, l_b, is 50 mm for $F_{d,u} - F_{d,p}$ load combination,

$$\sigma_{t,90} = \frac{V_d}{l_b b_2} = \frac{26.64 \times 10^3}{50 \times 126} = 4.23 \text{ N/mm}^2$$

Total bearing of timber at support,

$\sigma_{t,90,tot} = 3.66 + 4.23 = 7.89 \text{ N/mm}^2 < f_{p,d} = 8.64 \text{ N/mm}^2 \therefore \text{satisfactory}$

(c) Concrete strength demand and inequalities:

Concrete axial stress due to axial force for $F_{d,p}$ load combination,

$$\sigma_1(x) = \frac{\gamma_1 E_{1,eff} a_1 M(x)}{(EI)_{ef}} = \frac{0.668(8182)(96.64)(46.08 \times 10^6)}{1.410 \times 10^{13}} = 1.73 \text{ N/mm}^2$$

Concrete axial stress due to axial force for $F_{d,u} - F_{d,p}$ load combination,

$$\sigma_1(x) = \frac{\gamma_1 E_1 a_1 M(x)}{(EI)_{ef}} = \frac{0.549(34000)(67.46)(53.28 \times 10^6)}{3.262 \times 10^{13}} = 2.06 \text{ N/mm}^2$$

Total concrete axial stress due to axial force,

$\sigma_{1,tot} = 1.726 + 2.056 = 3.78 \text{ N/mm}^2$

Concrete axial stress due to bending moment for $F_{d,p}$ load combination,

$$\sigma_{m,1}(x) = \frac{1}{2} \cdot \frac{E_{1,eff} h_1 M(x)}{(EI)_{ef}} = \frac{0.5(8182)(65)(46.08 \times 10^6)}{1.410 \times 10^{13}} = 0.87 \text{ N/mm}^2$$

Concrete axial stress due to bending moment for $F_{d,u} - F_{d,p}$ load combination,

$$\sigma_{m,1}(x) = \frac{1}{2} \cdot \frac{E_1 h_1 M(x)}{(EI)_{ef}} = \frac{0.5(34000)(65)(53.28 \times 10^6)}{3.262 \times 10^{13}} = 1.81 \text{ N/mm}^2$$

Total concrete axial stress due to bending moment,

$$\sigma_{m,1,tot} = 0.869 + 1.805 = 2.67 \text{ N/mm}^2$$

Concrete total upper fibre stress, $\sigma_{c,tot} = - \sigma_{1,tot,} - \sigma_{m,1,tot}$

$= -3.78 - 2.67 = -6.46 \text{ N/mm}^2 < f_{cd} = 29.8 \text{ N/mm}^2 \therefore$ satisfactory

Concrete total lower fibre stress, $\sigma_{t,tot} = - \sigma_{1,tot} + \sigma_{m,1,tot}$

$= -3.78 + 2.67 = -1.11 \text{ N/mm}^2$ (compression) $< f_{ctd} = 1.87 \text{ N/mm}^2 \therefore$ satisfactory

(d) Connection strength demand and inequalities:

Maximum force in connection at support for $F_{d,p}$ load combination,

$$F_{(x=0)} = \frac{\gamma_1 E_{1,eff} A_1 a_1 s_{min}}{(EI)_{ef}} \cdot V_{max} = \frac{0.668(8182)(78000)(96.64)(831)}{1.410 \times 10^{13}} \times 23.04 \times 10^3$$

$= 55.9 \text{ kN}$

Maximum force in connection at support for $F_{d,u} - F_{d,p}$ load combination,

$$F_{(x=0)} = \frac{\gamma_1 E_1 A_1 a_1 s_{min}}{(EI)_{ef}} \cdot V_{max} = \frac{0.549(34000)(78000)(67.46)(831)}{3.262 \times 10^{13}} \times 26.64 \times 10^3$$

$= 66.6 \text{ kN}$

Total maximum force in connection at support,

$$F_{(x=0),tot} = 55.95 + 66.63 = 122.58 \text{ kN} < F_d = 129 \text{ kN} \therefore$$ satisfactory

Force in connection at L/4 for $F_{d,p}$ load combination,

$$F_{(x=L/4)} = \frac{\gamma_1 E_{1,eff} A_1 a_1 s_{max}}{(EI)_{ef}} \cdot V_{L/4}$$

$$= \frac{0.668(8182)(78000)(96.64)(1394)}{1.410 \times 10^{13}} \times 11.52 \times 10^3 = 46.9 \text{ kN}$$

Force in connection at L/4 for $F_{d,u} - F_{d,p}$ load combination,

$$F_{(x=L/4)} = \frac{\gamma_1 E_1 A_1 a_1 s_{max}}{(EI)_{ef}} \cdot V_{L/4}$$

$$= \frac{0.549(34000)(78000)(67.46)(1394)}{3.262 \times 10^{13}} \times 13.32 \times 10^3 = 55.9 \text{ kN}$$

Total maximum force in connection at support,

$$F_{(x=0),tot} = 46.936 + 55.89 = 102.3 \text{ kN} < F_d = 129 \text{ kN} \therefore \text{satisfactory}$$

(4) Verification for serviceability limit state in the long-term:

(a) Bending stiffness properties for serviceability limit state long-term verifications (similar to the bending stiffness properties for ultimate limit state long term verifications throughout the service life of the structure):

Effective flexural stiffness,

$$(EI)_{ef} = E_{1,eff} I_1 + E_{2,eff} I_2 + \gamma_1 E_{1,eff} A_1 a_1^2 + E_{2,eff} A_2 a_2^2 = 1.41 \times 10^{13} \text{ Nmm}^2$$

(b) Deflection inequalities:

Quasi-permanent part of the load, $F_{d,p} = G + \psi_2 Q = 3.6 + (0.4 \times 5.4) = 5.76$ kN/m

Mid-span long-term deflection due to quasi-permanent part of the load,

$$u_{final,d,p} = \frac{5F_{d,p} l^4}{384(EI)_{ef}} = \frac{5(5.76)(8000)^4}{384(1.410 \times 10^{13})} = 21.8 \text{ mm}$$

Difference between the rare and the quasi-permanent load,

$$F_{d,r} - F_{d,p} = (1 - \psi_2)Q = (1 - 0.4) \times 5.4 = 3.24 \text{ kN/m}$$

Instantaneous mid-span deflection due to the $F_{d,r} - F_{d,p}$ load,

$$u_{inst,d,r-d,p} = \frac{5(F_{d,r} - F_{d,p})l^4}{384(EI)_{ef}} = \frac{5(3.24)(8000)^4}{384(1.410 \times 10^{13})} = 12.3 \text{ mm}$$

Total long-term deflection, $u_{final,d,p} + u_{inst,d,r-d,p} = 21.8 + 12.3 = 34.0$ mm

$$< u_{allow} = \frac{span}{200} = 40.0 \text{ mm} \quad \therefore \text{satisfactory}$$

7.9   Conclusion

A design method and the construction of a novel semi-prefabricated LVL-concrete composite floor have been presented. The design method is based on the Annex B elastic formulas of the Eurocode 5 for composite beams with flexible connection. Due to the time-dependent phenomena, both ultimate and serviceability limit states must be checked at two stages: (1) in the short-term, just after construction, where no creep has been developed yet, and (2) in the long-term, at the end of the service life, where allowance for creep has to be made. The actual non-linear behaviour of the connection system is allowed for by using different secant slip moduli for serviceability and ultimate limit states. The creep of all component materials (concrete, timber and connection) is considered in long-term verifications by reducing the actual elastic moduli of materials (effective modulus method). The chapter is complemented by a design worked example, carried out in accordance with the New Zealand Standards.

8   Conclusions

"Of making many books there is no end, and much study wearies the body. Now all has been heard; here is the conclusion of the matter: Fear God and keep his commandments, for this is the whole duty of man. For God will bring every deed into judgement, including every hidden thing, whether it is good or evil." – King Solomon (Ecclesiastes 12:12-14)

The main objective of this Ph.D. project has been to study and quantify the behaviour of timber-concrete composite floors in the short- and long-term divided into 5 different experimental phases. The short-term herein refers to the response of the composite floors to collapse load in the ultimate limit state while long-term refers to the response of the composite floors to sustained load in the serviceability limit state condition. In meeting this main objective, 9 sub-objectives have been outlined in Chapter 1 and summarised in this chapter.

8.1   Selected best connection types

Achieving sub-objective:

> *1) To identify the best types of connection system to be used in TCC floors in New Zealand. The basic criteria of selection are structural performance, ease of manufacturing and cost effectiveness.*

A parametric investigation on 15 types of connection system has been undertaken, and presented in Chapter 3. As a result, 3 best types of connection system have been identified to be used in TCC floors in New Zealand: this was presented in Chapter 4. These connection types were $300l \times 50d \times 63w$ mm rectangular notches cut in the LVL and reinforced with a 16 mm diameter coach screw (R300), $30°\_60° \times 137l \times 60d$ mm triangular notches reinforced with the same diameter coach screw (T), and two $333l \times 136d \times 1t$ mm toothed metal plates pressed on the lateral surface of the LVL joist (P), where l, d, w, and t are the length, depth, width and thickness, respectively.

Achieving sub-objective:

> *2) To determine the characteristic strength and secant slip moduli of the chosen types of connection.*

The characteristic shear strength and mean secant slip moduli of the 3 best connection types was presented in Chapter 4 and summarised in Table 8-1.

Table 8-1. Characteristic strength and secant slip moduli values for a single connector

Type of connection	Mean secant slip moduli (kN/mm)			Characteristic shear strength, R_k (kN)
	$K_{0.4}$	$K_{0.6}$	$K_{0.8}$	
T (1-LVL)	145.8	138.8	115.9	70.4
R300 (1-LVL)	247.2	241.4	194.2	115
P (2-LVL)	463.7	394.6	256.8	116

Achieving sub-objective:

> *3) To establish the short-term behaviour of the selected connections by defining the pre- and post-peak responses subjected to collapse load.*

The detailed study undertaken to achieve this sub-objective is described in Chapter 4.

It was found that the length of the notch significantly enhances the strength performance of the connection, while a coach screw improves the slip modulus at ultimate limit state, the post-peak behaviour, and enables a more ductile failure to take place. The 300 mm notch reinforced with a coach screw is 3 times stronger and 8.5 times stiffer than a connection without a notch but just with the coach screw; 1.9 times stronger and 3 times stiffer than a 150 mm reinforced notch connection. The 300 mm long rectangular reinforced notch connection stands out as the best connection among those tested due to the high strength and secant slip moduli, while the 2 × 333 mm toothed metal plate connection appeared to be the most practical and labour cost effective since it does not involve any notching. However, this connection system requires a readily available hydraulic press of industrial size for this system to be used in floor construction. On the other hand, the triangular notch reinforced with a coach screw has the advantage of easier and faster construction requiring only two cuts. Neither of the notched connections exhibited a very brittle failure due to the use of the coach screw, whereas a more brittle failure was observed in the toothed metal plate connection characterized by tearing of the plate.

Defined analytical pre-peak and post-peak load-slip relationship of the 3 selected connections, which was related to the failure mechanism and behaviour of the connections, were presented in Chapter 4 Clause 4.6.5.

Achieving sub-objective:

    4) To derive an analytical model for the strength evaluation of the selected connections based on the different possible modes of failure.

The details to achieving this sub-objective are found in Chapter 4 Clause 4.7 and Appendix 4.

Considering among all possible failure mechanisms, shearing of the concrete in the shear plane as the most important one, analytical formulae for the strength evaluation of the notched connection were derived according to New Zealand Standards and Eurocodes.

The formulas were found to predict the experimental failure load with acceptable accuracy in all cases, with the closest agreement achieved when a new reduction factor was introduced in the Eurocodes formulas to take into account the length of the notch and the diameter of the coach screw.

8.2   Semi-prefabricated timber-concrete composite floor system

Achieving sub-objective:

  5) *To propose a semi-prefabricated construction method for TCC floors which ensure easy and fast erection*

A floor solution suitable for medium to large span floors in multi-storey timber buildings was first presented in Chapter 3. The performance requirements of effective acoustic separation, adequate fire resistance, and reduced susceptibility to vibrations indicated the use of a concrete topping as highly desirable. In order to exploit the stiffness and strength contribution of the concrete, a shear connection system has been used, so as to obtain composite action between the concrete topping and the timber beam. The proposed solution is a M-section module, 2400 mm wide, semi-prefabricated timber-concrete composite system where timber panels made from LVL joists and plywood sheets are prefabricated off-site, craned into position, and used as permanent form for the concrete topping which is poured on site. This solution has the advantages of the prefabrication and allows, at the same time, the construction of a monolithic floor from the concrete topping poured on site.

The construction of this novel semi-prefabricated LVL-concrete composite floor in a large-scale, two-storey, experimental post-tensioned timber building has been presented in Chapter 7.

8.3   Short-term behaviour of TCC floor

Achieving sub-objective:

  6) *To investigate the short-term ultimate and serviceability limit state behaviour of TCC floor beams under collapse load, the effects of concrete strength and construction sequence or method such as leaving connection pockets during*

> *concreting and grouting them later.*

Chapter 5 described short-term collapse test conducted on eleven 8 and 10 m LVL-concrete composite floor T-beams represented by different variables such as connection types, concrete, and design level corresponding to number of connections. 6 beams were well-designed and 5 were under-designed. Well-designed beams refer to beams that fully comply with all inequalities at ULS and SLS. Under-designed beams refer to beams where the maximum demand of shear force in the connection was about 1.3 times the resistance at ULS.

The effective bending stiffness method or γ-method according to Annex B of Eurocode 5 was used to design the beams with 3 kN/m^2 design live load. This method has been described in Chapter 7 and complemented by a full worked example.

All well-designed beams exhibited more than 95% degree of composite action regardless of connection type. They also showed redistribution of stress in the connections and thus enable strength recovery in the event the outer connections fail. Therefore, a well-designed system is highly recommended.

All well-designed beams with high degree of composite action exhibited an experimental ULS and SLS imposed load capacities very close to that of a full composite (approximately 0.9 times).

Therefore, a 15% increment correction factor to the deflection or a 13% reduction to the effective bending stiffness, (EI), calculated using the transformed section method can be proposed for all well-designed beams.

All experimental ULS imposed load capacities are about 3 times larger than the analytical capacities regardless of the beams being under-designed or well-designed. In other words, the γ-method underestimates the short-term ULS capacity for all cases in this experiment.

In most cases, the analytical prediction underestimated the experimental SLS live load by an average of less than 10%. In other words, the γ-method provided a reasonably accurate prediction of the SLS imposed load.

The use of 300 mm rectangular notch with coach screw connection in the composite beam is recommended for two main reasons: (1) High stiffness and strength even past the ULS load level; and (2) Less number of connectors along the beam. Triangular notched connection is another alternative. Although it may require more connectors than that of a 300 mm notch for the same design level, a triangular notch is easier and faster to cut, particularly if CNC machines were not available. Metal plate connection is practical in construction. The disadvantage of a beam built with this connection type is that the very good initial stiffness shown decreased quickly (due to brittle failure) beyond the ULS load level. Such behaviour can be improved by increasing the plate thickness.

The strength of concrete is important especially in notched-connected beams since it was the concrete within the notches that provided the shear transfer between the timber and concrete.

Leaving connection pockets during concreting and grouting them later did not show any improvement. Instead, the strength and stiffness of such beam was 0.86 times lower than one with connections cast all at the same time. The actual cause of this phenomenon is not fully known. Too early removal of prop (in this case the props were left for 3 days) before the grouted notches developed enough strength could be a possible reason.

8.4   Long-term behaviour of TCC connection and floor

Achieving sub-objective:

> 7) *To establish the long-term behaviour of the chosen connections by determining the creep coefficient.*

Long-term tests were conducted in an uncontrolled, unheated indoor environment using three types of connection and three 8 m span TCC beams under sustained load for 1.34 and 1.56 years, respectively. The results are presented in Chapter 6.

The creep coefficients, $\phi(t,t_0)$, for the connection specimens were extrapolated to the end of service life (50 years). The corresponding creep coefficients were k_{def} = 2.1 for the triangular notched and coach screw connection (T), k_{def} = 1.6 for the rectangular notch and coach screw connection (R) and k_{def} = 5.7 for the toothed metal plate connection (P).

Achieving sub-objective:

8) *To investigate the long-term behaviour of TCC floor beams under sustained load at serviceability limit state condition considering the effect of environmental changes; propped and un-propped; and concrete with different level of drying shrinkage.*

Two of the beam specimens had connection type $300l \times 50d \times 63w$ mm rectangular notches cut in the LVL and reinforced with a 16 mm diameter coach screw (R300). Of these, beam H had normal weight concrete and beam I had low shrinkage concrete, with half the drying shrinkage of normal weight concrete. The third, beam J, had connection type $2 - 333l \times 136d \times 1t$ mm toothed metal plates pressed on the lateral surface of the LVL joist (P) and low shrinkage concrete.

The specimens were exposed to environmental conditions characterized by either low temperature with high relative humidity (RH) or high temperature with low RH, conditions considered to be reasonably severe with relatively high daily fluctuations of temperature in the cooler months (maximum of 5.8 ºC) and of RH in the warmer months (maximum of 29.7%). The equilibrium moisture content dropped to approximately 7% in the warmer months and rose to approximately 25% in the cooler months, which exposed the specimens to an environmental condition classed as marginal to service class 3 according to Eurocode 5.

The relative connection slips and beam deflections fluctuated in response to the environmental changes. Large slips and deflections were induced by the low temperatures and equivalent high equilibrium moisture content during the cooler months, while in the warmer months with higher temperatures and low equilibrium moisture content, they remained more consistent.

Superimposed load induced an instantaneous 30 to 40% increase in beam deflections. A significant portion of the deflection occurred in the first quarter of the year and, most of the remainder (with annual fluctuations) until 1.2 years after which the deflections remained constant.

The mid-span deflections were extrapolated to the end of service life (50 years), with the final deflection for the beams predicted to be 52.0, 44.9 and 42.9 mm for beams H, I and J, respectively. Although the predicted final long-term deflections exceeded the commonly accepted limit of 40 mm (span/200), the environmental conditions were deliberately severe. Also, the extrapolation was based on a relatively short duration experiment and there was difficulty fitting a logarithmic curve to fluctuating experimental results which are likely to introduce additional error.

Two analytical methods, "Effective Modulus Method" proposed by Ceccotti (1995) and "effective creep coefficient method" recommended by Schänzlin and Fragiacomo (2007), were used to predict deflections at the end of service life. These deflections significantly underestimated the extrapolated experimental deflections. A possible reason for this underestimation is that the effects of drying shrinkage of concrete and, shrinkage/swelling of concrete and timber due to thermal expansion (elastic strains effects) were not considered in these methods.

Low shrinkage concrete (650 microstrain at 28 day) was effective in reducing the total deflection by 5 mm at 28 day when compared to normal weight concrete, corresponding to span/1600. High concrete shrinkage, in fact, increases the overall deflection of composite beams, especially when the connection is very stiff like in the case under study.

The effect of beam propping was investigated in Chapter 3 as part of some preliminary studies carried out. Un-propped beam sagged 11 mm at the time of casting. Props were removed after 7 days in propped beams. An instantaneous 6 to 10 mm deflection increment was recorded when the prop was removed. However, at 28 day, an un-propped beam sagged 5 mm more than a propped beam, corresponding to a deflection increment of span/1600.

On the whole, propping of beams at mid-span was important to minimise permanent deflection and enable initial composite action to be developed before sustaining the full self-weight of the concrete slab. Nevertheless, after the removal of props, deflection fluctuations in all beams (both propped and un-propped versions) follow a similar trend due to RH and temperature changes.

The time-dependent behaviour and creep mechanism in TCC are known to be very complex because the timber, concrete and connection all creep differently. Some creep rates are affected by environmental conditions so stresses are redistributed within the three components. Creep is inevitable so the long-term deflections of TCC structures are most effectively minimized by reducing initial deflections as much as possible through propping or pre-cambering the timber joist, and by using low shrinkage concrete. The other alternative is to precast the concrete slab and allow it to shrink before being connected to the timber joist.

8.5   Design of TCC floors and span tables

Achieving sub-objective:

> 9) *To develop design example and span tables for TCC floor beams that satisfy both the ultimate and serviceability limit state in the short- and long-term.*

A design method of TCC floor and a full worked example carried out in accordance with the New Zealand Standards were presented in Chapter 7. This design method known as the γ-method was based on the Annex B elastic formulas of the Eurocode 5 for composite beams with flexible connection. Due to the time-dependent phenomena, both ultimate and serviceability limit states were checked at two stages: (1) in the short-term, just after construction, where no creep has been developed yet, and (2) in the long-term, at the end of the service life, where allowance for creep has to be made. The actual non-linear behaviour of the connection system was allowed for by using different secant slip moduli for serviceability and ultimate limit states. The creep of all component materials (concrete, timber and connection) was considered in long-term verifications by reducing the actual elastic moduli of materials (effective modulus method).

Design span tables for the proposed M-section module, 2400 mm wide, semi-prefabricated LVL-concrete composite floors for up to 15 m long have been developed, given in Appendix 10. The span tables are ready for use by a practicing engineer without needing to carry out long design calculations. This is an important contribution of this thesis to the construction industry with the main objective to promote the use of timber-concrete composite floor systems in multi-storey timber buildings. The span tables give the safe imposed load in kN/m^2 for M-section modules with 3 connection types: (1) 300 mm long rectangular notch cut in the LVL joist and reinforced with a 16 mm diameter coach screw (R300); (2) triangular notch reinforced with the same coach screw (T); and (3) 2 – 333 mm long toothed metal plates (P).

8.6   Research needs

Solution for large long-term deflections in long span floors

The important issue with such composite system, primarily long span floors, is the large deflections in the long-term experienced over the service life of the structure. This deflection tends to increase significantly, possibly beyond the commonly accepted limit of span/200 when the structure is exposed to extreme environmental changes. In order to minimize these deflections, it is recommended that reduced shrinkage concrete be used and spans be propped at mid-span as carried out in this project (in Chapter 3). Other possible more practical method of reducing the deflections is by pre-cambering the floor joist, and in this case, it involves a modification in the cutting of the LVL at the factory. Alternatively, during the prefabrication of the units, the LVL joists can be clamped downwards at each end over a central support, forcing the joints to bend, and then by nailing or screwing the permanent formworks, in this case, the plywood, to the LVL flange. Another available solution is to increase the size of the LVL joist in order to minimise the effect of an un-propped floor. The final choice, however, would depend on the cost and savings achievable from each of the aforementioned solutions.

Accurate prediction of long-term deflections

It is recommended that long-term tests be carried out for a minimum of 3 years and ideally for 5 years (as opposed to the duration of 1.56 years in this project, presented in

Chapter 6), and that advanced numerical models be used to extrapolate experimental results to the end of the service life in order to provide more conclusive experimental-analytical comparisons and more confidence in design recommendations.

A long-term test should be conducted in a more representative service environment with an equilibrium moisture content of 8 to 12% found in air-conditioned and heated building.

The effect of inelastic strains and stresses due to drying shrinkage of concrete and environmental conditions causes redistribution of internal forces from the concrete to the timber. This, over time in the long-term and under load, depending on the environmental changes may incur excessive deflection on TCC floor. Such deflection was not accounted for in the existing γ-method and therefore in the span tables given in Appendix 10. Hence a method, possibly an advanced numerical model is needed to accurately quantify such deflection.

Cost and industrial implementation

The cost of making the proposed M-section semi-prefabricated TCC floors for the 3 connection types has not been considered in this project. Initial feedbacks from some industrial collaborators for the construction of a large-scale, two-storey, experimental post-tensioned timber building which included this floor system (mentioned in Chapter 7) was that the cutting of the notches was too labour intensive and time consuming, given that it was done manually. However, on-site assembly was rapid. Each floor unit was held by overhead crane for approximately 2 minutes, equating to a floor coverage rate of 486 m^2/hour. Floor units were light enough to be manoeuvred manually. A computer aided CNC machine is essential to reduce the amount of time and costs to cut the notches. The help of the industry is needed to market and implement this composite floor system.

Other research needs that were beyond the scope of this thesis

---

1) Numerical analyses – numerical finite element investigations in both the short- and long-term to calibrate the model on the experimental results of this project and to

predict the behaviour of composite systems with different geometrical and mechanical properties in the short- and long-term.

2) Dynamic behaviour – behavioural response of composite floors subjected to seismic loading considering the diaphragm action and floor-to-mainframe connection.

3) Fatigue behaviour – behavioural response of connections and floor beams subjected to 1 to 2 million cycles of repeated loads to investigate possible applications of the system for short-span girder bridges.

4) Vibrations – behavioural response of medium to long span floors subjected to vibration.

5) Acoustics – solution for inter-storey sound and impact transmission.

6) Fire resistance – behavioural response of composite floors to fire.

References

ABAQUS Version 6.0 (2000) Hibbitt, Karlsson & Sorensen, Inc.

Abd Ghafar H, Deam B, Fragiacomo M, Buchanan A (2008) Vibration performace of LVL-concrete composite floor system. In: Proceedings of 10th World Conference on Timber Engineering, Miyazaki (Japan), CD copy.

Aicher S, Klock W, Dill-Langer G, Radovic B (2003) Nails and nailplates as shear connectors for timber-concrete composite constructions. Otto-Graf-Journal 14:189-209.

Aldi P (2008) Timber-concrete composite beams: a numerical approach to investigate the behaviour of grooved connections. In: Proceedings of the 7th FIB PhD Symposium. Stuttgart (Germany), CD copy.

ANSYS (2007) Release 11.0 Academic Teaching Advanced. ANSYS Inc. Canonsburg PA 15317 USA.

AS/SNZ Standards Australia and Standards New Zealand (2002) AS/NZS1170 – Structural design actions – Part 0: General principles. Canberra, Australia.

Balogh J, Gutkowski R (2008) Modelling of shear transfer in wood-concrete notch connections. In: Proceedings of 10th World Conference on Timber Engineering, Miyazaki (Japan), CD copy.

Balogh J, Fragiacomo M, Gutkowski RM, Fast RS (2008) Influence of repeated and sustained loading on the performance of layered wood-concrete composite beams. J Struct Eng ASCE 134(3) 430-439.

Bathon L, Bletz O, Schmidt J (2006) Hurricane proof buildings - an innovative solution using prefabricated modular wood-concrete-composite elements. In: Proceedings of 9th World Conference on Timber Engineering, Portland, Oregon (USA), CD copy.

Benitez MF (2000) Development and testing of timber/concrete shear connectors. In: Proceedings of the World Conference on Timber Engineering, Vancouver, BC, Canada, paper 8.3.2.

Blakemore P (2003) The use of hand-held electrical moisture meters with commercially important Australian hardwoods, Part 2 for Forest Wood Products Research and

Development Corporation. CSIRO Forestry and Forest Product, Project No. PN 01.1306, Australia, p 191.

Bonamini G, Ceccotti A, Uzielli L (1990) Short- and long-term experimental tests on antique larch and oak wood-concrete composite elements. In: Proceedings of CTE Conference, Bologna (Italy), 241-251 (in Italian).

Bou Said E, Jullien JF, Ceccotti A (2004) Long term modelling of timber-concrete composite structures in variable climates. In: Proceedings of the 8th World Conference on Timber Engineering, Lahti (Finland), 14-17 June, Vol 2, 143–148.

Brunner M, Romer M, Schnüriger M (2007) Timber-concrete-composite with an adhesive connector (wet on wet process). J Materials and Structures RILEM 40(1) 119-126.

Buchanan AH (1986) Combined bending and axial loading in lumber. J Struct Eng 112(12) 2592-2609.

Buchanan AH (2007) Timber Design Guide – Chapter 25: Timber flooring by Fragiacomo M, Yeoh D, Davison R, Banks W. New Zealand Timber Industry Federation Inc., Wellington, 275-288.

Capozucca R (1998) Bond stress system of composite-concrete timber beams. J Materials and Structures RILEM 31(213) 634-640.

Carradine DM, Newcombe MP, Buchanan A (2009) Using screws for structural applications in laminated veneer lumber. In: Proceedings of the Meeting fourty-two of the Working Commission W18-Timber Structures, CIB, International Council for Research and Innovation, Dübendorf (Switzerland), Paper No CIB-W18/42-7-7, 10 pp.

CEB Comité Euro-International du Béton (1993) CEB_FIP model code 90. CEB Bulletin. No. 213/214, Lausanne, Switzerland.

Ceccotti, A (1995) Timber-concrete composite structures. In: Blass HJ et al. (editor) Timber Engineering, Step 2, 1st edition. Centrum Hout, The Netherlands. E13/1-E13/12.

Ceccotti A (2002) Composite concrete-timber structures. Progress in Structural Engineering and Materials 4(3) 264-275.

Ceccotti A, Fragiacomo M, Giordano S (2006) Long-term and collapse tests on a timber-concrete composite beam with glued-in connection. J Materials and Structures RILEM 40(1) 15-25.

Ceccotti A, Fragiacomo M, Gutkowski RM (2002) Design of timber-concrete composite structures according to EC5-2002 version. In: Proceedings of the Meeting thirty-five of the Working Commission W18-Timber Structures, CIB, International Council for Research and Innovation, Kyoto (Japan), September, CIB-W18/35, 10 pp.

CEN Comité Européen de Normalisation. (1991) EN 26891 – Timber structures – Joints made with mechanical fasteners – General principles for the determination of strength and deformation characteristics. Brussels, Belgium.

CEN Comité Européen de Normalisation (2004a) Eurocode 2 – Design of concrete structures – Part 1-1: General rules and rules for buildings. Brussels, Belgium.

CEN Comité Européen de Normalisation (2004b) Eurocode 5 – Design of timber structures – Part 1-1: General rules and rules for buildings. Brussels, Belgium.

CEN Comité Européen de Normalisation. (2004c) Eurocode 5 – Design of timber structures – Part 2: bridges. Brussels, Belgium.

Chassagne P, Bou Saïd E, Jullien FJ, Galimard P (2005) Three dimensional creep model for wood under variable humidity - Numerical analyses at different material scales. J Mechanics of Time-Dependent Materials 9(4) 1-24.

CHH Carter Holt Harvey (2007a) New Zealand factory production data for LVL Truform recipe from January to May 2007.

CHH Carter Holt Harvey (2007b). USA factory production data for two grades of LVL.

CHH Carter Holt Harvey (2009) LVL Specific Design Information. Technical Bulletin. New Zealand, 2009, 12 pp.

Clouston P, Bathon L, Schreyer A (2005) Shear and bending performance of a novel wood-concrete composite system. J Struct Eng ASCE 131(9) 1404-1412.

Cone CM (1963) A composite timber-concrete bridge. TDA Bulletin, New Zealand Forest Service, 1(9) Feb 1963.

Cook JP (1976) Composite construction methods. J Construction Division, Proceedings of the American Society of Civil Engineers, 102(CO1), March 1976, pp 21 – 27.

Deam B, Fragiacomo M, Buchanan A (2007) Connections for composite concrete slab and LVL flooring systems. J Materials and Structures RILEM 41(3) 495-507.

Deam B, Fragiacomo M, Gross LS (2008) Experimental behaviour of prestressed LVL-concrete composite beams. J Struct Eng ASCE 134(5) 801-809.

Dias AMPG (2005) Mechanical behaviour of timber-concrete joints. PhD Thesis, University of Coimbra, Portugal, ISBN 90-9019214-X.

Dias AMPG, Lopes SMR, Van de Kuilen JWG, Cruz HMP (2007a) Load-carrying capacity of timber-concrete joints with dowel-type fasteners. J Struct Eng ASCE 133(5) 720–727.

Dias AMPG, Van de Kuilen JW, Lopes S, Cruz H (2007b) A non-linear 3D FEM model to simulate timber-concrete joints. J Adv Eng Softw 38, 522-530.

Döhrer A, Rautenstrauch K (2006) Connectors for timber-concrete composite-bridges. In: Proceedings of the Meeting thirty-nine of the Working Commission W18-Timber Structures, CIB, International Council for Research and Innovation. Florence (Italy), August, 39-7-3, 10 pp.

Finnish Road Administration (1999)
http://www.underwater.pg.gda.pl/didactics/ISPG/Mosty/Vihantasalmi%20bridge.htm

Fragiacomo M (2005) A finite element model for long-term analysis of timber-concrete composite beams. J Structural Engineering and Mechanics 20(2) 173-179.

Fragiacomo M (2006) Long-term behaviour of timber-concrete composite beams. II: Numerical analysis and simplified evaluation. J Struct Eng ASCE 132(1) 23-33.

Fragiacomo M, Ceccotti A (2004) A simplified approach for long-term evaluation of timber-concrete composite beams. In: Proceedings of the 8th World Conference on Timber Engineering, Lahti (Finland), 14-17 June, Vol 2, 537-542.

Fragiacomo M, Ceccotti A (2006) Long-term behaviour of timber-concrete composite beams. I: Finite element modeling and validation. J Struct Eng ASCE 132(1) 13-22.

Fragiacomo M, Schänzlin J (2000) Modelling of timber–concrete floor structures. Cost Workshop "Timber construction in the new millennium", Venice (Italy), September 29.

Fragiacomo M, Amadio C, Macorini L (2004) A finite element model for collapse and long-term analysis of steel-concrete composite beams. J Struct Eng ASCE 130(3) 489-497.

Fragiacomo M, Amadio C, Macorini L (2007a) Short- and long-term performance of the "Tecnaria" stud connector for timber-concrete composite beams. J Materials and Structures RILEM 40(10) pp 1013-1026.

Fragiacomo M, Gutkowski M, Balogh J, Fast RS (2007b) Long-term behaviour of wood-concrete composite floor/deck systems with shear key connection detail. J Struct Eng ASCE 133(9):1307-1315.

Frangi A, Erchinger C, Fontana M (2008) Charring model for timber frame floor assemblies with void cavities. J Fire Safety 43(8) 551-564.

Frangi A, Fontana M (2001) A design model for the fire resistance of timber-concrete composite slabs. In: Proceedings of the IABSE Conference on Innovative Wooden Structures and Bridges, August 29-31, Lahti (Finland).

Frangi A, Fontana M (2003) Elasto-plastic model for timber concrete composite beams with ductile connection. IABSE Structural Engineering International, 13(1) 47-57.

Gaunt D, Penellum B (2004) Phase 1 Truform in-grade testing for Carter Holt Harvey, New Zealand Forest Research Institute Limited, New Zealand, Report TE03-037, 6 pp.

Gelfi P, Giuriani E, Marini A (2002) Stud shear connection design for composite concrete slab and wood beams. J Struct Eng 128(12) 1544–1550.

Gerber C, Crews K, Yeoh D, Buchanan A (2008) Investigation on the structural behaviour of timber concrete composite connections. In: Proceedings of the 20th Australasian Conference on the Mechanics of Structures and Materials, Queensland (Australia), CD copy.

Grantham R, Enjily V, Fragiacomo M, Nogarol C, Zidaric I, Amadio C (2004) Potential upgrade of timber frame buildings in the UK using timber-concrete composites. In: 8th World Conference on Timber Engineering, Lahti (Finland), 14-17 June, Vol 2, 59-64.

Gutkowski R, Brown K, Shigidi A, Natterer J (2004) Investigation of notched composite wood-concrete connections. J Struct Eng 130(10) 1553-1561.

Gutkowski R, Brown K, Shigidi A, Natterer J (2008) Laboratory tests of composite wood-concrete beams. J Construction and Building Materials 22(6) 1059-1066.

Gutkowski RM, Thompson W, Brown K, Etournaud P, Shigidi A, Natterer J (1999) Laboratory testing of composite wood-concrete beam and deck specimens. In: Proceedings of the RILEM Symposium on Timber Engineering, Stockholm (Sweden), 263-272.

Hanhijärvi A (1995) Modelling of creep deformation mechanisms in wood. PhD Thesis, Helsinki University of Technology. Technical Research Centre of Finland. VTT Publications, Espoo (SF).

Hanhjiärvi A (2000) Advances in the knowledge of the influence of moisture changes on the long-term mechanical performance of timber structures. J Materials and Structures RILEM 33(225) 43-49.

Holschemacher K, Klotz S, Weibe D (2002) Application of steel fibre reinforced concrete for timber-concrete composite constructions. LACER 7, 161-170.

ISO834 (2000) Fire resistance testing. International Standards Organization, Geneva (Switzerland).

Kavaliauskas S, Kvedaras K, Gurksnys K (2005) Evaluation of long-term behaviour of composite timber-concrete structures according to EC. Technological and Economic Development of Economy, XI(4) pp 292-296.

Kenel A, Meierhofer U (1998) Long-term performance of timber-concrete composite structural elements. Report. No. 115/39, EMPA, Dübendorf, Switzerland (in German).

Koh HB, Mohamad Diah AB, Lee YL, Yeoh D (2008) Experimental study on shear behaviours of timber-lightweight concrete composite shear connectors. In: Proceedings of the 3rd Brunei International Conference on Engineering and Technology, Bandar Seri Begawan (Brunei), CD copy.

Kreuzinger H (1999) Holz-beton-verbundbauweise timber–concrete composite structures. *Informationsdienst Holz. Fachverlag Holz.*, Du¨sseldorf, Germany (in German).

Kuhlmann U, Aldi P (2008) Fatigue of timber-concrete-composite beams: characterization of the connection behaviour through push-out tests. In: Proceedings of 10th World Conference on Timber Engineering. Miyazaki (Japan), CD copy.

Kuhlmann U, Michelfelder B (2004) Grooves as shear-connectors in timber-concrete composite structures. In: Proceedings of the 8th World Conference on Timber Engineering, Lahti (Finland), 1, 301-306.

Kuhlmann U, Michelfelder B (2006) Optimised design of grooves in timber-concrete composite slabs. In: Proceedings of the 9th World Conference on Timber Engineering, Portland, Oregon (USA), CD copy.

Kuhlmann U, Schänzlin J (2001) Grooves as shear connectors for timber-concrete composite decks. In: Proceedings of the RILEM Conference on Joints in Timber Structures, Stuttgart (Germany), September 12-14, 283-290.

Lukaszewska E (2009) Development of prefabricated timber-concrete composite floors. PhD Thesis, Lulea University of Technology, Sweden.

Lukaszewska E, Fragiacomo M (2008) Static performance of prefabricated timber-concrete composite systems. In: Proceedings of the 10th World Conference on Timber Engineering, Miyazaki (Japan), CD copy.

Lukaszewska E, Fragiacomo M, Frangi A (2007) Evaluation of the slip modulus for ultimate limit state verifications of timber-concrete composite structures. In: Meeting forty of the Working Commission W18-Timber Structures, CIB, International Council for Research and Innovation, Bled (Slovenia), August 28-31, Paper No CIB-W18/40-7-5, 14 pp.

Lukaszewska E, Johnsson H, Fragiacomo M. (2008) Performance of connections for prefabricated timber-concrete composite floors. J Materials and Structures RILEM 41(9) 1533-1550.

Lukaszewska E, Fragiacomo M, Johnsson H. (2009a) Laboratory tests and numerical analyses of prefabricated timber-concrete composite floors. J Struct Eng ASCE, accepted for publication, June 2009.

Lukaszewska E, Fragiacomo M, Johnsson H (2009b) Time-dependent behaviour of prefabricated timber-concrete composite floors. Part 1: Experimental testing. J Engineering Structures Elsevier, submitted May 2009, under review.

McCullough B (1943) Oregon tests on composite (timber-concrete) beams. J American Concrete Institute 14(5) 429-440.

Meierhofer U (1993) A timber/concrete composite system. Structural Engineering International 3(2) 104-107.

Mettern C (2003) Structural timber-concrete composites – advantages of a little known innovation. The Structural Engineer, 18 February 2003, 17-19.

Miotto J, Dias A (2008) Glulam-concrete composite structures: experimental investigations into the connection system. In: Proceedings of the 10th World Conference on Timber Engineering, Miyazaki (Japan), CD copy.

Möhler K. (1956) On the load carrying behavior of beams and columns of compound sections with flexible connections. Habilitation, Technical Univ. of Karlsruhe, Germany (in German).

Muller P (1922) Decke aus hochkantig stehenden Holzbohlen oder Holzbrettern und Betondeckschicht. Patentschau aus dem Betonbau und den damit verwandten Gebieten. Auszuge aus den Patentschriften. Beton und Eisen, H. XVII, S. 244 (in German).

Mungwa MS, Jullien JF, Foudjet A, Hentges G (1999) Experimental study of a composite wood-concrete beam with the INSA-Hilti new flexible shear connector. J Construction and Building Materials 13(7) 371-382.

Murray R (2009) Fatigue analysis of timber-concrete composite connections. Research report, University of Canterbury, New Zealand.

Natterer J (2002) New technologies for engineered timber structures. Prog. Struct. Engng Mater. 4, 245-263.

Natterer J, Hamm J, Favre P (1996) Composite wood-concrete floors for multi-story buildings. In: Proceedings of the International Wood Engineering Conference, New Orleans, Louisiana, (USA), 3, 431-435.

Newcombe M, van-Beerschoten WA, Carradine D, Pampanin S, Buchanan A, Deam B, Fragiacomo M (2009) In-plane experimental testing of timber-concrete composite floor diaphragms. In: Proceedings of New Zealand Society of Earthquake Engineering Conference, Christchurch (New Zealand), CD copy.

Ollgard G, Slutter G, Fischer W (1971) Shear strength of stud connectors in lightweight and normal weight concrete. AISC Eng J 8, 55-64.

O'Neill J (2009) The fire performance of timber-concrete composite floors. Master Thesis, University of Canterbury, New Zealand.

Owen B (1963) Handbook of Statistical Tables. Addison-Wesley Publishing Company, Inc. Reading, Massachussetts.

Persaud R, Symons D (2005) Design and testing of a composite timber and concrete floor system. The Structural Engineer 84(4) 22-36.

Pillai U, Ramakrishnan P (1977) Nail shear connectors in timber-concrete composites. J Institution of Engineers (India) Civil Engineering Division 58(CI 1) 34-39.

Pincus P (1970) Behaviour of wood concrete composite beams. J Structural Division ASCE 96(7) 2009-2019.

Priestley MJN (1970) Shear tests on timber-concrete composite construction. Ministry of Works, Central Laboratories, New Zealand Forest Service, Report 364, 18th August 1970.

Ranta-Maunus A (2000) Creep of timber during eight years in natural environments. In: Proceedings of the 6th World Conference on Timber Engineering, Whistler Resort, British Columbia (Canada), 31 July–3 August, Paper No 8-5-2, CD.

Richart FE, Williams CB (1943) Tests of composite timber-concrete beams. J American Concrete Institute 14(4) 253-276.

Schänzlin J (2003) Time dependent behaviour of composite structures of board stacks and concrete. PhD Thesis, University of Stuttgart (in German).

Schänzlin J, Fragiacomo M (2007) Extension of EC5 Annex B formulas for the design of timber-concrete composite structures. In: Meeting forty of the Working Commission W18-Timber Structures, CIB, International Council for Research and Innovation, Bled (Slovenia), August 28-31, 2007, Paper No CIB-W18/40-10-1, 10 pp.

Schänzlin J, Fragiacomo M (2008) Modelling and design of timber-concrete-composite structures in the long-term. In: Proceedings of the 10th World Conference on Timber Engineering, Miyazaki (Japan), June 2-5, 2008, CD copy.

Schaub O (1939) Verbunddecke aus Holzrippen und Betonplatte. Patentschrift Nr. 673 556 Deutsches Patentamt (in German).

Seibold E (2004) Feasibility study for composite concrete/timber floor systems using laminated veneer lumber in New Zealand. Research report. University of Canterbury, New Zealand.

SIKA (2008) Product Data Sheet SIKA 212/215 Version no: 05/04 (reprinted 08/05) http://www.sika.co.nz/nz_con_contds_sika_grout_212_215_0805.pdf

Sipari P (2000) Sound insulation of multi-storey houses – a summary of Finnish impact sound insulation results. J Building Acoustics 7(1) 15-30.

Smith T, Fragiacomo M, Pampanin S, Buchanan A (2009) Construction time and cost estimates for post-tensioned multi-storey timber buildings. In: Proceedings of ICE Construction Materials – Special issue on timber structures, in print.

Smith T, Pampanin S, Fragiacomo M, Buchanan A (2008) Design and construction of prestressed timber buildings for seismic areas. In: Proceedings of the 10th World Conference on Timber Engineering, Miyazaki (Japan), June 2-5, 2008, CD copy.

SNZ Standards New Zealand (1986) NZS 3112 – Specification for methods of test for concrete. Wellington, New Zealand.

SNZ Standards New Zealand (1993) NZ3603 – Design timber structures. Wellington, New Zealand.

SNZ Standards New Zealand (2006) NZ3101 – Concrete structures standard – Part 1: The design of concrete structures. Wellington, New Zealand.

Steinberg E, Selle R, Faust T (2003) Connectors for timber-lightweight concrete composite structures. J. Struct Eng 129(11) 1538-1545.

TICOMTEC Holz-Verbund-Systeme (2007) http://www.hbv-system.de

To LG (2009) 3D finite element modelling of time-dependent behaviour of wood concrete composite beams. PhD Thesis, Colorado State University, Fort Collins (USA).

Toratti T (1992) Creep of timber beams in variable environment. PhD Thesis, Helsinki University of Technology, Laboratory of Structural Engineering and Building Physics.

Toratti T (2004) Service limit states: Effects of duration of load and moisture on deformations. Cost E24 Reliability of Timber Structures, Florence, 27-28 May 2004, 11 pp.

Toratti T, Kevarinmäki A (2001) Development of wood-concrete composite floors. In: Proceedings of the Innovative wooden structures and bridges Conference, International Association for Bridge and Structural Engineering, Lahti (Finland), 513-518.

Turrini G, Piazza M (1983a) A technique for stiffness and strength upgrading of wooden floors. Recuperare, 5, 224–237 (in Italian).

Turrini G, Piazza M (1983b) Static behaviour of timber-concrete composite structures. Recuperare, 6, 214–225 (in Italian).

Van der Linden M (1999) Timber-concrete composite floor systems. PhD Thesis, Delft University Press, The Netherlands.

Weaver CA, Davids WG, Dagher HJ (2004) Testing and analysis of partially composite fibre-reinforced polymer-glulam concrete bridge girders. J Bridge Eng 9(4) 316–325.

Yeoh D, Fragiacomo M, Abd Ghafar H, Buchanan A, Deam B, Crews K (2008a) LVL-concrete composite floor systems: an effective solution for multi-storey timber buildings. In: Proceedings of the Australasian Structural Engineering Conference, Melbourne (Australia), CD copy.

Yeoh D, Fragiacomo M, Aldi P, Mazzilli M, Kuhlmann U (2008b) Performance of notched coach screw connection for timber-concrete composite floor system. In: Proceedings of the 10th World Conference on Timber Engineering, Miyazaki (Japan), CD copy.

Yeoh D, Fragiacomo M, Buchanan A, Crews K, Haskell J, Deam B (2008c) Development of semi-prefabricated timber-concrete composite floors in Australasia. In: Proceedings of the 10th World Conference on Timber Engineering, Miyazaki (Japan), CD copy.

Yeoh D, Fragiacomo M, Banks W, Newcombe MP (2009a) Design and construction of a LVL-concrete composite floor. J Structures and Buildings ICE – Timber special issue, submitted October 2009, under review.

Yeoh D, Fragiacomo M, Buchanan A, Deam, B (2009b) Experimental behaviour at ultimate limit state of a semi-prefabricated timber-concrete composite floor system. In: Proceedings of the International Symposium on Timber Structures from Antiquity to the Present, Istanbul (Turkey), June 25-27, 287-298.

Yeoh D, Fragiacomo M, Buchanan A, Gerber C (2009c) Preliminary research towards a semi-prefabricated LVL-concrete composite floor system for the Australasian market. Australasian J Struct Eng 9(3) 225-240.

Yeoh D, Fragiacomo M, Deam B (2009d) Long-term behaviour of LVL-concrete composite connections and beams under sustained load. J Materials and Structures RILEM, submitted December 2009, under review.

Yeoh D, Fragiacomo M, De Franceschi M, Buchanan A (2009e) Experimental tests of notched and plate connectors for LVL-concrete composite beams. J Struct Eng ASCE, submitted August 2009, under review.

Yeoh D, Fragiacomo M, De Franceschi M, Koh HB (2009f) The state-of-the-art on timber-concrete composite structures – a literature review. J Struct Eng ASCE, submitted August 2009, under review.

Yeoh D, Fragiacomo M, Deam B (2010) Experimental limit state behaviour of LVL-concrete composite floor beams. J Eng Struct Elsevier, submitted January 2010, under review.

Appendices